Alma Mater Studiorum – Università di Bologna

DOTTORATO DI RICERCA IN

SCIENZE DELLA TERRA

Ciclo XXVIII

Settore Concorsuale di afferenza: 04/A2

Settore Scientifico disciplinare: GEO/02

The Pleistocene-Holocene transition in the Po Plain (Italy): stratigraphic architecture and sequence stratigraphy from a highly-subsiding basin

Presentata da: ***Bruno Campo***

Coordinatore Dottorato	**Relatore**
Prof. Jo Hilaire Agnes De Waele	***Prof. Alessandro Amorosi***

Esame finale anno 2016

INDEX

1. INTRODUCTION

In the last decades of the twentieth century, among the international scientific community it has become evident the huge impact of human activities upon the environment. Specific attention has been paid to climate changes over very short time scales, especially after the first studies on the “greenhouse” effect (Mitchell, 1989; Smith and Tirpak, 1989; IPCC Scientific Assessment, 1990; Peiji, 1991).

In order to make predictions about climate, sea-level changes and their effects on coastal regions, the first step has been to look at the continental stratigraphic record, which represents an authentic physical record of global change (Burke et al., 1990). Several studies focused on the magnitude and frequency of past global changes to provide useful historical trends for a reliable understanding of climate evolution and its possible impact.

The interest for continental strata, and in particular, for the allogenic factors (tectonics, climate, eustacy) controlling the stratigraphic architecture at different time-scales, was energized by the contemporaneous development of sequence stratigraphic concepts, such as the response of depositional systems to sea-level changes (Jervey, 1988; Posamentier and Vail, 1988; Posamentier et al., 1988) and the debate concerning the controversial linkage between alluvial and coeval shoreline (Shanley and McCabe, 1994).

In this framework several fluvial models were developed (Miall, 1991; Schumm, 1993; Wright and Marriott, 1993; Helland-Hansen and Gjelberg, 1994; Helland-Hansen and Martinsen, 1996; Leeder and Stewart, 1996; Milana, 1998; Marriott, 1999; Posamentier and Allen, 1999), but none was able to really isolate and quantify the role played by every single forcing factor.

More recently, climate (Legarreta and Uliana, 1998; Bridgland, 2000; Aqrawi, 2001; Lewis et al., 2001; Macklin et al., 2002; Vandenberghe, 2003) and tectonics (Martinsen et al., 1999; Marzo and Steel, 2000; Adams and Bhattacharya, 2005; Hickson et al., 2005) have been identified as the major factors controlling fluvial architecture.

Another discussion was opened on the landward propagation of the effects produced by changes in relative sea-level on fluvial systems: several alluvial systems around the world, with different characteristics (sediment supply, gradient etc…) have shown values ranging between few tens of km up to several hundreds of km, updip from the shoreline (Schumm, 1993; Blum and Törnqvist, 2000; Cattaneo and Steel, 2003, Holbrook et al., 2006; Shen et al., 2012).

Furthermore, a good understanding of alluvial deposits (both ancient and modern) in terms of stratigraphic architecture and sediment-body geometries may turn out useful

for practical purposes, such as hydrocarbon and groundwater exploration. Since the last decades have been characterized by an increased demand for natural resources due to human activities, accurate characterizations and delineations of reservoir/aquifer geometries could significantly reduce costs and improve profits.

High-resolution stratigraphic studies, however, represent a difficult task when limited by tectonic deformation and poor knowledge of climate, eustacy and fossil record. On the other hand, in Quaternary successions, tectonic deformation is irrelevant and both climatic and eustatic histories are well known, especially after the development of Quaternary paleoclimatology.

Studies on oxygen-isotope records in deep-sea sediments (Shackleton and Opdyke, 1973; Imbrie et al., 1984; Chappell and Shackleton, 1986; Shackleton, 1987) documented the cyclic alternation of glacial and interglacial phases which definitively led to the acceptance of the Milankovitch theory of climate change (Hayes et al., 1976; Imbrie and Imbrie, 1979): global variations in ice volume and sea-level, following periods of 400-100-43-23 and 19 ky as predicted by the Milankovitch theory of orbital forcing. Middle and Late Pleistocene, for example, have been characterized by the alternation of full glacial-interglacial cycles with a periodicity of 100 ky.

Additional works on the marine record and ice cores proved the superimposition on 100 ky Milankovitch cycles of important (not completely understood) climate changes at time scales of 10^3-10^4 (Behl and Kennet, 1996; Bond et al.,1993, 1997), showing the complexity of the Pleistocene-Holocene transition.

An equivalent cyclicity, in the Milankovitch and sub-Milankovitch bands, was observed in the late Quaternary deposits of the highly subsiding Po Plain, characterized by distinctive cyclic changes in lithofacies and channel stacking patterns.

Recent studies, based on pollen data and radiocarbon dating, have documented a glacio-eustatic control on the stratigraphic architecture of the Po coastal plain (Amorosi et al, 1999a; 2004; Amorosi and Colalongo, 2005; Amorosi, 2008) and of the central Po Plain (Amorosi et al., 2008a). In particular, five vertically stacked, 4th order transgressive-regressive (T-R) sequences (*sensu* Embry, 1995) were recognized across the whole Po basin from the proximal Apenninic margin, down to the distal coastal plain succession.

Beneath the modern coastal plain (see Amorosi and Colalongo, 2005), because of the high-subsidence rates, these sequences reach a maximum thickness of 100 m, and consist of basal aggradational coastal plain deposits overlain by transgressive sands, interpreted as retrograding barrier-lagoon-estuary systems during rapid sea-level rise under interglacial conditions (transgressive systems tract, TST). The upward vertical transition to shallow-marine and alluvial sediments reflects the delta and strandplain

progradation (highstand systems tracts, HST). Thick (up to 60 m) alluvial successions reveal long phases of sea-level fall during glacial periods (falling stage and lowstand systems tracts or FSST and LST).

In landward position, within fully alluvial strata, T-R sequences have been identified on the basis of abrupt changes in lithofacies and fluvial channel stacking patterns: basal silty-clay overbank deposits with individual fluvial channel sands (TST), grade upwards into increasingly amalgamated and laterally extensive fluvial bodies (HST, FSST and LST). Pollen analysis highlighted the association between the lowermost, organic-rich portion of the overbank deposits and major phases of channel abandonment and floodplain aggradation taking place at the onset of warm-temperate (interglacial) climatic conditions (Amorosi et al., 2008a). Lack of pollen data from the sandy sheet-like sediments prevented the climatic characterization of the upper regressive interval of the sequence.

Amorosi and Colalongo (2005) postulated the possible correlation between cyclic facies changes and the marine oxygene-isotope record, documenting strict relationships between the stratigraphic architecture of T-R sequences and glacial-interglacial cyclicity. They suggested transgressive surfaces (TSs) as the key feature for stratigraphic correlations due to their high traceability throughout the basin. The TSs physically mark abrupt landward shifts of facies, and have a characteristic warm-temperate pollen signature.

Previous work on the stratigraphic characterization of the Emilia-Romagna (E-R) coastal plain subsurface has focused on cross-sections perpendicular to the modern shoreline (Rizzini, 1974; Amorosi and Milli 2001; Amorosi et al., 1999b, 2003), with the aim of providing high-resolution descriptions of T-R coastal wedges; however, no long stratigraphic cross-sections have been constructed along strike, to ensure 3D stratigraphic reconstructions.

Furthermore, though Amorosi and Colalongo (2005) documented the linkage between shoreline deposits with coeval alluvial successions on the basis of the landward TS traceability, there is scarce physical evidence in terms of facies distribution, to answer the question “how far inland sea-level changes affected alluvial architecture beneath the Po Basin at the Pleistocene-Holocene transition”.

The aim of this work is to focus on the Pleistocene-Holocene transition with examples from the Po Plain: specifically, we want to enhance the present high-resolution stratigraphic framework providing two new long cross sections. Through the first one (ca. 100 km long), parallel to the modern E-R shoreline, we want:

- to investigate the lateral extent of the vertical transition between Late Pleistocene alluvial deposits and Holocene coastal sediments;

- to document facies distribution, geometries and lateral continuity of the Holocene T-R coastal wedge, from the area where the present shoreline meets the Apenninic margin to the modern Po Delta;
- to offer a generalized sequence-stratigraphic interpretation of the Pleistocene-Holocene sedimentary succession for the time "window" suited to radiocarbon analysis (last 45 ky BP).

With the second cross-section (ca. 120 km-long), along the modern Po River we want:

- to investigate a fully alluvial succession extending ca. 130 km updip from the modern shoreline;
- to describe the contrasting stratigraphic architecture between amalgamated Late Pleistocene fluvial sands and a Holocene mud-dominated succession with isolated fluvial-channel bodies;
- to check the "glacial age" of these multi-storey sand bodies through new radiocarbon dates;
- to identify the "landward limit of sea-level influence" of Blum and Törnqvist (2000), during the post-glacial sea-level rise, on the basis of horizontal facies distribution/variation coupled with additional radiocarbon dating.

We noticed that the overall stratigraphic architecture that characterize the Pleistocene-Holocene transition in the subsurface of the Po Plain has similarities with the incised valley fills (ivfs) of late Quaternary age described by Blum and Törnqvist (2000), Hori et al. (2002) and Tanabe et al. (2006).

In Italy, thick paleovalley systems have been identified from the high-gradient Tyrrhenian Sea coast: these studies include the Tiber River Delta (Milli et al., 2013) and the Roma Basin (Milli, 1997; Milli et al., 2008; Mancini et al., 2013); the Arno valley and Serchio river mouth in Tuscany (Amorosi et al., 2008c, 2009, 2013); the Volturno coastal plain (Amorosi et al., 2012).

Ivfs represent expanded stratigraphic successions accumulated within incisions cut by rivers during sea-level fall, in correspondence of glacial periods. Sea-level rise, during interglacial conditions, produces the progressive drowning and filling of the valley with low net-to-gross transgressive and highstand deposits above amalgamated (lowstand) fluvial channel bodies (Dalrymple et al., 1994; Zaitlin et al., 1994; Boyd et al., 2006). Paleovalley systems also include paleosol development in the subaerially exposed interfluves during sea-level fall (Blum et al., 2013). Paleosols are considered as key elements for subdivision and mapping of continental strata on a variety of time

scales (Choi, 2005; Buck et al., 2010) and sequence stratigraphic models have predicted the presumed position of paleosols within non-marine deposits (Van Wagoner et al., 1990; Wright and Marriott, 1993; Cleveland et al., 2007; Varela et al., 2012). One of the most prominent features are paleosols formed at interfluves sequence boundaries, adjacent to paleovalley systems (Aitken and Flint, 1996; McCarty and Plint, 1998), which in late Quaternary interfluves mark the depositional hiatus between Pleistocene and overlying Holocene deposits.

In this perspective, pushed by new-fresh data available from continuously cored boreholes, we specifically selected a mud-prone, distal alluvial succession between the Apenninic margin and the Po channel belt (i.e. interfluve), with specific focus on paleosol stratigraphy. The aim was to test a new method for paleosol identification in unconsolidated deposits (coupled with accurate facies analysis), using geotechnical properties deriving from simple pocket penetrometer tests. Paleosol identification, in fact, can be used for high-resolution stratigraphic correlations of Late Pleistocene-Holocene alluvial successions (Bruno et al., 2013; Amorosi et al., 2014).

On the other hand, no major valley systems attributable to the Po River have been observed along the low-gradient north-Adriatic shelf (Trincardi et al., 1994), whereas an important erosional feature (the Manfredonia incised-valley-system) was identified in the Adriatic offshore, south to the Gargano Promontory (Maselli and Trincardi, 2013; Maselli et al., 2014). For this reason, we moved to another coastal plain, about 300 km south of the Po Plain, where we had the opportunity to investigate, for the first time, an Adriatic incised-valley system buried onshore (the Biferno paleovalley). Through the high-resolution reconstruction of the Biferno coastal deposits we compared two coeval (Late Pleistocene-Holocene) Adriatic coastal successions that diverge in terms of shelf gradient and proximity to the lowstand Po Delta.

In densely populated alluvial setting, such as the Po Plain, stratigraphic studies and methods (i.e., facies analysis, sequence stratigraphy etc…) can also be applied for practical purposes, including aquifer identification and their subsurface spatial distribution. From a hydrostratigraphic point of view, the peculiar cyclicity observed in the Po Plain deposits has important implications: each T-R cycle has been associated to an aquifer system (Amorosi and Pavesi, 2010): the muddy, transgressive portion is the aquitard (permeability barrier), whereas the “regressive” deposits form the aquifer. During this research, we had the opportunity to collaborate with hydeogeologists (Prof. Gargini research group, University of Bologna) who have been dealing with potential aquifer contamination in the city of Ferrara.

The aim of this multi-proxy study was to show the effectiveness of integrating hydrogeological and sequence-stratigraphy data, in order to interpret contaminant

concentration distribution and transformation in space and time. Through detailed facies analysis along a ca. 6 km-long cross-section, we highlight the stratigraphic role of swamp, organic-rich layers for contaminant enhancement (through reaction with organic matter) and dispersal.

This three years research is the result of a collaboration of the University of Bologna (Department of Biology, Earth and Environmental Sciences) with:

- The Geological, Seismic and Soil Survey of Regione Emilia-Romagna, which made available more than 1,686 stratigraphic descriptions, including continuously drilled core and drilling logs, radiocarbon dates, pollen profile and pocket penetration values. This vast database was implemented with 25 continuous cores drilled during 2012-2015.
- The University of Molise (Prof. Rosskopf research group), which made available the stratigraphic dataset for the study of the Biferno coastal Plain.

2. GEOLOGICAL SETTING

2.1. Structural setting

The Po Plain is the superficial expression of the foreland basin bounded by two fold-and-thrust belts of opposite vergence: the S-verging Alps to the north and the N-NE verging Apennines to the south (Fig 1).The evolution of these mountain chains took place in the framework of the Eurasia-Africa convergence since the Cretaceous (Carminati and Doglioni, 2012). Recent studies based on GPS have documented a rate of 3-8 mm/y for the ongoing motion between Africa and Eurasia plates (Serpelloni et al., 2007).

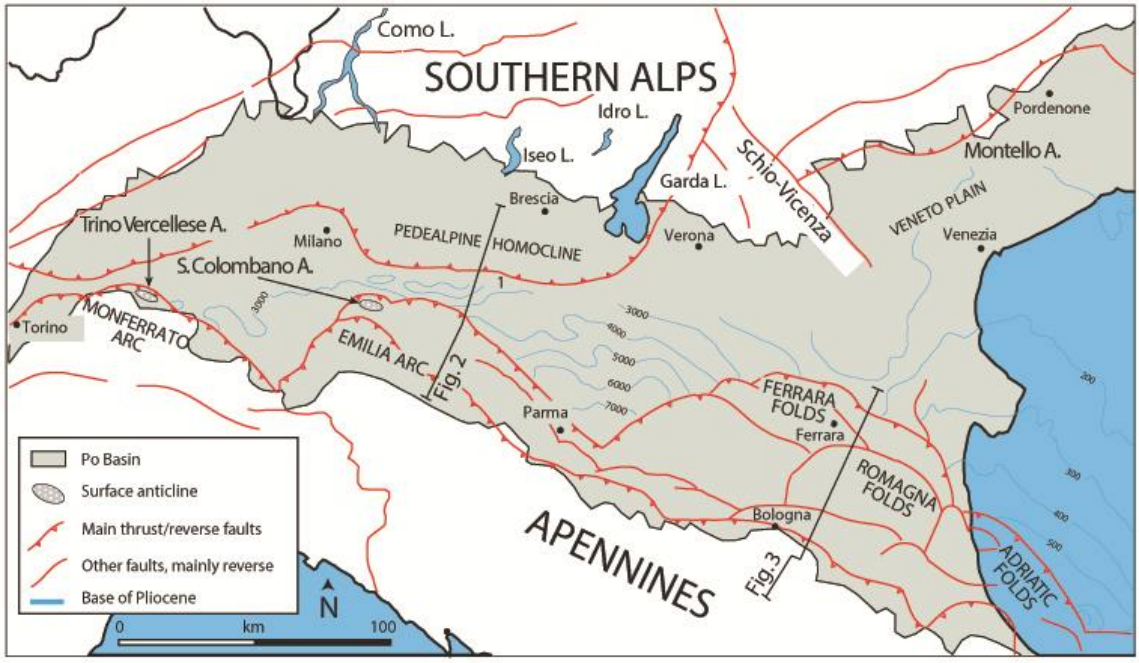

Fig. 1 - Structural map of the Po Basin. Modified from Burrato et al. (2003).

The origin of the Southern Alps is connected to the southward-dipping subduction of the European plate beneath the Adriatic plate (Vannoli et al., 2015). The Eocene-upper Miocene crustal flexuring by the S-verging southern Alpine thrusts led to the formation of the S-Alpine foredeep with the deposition of a thick molasse succession (Stefani et al., 2007).

The Apennines are related to the WSW-dipping subduction of the Adriatic plate under the Tyrrhenian lithosphere (Carminati et al., 2005), which started in the Late Oligocene along the retrobelt of the Alps (Gueguen et al., 1998).The Apennine thrust fronts, foredeep basins and extensional back-arc tectonics migrated progressively to the east as a consequence of the radial retreat of the subduction process (Doglioni et

al., 1999). The Cenozoic passive margin sedimentary cover of the subducting Adria microplate was piled up by the subduction hinge rollback to form the Apennines accretionary prism (Carminati and Vadacca, 2010).

The Po Plain lies on the remains of the Adriatic plate and represents the foreland of both the S-Alps and the N-Apennines. Both thrust belts are buried beneath the modern alluvial plain (Fig. 2), because of the fast subsidence rates induced by the tectonic loading of the two chains. North to the Po River, the S-Alps front runs from Milano to the Garda Lake, defining a single wide arc connected to the Giudicarie thrust system (Castellarin and Cantelli, 2000; Massironi et al., 2006) and deforming the S-sloping Pedealpine homocline (Burrato et al., 2003). It has been associated with high angle back-thrust and small topographic highs cropping out in the northern sector of the plain (Livio et al., 2009). The most noticeable tectonic structures expressed at the surface are the Trino Vercellese Anticline, the San Colombano Anticline and the Montello Anticline in the Veneto Plain (Burrato et al., 2003).

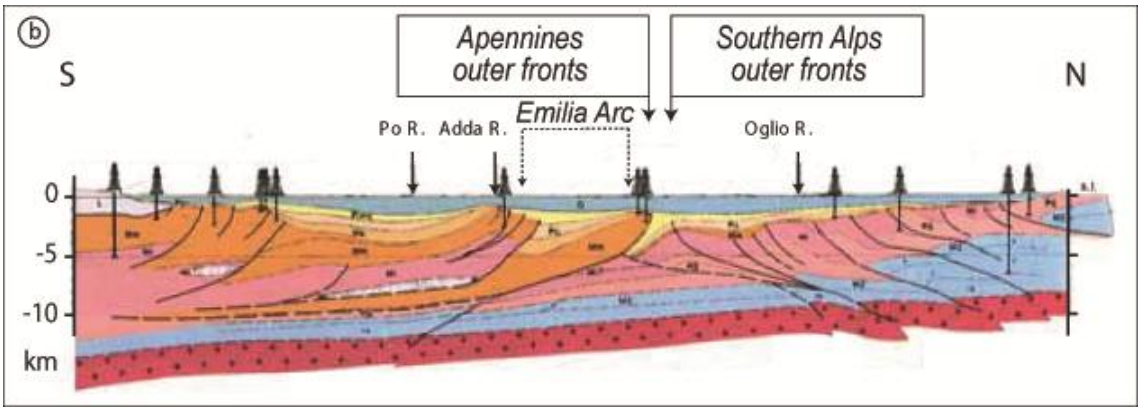

Fig. 2 - Apenninic (to the south) and Alpine (to the north) thrust fronts beneath the Po Plain. Modified from Burrato et al. (2003).

South to the Po River, several studies have documented the structure of the Apennine fold-and-thrust belt (Fig. 3), which involved Mesozoic to Neogene sediments of Adria and the older basement (Picotti and Pazzaglia, 2008; Mazzoli et al., 2015).

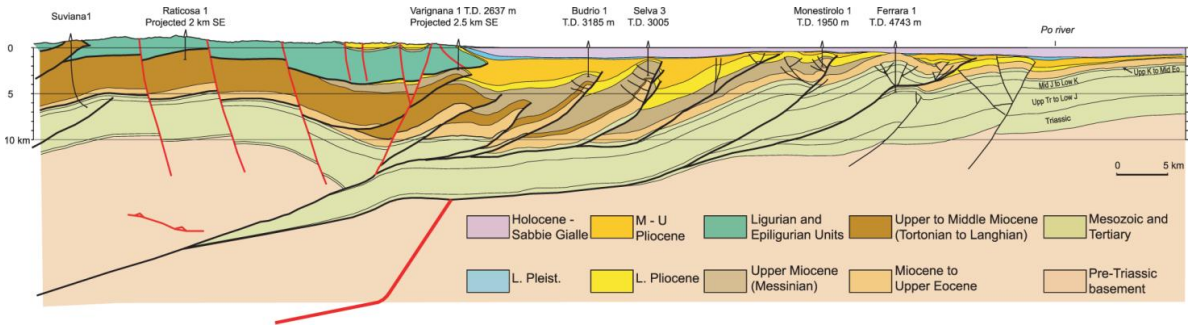

Fig. 3 - Buried structures beaneth the Po Plain, south to the Po River: the Apenninic fold-and-thrust belt. Modified from Picotti and Pazzaglia (2008).

Extensive oil exploration campaigns carried out by Agip (i.e. Pieri and Groppi, 1981) allowed the mapping of the main buried tectonic elements forming the Apennines outer fronts. Three arcs of blind, north-verging thrusts were identified beneath the Po Plain (Figs. 1 and 4):

1. the Monferrato Arc (Elter and Pertusati, 1973) is the inner and westernmost arc characterized by a last, Late Pleistocene important diastrophic phase;
2. the Emilia Arc is the central arcuate system thrust, also showing its latest and most important phase during the Late Pliocene (Castellarin and Vai, 1986);
3. the Ferrara-Romagna is the easternmost and the most external arc.

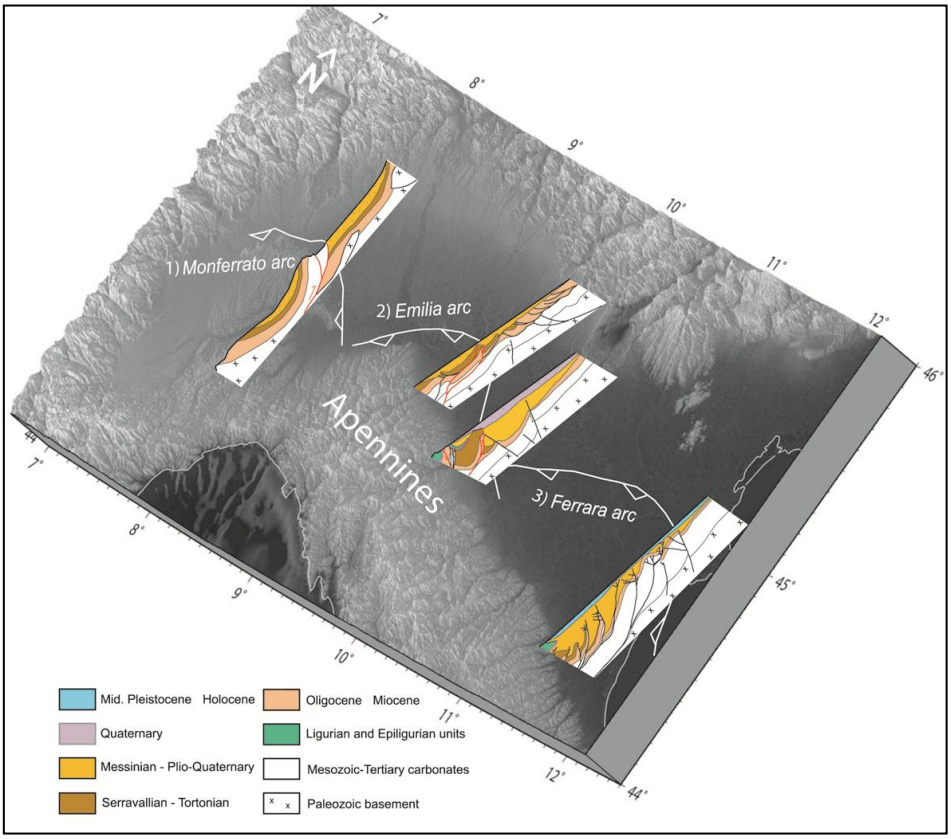

Fig. 4 - The Apennines outer fronts buried beneath the Po Plain: Monferrato, Emilia and Ferrara Arcs. Modified from Picotti and Pazzaglia (2008).

The Ferrara-Romagna arc is subdivided into the lower-rank Ferrara folds (or “Dorsale Ferrarese”), Romagna folds (the innermost system) and Adriatic folds (Burrato et al., 2003). The latter are buried in the Adriatic offshore, and their outer structures are covered by Late Pleistocene and Holocene deposits (Mazzoli et al., 2015).

The activity of the more external Apennine thrusts (Ferrara arc and Mirandola anticline) has recently been proved by earthquakes ca. Mw. 6 (may-june 2012)

generated in the Mirandola area (Galli et al., 2012). Another important structure is the Apenninic mountain front or Pedeapenninic Thrust Front (PTF) of Boccaletti et al., (1985), which lies at the foot of the N-Apennines (Fig. 5). It has been interpreted as an emergent to blind thrust fault by Boccaletti et al. (2004); on the other hand, Picotti and Pazzaglia (2008) showed that the present-day compression is due to a steep blind ramp, located between 15-18 km depth.

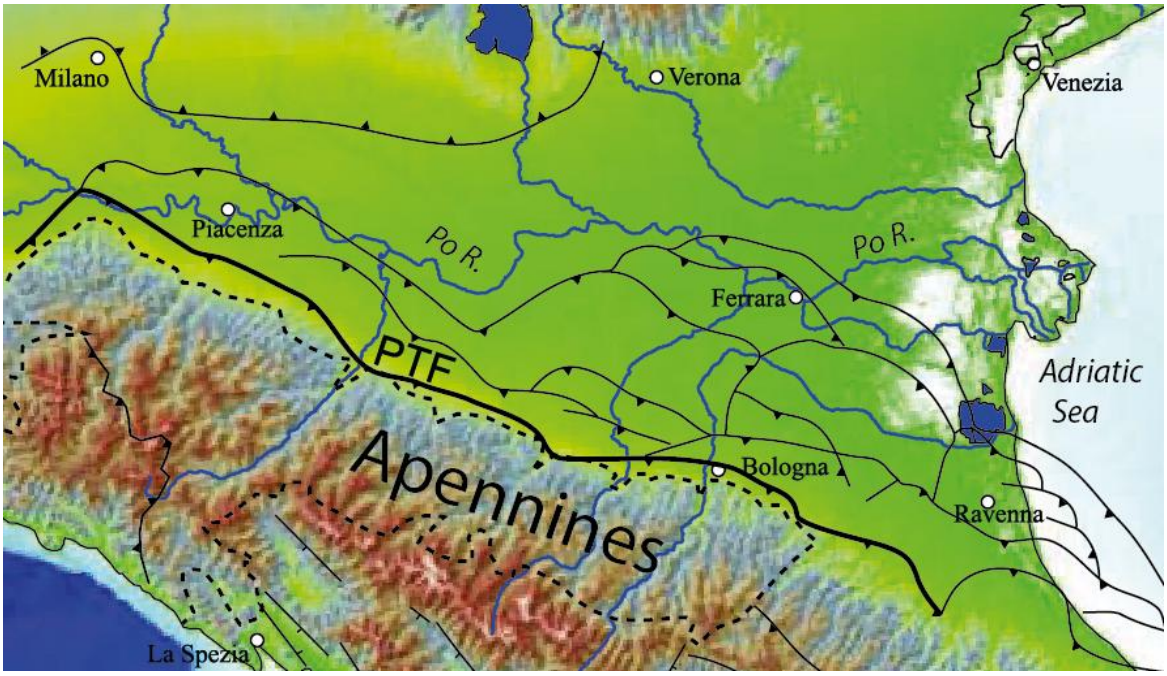

Fig. 5 - The apenninic mountain front or Pedeapenninic Thrust Front (PTF) of Boccaletti et al. (1985) lies at the foot of the N-Apennines.

The overall subsiding trend that characterizes the Po Basin is related to crustal flexuring generated by the Apennines, as documented by Carminati et al. (2005). Long-term subsiding rates range between 0.4-2.4 mm/y (Carminati et al., 2005), the highest values characterizing the modern Po Delta, as shown in Figure 6a (Carminati and Martinelli 2002; Antonioli et al., 2009). Vertical velocities depend on long-term geological processes and their components, such as sediment compaction, sediment loading and tectonic loading. Present-day vertical movements (Fig. 6b) are more related to the “anthropogenic component”, including the relatively recent water pumping and hydrocarbon extraction activities, which led to maximum values of 70 mm/y (Carminati and Martinelli 2002; Baldi et al., 2009). The present-day natural subsidence is still affected by the effects of the post-Last Glacial Maximum deglaciation (Mitrovica and Davis, 1995; Carminati et al., 2005).

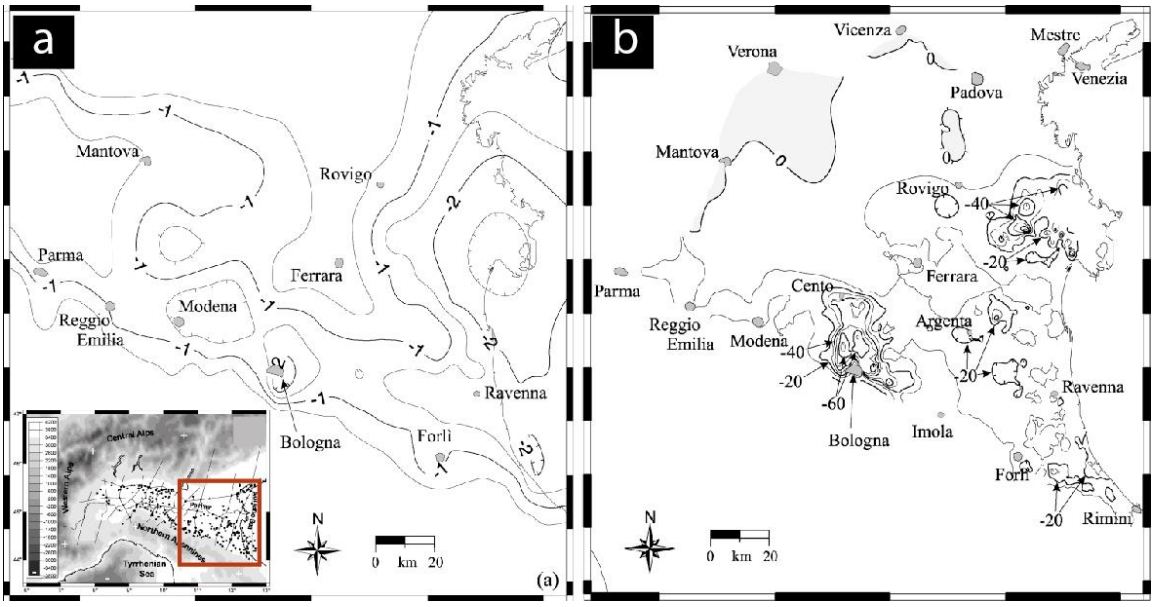

Fig.6 - a) Long-term subsidence (last 1.43 My); b) present-day subsidence. Modified from Carminati and Martinelli (2002).

2.2. Depositional architecture

In the Po Valley Basin, subsurface geology has been investigated and described on the basis of seismic data collected for hydrocarbon exploration (Pieri and Groppi, 1981; Dalla et al., 1992; Muttoni et al., 2003). The clastic sequence deposited between the Tertiary and the Quaternary shows an overall regressive evolution from Pliocene open-marine to Quaternary shallow-marine and alluvial deposits. The thickness of the Plio-Pleistocene foredeep in the S-Alps ranges between 2-6 km (Doglioni, 1993; Bertotti et al., 1998; Burrato et al., 2003); between 7-8.5 km in the deepest depocenters of the N-Apennines (Pieri and Groppi, 1975; Consiglio Nazionale delle Ricerche, 1992; Carminati and Vadacca, 2010).

Additional studies based on the integration between seismic data and well-log interpretation (Regione Emilia-Romagna and Eni-Agip, 1998; Regione Lombardia and Eni Divisione Agip, 2002) described the large-scale stratigraphic architecture of the Po basin. South to the Po River (Regione Emilia-Romagna and Eni-Agip, 1998) the Plio-Quaternary basin fill was divided into six depositional sequences (third-order *sensu* Mitchum et al., 1977 - Fig. 7), identified as unconformity-bounded stratigraphic units (UBSU): each unconformity represents a phase of basin re-organization and the basin fill shows progressively decreasing deformation from the bottom to the top (Amorosi et al., 2008a).

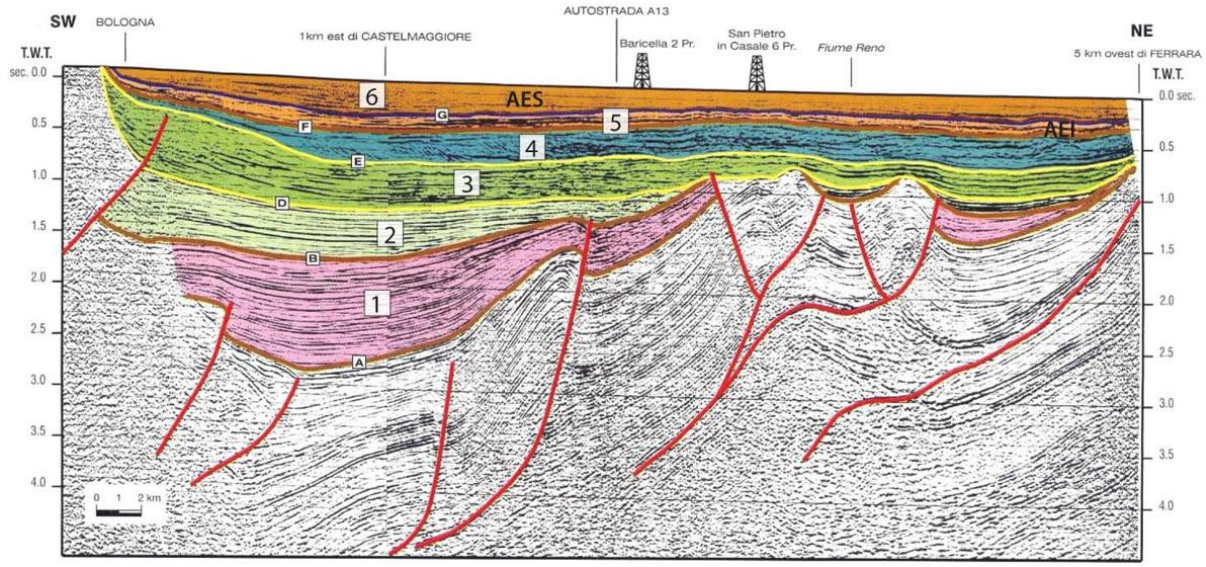

Fig. 7 - The Plio-Quaternary basin fill has been divided into six depositional sequences (third-order sequences sensu Mitchum et al., 1977) identified as unconformity-bounded stratigraphic units (Regione Emilia-Romagna and ENI-AGIP, 1998).

The uppermost UBSU (Fig. 7 - Emilia-Romagna Supersynthem of Regione Emilia-Romagna, 1998; Po Supersynthem of Amorosi et al., 2008a), coinciding with cycle Qc of Ricci Lucchi et al. (1982) has been estimated post-0.87 Ma by Muttoni et al. (2003). Its maximum thickness is ca. 800 m beneath the Adriatic coastal plain (Amorosi et al., 2008a). The Po Supersynthem is made up of two lower-rank units: the “Lower Po Synthem” and the “Upper Po Synthem” (Fig. 8) separated by an unconformity of tectonic origin dated ca. 0.45 Ma (Molinari et al., 2007). The lower Po Synthem has been termed AEI by RER and Eni-Agip (1998); the upper Po Synthem as AES.

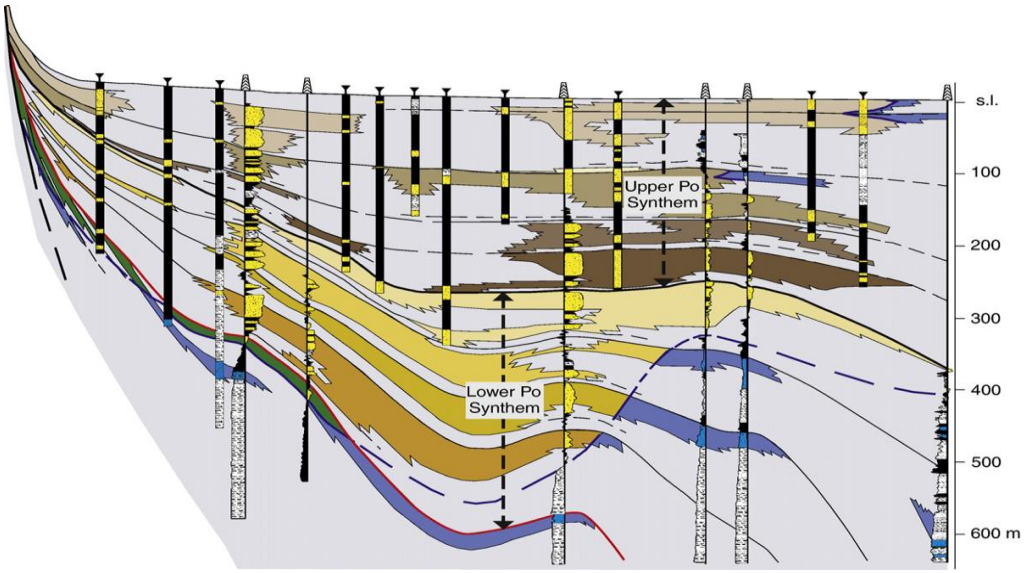

Fig. 8 - The Po Supersynthem is made up of two minor units: the “Lower Po Synthem” and the “Upper Po Synthem” separated by an unconformity of tectonic origin dated ca. 0.45 Ma (Amorosi et al., 2008a).

High-resolution stratigraphic studies have documented major influence by the Milankovitch-scale (ca. 100 ky) cyclicity upon the depositional architecture of the Upper Po Synthem (Amorosi et al., 1996, 1999a, 2001, 2004, 2008a - Fig.8). In particular, repeated alternation of coastal and alluvial deposits beneath the modern coastal plain (Amorosi et al., 2003, 2004, 2005, 2008b); or equivalent cyclicity in lithofacies and channel bodies stacking pattern within fluvial deposits (Amorosi et al., 2008a) allowed further partitioning of the Upper Po Synthem into 4th order depositional cycles or transgressive-regressive (T-R) sequences of Embry (1993, 1995) and Johnson et al. (1985). Each cycle shows distinctive upstream facies changes and peculiar pollen signature throughout its basinal extent.

Five T-R sequences were identified beneath the Po Plain (Figs. 8 and 9), allowing the subdivision of the Upper Po (ER) Synthem in subunits (Subsynthems, AES 4-8 of the Geological Mapping of Italy at 1:50,000 scale): each Subsynthem corresponds to a T-R sequence (Tab. 1). The uppermost T-R sequence, which developed after the LGM, is incomplete and lacks its regressive high net-to-gross portion.

The subsurface of the modern coastal plain is characterized by the cyclic alternation of marine and alluvial deposits Amorosi et al. (1999a, 2003, 2004, 2005, 2008b). The former are characterized by the typical “wedge-shaped” geometry due to the backstepping of beach/barrier-lagoon systems, followed by progradation of delta systems and re-establishment of alluvial conditions.

The base of each cycle is bounded by the transgressive surface (TS) in correspondence of significant landward shifts of facies, showing high-lateral traceability across the whole Po basin (Fig. 9 - Amorosi, 2008).

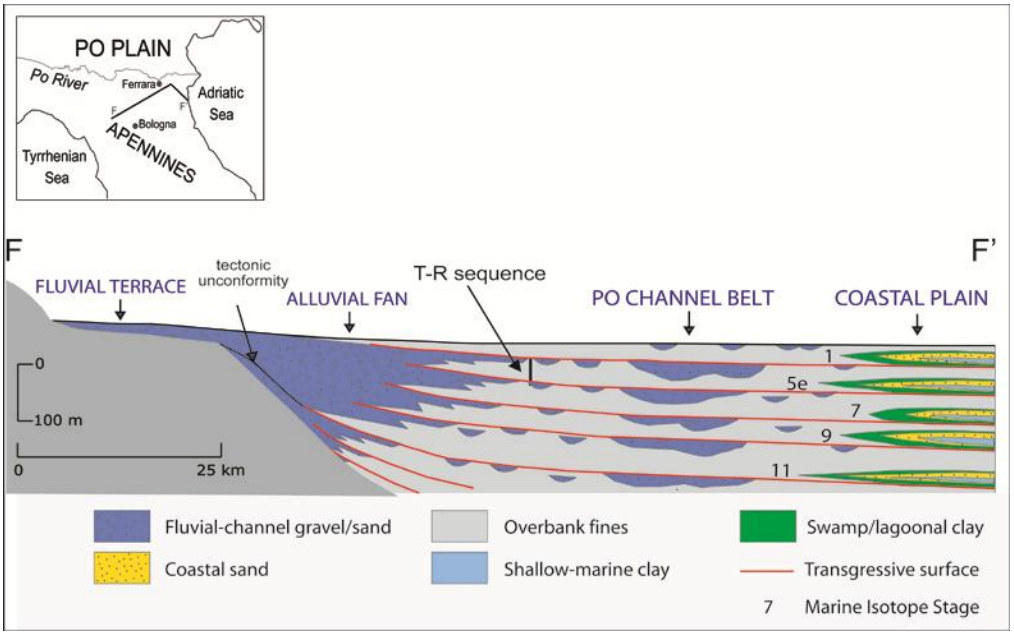

Fig. 9 - Basin-scale linkage between coastal and alluvial depositional systems (Amorosi, 2008).

Correlation between T-R cycles and the oxygen isotope curve and sea-level curve was achieved through combined radiocarbon dates and pollen data, as shown in Fig. 10 (Amorosi et al., 1999a; Amorosi, 2008). Pollen data proved that shoreline transgression took place at the onset of the interglacial intervals, whereas the re-establishment of alluvial conditions was connected with transition to glacial periods (Amorosi et al., 2004, 2008a).

Hence, it was proved the glacio-eustatic control on the stratigraphic architecture of T-R sequences.

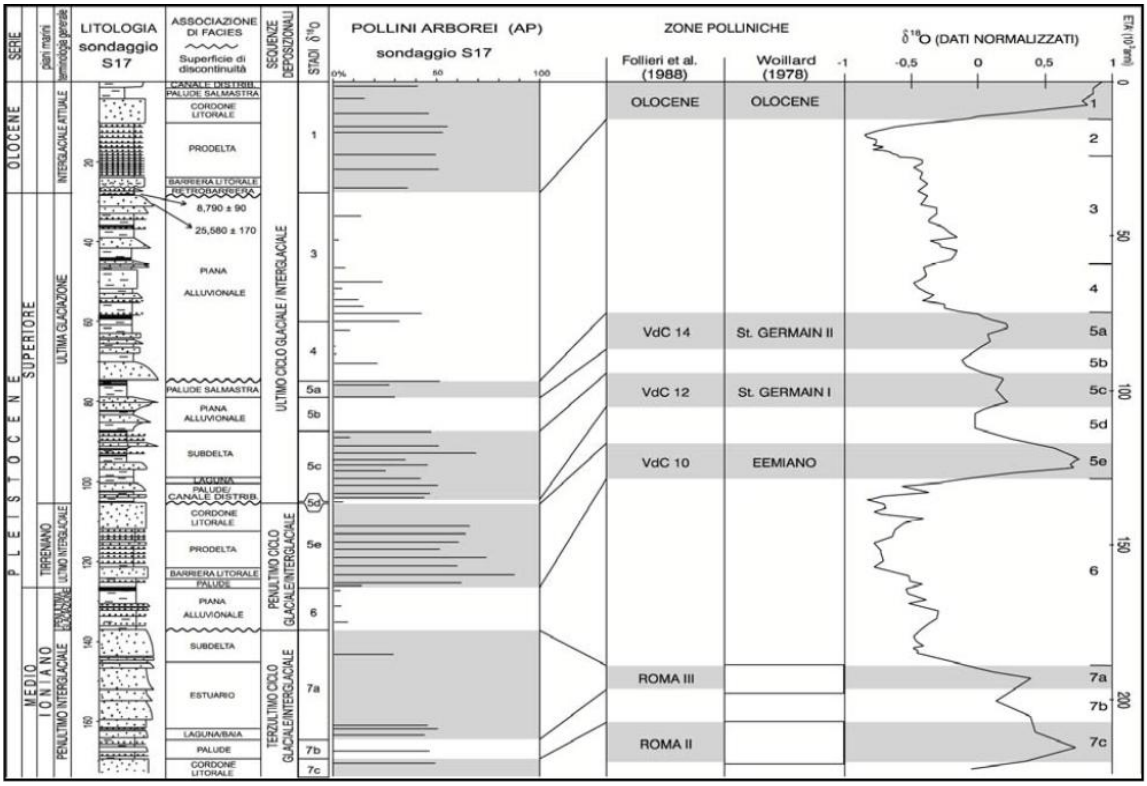

Fig. 10 - Correlation between stratigraphy, facies associations, curve of arboreal pollens (AP) recorded from a ca. 140 m deep core (223 S17), pollen zones from European series, and the oxygen-isotope record of Martinson et al. (1987). From Amorosi et al. (1999a).

In terms of sequence stratigraphy, each T-R sequence is the result of a single (100 ky) glacio-eustatic fluctuation, allowing its internal subdivision in systems tracts.

In the coastal sector, above the TS, the transgressive systems tract (TST) is characterized by the “classic” retrogradational stacking pattern showing backstepping beach/barrier-lagoon systems.

The uppermost portion of the T-R sequence, made up of dominant alluvial muds with subordinate fluvial channel sands, represents the transition from interglacial to glacial deposits, and includes falling-stage (FSST of Plint and Nummedal, 2000) and lowstand systems tracts (LST). These systems tracts are characterized by channel

incision and soil development in the interfluves, with deposition of fluvial sediments, locally channel-belts, in the lower part of the fluvial incisions.

Millennial-scale depositional cycles (i.e. parasequences, *sensu* Van Wagoner et al., 1990) have been identified within coastal deposits ofthe TST and HST by several studies (Amorosi and Milli, 2001; Amorosi et al., 2005; Correggiari et al., 2005; Stefani and Vincenzi, 2005): these cycles are bounded by flooding surfaces and show characteristic shallowing-upward trends, suggesting a step-wise sea-level rise during the Holocene with intermittent phases of landward shift in facies followed by generalized progradation (Fig.11).

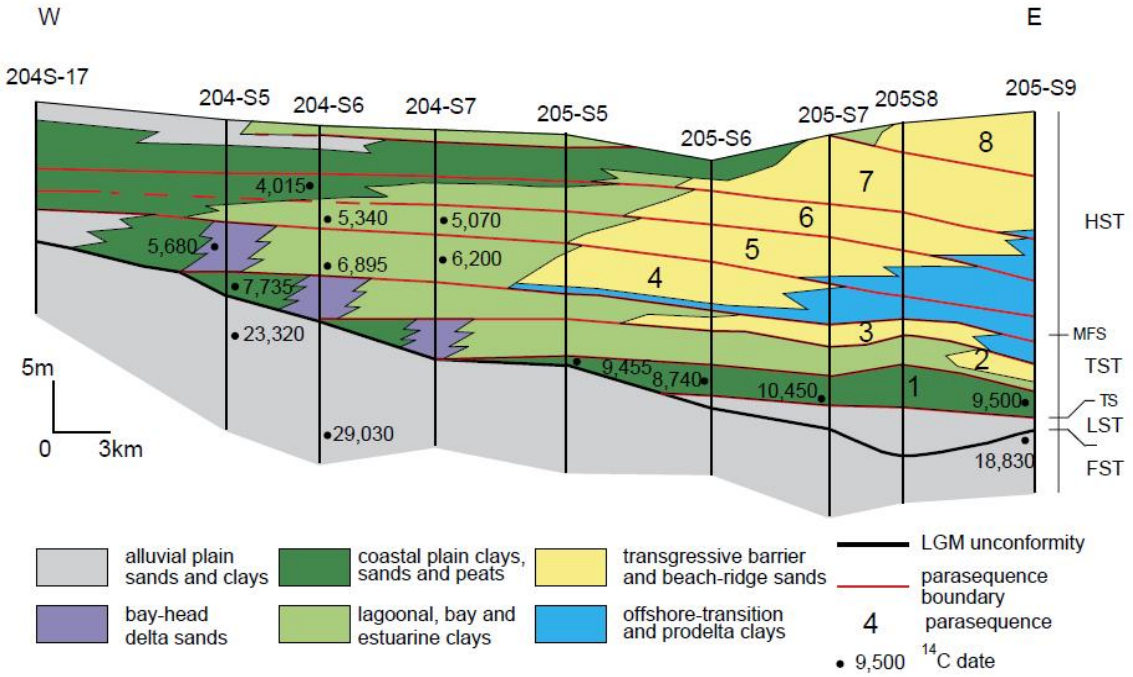

Fig. 11 - Parasequence architecture beneath the E-R coastal plain (Amorosi et al., 2005).

The transition to the highstand systems tract is the MFS (Maximum Flooding Surface). This stratigraphic surface, which is placed at the turnaround from deepening-upward to shallowing-upward trends, defines the beginning of the progradation of wave-influenced deltas and adjacent strandplains (Amorosi et al., 1999b, 2003).

The landward prosecution of the T-R coastal wedge in the “alluvial portion” of the basin (central Po Basin), is represented by equivalent cyclic sequences (Fig. 9). Each sequence consists of basal overbank deposits with lens-shaped fluvial-channel sands that are replaced upsection by increasingly amalgamated and laterally extensive fluvial-channel sand bodies (Fig. 12 - Amorosi et al., 2008a).

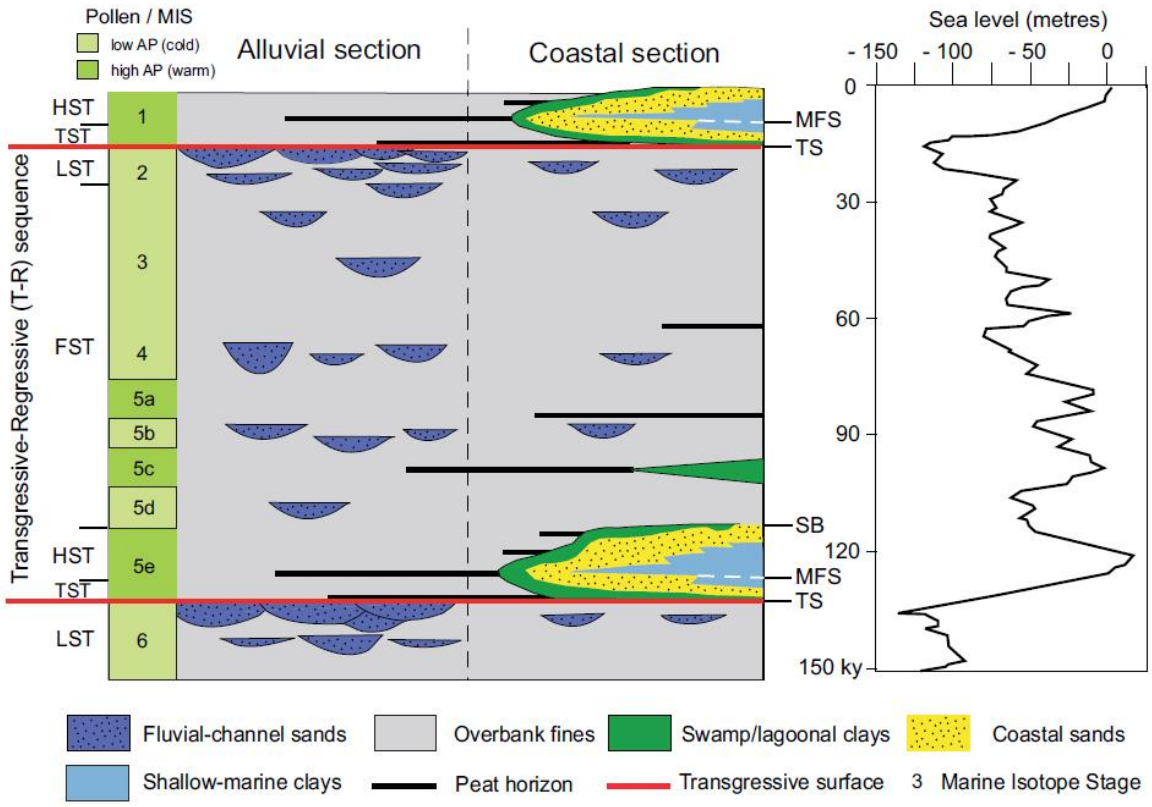

Fig. 12 - Contrasting facies architecture in proximal (alluvial) and distal (coastal) sectors of the Po Basin. From Amorosi and Colalongo (2005).

Correlation of numerous stratigraphic information documented the regional development (hundreds of square km) of coarse-grained fluvial-channel belt sand bodies displaying high degree of channel clustering. Laterally extensive organic-rich deposits cap the multi-storey sand bodies, forming the base of the overlying fine-grained deposits (TST). The identification of the diagnostic pollen signal of thermophilous forest expansion within these organic clays just a few meters above the laterally extensive fluvial channel sands, suggested that the major phases of channel abandonment and floodplain aggradation occurred at the onset of warm-temperate (interglacial) climatic conditions, corresponding to phases of rapid sea-level rise (Amorosi et al., 2008a). Increased accommodation rates accompanying sea-level rise coupled with ongoing subsidence caused accumulation of large volumes of fine-grained material, and the preservation of poorly interconnected, thin fluvial-channel bodies. The upward decrease in fine-grained sediments along with the increase in the thickness of fluvial-channel deposits, suggest decreasing accommodation during highstand setting (HST).

Amorosi and Colalongo (2005) and Amorosi (2008) assigned the amalgamated fluvial sands to forced regression (FSST) and lowstand (LST) (Figs. 12 and 13). Under very-low accommodation conditions, fluvial erosion is the dominant process and alluvial

sedimentation is restricted to thin channel-belt sand bodies (Shanley and McCabe, 1993, 1994; Olsen et al., 1995; Plint et al., 2001; Blum and Aslan, 2006), mostly due to lateral migration of river channels and contemporaneous scour-and-fill episodes. In a highly subsiding basin, such as the Po Plain, tectonic subsidence played a fundamental role in the accumulation and preservation of multi-storey deposits. In terms of key stratigraphic surfaces, the drastic change from glacial, amalgamated fluvial sands to interglacial organic-rich muds has been interpreted as the landward equivalent of the TS identified seaward (Amorosi and Colalongo, 2005; Amorosi, 2008 – Fig.13): widespread organic-rich paludal deposits represent an important landward shift in facies, in line with the classic sequence stratigraphic definition of the TS as the first significant marine flooding surface (Van Wagoner et al., 1987).

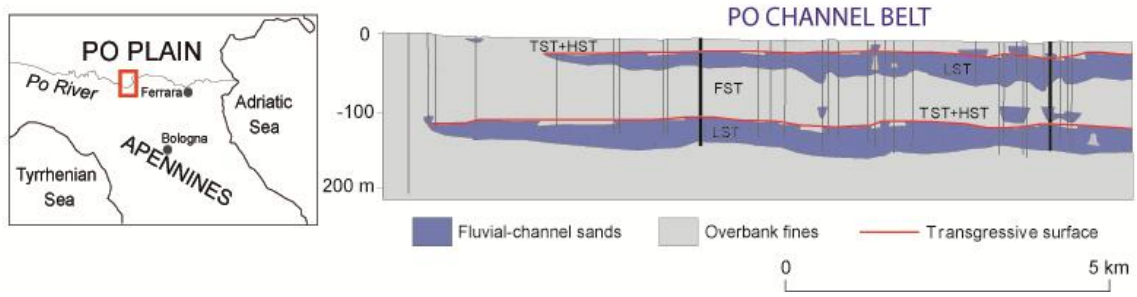

Fig. 13 - Cyclic facies architecture of late Quaternary deposits beneath the modern Po River. Modified from Amorosi (2008).

A similar cyclic alternation between amalgamated coarse-grained (mostly gravel) deposits and basal fine-grained dominated units, the latter connected to warm-temperate conditions by pollen data (Amorosi et al., 2001), was documented in the proximal area of the southern Po Basin. Here, at the Apenninic margin, alluvial fan deposits (Amorosi et al., 1996) consist of amalgamated and vertically stacked gravel bodies thickening in seaward direction (Fig. 14). These gravel deposits show a pollen signature that reflects transition to cold-climate (glacial) vegetation and, along with the basal clayey unit, represent the most landward equivalent of the T-R cycle.

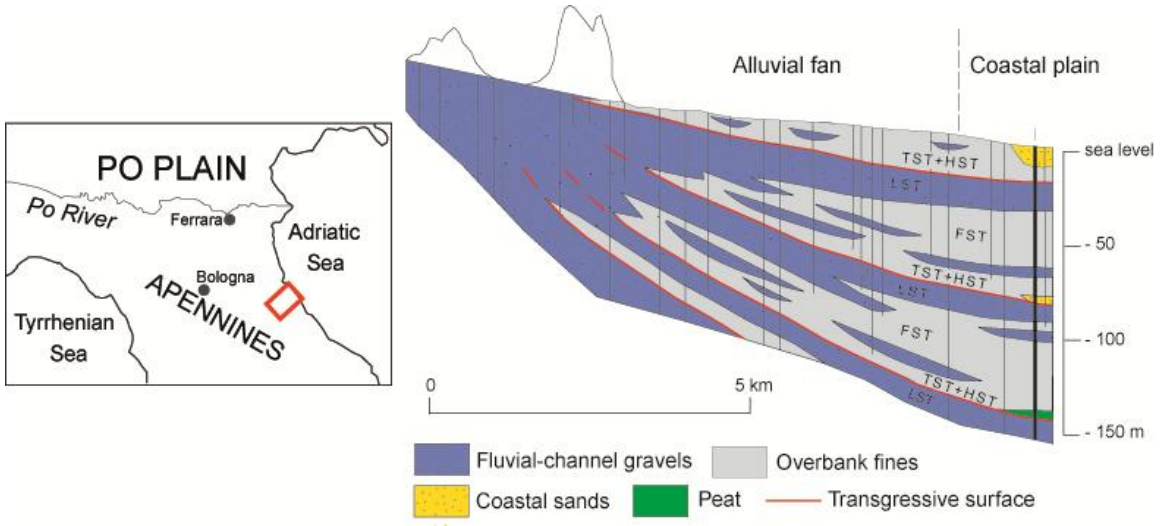

Fig. 14 - In proximal locations (Apenninic margin) alluvial fan deposits consist of amalgamated and vertically stacked gravel bodies thickening in a seaward direction (from Amorosi, 2008).

The stratigraphic architecture of the Quaternary Po Basin fill has important practical implications from a hydrostratigraphic point of view: facies connotation and geometric characterization of major aquifers are useful to evaluate volumes and characteristics of groundwater resources (Amorosi and Pavesi, 2010). In this framework, each T-R cycle corresponds to an aquifer system.

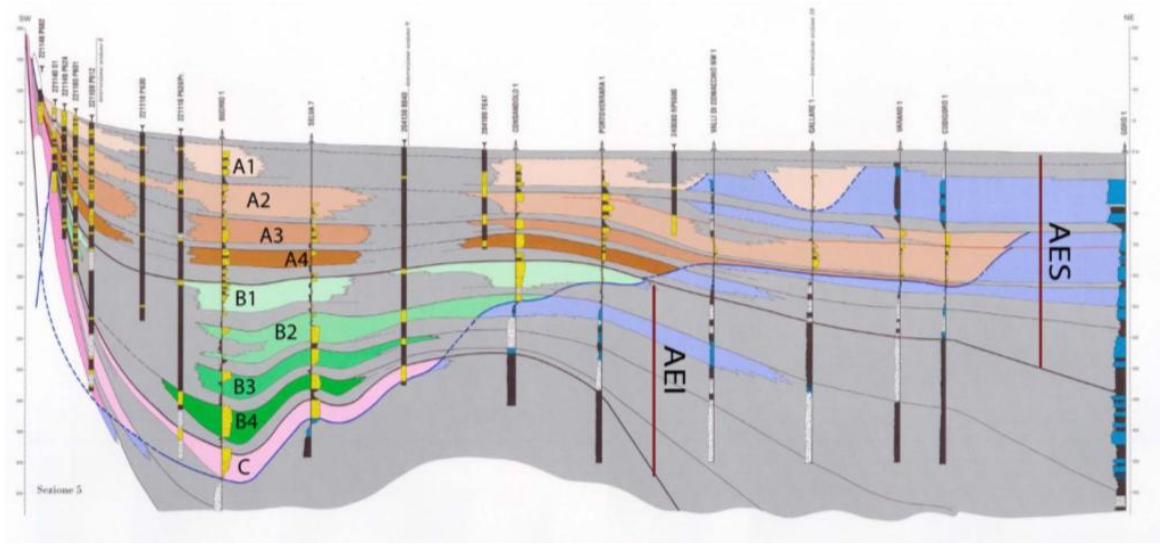

Fig. 15 - Hydrostratigraphic cross-section of the southern Po Basin from the Apenninic margin to the coastal sector: aquifer systems (A4 to A1 and B4 to B1) correspond to T-R sequences (Emilia-Romagna and Eni-Agip, 1998).

STRATIGRAPHIC UNITS (Geological Map of Italy to scale 1:50,000)			HYDROSTRATIGRAPHIC UNITS (Regione Emilia-Romagna and Eni-Agip, 1998)	
Supersynthem	**Synthem**	**Sub-synthem**	**Aquifer group**	**Aquifer systems**
Emilia-Romagna Supersynthem	Upper Emilia-Romagna Synthem (AES)	AES8	A	A0
		AES7		A1
		AES6		A2
		AES5		A3
		AES4		A4
	Lower Emilia-Romagna Synthem (AEI)		B	B1
				B2
				B3
				B4
Imola Sands (IMO)			C	

Table 1 - Nomenclature of the southern Po Basin depositional units: stratigraphic and hydrostratigraphic correlations (from Emilia-Romagna and Eni-Agip, 1998).

In particular, the laterally extensive coarse-grained units represent the major aquifer systems (A1-A4 and B1-B4 in Fig. 15) of RER and Eni-Agip (1998); whereas the overbank muddy-units form important permeability barriers (i.e. *aquitards*). Along the entire Po Basin, from proximal to distal positions (Apenninic margin to coastal plain), the major aquifers are represented by amalgamated alluvial fans, vertically-stacked Po channel belts and nearshore sands (Fig. 16 - Amorosi, 2008).

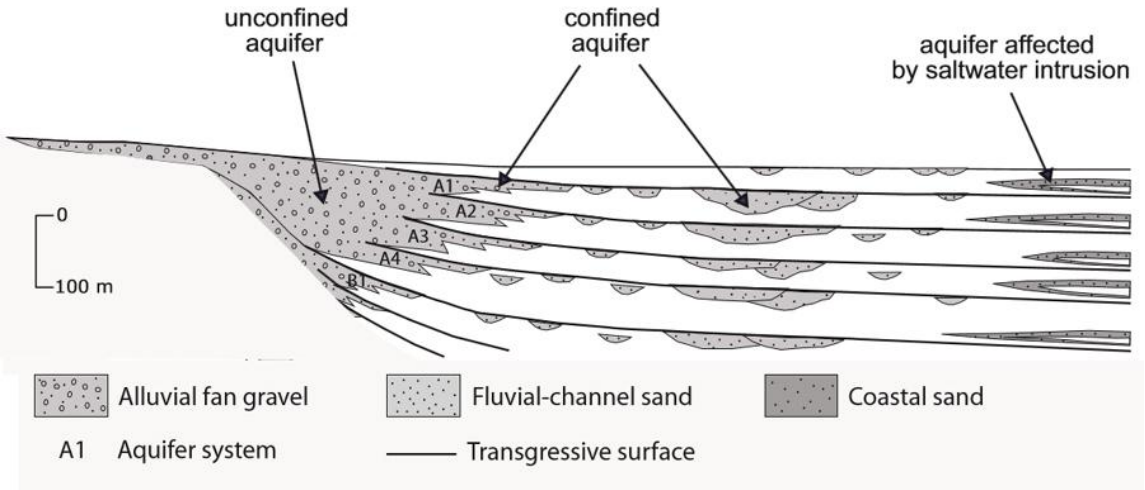

Fig. 16 - Along the entire Po Basin, from the Apenninic margin to the coastal plain, the major aquifers are represented by amalgamated alluvial fans, vertically-stacked Po channel belts and nearshore sands. Modified from Amorosi (2008).

2.3. The Po River catchment and its evolution since the LGM

The Po Plain is the largest alluvial plain in Italy, elongated in W-E direction, from the Alps to the Adriatic Sea (Fig. 17). It is drained by the Po River, the longest river in Italy,

which originates from the western Alps and flows eastward across the modern alluvial plain for 691 km. It counts on 141 tributaries, both from the Alps and the Apennines which supply different volumes and type of sediment to the Po River, depending on their source area (Alps vs Apennines, see Amorosi et al., 2002).

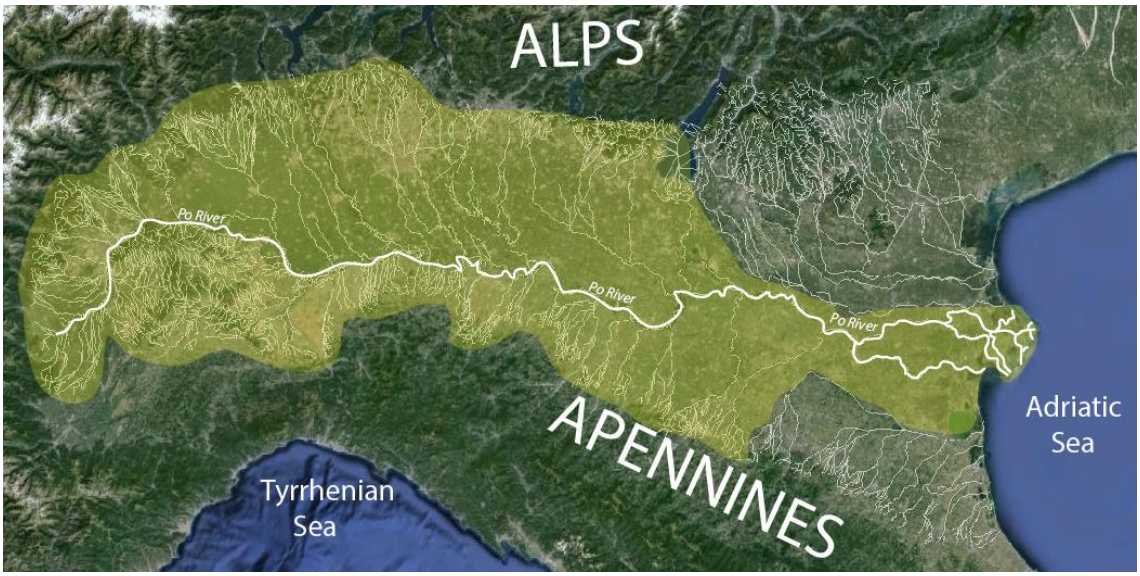

Fig. 17 - The modern Po River course across the Po Plain. In yellow the Po River catchment with its Alpine and Apenninic tributaries.

The Po River represents the main resource of fresh water for the Adriatic Sea, and the average discharge measured at Pontelgoscuro (Fe) is 1.525*10³ m³/s (Maselli et al., 2011). Upstream to this location, at a distance of ca. 100 km by the modern shoreline, the gradient of the Po Plain steepens. Downstream of Pontelagoscuro, the river enters the coastal region, flattening its profile (Fig.18) and developing the present-day delta which consists of six major distributary channels: Pila, Levante, Maestra, Tolle, Goro, Gnocca (Fig. 19). Two additional branches, south of the modern delta, are Po di Volano and Po di Primaro, this latter occupied at present by the Reno River.

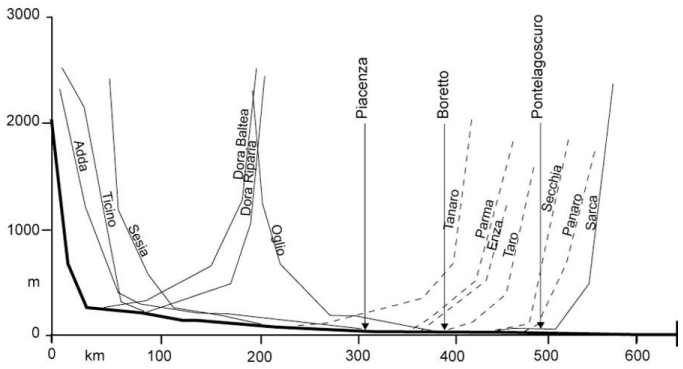

Fig. 18 - Po River gradient (modified from Correggiari et al., 2005).

Fig. 19 - Modern Po Delta branches.

The present-day delta, in fact, evolved only in the last 500 y, after the Porto Viro diversion (1599-1606 AD), with progradation of the shoreline of about 30 km (Correggiari et al., 2005). Since the 1600 AD, though the relative importance of the individual lobes changed through time, and delta lobes underwent retreat once another lobe was dominant, the Po Delta can be considered supply-dominated as a whole (Cerreggiari et al., 2005).

In the past, during the Bronze age (ca. 3.5 ky BP), the Po Delta was a wave-dominated delta and extended southward in the coastal area between Ravenna and Adria, with numerous outlets and branches which evolved because of natural avulsion. It formed a cuspate delta, as suggested by the preservation of several stranded sand ridge systems (Bondesan et al., 1995; Correggiari et al., 2005). In the late Bronze Age (ca. 3 ky BP), the Po River system consisted of two main branches: Po di Adria to the north and Po di Spina to the south (Fig. 20A). During the Roman Age (2500-1500 BP), the whole system was located south of the present delta and developed the Po di Eridano and Po di Olano branches (Fig. 20B). The Po di Primaro was the most important branch to the south during the Middle Age (500-1500 AD), along with the Po di Ariano to the north (Fig. 20C), which evolved in the Po di Volano (Fig. 20D). The major historical natural avulsion, named “Rotta di Ficarolo” (1152 AD), shifted the entire Po River system up to the north (Fig. 20E), leading to the formation of Po delle Fornaci and Po di Ariano-Goro.

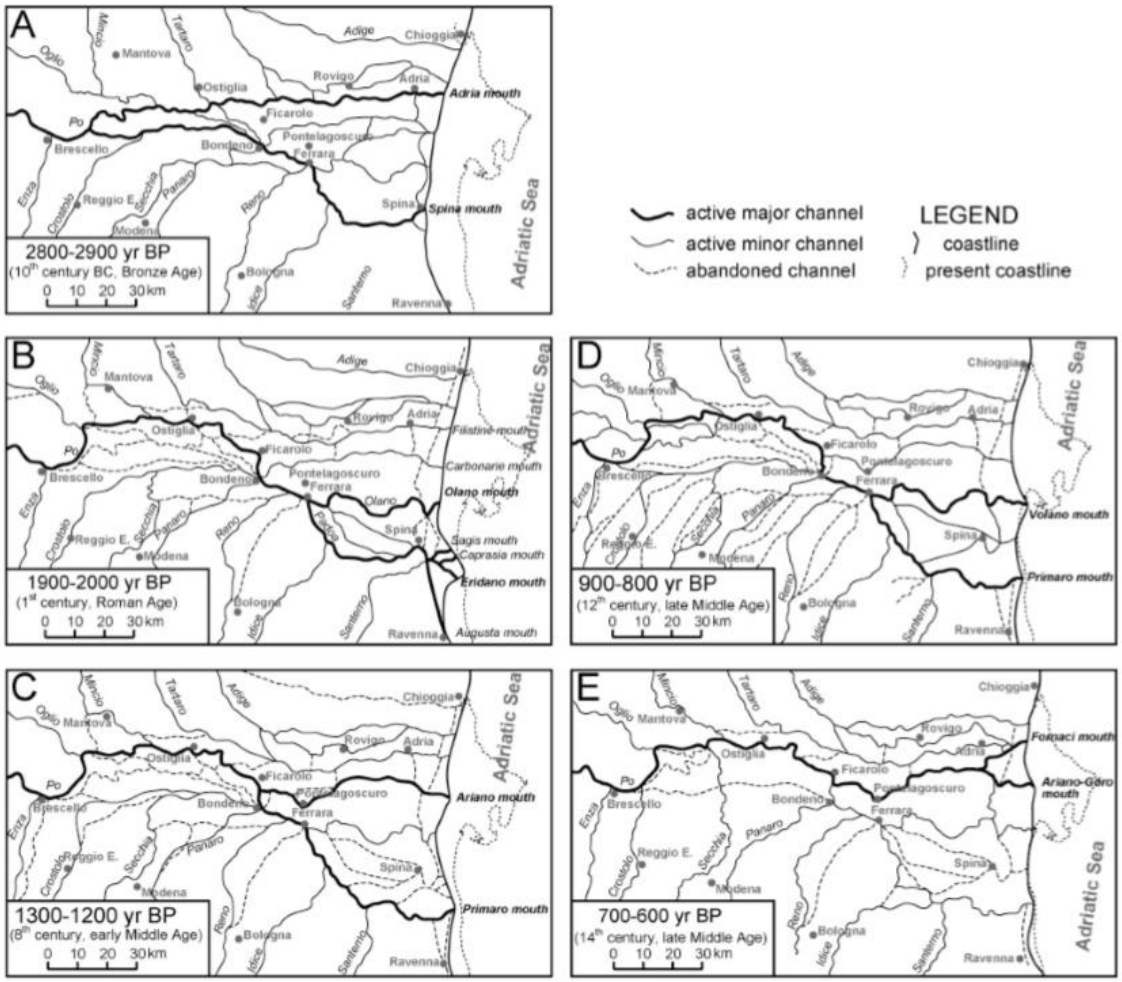

Fig. 20 - Pre-Modern Age Po delta evolution: A) End of Bronze Age (Po di Spina and Po di Adria); B) Roman Age (Po di Eridiano and Po di Olano); C) Middle Age (Po di Primaro and Po di Ariano); D) During the Middle Age Po di Ariano evolved in the Po di Volano ; E) After the Ficarolo avulsion in the 12th century, Po di Primaro was abandoned and the main trunk of the Po moved to the north (from Correggiari et. al., 2005).

During the Last Glacial Maximum (24-19 ky BP), the Po River and its tributaries reached the central Adriatic basin, because of the sea-level lowstand (Correggiari et. al, 1996; Cattaneo and Trincardi, 1999), with establishment of alluvial conditions throughout the subaerially exposed North Adriatic shelf (Fig. 21 - Maselli et al., 2011). As a consequence, the Po River drainage systems reached 190,000 km², more than twice larger than the present one (74,500 km²).

Kettner and Syvitski (2008) used a numerical model to make discharge predictions, based on climate and drainage characteristics. They estimated an average suspended sediment flux of 46.6 Mt/y and an average bedload of 0.83 Mt/y of the Po River during the Late Pleistocene (21-10 ky BP). These values are 75% bigger than those related to the Holocene (10-0 ky BP): for this period, the model calculated a suspended sediment flux of 26.7 Mt/y and a bedload of 0.53 Mt/y. However, considering the sediment yield with load sediment normalized to unit area, simulations showed higher values for the

sediment yield during the Holocene (336 t/km²*y vs 283 t/km²*y calculated for the Late Pleistocene) due to an increase in precipitation during the warmer Holocene.

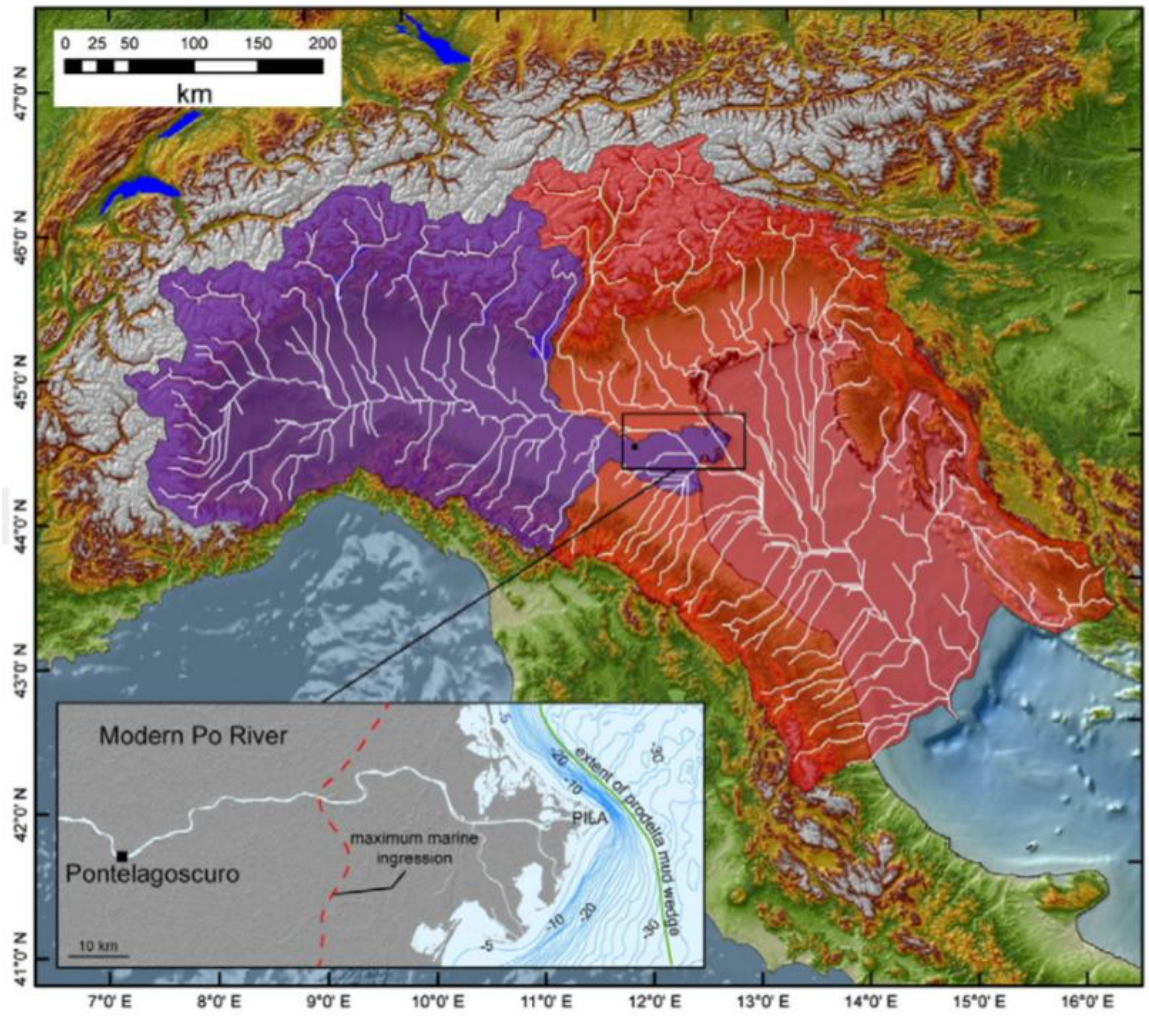

Fig. 21 - In red: the Po River catchment area during the last sea-level lowstand (Last Glacial Maximum). In violet: the modern Po River catchment area. Modified from Maselli et al. (2011).

3. METHODS

The high-resolution stratigraphic investigation was carried out through the construction of 2D cross-sections at different scales (up to 123 km long). Data spacing ranges between 0.3 to 2 km and the average depth of investigation is about 50 meters.

Detailed stratigraphic correlations were based on a large borehole data base from various sources and supported by multi-proxy investigation of core descriptions available, along with geotechnical, hydrogeological, petrographic and geochemical data, as well as radiocarbon dating. New fresh cores were collected to calibrate older data and to implement the chronostratigraphic framework (^{14}C samples). Accurate facies analysis was carried out in order to make reliable stratigraphic interpretations, taking into account both horizontal and vertical relationships between different lithofacies.

3.1. Geological dataset

The study has counted on different databases, listed below:

1) Regione Emilia-Romagna (RER) database
2) Regione Lombardia database
3) Italferr S.p.A. (*Ferrovie dello Stato Italiane* Group)
4) Università del Molise and Cosib (*Consorzio per lo sviluppo industriale della valle del Biferno*)

The Geological Mapping Project (at 1:50,000 scale) pushed for a vast drilling campaign carried out by the Regione Emilia Romagna and Regione Lombardia Geological Surveys in the Po Plain during the last 20 years, allowing the collection of several thousands of new stratigraphic information. All these data are stored in *pdf* format at the Geological, Seismic and Soil Survey of Regione Emilia-Romagna and Regione Lombardia, respectively.

As regards the data used in this work, a total of 1,686 stratigraphic data were taken from the RER database, and 116 from the Regione Lombardia database.

The RER database (Fig. 22) has recently been implemented with additional continuously cored boreholes, drilled: to study the sand liquefaction after the 2012 5.9 Mw earthquake (22 new continuous cores); to map the saltwater intrusion along the coast (3 cores); for other purposes (6 cores).

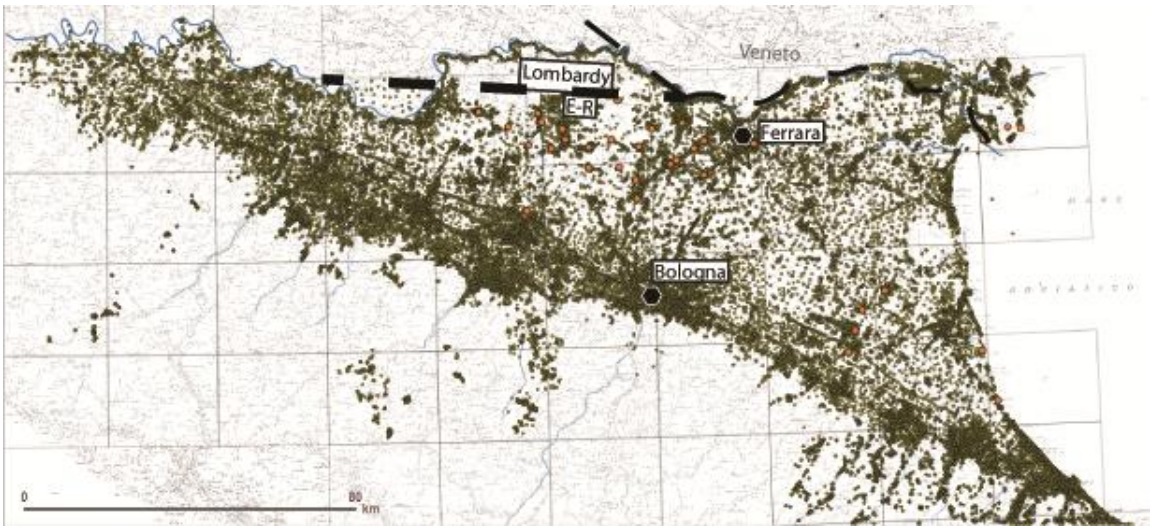

Fig. 22 - The Emilia-Romagna and Lombardy (Oltre Po Mantovano) dataset. In orange, the new continuous cores recovered by the RER Geological Survey during 2012-2015.

The Italferr S.p.A. (*Ferrovie dello Stato Italiane* Group) dataset includes 19 continuous cores and 7 cone penetration tests CPT (Fig. 23). Two additional continuously drilled boreholes (S1 and S14, Fig. 23) were collected: S14 was provided by Cosib (*Consorzio per lo sviluppo industriale della valle del Biferno*); S1 was specifically drilled for this work.

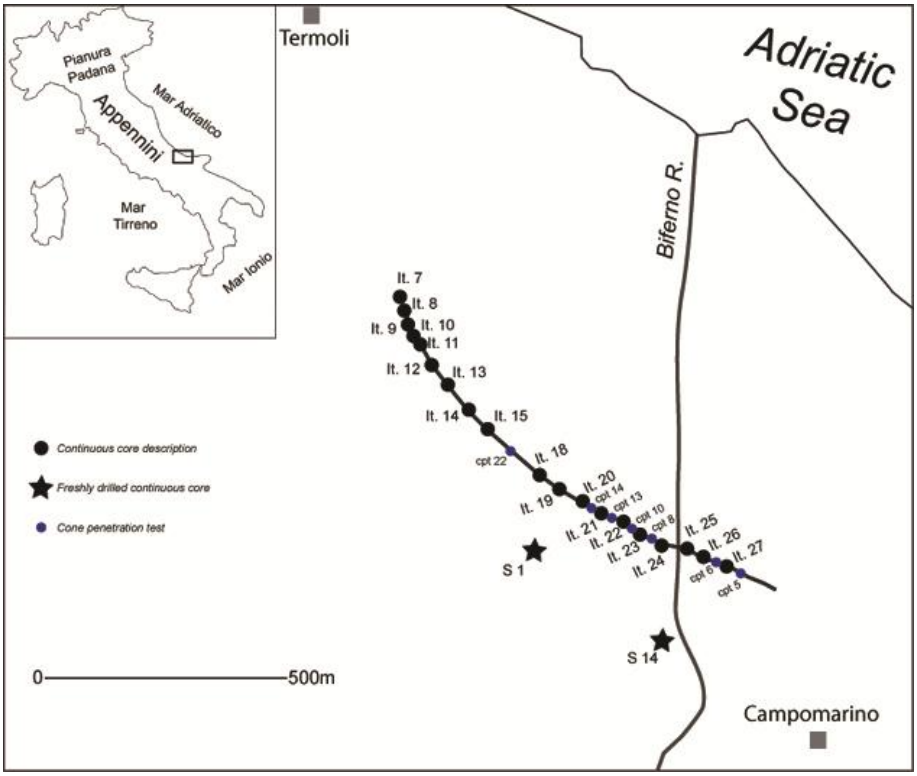

Fig. 23 - The Biferno coastal plain database: continuously cored borehole descriptions (black dots); freshly-drilled continuous cores (black stars); cone penetration tests (blue dots).

As a whole, the geological dataset is composed of different types of stratigraphic information, depending on the different methods of investigations, with peculiar vertical resolution, range of depth, and quality of descriptions. Listed below are the main sources of data:

- *Continuously cored boreholes* (20-50 m deep): are fundamental tools for statigraphic reconstructions, because facies analysis on cores guarantees high-resolution stratigraphic information such as: lithology, grain-size tendencies, colors, contacts, accessory materials (roots, wood and plants fragments, carbonate nodules, bioturbation, fossil content), pedogenic features, pocket penetrometer and torvane test values. Locally, are also included uncalibrated radiocarbon dates, as shown in Fig. 24, which represent examples of high-resolution core description used for the geological mapping of Italy (at 1:50,000 scale) by the RER Geological Survey (CARG Project). CARG stratigraphic logs may provide stratigraphic, pedological, geotechnical (pocket penetrometer and torvane test measurements), paleoclimatic, paleobotanic and paleontological information.

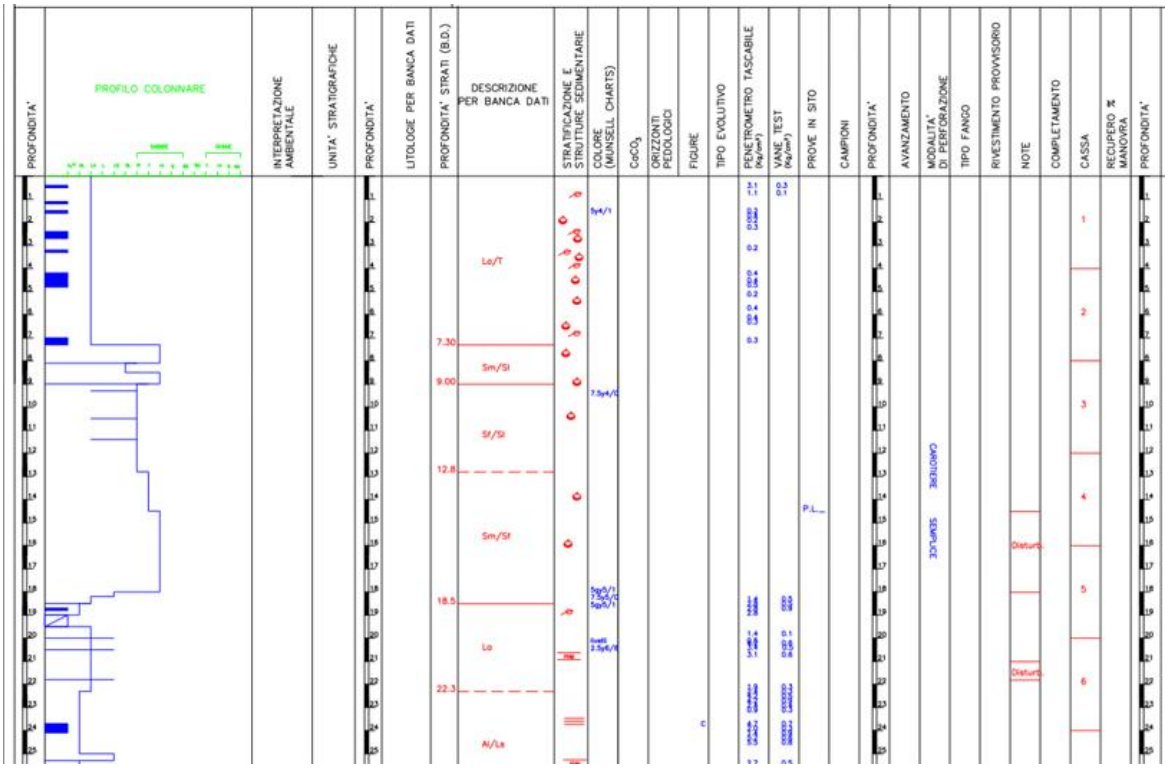

Fig. 24 -Typical stratigraphic log description from CARG Project (RER Geological Survey database).

Other stratigraphic descriptions are less detailed, because realized for non-stratigraphic purposes, such as hydrogeological surveys, and may lack information

about accessory materials, consistency, pocket penetrometer and vane test values (Fig. 25).

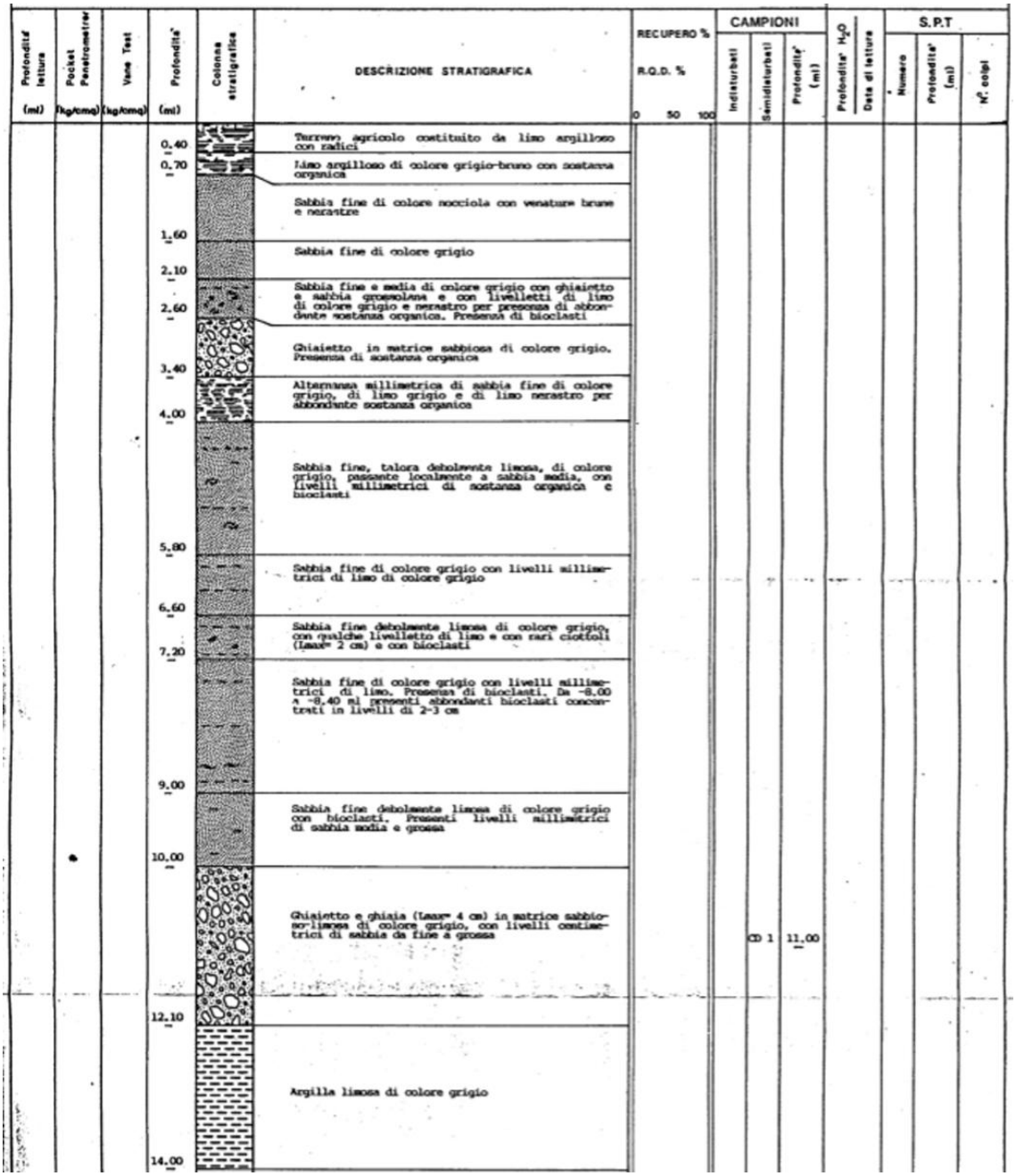

Fig. 25 - Example of common stratigraphic description from the RER Geological Survey database.

Some of the cores were directly studied during this research, such as those drilled during the sand liquefaction campaign, carried out by RER Geological Survey during the 2012 (Fig. 26). Samples were collected from freshly-drilled cores for laboratory analyses (radiocarbon dating, paleontological and geochemical characterization).

Fig. 26 - Freshly-drilled core directly observed during this study.

- *Water wells* (30-450 m deep) were drilled for hydrological purposes. Because of their intrinsic scarce vertical resolution, their related stratigraphic descriptions are mostly restricted to basic grain-size (sand= aquifers; clay=aquitard) information (Fig. 27). Rarely, they may include annotations on color, grain size and organic matter content. These descriptions were utilized to identify thick fluvial-channel bodies, especially the deepest ones, lying more than 50 m below the ground surface.

Profondità		Colonna Stratigr.	Descrizione litologica
Da m	A m		
00.00	05.00		TERRENO DI RIPORTO
05.00	30.00		ARGILLA E SABBIA
30.00	38.00		SABBIA
38.00	140.00		ARGILLA
140.00	165.00		SABBIA
165.00	170.00		ARGILLA

Fig. 27 - Example of water well description (RER Geological Survey database).

- *Cone penetration tests (CPT) and piezocone penetration tests (CPTU)* are efficient indirect investigations commonly utilized for geotechnical investigations, that provide cone resistance (Qc), slevee friction (Fs) and pore pressure values (U). These tests are relatively “low-cost” and are characterized by high vertical resolution (Fig. 28). The depth of investigation is up to 15 m for CPT

tests, and up to 36 m for CPTU tests. Recent studies on late Quaternary deposits have revealed the efficiency of cone penetration tests for facies characterization and subsurface stratigraphic correlations (Amorosi and Marchi, 1999; Styllas, 2014; Amorosi et al., 2015). For detailed information on the stratigraphic use of this technique, the reader may refer to Amorosi and Marchi (1999).

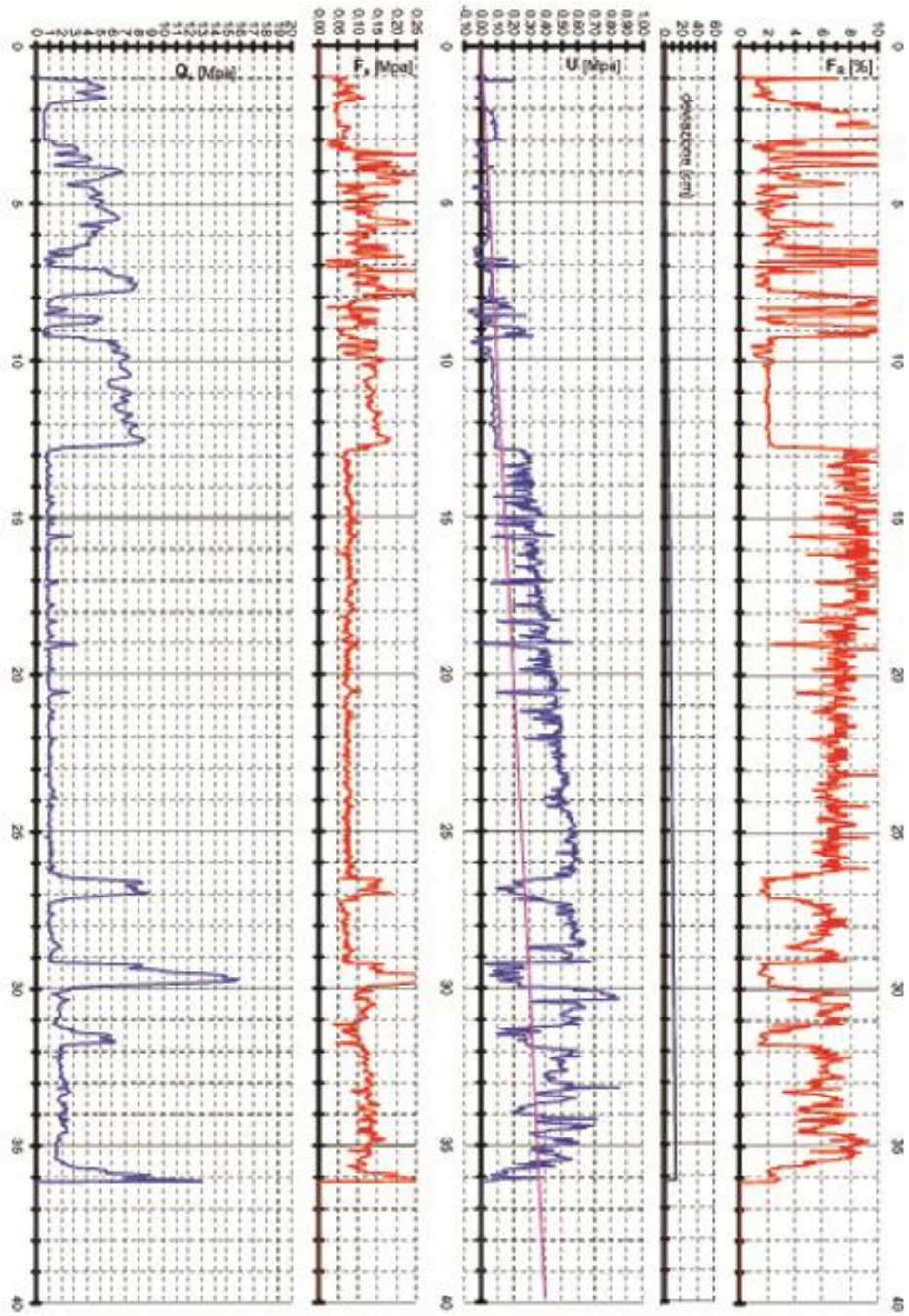

Fig. 28 - Example of CPTU test from the RER Geological Survey database.

All stratigraphic information stored as archived material was re-interpreted from a sedimentological point of view, leading to facies interpretation of simple lithologic descriptions.

Specific attention was paid to accessory components that might reveal information useful to the reconstruction of the depositional environments. Subaerial exposure or pedogenesis was detected through careful examination of several features, such as consistency, color, carbonate concretions, Fe and Mg oxides, presence of organic matter and high pocket penetrometer values.

For each re-interpreted element of the dataset, the resulting stratigraphic log was associated to its depositional facies interpretation (Fig. 29) and plotted in cross-sections.

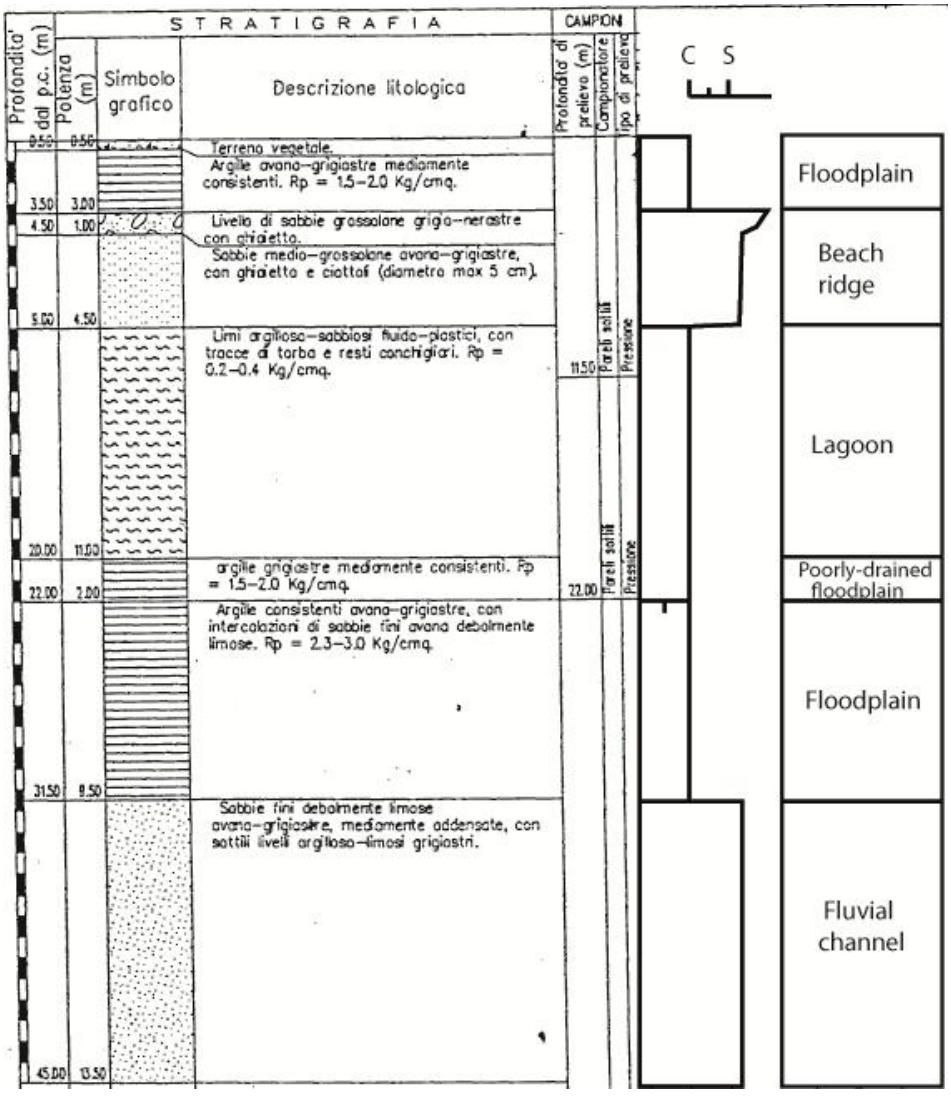

Fig. 29 - Example of re-intepretation of core description stored in the geological RER Geological Survey database. On the right, stratigraphic log and resulting facies interpretation.

Uncalibrated radiocarbon dates archived in the dataset, were calibrated using two calibration programs: Calib 7.1 (referenced as Stuver and Reimer, 1993), with the Intcal13 and Marine13 datasets (Reimer et al., 2013); Oxcal 4.2 (Ramsey, 2009), with the Intcal13 calibration curve and Marine13 datasets (Reimer et al., 2013), as shown in Figure 30.

Organic-rich samples from fresh cores observed were dated:

- at the Laboratory of Ion Beam Physics (ETH, Zurich, Switzerland);
- at CIRCE Laboratory (Caserta, Italy);
- at the Laboratory of Korea Institute of Geoscience and Mineral Resources (KIGAM, Republic of Korea)

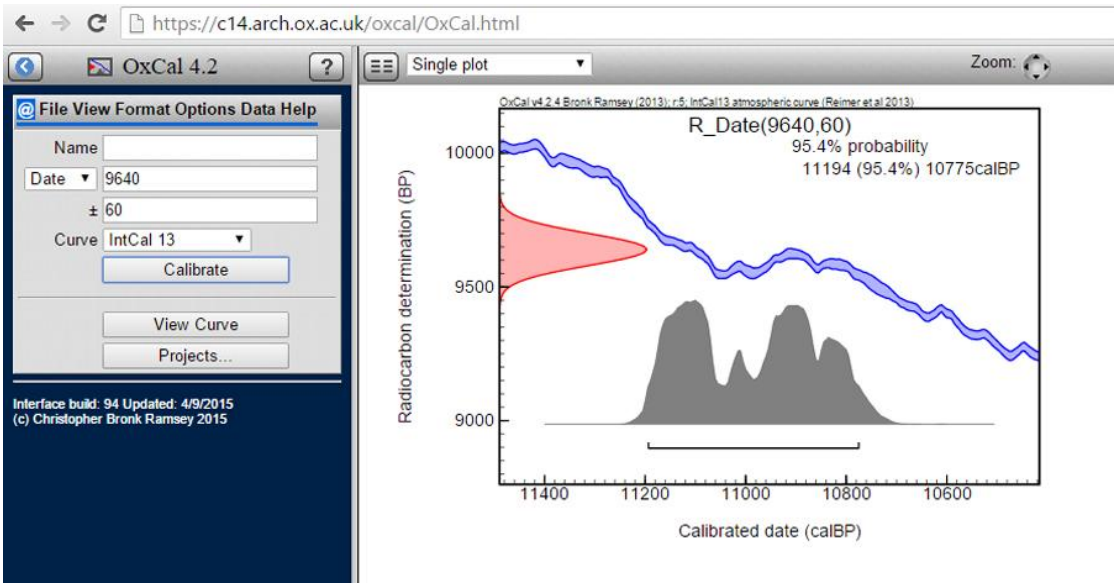

Fig. 30 - Oxcal 4.2: free online source at https://c14.arch.ox.ac.uk/oxcal/OxCal.html.

4. STUDY AREA SUMMARY

This work focuses on the Late Pleistocene-Holocene transition in the southern Po Basin. Five areas were investigated, with the aim of unraveling the role of different allogenic factors (climate, eustacy, sediment supply, etc...) on stratigraphic architecture in the last 45 ky. The study starts from the distal portion of the basin (i.e., the coastal plain deposits), and then moves to two increasingly internal areas (Central Po Plain), > 100 km landward from the modern Adriatic coastline: the alluvial sector characterized by the Po channel belt deposits (study area 2 - Fig. 31), and the mud-prone interfluvial succession between the Apenninic margin and the Po channel belt (study area 3 - Fig. 31).

The fourth study area (Biferno coastal plain) is also located along the Adriatic coast, but ca. 300 km south of the Po Plain. Through the reconstruction of the Biferno coastal deposits, we had the opportunity to document two coeval (Late Pleistocene - Holocene) coastal sedimentary successions, diverging in terms of shelf gradient and proximity to the LGM-lowstand Po Delta.

Study area 5, broadly coincides with the Ferrara urban perimeter, was selected to show how high-resolution stratigraphic studies can be used for practical purposes.

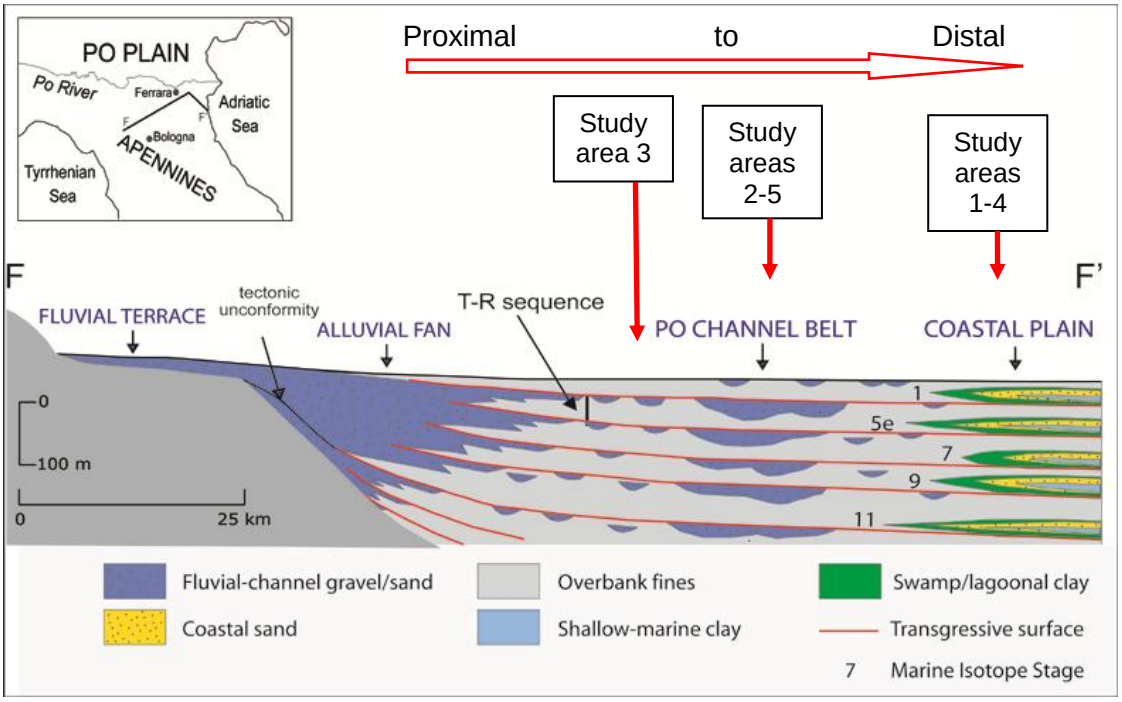

Fig. 31 - Approximate location of the study areas across the Po Plain. Modified from Amorosi (2008).

4.1. Study area 1

Sequence stratigraphy and late Quaternary paleoenvironmental evolution of the Adriatic coastal plain (northern Italy)

Bruno Campo, Alessandro Amorosi, Stefano Claudio Vaiani

Study area 1 (Fig. 32) includes the Emilia-Romagna coastal plain sector, between the city of Cesenatico and the modern Po Delta.

In this work we used 15 high-resolution core descriptions, 29 conventional continuous core descriptions, 16 stratigraphic data from water wells and 54 cone penetration tests from the Regione Emilia-Romagna database and from previous published studies (Amorosi et al., 1999a, 1999c, 2003).

Stratigraphic dates were calibrated, in terms of facies interpretation, to the freshly-drilled continuous core “Cervia 2”. The study was supported by detailed microfossil analyses, which refined facies interpretation. The chronostratigraphic framework was based on a total of 29 published ^{14}C dates (Amorosi et al., 1999a, 2003; Geological Map of Italy at 1:50,000 scale, Sheet 187, 205, 223, 240-241, 256; Scarponi et al., 2013) and on four new radiocarbon ages from cores “Cervia 2”, 240 S6, and 223 S17.

Detailed stratigraphic correlations between the cores allowed the construction of a ~ 93 km-long cross-section parallel to the present shoreline and transversal to the Holocene transgressive-regressive coastal wedge. Stratigraphic relationships documents along-strike changes in facies architecture, across the Late Pleistocene (45-12.5 ky BP) alluvial succession, and the Holocene (12.5 ky BP to Present) marine-influenced deposits. High-resolution facies analysis, along with a well-constrained chronostratigraphic framework, led to the accurate paleoenvironmental reconstruction of the last 45 ky BP depositional history along the transect. We also provide a sequence stratigraphic interpretation for the whole sedimentary succession.

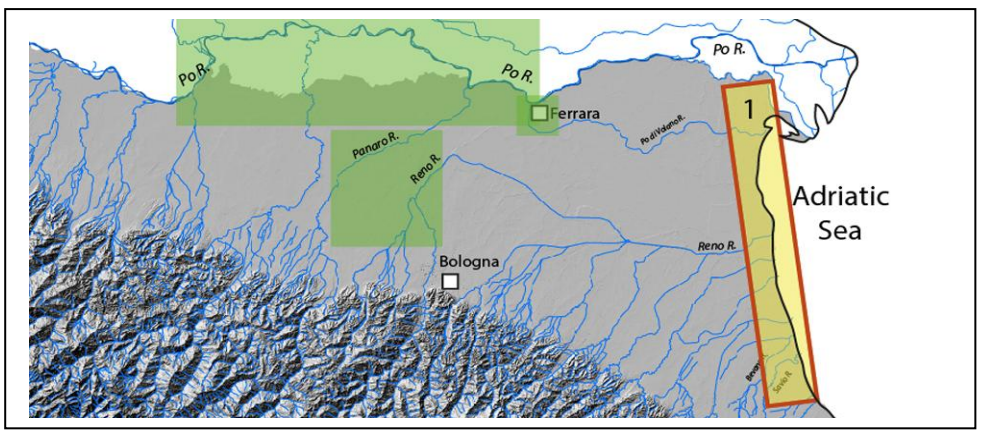

Fig. 32 - Location of study area 1 (yellow rectangle).

4.2. Study area 2

Contrasting alluvial architecture of Late Pleistocene and Holocene deposits along a 120-km transect from the central Po Plain (northern Italy)

Bruno Campo, Alessandro Amorosi, Luigi Bruno

In this study, we moved our research landward, ca. 90 km updip from the modern Adriatic coastline (Fig. 33). The construction of a ~120 km-long transect, roughly coincident with the southern bank of the modern Po River, documents for the first time the Pleistocene-Holocene stratigraphy of a fluvial-dominated sector (Last Glacial Maximum to the Present) in the Central Po Plain. Based on 28 radiocarbon dates, facies interpretation from 60 high-quality core descriptions (performed by the Regione Emilia-Romagna Geological Survey) and three freshly-drilled continuous cores, the contrasting stratigraphic architecture of Late Pleistocene (LP) and Holocene (H) deposits was highlighted. Changes in lithofacies and channel stacking patterns reveal the vertical superposition of amalgamated fluvial-channel sands (LP) and mud-dominated deposits (H), with isolated fluvial-channel bodies.

We also attempted to establish the link between facies architecture, sea-level fluctuations (lowstand vs highstand) and climate changes (glacial vs interglacial conditions).

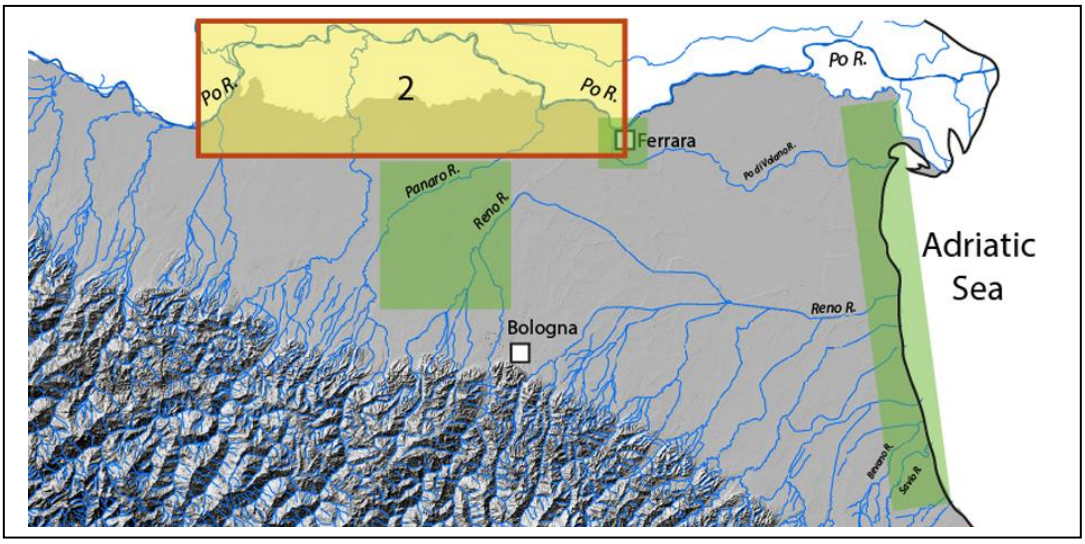

Fig. 33 - Location of study area 2 (yellow rectangle).

4.3. Study area 3

The value of pocket penetration tests for the high-resolution stratigraphy of late Quaternary deposits

Alessandro Amorosi, Luigi Bruno, ***Bruno Campo***, Agnese Morelli

The third study area (ca. 6,750 km^2) is located in south of the study area 2 of the Po Plain, between the Po River channel belt and the Apenninic margin (Fig. 34).

We properly selected a mud-prone alluvial succession (Panaro and Reno River interfluve), to test a new method for paleosol identification, on the basis of geotechnical properties generated from simple pocket penetrometer (Pp) values.

In order to test this new technique, three freshly-drilled cores were used as reference cores for facies analysis, and additional 40 stratigraphic logs (from the Regione Emilia Romagna database) provided with Pp values.

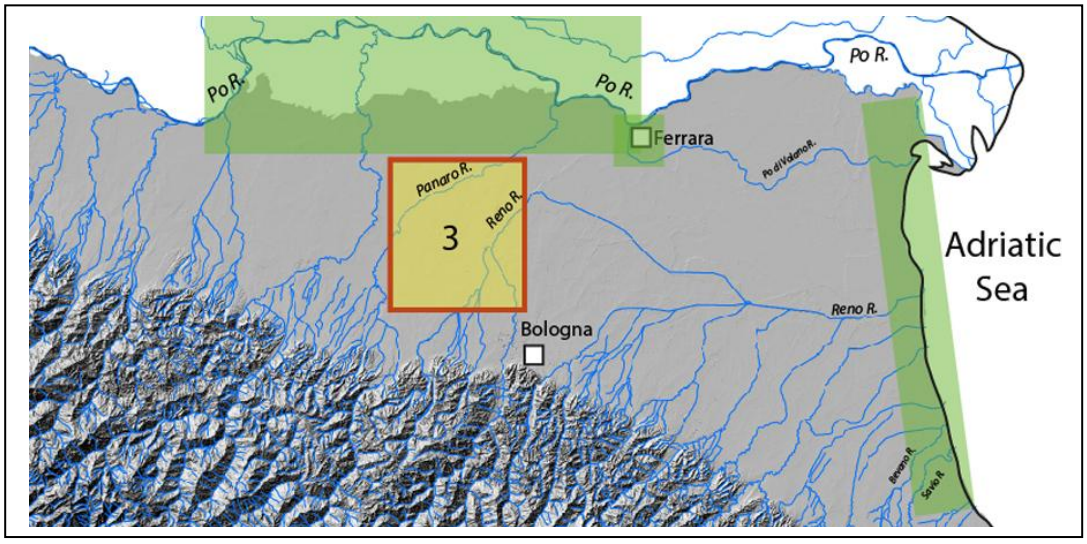

Fig. 34 - Location of study area 3 (yellow rectangle).

4.4. Study area 4

A late Quaternary multiple paleovalley system from the Adriatic coastal plain (Biferno River, Southern Italy).

Alessandro Amorosi, Vito Bracone, ***Bruno Campo***, Carmine D'Amico, Veronica Rossi, Carmen M. Rosskopf

Study area 4 is located along the Adriatic coast, ca. 300 km to the south of the modern Po coastal plain (Fig. 35). In this study, we depicted the high-resolution facies architecture of the Biferno valley fill (Late Pleistocene-Holocene) through a multi-proxy approach including geomorphological, stratigraphic, sedimentological and paleontological (benthic foraminifers, ostracods and molluscs) information. The extremely high data density (2 new continuously cored boreholes, high-quality core descriptions, and cone penetration tests) allowed the construction of a ca. 2 km-long cross section parallel to the modern Adriatic shoreline. We also provided a sequence stratigraphic interpretation of the investigated coastal succession.

This study represents an opportunity to compare two coeval successions located in a different geological setting (Po Plain and Biferno coastal plain) along the Adriatic coast.

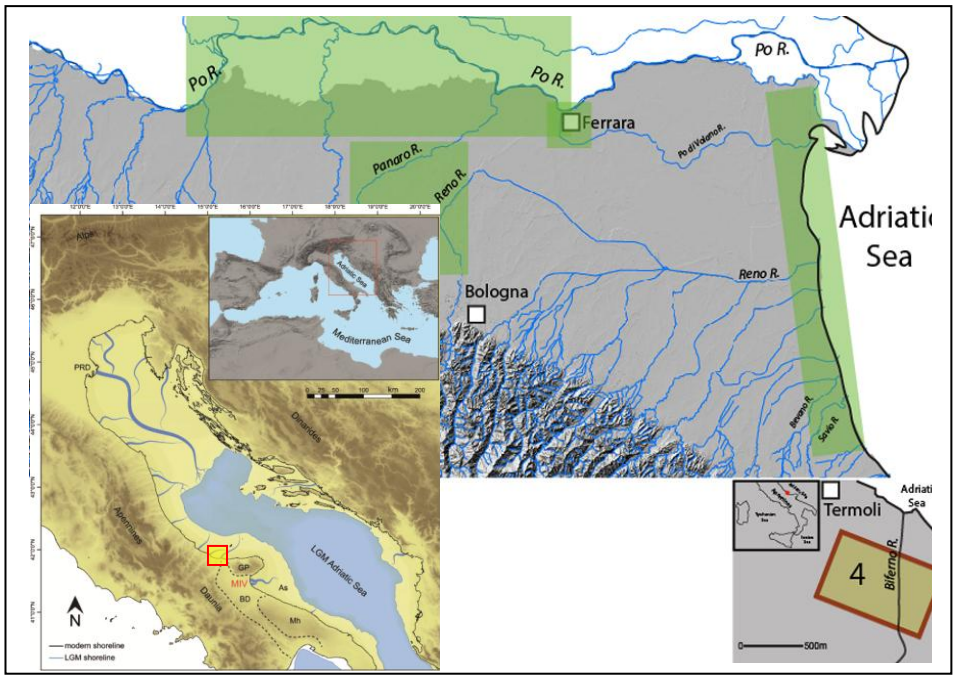

Fig. 35 - Location of study area 4 (yellow rectangle on the right). On the left, the LGM paleoenvironmental reconstruction from Maselli et al. (2014). In the red rectangle, the LGM Biferno area.

4.5. Study area 5

Origin of VC-only plumes from naturally enhanced dechlorination in a peat-rich hydrogeologic setting

Maria Filippini, Alessandro Amorosi, ***Bruno Campo***, Sara Herrero-Martìn, Ivonne Nijenhuis, Beth L. Parker, Alessandro Gargini

The fifth study area corresponds to the city of Ferrara (Fig. 36). This study was carried out to show how high-resolution sequence stratigraphic studies on unconsolidated sediments (Late Pleistocene-Holocene) may be useful for practical purposes. The research was developed in collaboration with a team of hydrogeologists (Prof. Alessandro Gargini and Dr. Maria Filippini, University of Bologna): we provided a 6 km-long cross section, depicting the stratigraphic architecture and the facies distribution beneath the city of Ferrara. Through the combination of hydrostratigraphic and stratigraphic-sedimentological data, we investigated the causes of VC-only plumes (with uncertain source location) in the aquifers; we also proved that reductive dechlorination of PCE and TCE takes place during contaminant migration through peat-rich layers (swamp deposits) related to the Holocene transgression.

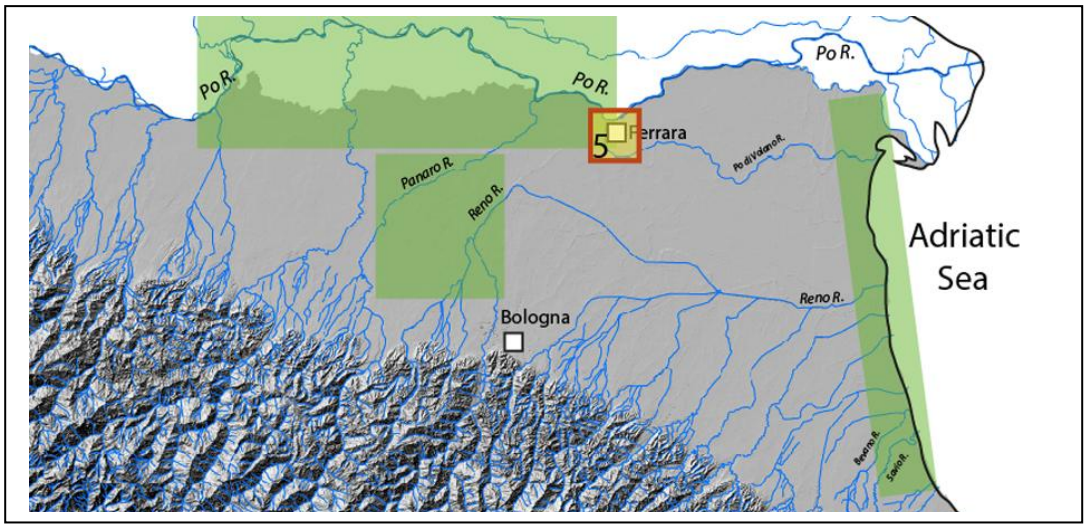

Fig. 36 - Location of study area 5 (yellow rectangle).

5. MANUSCRIPTS

5.1. Paper 1 (Study area 1)

Sequence stratigraphy and late Quaternary paleoenvironmental evolution of the Adriatic coastal plain (northern Italy)*

Bruno Campo, Alessandro Amorosi, Stefano Claudio Vaiani

*Submitted to ***Paleo3***

Sequence stratigraphy and late Quaternary paleoenvironmental evolution of the Adriatic coastal plain (northern Italy)

Bruno Campo[a1], Alessandro Amorosi[a], Stefano Claudio Vaiani[a]

[a] *Dipartimento di Scienze Biologiche, Geologiche e Ambientali, University of Bologna, Via Zamboni 67, 40127 Bologna, Italy*

Abstract

Integrated sedimentological and micropaleontological data were used for the construction of a 93 km-long stratigraphic cross-section parallel to the modern Adriatic shoreline (northern Italy). The stratigraphic panel, transversal to the Holocene transgressive-regressive coastal wedge for most of its length, highlights for the first time along-strike changes in facies architecture. Close to the Apenninic margin, the Late Pleistocene alluvial deposits (ca. 45-12.5 kyr BP) consist of pedogenized floodplain muds that are replaced beneath the modern Po Delta by a laterally continuous, ~20 m-thick channel-belt sand body. A major paleosol, younger than 34 kyr cal BP, is inferred to have formed in response to sea-level fall and river downcutting at the onset of the Last Glacial Maximum (MIS 3-MIS 2). Another paleosol (12.5-10 kyr BP), associated to the Younger Dryas (YD) cold event, marks the transition from latest Pleistocene alluvial deposits to overlying Holocene coastal facies. In terms of sequence stratigraphy, the lower paleosol represents the sequence boundary and the coeval, amalgamated channel-belt deposits form the lowstand systems tract. The transgressive surface coincides with a weakly-developed paleosol (18.5-16 kyr BP) that marks a major phase of channel abandonment induced by early sea-level rise. The YD paleosol allows subdivision of the transgressive systems tract (TST) into lower and upper TST. The lower TST, well developed in the south and in the north, is characterized by thin poorly-drained floodplain deposits; the upper TST, showing vertical transition to coastal and shallow-marine clays, has diagnostic 'marine' signature, and is laterally continuous, with no significant thickness changes. The maximum flooding surface marks the turnaround from a deepening-upward to shallowing-upward trend. The highstand systems tract includes a prograding succession of prodelta clays and overlying delta-front sands. The late Holocene beach-ridge sand body is continuous for

[1] Corresponding author. Fax +39 051 2094522. Phone +39 051 2094564.
E-mail addresses: bruno.campo2@unibo.it (B. Campo), alessandro.amorosi@unibo.it (A. Amorosi), stefano.vaiani@unibo.it (S.C. Vaiani).

> 93 km, suggesting that prograding delta systems had wave-dominated, arcuate geometry, with transition to laterally continuous strandplains.

Keywords: late Quaternary, coastal plain deposits, sequence stratigraphy, paleoenvironmental evolution, Po Plain

1. Introduction

Coastal depositional systems have been extensively investigated since the beginnings of sequence stratigraphy (Vail, 1987; Posamentier et al., 1988; Galloway, 1989) and their successive developments (Dalrymple et al., 1992; Posamentier et al., 1992; Allen and Posamentier, 1993; Catuneanu, 2006; Neal and Abreu, 2009). In particular, late Quaternary coastal successions represent ideal natural laboratories that may offer a very high-resolution chronologic framework to a number of possible ancient analogs, for several reasons: (i) Late Pleistocene and Holocene sea-level fluctuations are well established; (ii) sedimentary successions are generally poorly deformed by tectonic activity; (iii) radiocarbon dating provides the basis for very accurate stratigraphic correlations, and (iv) the species that make up the fossil record are readily comparable to the modern ones.

The subsurface of the Po coastal plain (Fig. 1), in northern Italy, has been extensively investigated in the past 30 years, and several studies carried out for different purposes (coastal hazard mitigation, aquifer characterization, geological mapping, etc…) have led to the high-resolution reconstruction of late Quaternary facies architecture. These studies, however, have been conducted on relatively small areas of the Adriatic coastal plain (Amorosi et al., 1999a, 2003, 2004; Amorosi and Colalongo, 2005; Stefani and Vincenzi, 2005). Based on a series of stratigraphic cross-sections perpendicular to the coastline, Amorosi et al. (1999a, 2003) identified the characteristic wedge-shaped stratigraphic architecture of the Holocene coastal deposits, between Ravenna and Comacchio (Fig. 1). Amorosi et al. (2004) and Amorosi and Colalongo (2005) enhanced this stratigraphic framework, pointing out a characteristic (transgressive-regressive, T-R) cyclicity of coastal and alluvial deposits from the same area (Figs. 1 and 2a). On the basis of combined radiocarbon and pollen data, a major glacio-eustatic control on sedimentation, falling in the Milankovitch band (~100 kyr) was documented for the youngest two T-R cycles (Fig. 2b). Following Embry (1995), Amorosi and Colalongo chose the transgressive surfaces (TSs) as the most prominent markers for stratigraphic correlations, because of their high subsurface traceability across the basin. The TSs mark the landward shifts of barrier-lagoon systems,

corresponding to dramatic facies changes from pedogenized lowstand alluvial plain strata to overlying back-barrier deposits. Each coastal wedge, thus, includes transgressive (TST) and progradational (HST) deposits, separated by the maximum flooding surface (MFS). The upper parts of the T-R cycles mark the transition to alluvial deposits, which represent the falling-stage and lowstand systems tracts (FSST and LST). Widespread alluvial plain aggradation, even during periods of sea-level fall was favored by high rates of tectonic subsidence (Amorosi et al., 2004).

This paper is based on a > 90 km-long stratigraphic cross section, parallel to the present Adriatic coastline, from Cesenatico to the modern Po Delta (Fig. 1). Through this stratigraphic panel, for the first time we show the along-strike stratigraphy of the late Quaternary (last 45 kyr) coastal succession of the Po Plain. The objectives of this study are:

- to investigate along-strike variations in stratigraphic architecture of the Holocene T-R wedge;
- to offer the sequence-stratigraphic interpretation of the whole late Quaternary succession, through the identification and lateral tracing of all key surfaces;
- to check the extent to which proximity to the Apenninic chain influenced coastal evolution with respect to the modern delta area.

Long stratigraphic cross-sections (> 50 km) parallel to the coastline, though reported from the rock record (Forzoni et al., 2015; Hampson et al., 2011), are uncommon in late Quaternary studies and lacking from the Mediterranean area. Literature examples are from McFarlain Jr. (1961), who reconstructed three cross-sections transversal to the Mississippi Delta; Goodbred Jr. and Kuehl (2000) and Goodbred Jr. (2003), who studied stratigraphy and evolution of the Ganges-Brahmaputra delta through several >100 km long sections; Hijma et al. (2009), who documented the stratigraphic evolution of the Rhine mouth through ca. 50 km long cross-sections. Additional case studies are from the East Asian coastal plains, including the Yangtze delta (Li et al., 2002) and the Mekong delta (Ta et al., 2005).

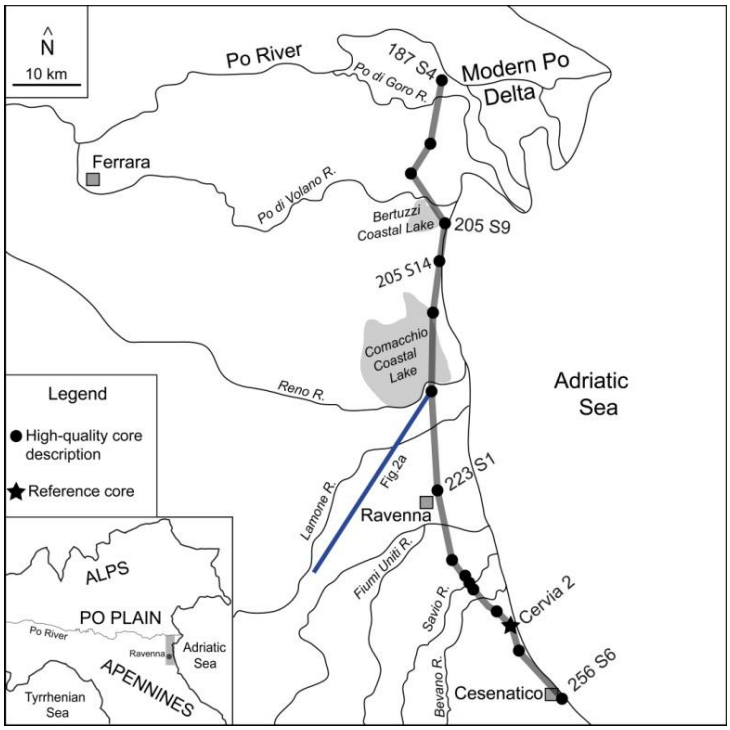

Fig. 1 - Study area with indication of the section trace of Figures 4 and 6. Sixteen continuous cores for which facies interpretation is available are shown along the transect. The blue line indicates the trace of the section in Fig. 2a.

2. Geological setting

The Emilia-Romagna coastal plain is the seaward portion of the wider Po Plain, a peri-sutural basin bounded by the Alps to the north and the Apennines to the south (Fig. 1). Following accurate hydrocarbon exploration campaigns, the thickness of the Pliocene and Quaternary basin fill has been estimated to be ca. 700-800 m (Castellarin and Vai, 1986; Pieri and Groppi, 1981). Further detailed stratigraphic investigation carried out by Regione Emilia-Romagna and Eni-Agip (1998) south to the Po River identified six depositional sequences bounded by third-order, seismic-scale unconformities. The youngest sequence (ca. 0.87 Myr-Present, - Muttoni et al., 2003) was subdivided into eight lower-rank (fourth-order) depositional cycles, equivalent to the transgressive-regressive (T-R) cycles of Amorosi and Colalongo (2005).

In the Po coastal plain, the T-R cycles consist of repeated alternations of coastal and alluvial deposits. Two wedge-shaped coastal sand bodies were reconstructed between 0-30 m and 100-130 m depth, respectively, separated by a thick mud-dominated alluvial succession (Amorosi et al., 2004 - Fig. 2a). Pollen characterization proved a glacio-eustatic control on facies architecture (Fig. 2b), with a major influence by the Milankovitch-scale periodicity (ca. 100 kyr). In particular, the expansion of broad-leaved forests reconstructed from the coastal deposits was associated to the Marine Isotope Stage (MIS) 5e and MIS 1 interglacials; whereas the thick alluvial succession

between the two coastal wedges was assigned to the MIS 4 to MIS 2 glacial period (Amorosi et al., 1999b, 2004; Amorosi and Colalongo, 2005).

In terms of sequence stratigraphy, the two coastal wedges have been interpreted to represent the landward migration of barrier-lagoon systems and the following progradation of wave-influenced deltas; for this reason, they include the transgressive systems tract (TST in Fig. 2) and the highstand systems tract (HST). The intervening alluvial deposits represent the falling stage systems tract (FSST of Plint and Nummedal, 2000) and the lowstand systems tracts (LST), which accumulated under the influence of high tectonic subsidence rates (Amorosi and Milli, 2001). The transgressive surface (TS) marks the abrupt facies transition from stiff pedogenized alluvial deposits (LST) to overlying back-barrier strata (TST). The laterally extensive erosional surface separating back-barrier deposits from transgressive sands, was interpreted as the ravinement surface or RS (*sensu* Swift and Nummedal, 1987). The maximum flooding surface (MFS) is located at the transition between retrogradational to progradational stacking patterns.

The anatomy of the Holocene coastal wedge has been described by Amorosi et al. (1999a, 2003), Bondesan et al. (1995) and Rizzini (1974) from the Romagna coastal plain to the modern Po delta. Through the reconstruction of beach-ridge/drainage system evolution, the role of autogenic processes to sedimentary evolution has been established (Bondesan et al., 1995; Ciabatti, 1967; Correggiari et al., 2005a, 2005b; Stefani and Vincenzi 2005; Veggiani, 1974).

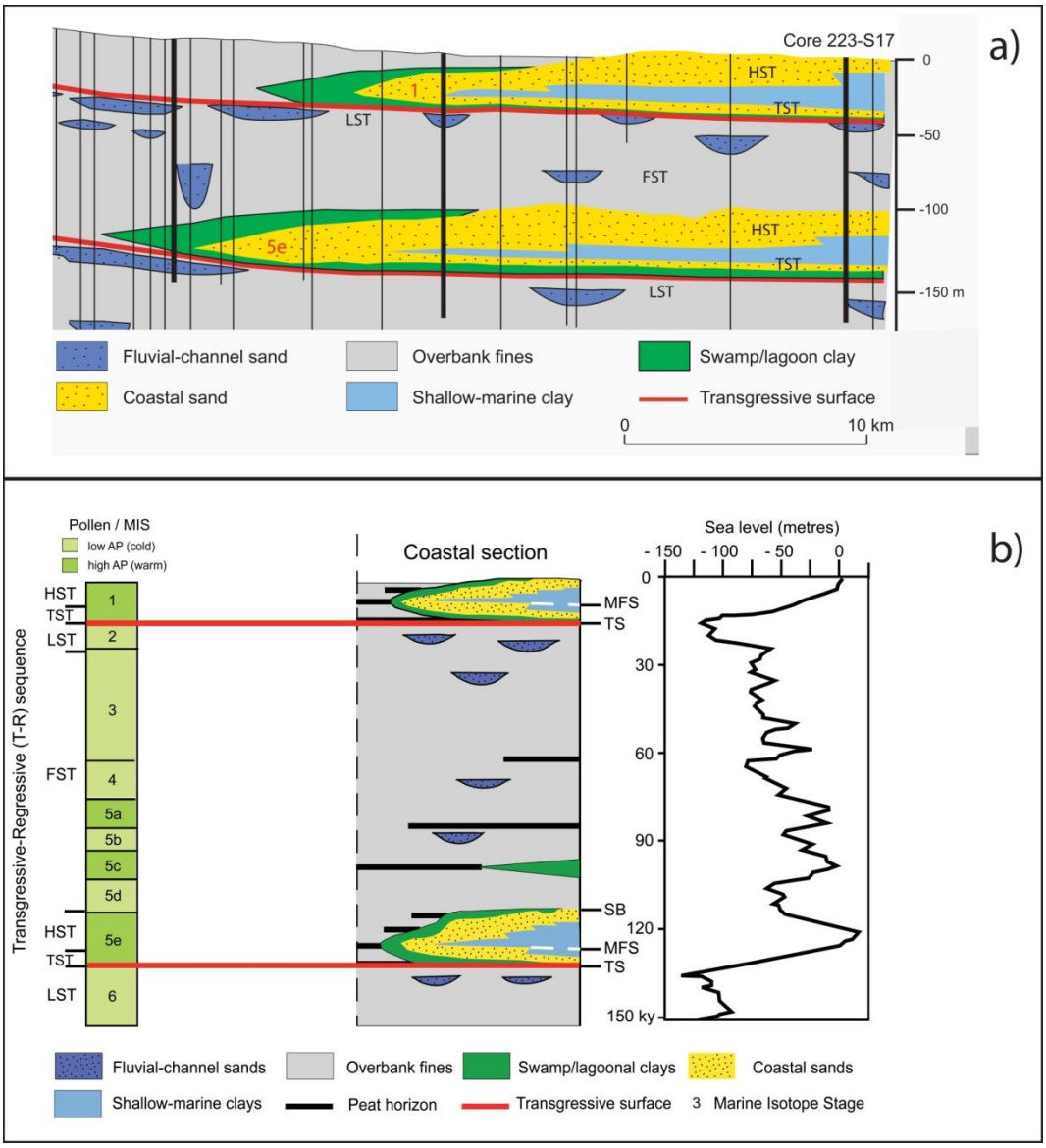

Fig. 2 - a) Cyclic facies architecture beneath the Po coastal plain: wedge-shaped coastal wedges alternating with thick packages of alluvial deposits (FST+LST). In red, the transgressive bounding surfaces. For section trace, see Fig. 1. b) Schematic representation of the last two T-R cycles (post 125 kyr BP) in relatively proximal (alluvial section) and distal (coastal section) positions. The relations between stratigraphic architecture, climate-change, sea-level fluctuations (sea-level curve after Bard et al., 1990) and sequence stratigraphy are shown. MIS: Marine Isotope Stage; AP: arboreal pollen (excluding Pinus); SB: sequence boundary; TS: transgressive surface; MFS: maximum flooding surface. Modified from Amorosi (2008).

3. Methods

A total of 114 stratigraphic data were selected from the Emilia-Romagna Geological Survey database: these data include 15 high-resolution, sedimentological core descriptions (at ca. 45 m depth), 29 conventional (lithologic) core descriptions (ca. 30 m deep), 16 stratigraphic data from water wells (> 50 m deep), and 54 cone penetration tests (10-36 m deep). All stratigraphic data were used for the construction

of a 93-km-long stratigraphic cross-section parallel to the modern Adriatic shoreline (Fig. 1).

High-resolution, sedimentological core descriptions include all relevant information for facies interpretation, such as grain-size, color, accessory materials, pedogenic features, pocket penetrometer values and radiocarbon dates. Conventional core descriptions include basic grain-size characteristics, but lack geotechnical information, soil characteristics, radiocarbon dates and fossil annotations. Despite their poor-quality, water well descriptions were used, as they offer basic lithologic (clay/sand) distinctions that are useful to identify thick sand bodies in the subsurface. Finally, data from cone penetration tests (CPT) and piezocone penetration tests (CPTU) were utilized, as they may serve to perform detailed facies characterization and subsurface stratigraphic correlations (Amorosi and Marchi, 1999; Amorosi et al., 2015; Sarti et al., 2012). For facies calibration of CPTU tests, we used the freshly drilled continuous core “Cervia 2”, 52.5 m long (Fig. 1).

Microfossil (foraminifer and ostracod) analyses from cores 256-S6, 240-S6, 187-S6 and 187-S4, integrating a review of paleontological data from cores 240-S8, 223-S1, 223-S17, 205-S4, 205-S9, 205-S14 and 187-S1 (Amorosi et al., 1999a, 1999b, 2003, 2004; Vaiani, 2010), were carried out to refine facies interpretation. Paleoenvironmental interpretation of microfaunal assemblages is based mainly on the recent distribution of observed taxa in the Mediterranean, specifically the Northern Adriatic Sea (Donnici and Serandrei Barbero, 2002; D'Onofrio, 1969; Jorissen, 1988; Montenegro and Pugliese, 1996; Rossi and Horton, 2009). Further information was obtained by comparison with assemblages from other subsurface successions of the Po coastal plain (e.g. Di Bella et al., 2011, 2013; Dinelli et al., 2013; Fiorini, 2004).

The chronologic framework is based on a total of 29 published ^{14}C dates on peat, organic-rich layers, shells, wood and plant fragments (Amorosi et al., 1999a, 2003; Geological Map of Italy at 1:50,000 scale, Sheet 187, 205, 223, 240-241, 256 – Tab. 1). One sample from core “Cervia 2” was dated at the Laboratory of Korea Institute of Geoscience and Mineral Resources (KIGAM, Republic of Korea). One sample from core 223-S17 was dated at the Laboratory of Ion Beam Physics (ETH, Zurich, Switzerland). Two samples from core 240-S6 were dated at CEDAD (University of Salento, Italy). All radiocarbon dates were calibrated by Oxcal 4.2 (Ramsey, 2009), with the Intcal13 calibration curve and Marine13 (Reimer et al., 2013) with a ΔR value of 139 ± 28 yr (Langone et al., 1996).

Tab. 1 – List of radiometric ages. (* Geological Map of Italy at 1:50,000 scale).

Core	*Depth in core (m)*	*Material*	*Conventional ^{14}C age (yr BP)*	*Calibrated age 2σ range (yr BP)*	*Calibrated age mean (yr BP)*	*σ*	*References*
256 S6	19.9	Organic clay	9,730±50	11,245-11,075	11,145	90	Sheet 256*
256 S6	32	Organic clay	29,780±320	34,545-33,375	33,925	280	Sheet 256*
256 S6	38	Wood	33,140±410	38,445-36,320	37,370	580	Sheet 256*
241 S1	10.1	Organic clay	5,840±50	6,755-6,500	6,645	65	Sheet 240-241*
241 S1	14.9	Organic clay	9,520±50	10,905-10,655	10,875	135	Sheet 240-241*
241 S1	23.7	Organic clay	14,290±60	17,610-17,175	17,400	110	Sheet 240-241*
241 S1	39.8	Organic clay	38,390±560	43,320-41,745	42,520	395	Sheet 240-241*
240 S8	21	Organic clay	8,840±100	10,195-9,600	9,915	165	Sheet 240-241*
240 S8	30.5	Organic clay	13,270±50	16,145-15,755	15,955	100	Sheet 240-241*
Cervia2	16.45	Organic clay	6,720±40	7,665-7,555	7,585	35	This paper
240 S6	21.55	mollusk shell	7,384±45	8,037-7,856	7,958	45	This paper
240 S6	23.60	mollusk shell	7,358±45	8,013-7,843	7,932	45	This paper
223 S1	16.1	Organic clay	3,305±60	3,645-3,395	3,535	70	Amorosi et al., 1999a
223 S1	25.6	Wood	8,160±60	9,290-8,995	9,125	90	Sheet 223*
223 S1	25.6	Wood	8,170±50	9,270-9,010	9,130	80	Amorosi et al., 1999a
223 S1	32.8	Organic clay	25,580±170	30,315-29,260	29,755	270	Amorosi et al., 1999a
223 S1	45	Wood	33,530±440	38,855_36,550	37,785	605	Sheet 223*
223 S17	23.6	Shell	4,400±35	4,505-4,230	4,365	70	This paper
205 S4	8.65	Shell	1,460±55	993-719	858	68	Amorosi et al., 2003
205 S4	10-10.1	Shells/Lentidium	1,390±30	897-699	797	53	Scarponi et al., 2013
205 S4	31.5-31.75	Shells/Lentidium	8,485±30	9,382-9,121	9,231	63	Scarponi et al., 2013
205 S4	32.5-32.6	Shells/Lentidium	8,575±30	9,442-9,278	9,361	45	Scarponi et al., 2013
205 S4	34.4	Organic clay	15,280±380	19,455-17,700	18,545	430	Amorosi et al., 2003
205 S14	3-3.1	Shells/Lentidium	1,080±25	621-487	547	36	Scarponi et al., 2013
205 S14	31.7	Organic clay	10,480±40	12,570-12,375	12,430	100	Amorosi et al., 2003
205 S9	8.4	Organic clay	2,013±57	2,125-1,860	1,975	70	Amorosi et al., 2003
205 S9	26.9-27	Shells/Lentidium	7,975±30	8,382-8,192	8,298	50	Scarponi et al., 2013
205 S9	26.9-27	Shells/Varicorbula	8,075±30	8,501-8,316	8,398	45	Scarponi et al., 2013
205 S9	31.2	Plant fragments	9,500±80	11,110-10,570	10,840	160	Amorosi et al., 2003
205 S9	35.3	Wood	18,830±140	23,035-22,410	22,710	165	Amorosi et al., 2003
187 S1	25.85	Plant fragments	8,250±60	9,420-9,070	9,230	100	Sheet 187*
187 S1	50.05	Peat	41,790±1000	47,495-43,440	45,390	1,005	Sheet 187*
187 S4	25.45	Peat	8,020±70	9,035-8,635	8,875	115	Sheet 187*

4. Facies associations

Facies characterization of late Quaternary deposits along the Adriatic coastal plain relies upon the detailed sedimentological and micropalaeontological study of high-quality cores in Fig. 1. Nine facies associations were identified on the basis of core

data (Fig. 3). The description of the facies associations, follows the stratigraphic order, from bottom to top.

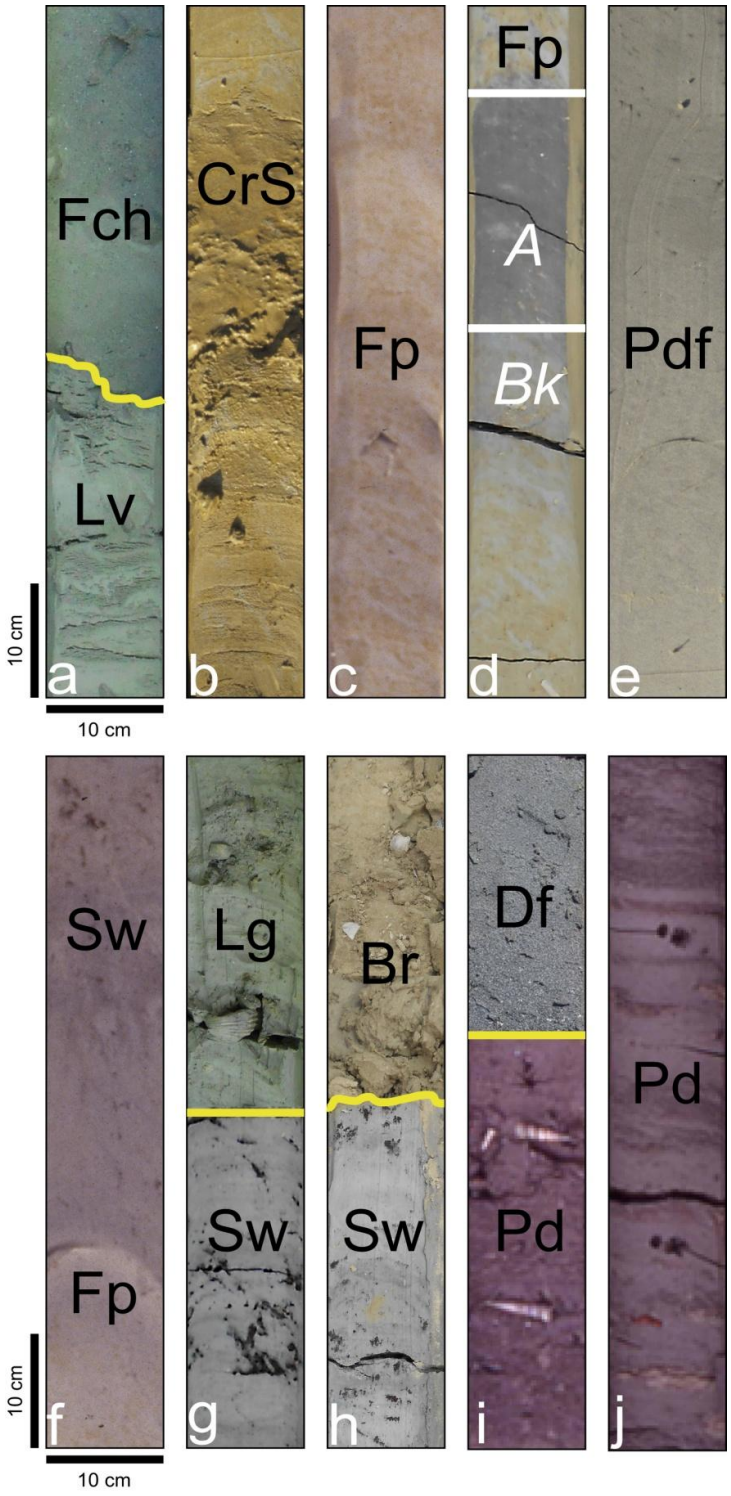

Fig. 3 - Representative core photographs depicting the major facies associations and lithofacies identified in cores (256-S6, 241 S1, 240 S6, "Cervia 2", 223-S1 and 223-S17). a: mud and silty sand alternations of levee (Lv) sediments and overlying fluvial channel (Fch) sands with erosional base (yellow line); b: crevasse splay (CrS) deposit with diagnostic CU trend; c: massive and mottled floodplain (Fp) silty clays; d: pedogenized floodplain deposit (Fp) with weakly-developed paleosol consisting of A-horizon (organic-rich) and Bk horizon (calcic); e: massive and gray poorly-drained floodplain (Pdf) silty clays; f: vertical transition from stiff floodplain (Fp) clays to overlaying soft and organic-rich swamp (Sw) deposits; g: swamp (Sw) sediments capped by lagoonal (Lg) silty clays with shell fragments (Cerastoderma); h: organic-rich swamp (Sw) clays and beach ridge (Br) sands with bioclasts and erosional base (yellow line); i: massive and bioturbated prodelta (Pd) deposit with gastropods (turritella) overlain by medium to coarse gray delta front (Df) sands; j: soft prodelta (Pd) muds with mm-cm sandy layers.

4.1. Fluvial channel facies association

4.1.1. Description

This facies association is just a few m thick in the southern part of the study area, but about 20 m thick across 30 km in the northern portion of the transect (Fig. 4). It is composed of gray, well sorted, coarse to fine sand, with fining-upward (FU) tendency and erosional base (Fig. 3a). Wood, plant debris and abraded or broken specimens of foraminifera are rare, but locally present. The upper boundary to the overlain mud is either sharp or transitional, and the entire succession is commonly capped by peat or organic-rich layers. Piezocone penetration tests display high tip-resistance (Qc > 5 MPa), typically decreasing from base to top, along with negative pore pressure values.

4.1.2. Interpretation

The combination of lithology, sedimentological features and geotechnical characteristics allows for interpretation of these deposits as fluvial-channel facies association (Miall, 1992). Negative pore pressure values, indicating high permeability, are typical for this type of depositional facies (Amorosi and Marchi, 1999). The presence of wood, plant debris and poorly preserved foraminifers, interpreted as reworked from older units, also supports this interpretation. The transitional or sharp boundary to the overlying peats or organic-rich muds may reflect gradual or abrupt channel abandonment, respectively, with development of standing bodies of water.

4.2. Crevasse and levee facies association

4.2.1. Description

This facies association, 0.5-2.5 m thick (Fig. 4), is barren and characterized by two different lithofacies: (i) a rhythmical alternation of gray to brownish silty sand and silty clay, with scattered root fragments, bioturbation, iron and manganese oxides, and scarce carbonate nodules (Fig. 3a); (ii) medium-fine sand to silty sand bodies showing either FU or coarsening-upward (CU) tendencies, with erosional or transitional base, respectively (Fig. 3b). This facies is barren of fossils.

4.2.2. Interpretation

This facies association is interpreted as channel-related deposit, reflecting a broad variety of depositional sub-environments formed as the result of fluvial activity next to the channel axis. In particular, (i) the rhythmical alternation of silty sand and silty clay is thought to represent sedimentation on natural levees, the sand/mud ratio increasing

with decreasing distance from the river axis. Pedogenized features testify to subaerial exposure; (ii) sand bodies with gradual base, sharp top and CU trend represent crevasse splays; whereas sand bodies with erosional base and gradational FU tendency to the top are interpreted to be crevasse channels (Collinson, 1996; Miall, 1992).

4.3. Well-drained floodplain facies association

4.3.1. Description

This facies association, typically encountered in the southern part of the cross-section, about 20 m below the ground surface (Fig. 4), is up to 35 m thick, and consists of a monotonous succession of highly pedogenized, rooted and deeply bioturbated gray clay and silty clay with brownish-yellowish mottles (Figs. 3c and 3d). Iron and manganese mm-scale nodules are abundant. The dominant clay is mostly structureless, with faint horizontal mm- to cm- thick laminations. Silty sand to very fine sand intercalations are locally present. Stiff pedogenized horizons or weakly developed paleosols are common at various stratigraphic intervals. These paleosols are locally characterized by diagnostic clay layering, with upper, dark-gray organic enriched A-horizons and lower, whitish-gray Bk-horizons (Fig. 3d) with characteristic calcite and oxides nodules (mm to cm in diameter). Shell fragments of continental molluscs, commonly referable to *Hydrobia* and *Planorbis,* and valves of freshwater ostracods, such as *Candona* and *Ilyocypris* are locally observed within thin, organic-rich clays.

Pocket penetration values range between 1.8-3 kg/cm^2. *Qc* measurements in CPTU tests are 1.8-3 MPa. These values are higher in paleosols, especially in the Bk-horizon (3 to 6 kg/cm^2; >2.5 MPa).

Radiometric dating yielded ages between 45.5 and 11 kyr.

4.3.2. Interpretation

Lithology, geotechnical data and presence of pedogenized features allow the interpretation of this facies association as formed in a floodplain. Specifically, monotonous clay and silty clay deposits, along with the presence of roots, bioturbation and paleosols suggest a low-energy depositional environment characterized by common episodes of subaerial exposure in well-drained conditions (Amorosi et al., 2015a; 2014). The local occurrence of freshwater fossils is consistent with temporary development of ephemeral swamps and ponds. Weakly developed paleosols with A-Bk horizons are interpreted as Inceptisols (Soil Survey Staff, 2014), representing periods

of non-deposition possibly 2-4 kyr long (Amorosi and Marchi, 1999; Amorosi et al., 2014; Sarti et al., 2012).

4.4. Poorly drained floodplain facies association

4.4.1. Description

This facies association, with maximum thickness of 5 m (Fig. 4), is made up of gray to dark gray clay and silty clay. Thin layers of decomposed organic matter, a few cm-thick, are common, along with scattered mm-sized plant remains.

Shell fragments of continental mollusks (*Hydrobia* and *Planorbis*), commonly associated with freshwater ostracods, mainly *Candona* and *Ilyocypris,* are common within this facies association. No pedogenic features, such as manganese and iron nodules, brownish-yellowish mottled or paleosols were encountered.

Pocket penetration and cone tip resistance values range between 1.2-1.9 kg/cm² and 1.2-1.9 MPa, respectively.

Radiometric dating gave ages between 16 and 10 kyr.

4.4.2. Interpretation

The dominance of clay in this facies association reflects a low-energy depositional environment. The lack of Fe-Mn nodules and of traces of subaerial exposure, combined with the presence of a freshwater fauna suggest a poorly drained floodplain (Amorosi et al., 2016), where persistent influence of freshwater was favored by topographic depressions (ponds), river floods and/or high water table. Geotechnical measurements (pocket penetrometer and *Qc*) are consistent with a depositional environment where the water influence induced lower consistency than the well-drained floodplain.

4.5. Swamp/Inner estuary facies association

4.5.1. Description

This facies association, which forms an excellent stratigraphic marker across a significant portion of the study transect (Fig. 4), consists of very soft dark to gray clay (up to 4 m thick), with abundant organic matter, wood fragments and plant debris (Figs. 3f, 3g and 3h). Peat layers, 5-50 cm thick, are common within this facies association. Thin sand layers are locally encountered.

The fossil assemblage includes abundant freshwater ostracods, mainly *Candona* and *Pseudocandona* (Fig. 5A), with the local occurrence of *Ilyocypris*, in association with rare continental gastropods (see floodplain facies association).

Pocket penetration and cone tip resistance values are invariably < 1 kg/cm² (or MPa), with average value of 0.5 kg/cm² (or MPa). Peat layers may display higher values, up to 1.9 kg/cm² (or MPa).

Radiocarbon ages between 10.9 and 9.2 kyr cal BP were obtained from this facies association.

4.5.2. Interpretation

Lithofacies characteristics, geotechnical data, the fossil content and high amounts of organic matter are coherent with very low-energy, freshwater depositional environments deprived of any marine influence, such as swamps, coastal lakes, or the inner portion of an estuary (Amorosi et al., 1999a, 2003). Radiometric ages indicate that the development of paludal environments took place at the onset of the Holocene.

4.6. Lagoon/Outer estuary facies association

4.6.1. Description

This facies association displays maximum thickness of 11 meters (Fig. 4), and includes two lithofacies. Lithofacies (i) consists of mm-cm thick alternations of soft gray clay and silty clay rich in organic matter, wood fragments and brackish mollusks (mainly *Cerastoderma glaucum*), with subordinate, thin sand layers (Fig. 3g). The microfossil assemblage includes variable amount of ostracods, almost entirely represented by *Cyprideis torosa* (Jones, 1850) and foraminifera, mainly *Ammonia tepida* (Cushman, 1926) and *Ammonia parkinsoniana* (d'Orbigny, 1839), with subordinate *Cribroelphidium* spp. and *Haynesina germanica* (Ehrenberg, 1840) (Fig. 5B). Pocket penetrometer and cone tip resistance values are < 1.3 kg/cm² (or MPa).

This lithofacies shows vertical transition to lithofacies (ii), which is made up of very fine to medium gray sands, up to 1 m thick, with local sharp lower boundaries and overall CU tendency. The fossil assemblage includes mainly poorly preserved planktonic and benthic foraminifera.

This facies association occurs at three distinct stratigraphic levels: radiometric ages, along with pollen data chronologically constrain the lower interval to the Bølling-Allerød interstadial period (ca. 14-13 kyr BP) in core 240 S8 (Amorosi et al., 2004). The thick stratigraphic interval reconstructed in the southern part of the transect is dated between about 8 and 6.6 kyr BP. The upper interval is assigned to the last 2 kyr BP.

4.6.2. Interpretation

Sedimentological characteristics and fossil assemblages are indicative of a lagoonal/outer estuarine setting (Amorosi et al., 2003, 2004; Reinson, 1992; Tanabe et al., 2006). Clay-silt alternations in lithofacies (i) represent inner lagoonal/estuarine deposits because of the diagnostic microfossil assemblages, including taxa commonly present in recent lagoon with high freshwater influx (e.g. Athersuch et al., 1989; Debenay et al., 2000), such as those of Po River delta (e.g. Coccioni, 2000; D'Onofrio et al., 1976) and in lagoonal successions (e.g. Di Bella et al., 2011). The local increase in abundance and thickness of the sand intercalations is interpreted to reflect transition to outer lagoonal/estuarine sub-environments. The sandy deposits with CU trend (lithofacies ii), with poorly preserved fossil interpreted as transported from nearby environments or reworked from older units, are interpreted as flood-tidal delta or washover deposits.

4.7. Transgressive barrier facies association

4.7.1. Description

This facies association, < 4.5 m thick (Fig. 4), is made up of gray fine-medium to coarse sand, with typical FU trend and a well recognizable erosional lower boundary. A shell-rich layer (5-30 cm thick) at the base of the unit, includes shells and bioclasts of marine bivalves and gastropods (i.e., *Cardium, Venus,* and *Pecten*), and forms a laterally extensive stratigraphic marker across most of the study area. In relatively proximal areas, this facies association is amalgamated with the overlying beach-ridge facies association, whereas at seaward locations it is sharply capped by the mud-prone, prodelta-offshore facies association.

This facies association shows a microfossil assemblage dominated by benthic foraminifera. Low amounts of size-selected and locally poorly preserved specimens (mainly *Ammonia, Elphidium* and *Miliolacea*) are observed in the lower part of this unit and are locally replaced at the transition with the overlying shallow-marine facies association by a well preserved assemblage dominated by Miliolacea, such as *Adelosina cliarensis* (Heron-Allen and Earland, 1930), *Adelosina elegans* (Williamson, 1858)*, Quinqueloculina spp, Siphonaperta aspera* (d'Orbigny, 1826) and *Triloculina trigonula* (Lamarck, 1804), in association with abundant *Cribroelphidium* and *Elphidium*, mainly *Cribroelphidium lidoense (*Cushman, 1936), *Elphidium crispum* (Linnaeus, 1758) and *Elphidium macellum* (Fichtel and Moll, 1798) and subordinate *Ammonia* and *Textularia* species (Fig. 5C).

Radiometric dating provides the age of 8.3-8.4 kyr cal BP, for this facies association.

4.7.2. Interpretation

The lithologic characteristics of this facies association and the peculiar fossil assemblage indicate a high-energy littoral environment. The FU trend and microfossils distribution are consistent with a deepening-upward tendency from an upper shoreface sub-environment, with transported assemblages (poorly preserved foraminifera and mollusk bioclasts), to a lower shoreface/offshore-transition, with well preserved and *in situ* specimens. The remarkable concentration of selected Miliolacea (*Adelosina elegans, Adelosina cliarensis* and *Triloculina trigonula*), is considered to reflect bottom with vegetation cover (Sgarrella and Moncharmont Zei, 1993). The basal erosional surface is thought to be the consequence of the wave ravinement that cut through back-barrier deposits during the beach-barrier migration in response to rapid sea-level rise (Nummedal and Swift, 1987; Storms et al., 2008). The shell-rich layer has been interpreted as the transgressive lag marking the shoreface retreat during transgression (Amorosi et al., 1999a, 2003, 2008).

4.8. Shallow-marine facies association

4.8.1. Description

This facies association, up to 16 m thick, is continuously developed in the central and northern parts of the study transect (Fig. 4), and consists of two main lithofacies.

Lithofacies (i) includes the rhythmical alternation of silty clay and mm to cm-thick sand layers, with upward transition to massive and bioturbated soft grey clay. Sand layers, up to a few dm thick, with sharp lower boundaries are locally present. The microfossil assemblage (Fig. 5D) includes mainly benthic foraminifera, with high amount of *Cribroelphidium lidoense*, *Elphidium advenum* (Cushman, 1922)*, Elphidium macellum,* Miliolacea and *Textularia* associated with a variety of other taxa, such as *Ammonia*, *Asterigerinata*, *Lagena* and *Rosalina*. Within lithofacies (i) an upward increase in *Textularia*, paralleled by a decrease in *Ammonia*, is commonly observed (e.g. Amorosi et al., 1999b; Vaiani, 2010).

Lithofacies (i) is commonly overlain by lithofacies (ii): massive, bioturbated soft grey clay, with abundant wood and plant remains (Fig 3i). Sand layers, mm to cm-thick, are of very common occurrence, especially in the upper part of this facies association (Fig. 3j). Marine bivalves and gastropods, including *Turritella communis* (Risso, 1826), *Dentalium* sp. and *Murex* (Amorosi et al., 2003) are concentrated at distinct

stratigraphic levels (Fig. 3). Pocket penetrometer and cone tip resistance values are invariably < 1 kg/cm² or MPa. Similar to lithofacies (i), the microfossil assemblage (Fig. 5E) includes mainly benthic foraminifera, though with a lower number of species, and is dominated by *Ammonia tepida* and *Ammonia parkinsoniana* (with an increasing upward trend), and subordinate *Aubignyna perlucida* (Heron-Allen and Earland, 1913), *Cribroelphidium* spp., *Elphidium* spp., *Nonionella turgida* (Williamson, 1858), and *Quinqueloculina seminulum* (Linnaeus, 1758).

Two radiocarbon dates from this facies association yielded ages of 4.4 and 3.5 kyr cal BP.

4.8.2. Interpretation

From its lithologic character and the fossil content, this facies association is interpreted to reflect a low-energy, shallow-marine depositional environment (Amorosi et al., 1999a) with fluctuations in freshwater influence. Lithofacies (i) is interpreted to have formed in offshore-transition to offshore depositional environments (Amorosi et al., 2003), in which changes in lithofacies from clay/sand alternations to massive clay, along with microfossil distribution (specifically for *Textularia* and *Ammonia)* are consistent with progressively deeper marine conditions. Lithofacies (ii) is interpreted to represent a prodelta depositional environment (Amorosi et al., 2008). The occurrence of sand layers is considered to reflect fluvial flooding events. Benthic foraminifera are characterized by remarkable amounts of species indicative of a shallow prodelta with high organic matter (Van der Zwaan and Jorissen, 1991; Rossi and Horton, 2009); the observed trend of *Ammonia* species is interpreted as an upward increase in freshwater influence (Jorissen, 1988).

4.9. Beach-ridge/delta-front facies association

4.9.1. Description

This facies association, up to 19 m thick, forms a laterally extensive sedimentary body, continuous across the entire cross-section (93 km), which forms low-relief ridges that crop out in the modern coastal plain (Fig. 4). It consists of three vertically stacked lithofacies: lithofacies (i) is made up of very fine to fine sand, rich in shell fragments (Fig. 3h); lithofacies (ii) is mostly composed of medium to coarse sand, rich in bioclasts (Fig. 3i); lithofacies (iii) consists of fine to medium sand, with scattered plant debris and shell fragments. Thin intervals of lagoon facies association are intercalated with the sands in the northern part of the study area (Fig. 4). The microfossils assemblage is characterized by planktonic and benthic foraminifera, commonly abraded or broken.

Planktonic taxa locally include Miocene and Pliocene species (Amorosi et al., 2004), whereas benthic foraminifera show a variety of taxa, such as *Adelosina, Ammonia, Bolivina, Bulimina, Cassidulina, Cribroelphidium, Fissurina, Globocassidulina, Melonis* and *Uvigerina* (Fig. 5F).

Based on radiocarbon and archeological data (Ciabatti, 1967), this facies association dates from the last 3,000 years.

4.9.2. Interpretation

This laterally continuous, outcropping sand body accumulated during the last 3,000 years in response to widespread progradation of wave-dominated delta systems and adjacent strandplains. Lithology and sedimentological features testify to a high-energy marine setting. The vertical stacking of lithofacies (i) to (iii) is interpreted to reflect the overall shallowing-upward trend from lower shoreface (i) to upper shoreface (ii) and foreshore/backshore (iii) sub-environments (Amorosi et al., 1999a, 2008). The fossil assemblage, including a mixture of poorly preserved specimens from relatively deep (*Bolivina, Bulimina, Globocassidulina, Melonis*, *Uvigerina* and planktonics) and shallow (*Ammonia, Cribroelphidium* and *Elphidium*) marine environments, is considered transported from nearby environments and reworked from older units.

5. Facies architecture

Accurate correlation of tens of high-resolution stratigraphic data along the modern Adriatic coastline, between the Apenninic margin and the modern Po Delta, led to the construction of the 93 km-long stratigraphic cross-section shown in Fig. 4. The large density of stratigraphic information allowed extremely detailed along-strike documentation of the transgressive-regressive Holocene wedge described at length by previous work (Amorosi and Milli, 2001; Amorosi et al., 1999a, 2003, 2005; Rizzini, 1974; Stefani and Vincenzi, 2005). All those stratigraphic studies documented along-dip, T-R wedge-shaped geometry and facies distribution, but none took into account its transversal and regional extent, as shown in Fig. 4.

The Late Pleistocene sedimentary succession, between about 45 and 12.5 kyr BP, consists entirely of alluvial sediments: pedogenized floodplain muds, laterally associated with 5-10 m thick, fluvial sand bodies represent the dominant feature in the southern part of the transect (Fig. 4). In contrast, a laterally extensive, 20 m-thick channel-belt sand body, with high degree of channel clustering, is clearly identified in the north, beneath the modern Po River (Fig. 4). Levee and crevasse facies are strongly subordinate.

Three prominent, weakly-developed paleosols were recognized at the southern margin of the study area (Fig. 5). The lower paleosol, younger than 34 kyr BP (core 256 S6 in Fig. 4), occurs at ca. 30 m depth. Based on radiocarbon dates from the adjacent fluvial sands, this paleosol might be genetically-related to the erosional-based fluvial bodies (Fig. 4).

Another pedogenized horizon, dated to ca. 18.5-16 kyr BP (cores 241 S1 and 205 S4 in Fig. 4) was identified about 4 meters above, in the southern sector of the study area, where it can be continuously tracked for ca. 3 km. Stratigraphic and geometric relationships suggest high traceability of this paleosol into horizontally aligned tops of the amalgamated fluvial sands, across large parts of the transect. At the southernmost tip of the cross-section, the 18.5-16 kyr BP paleosol is overlain by well-drained floodplain deposits (ca. 5 m thick) with thin (< 1 m) poorly-drained floodplain deposits, with local development of brackish conditions (cores 240 S8 and S6).

The abrupt vertical transition from the Late Pleistocene alluvial succession to overlying coastal deposits of Holocene age is physically highlighted by a continuous and laterally traceable paleosol (5-6 km), dated around 12.5-10 kyr BP (Fig. 4). Pollen data from this pedogenized horizon clearly show high values in *Pinus* spectra (Amorosi et al., 2004). This paleosol shows high lateral traceability, especially in the southernmost portion of the cross-section (Fig. 4), whereas it is lacking to the north, between cores 187-S6 and 187-S4. In the central sector, it lies just a few decimeters above the top of the Late Pleistocene fluvial-channel bodies. In this part of the cross-section, the paleosol is more discontinuous and locally replaced by lens-shaped poorly-drained floodplain deposits.

The coastal succession of Holocene age exhibits gradual transition from poorly-drained floodplain deposits to organic-rich, paludal clays (10.9-9.2 kyr cal BP), up to lagoonal deposits (ca. 9 kyr cal BP). These back-barrier sediments, between core 223 S1 and 187 S4, are overlain by thin, transgressive barrier sands (ca. 8.4 kyr cal BP), which in turn are replaced upsection by a thick succession of laterally extensive offshore/prodelta muds (4.4-3.5 kyr cal BP). In the southernmost part of the study transect, where the cross-section typically develops an along-dip component, shallow-marine deposits are replaced landwards by nearshore and lagoonal deposits dated ca. at 8 kyr cal BP. The laterally extensive (> 90 km) and thick (ca. 10 m) sand sheet that caps the entire succession includes beach ridges and delta front facies associations (ca. 2 kyr BP to Present). These marine sands, which are locally outcropping, along with modern coastal lakes, ponds and floodplain/delta plain deposits form the modern coastal plain.

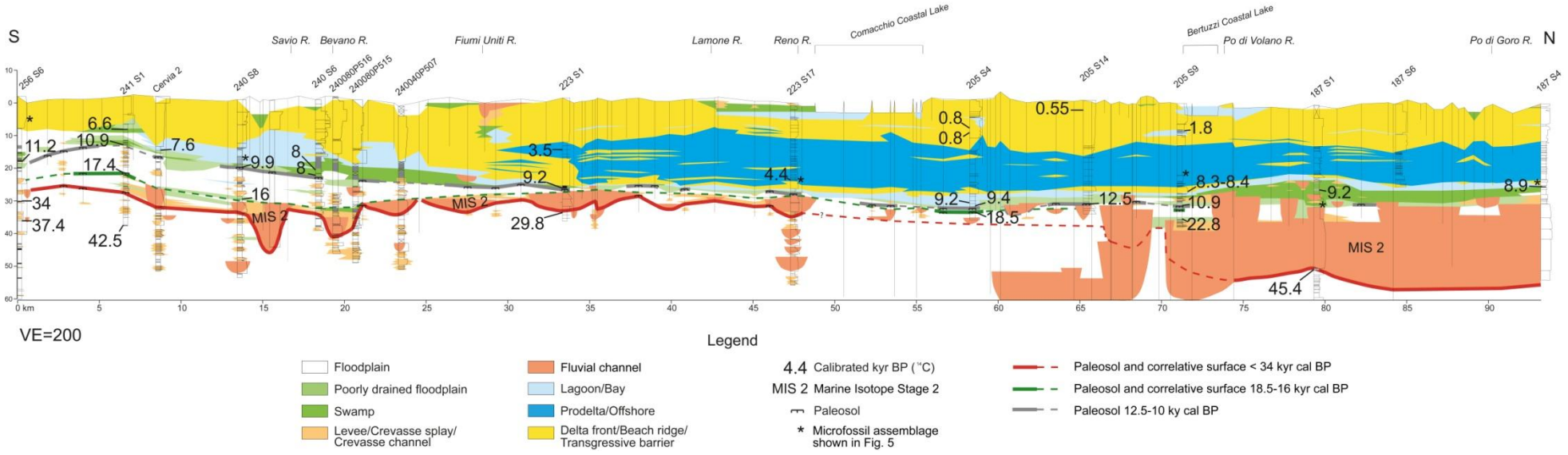

Fig. 4 - Stratigraphic architecture beneath the modern Adriatic coastal plain along a 93 km-long cross-section. For section trace, see Fig. 1.

Fig. 5 - Microfossil assemblages of selected facies associations. A: swamp, core 187-S1, -30.50 m core depth; B: lagoon, core 240-S8, -17.90 m core depth; C: transgressive barrier, core 187-S4, -24.50 m core depth; D: shallow marine (offshore-transition), core 223-S17, -23.60 m core depth; E: shallow marine (prodelta), core 205-S9, -22.05 m core depth; F: beach ridge, core 256-S6, -6.80 m core depth. Bar: 200 µm

6. Paleoenvironmental evolution

The chronologically well constrained stratigraphic framework along a ca. 100 km-long cross-section provides the basis for depicting the paleoenvironmental evolution of the entire Po coastal plain during the last 45 kyr. Previous stratigraphic interpretations

(Amorosi et al., 1999a, 1999b, 2003, 2005; Stefani and Vincenzi, 2005) may thus be refined in the light of a basin-scale view. Integrated microfossil analysis provides additional, valuable information for accurate paleoenvironmental reconstruction.

The presence of weakly developed paleosols in the southern part of the study area (Fig. 4), close to the Apenninic chain, has strong similarities with recent findings from the southern basin margin, where two major paleosols, related to the MIS 3-MIS 2 transition and the Younger Dryas cold event, respectively, were identified and mapped for tens of km (Amorosi et al., 2015a, 2015b, 2014). Between MIS 3 and MIS 2 (ca. 29.8 kyr cal BP), sea level dropped down to -120 m, and the Po Plain extended 300 km to SE across the north-Adriatic shelf (Maselli et al., 2014). This period was marked by climatic deterioration toward colder and drier conditions, with fluvial incision and consequent subaerial exposure of the interfluves and soil development (Amorosi et al., 2015b, 2014).

The age of the lower paleosol (younger than 34 cal kyr BP, but older than 18 cal kyr BP), along with radiocarbon dates from the adjacent, fluvial channel-belt sand bodies, which constrain fluvial activity between about 30-23 cal kyr BP (Fig. 4), suggest a possible linkage between pedogenesis and contemporary river incision at the onset of the Last Glacial Maximum (MIS 3-MIS 2 transition). Low accommodation under sea-level lowstand conditions (Fairbanks, 1989; Paltier and Fairbanks, 2006) and high sediment supply during a fully glacial period (Fontana et al., 2014) favored lateral channel migration and deposition of a laterally extensive fluvial body (Fig. 4).

When sea-level started to rise, ca. 19 kyr BP (Cattaneo and Trincardi, 1999; Clark et al., 2004), in response to meltwater pulses (MWP) 1A and 1B (Pellegrini et al., 2015; Storms et al., 2008), the Adriatic shelf was progressively drowned. MWP-1A (14.4-14 kyr cal BP) produced a considerable sea-level rise of ca. 20 m. However, the coastline remained hundreds of kilometers far from the study area (Amorosi et al., 2015b) which experienced sedimentation in an entirely alluvial environment, with scattered poorly-drained floodplain deposits and even brackish sedimentation in topographic depressions (core 240-S8). Soil development still took place on the interfluves (18.5-16 kyr cal BP paleosol of Fig. 4).

The establishment of colder and drier climatic conditions during the Younger Dryas event (Amorosi et al., 2004; Lehman et al., 1992) caused a new phase of river erosion and pronounced, albeit short-lived subaerial exposure in the interfluves. Under these conditions the YD paleosol was formed (12.5-10 kyr BP, gray line in Fig. 4; see also Amorosi et al., 2015a, 2015b, 2014,).

Climate ultimately turned warmer at the end of the YD period (Taylor et al., 1997) and the rapid sea-level rise that followed during the Holocene (MWP-1B -11.5-11.2 kyr

BP) produced a generalized drowning of the whole study area, including the interfluves: rapidly, poorly-drained and swampy environments back-stepped above the older, Pleistocene alluvial deposits (Fig. 4). Sea level continued to rise (9.4 and 7.6 kyr BP), and a beach-barrier-lagoon-estuary system migrated landward, leading to the establishment of shallow-marine conditions.

After sea-level reached its maximum, deltaic and coastal systems started to prograde due to increased sediment supply from the feeding distributary channels. In an along-strike transect, coastal progradation is revealed by the diagnostic shallowing-upward trend of the depositional facies. Progradation led to deposition of delta front sand onto prodelta clay. Superposed wave activity produced laterally extensive beach ridges, elongated parallel to the shoreline, which formed typically wave-dominated deltas (Amorosi and Milli, 2001). Fluvial avulsions on a centennial scale caused frequent delta lobe switching: under the effect of the ongoing subsidence, abandoned delta lobes were progressively drowned, leading to the establishment of marsh and coastal lakes that form the modern coastal plain.

7. Sequence Stratigraphy

The high-resolution stratigraphic framework depicted in the previous sections enables the sequence stratigraphic interpretation of the Late Pleistocene-Holocene succession of the Po coastal plain (Fig. 6).

7.1. Sequence Boundary

We tentatively place the sequence boundary (SB, Fig. 6) in coincidence of the major paleosol in the area. This paleosol can be interpreted as the classic “interfluve sequence boundary” (Plint et al., 2001; Van Wagoner et al., 1990), seen as a physical regional stratigraphic marker (Demko et al., 2004). This pedogenized horizon is associated to the abrupt sea-level fall and climate change that took place at the onset of the Last Glacial Maximum (MIS 3-MIS 2 transition), and that produced fluvial channel downcutting and soil development on the interfluves (see Amorosi et al. 2015a, 2015b, 2014). The coeval, amalgamated channel-belt sand bodies are interpreted as the lowstand systems tract (LST, Fig. 6), while the underlying (pre-LGM) deposits form the forced regressive systems tract (FSST).

7.2. Transgressive Surface

The concept of transgressive surface (TS) is still debated among the scientific community, and several authors have offered different terms and definitions (Catuneanu, 2009): from the "*Maximum Regressive Surface*" (Catuneanu, 2006; Catuneanu et al., 2011; Embry, 2002; Embry et al., 2007; Helland-Hansen and Gjelberg, 1994; Hellen-Hansen and Martinsen, 1996), which marks the change in shoreline trajectory from lowstand normal regression to transgression; to the "*Transgressive Surface"* of Posamentier and Vail, (1988) and Van Wagoner et al. (1988); the *"Top of Lowstand Surface*" of Vail et al. (1991); the "*Initial Transgressive Surface"* of Nummedal et al. (1993); the "*Conformable Transgressive Surface"* of Embry (1993, 1995); the *"Maximum Progradation Surface"* of Emery and Myers (1996); up to the recent concept developed by Neal and Abreu (2009), which identified the TS as the boundary between progradation to aggradation (LST) and retrogradation (TST).

Based on the age of the transgressive surface recognized in the offshore part of the Po-Adriatic system (Amorosi et al., 2015b), the TS along the study transect might coincide with the weakly developed paleosol (18.5-16 kyr cal BP) that marks the major phase of channel abandonment in Fig. 4, and that is overlain by a thin succession of continental deposits. This paleosol, which shares strong similarities with the transgressive surface of Tanabe et al. (2015), a hiatal surface at the base of an aggradational retrograding meandering system, is likely to represent the "correlative surface in nonmarine settings" of the *Maximum Regressive Surface* of Hellen-Hansen and Martinsen (1996). In the Po coastal plain, the 18.5-16 kyr paleosol most likely records the very last episode of subaerial exposure on the interfluves (depositional *hiatus*) before the onset of renewed fluvial sedimentation. Rapid-sea level rise probably modified the equilibrium profile of rivers throughout the Po Basin, which in turn triggered drainage system reorganization (Blum and Törnqvist, 2000) in the study area. As discussed by Amorosi et al. (2015b), an alternative position for the TS is above the prominent Younger Dryas paleosol, at the sharp facies contrast from well-drained floodplain deposits to paludal and estuarine deposits.

During the early phases of sea-level rise, additional accommodation space was created in the Po Basin, enhanced by high subsidence rates (ca. 1 mm/yr). Abundant glacial sediment was delivered because of the ice-decay, producing high aggradation rates (Bruno et al., 2016; Fontana et al., 2014). Under these conditions, rivers began to avulse significantly (Blum et al., 2013), depositing new sediment above the pedogenized interfluves (SB). As a result, fluvial-channel architecture changed from amalgamated (low accommodation during lowstand conditions) to increasingly more

isolated sand bodies (higher-accommodation starting from early transgression). Once sea-level approached the Po coastal plain (ca. 10 kyr BP, post-YD), the study area was drowned (late transgression).

As a result of sea-level rise, the transgressive systems tract (TST, Fig. 6) shows the typical deepening-upward tendency from basal alluvial deposits to overlying coastal and marine sediments. The Younger Dryas (YD) unconformity, corresponding to the highly-continuous paleosol dated 12.5-10 kyr BP, allows subdivision of the TST into lower TST (pre-YD) and upper TST (post-YD) (see Cattaneo and Trincardi, 1999 for the offshore portion of the system). Lower TST deposits display average thickness of 2.5 m in the north, and maximum thickness (ca. 5 m) in the south, close to the Apennine margin; on the other hand, these deposits are scarcely represented in the central sector (interfluve), and generally less than 1 m thick. The upper TST (ca. 6 m thick), instead, is continuous along the entire section, with no significant thickness changes along strike.

7.3. Maximum Flooding Surface

The maximum flooding surface (MFS, Fig. 6) marks the transition from a retrogradational (TST) to a progradational (HST) stacking pattern of facies (Van Wagoner et al., 1988), and corresponds to the end of transgression.

In the study area, given the along-strike orientation of the cross-section, the MFS has relatively flat geometry. This surface lies within a lithologically homogeneous, mud-prone succession, with poor physical expression. In the study area, it was tracked on the basis of paleontological (micro- and macrofossils) depth indicators, at the turnaround from a deepening-upward to shallowing-upward trend (Amorosi et al., 2003, 2004; Geological Map of Italy at 1:50,000 scale, Sheet 187). Close to the Apenninic margin, the maximum flooding surface occurs within coastal deposits, and is dated around 6.6 kyr cal BP (Fig. 6). At seaward locations (223-S17), this surface seems to be slightly younger (4.4 cal kyr BP) because of the distinct stratigraphic condensation effect at the transition between offshore and prodelta clay deposits. The highstand systems tract (HST) has homogeneous thickness across most of the study section, and thins to the north, with decreasing distance from the Apenninic margin (Fig. 6).

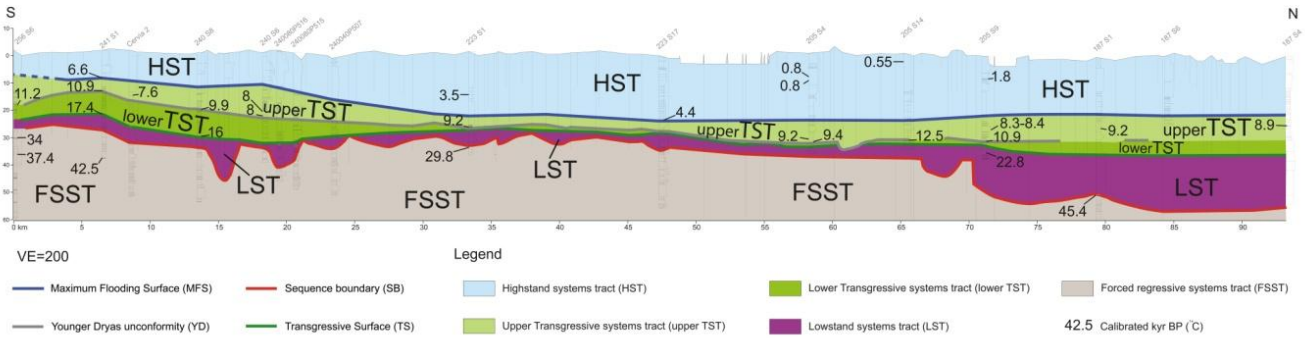

Fig. 6 - Sequence-stratigraphic interpretation of the stratigraphic panel shown in Fig. 4.

8. Conclusions

The construction of a > 90 km-long stratigraphic cross-section, transversal to the present Adriatic coastline, allowed, for the first time, to characterize the along-strike stratigraphy of the late Quaternary (last 45 kyr) coastal succession in the Po Plain.

Integrated sedimentological and micropaleontological analyses, coupled by radiocarbon dating, enabled the construction of a high-resolution stratigraphic framework. The results of this study led to refine previous stratigraphic interpretations, casting new light on the geometry of the Late Pleistocene alluvial deposits and the overlying transgressive-regressive (T-R) coastal wedge.

The Late Pleistocene sedimentary succession (ca. 45-12.5 kyr cal BP) consists almost entirely of well-drained floodplain deposits. At the southern margin of the study area, three prominent, weakly-developed paleosols were identified: (i) the lower paleosol (< 34 kyr BP), continuously tracked for more than 5 km, is genetically related to erosional-based fluvial bodies; (ii) another paleosol (18.5-16 kyr BP), which can be continuously followed for ca. 3 km, is locally traceable into the top of amalgamated fluvial sands; (iii) the upper paleosol (12.5-10 kyr BP), assigned to the Younger Dryas, is tracked discontinuously through a large part of the transect. This paleosol marks the abrupt transition from Late Pleistocene alluvial sediments to the overlying Holocene succession.

The lower part of the Holocene succession is characterized by the gradual transition from poorly-drained floodplain deposits to organic-rich, paludal clays (10.9-9.2 kyr cal BP), up to lagoonal sediments (ca. 9 kyr BP). These back-barrier deposits are replaced up-section by thin, transgressive sands (ca. 8.4 kyr BP), which in turn are overlain by a thick succession of laterally extensive offshore/prodelta muds (4.4-3.5 kyr cal BP). In the southern part of the study transect, shallow-marine deposits are in lateral transition with nearshore and lagoonal deposits, reflecting a local, along-dip component of the cross-section. The whole sedimentary succession is capped by a laterally extensive (>

90 km), 10 m-thick sand sheet, composed of beach-ridge and delta-front deposits (ca. 2 kyr BP to Present).

In terms of sequence stratigraphy, the lower paleosol is interpreted as the sequence boundary (SB). Radiocarbon ages suggest a possible link between pedogenesis and the abrupt sea-level fall/climate change (onset of LGM) that took place at the MIS 3-MIS 2 transition, and that produced river incision and soil development on the interfluves. The coeval amalgamated channel-belts (lowstand systems tract, LST) accumulated during the LGM when the shoreline was located 300 km to the south. The underlying (pre-LGM) alluvial deposits represent the forced regressive systems tract (FSST).

The transgressive surface (TS) marks a major phase of channel abandonment, and coincides with a weakly-developed paleosol dated at 18.5-16 kyr BP. Most likely this paleosol records the very last episode of subaerial exposure on the interfluves before sea-level rise induced the dramatic reorganization of the drainage system. The progressive drowning of the lowstand, north Adriatic alluvial plain is reflected by the typical deepening-upward tendency observed in the transgressive systems tract (TST), from alluvial to shallow-marine deposits. The YD paleosol allows TST subdivision into lower TST (pre-YD) and upper TST (post-YD). The early (Late Pleistocene) stages of transgression saw the onset of poorly-drained floodplain conditions along vast portions of the study area. Following deglaciation, the sea invaded the alluvial plain during the Holocene, and the upper TST consists of vertically stacked, coastal to shallow-marine deposits.

The Maximum Flooding Surface (MFS), dated at ca. 6.6 kyr cal BP at proximal locations, is placed at the turnaround from deepening-upward to shallowing-upward trends, and marks the generalized progradation of deltaic and coastal depositional systems. Based on the very high lateral continuity (> 90 km) of the late Holocene beach-ridge systems, we provide evidence for a wave-dominated (arcuate) delta morphology, with lateral transition to prograding strandplains.

Acknowledgements

We are grateful to Paolo Severi and Lorenzo Calabrese for the access to the database of the Emilia-Romagna Geological Survey. A special thanks to Luigi Bruno for his precious support during the recovery of the reference core and for providing additional radiocarbon information.

References

Allen, J.P., Posamentier, H.W., 1993. Sequence stratigraphy and facies model of an incised valley fill: the Gironde Estuary, France. Journal of Sedimentary Petrology 63, 378-392.

Amorosi, A., Marchi, N., 1999. High-resolution sequence stratigraphy from piezocone tests: an example from the Late Quaternary deposits of the southeastern Po Plain. Sedimentary Geology 128, 67-81.

Amorosi, A., Colalongo, M.L., Pasini, G., Preti, D., 1999a. Sedimentary response to Late Quaternary sea-level changes in the Romagna coastal plain (northern Italy). Sedimentology 46, 99-121.

Amorosi, A., Colalongo, M.L., Fusco, F., Pasini, G., Fiorini, F., 1999b. Glacio-eustatic control of continental-shallow marine cyclicity from Late Quaternary deposits of the south-eastern Po Plain (Northern Italy). Quaternary Research 52, 1-13.

Amorosi, A., Milli, S., 2001. Late Quaternary depositional of Po and Tevere river deltas (Italy) and worldwide comparison with coeval deltaic successions. Sedimentary Geology 128, 357-375.

Amorosi, A., Centineo, M.C., Colalongo, M.L., Pasini, G., Sarti, G., Vaiani, S.C., 2003. Facies architecture and Latest Pleistocene-Holocene depositional history of the Po Delta (Comacchio area) Italy. The Journal of Geology 111, 39-56.

Amorosi, A., Colalongo, M.L., Fiorini, F., Fusco, F., Pasini, G., Vaiani, S.C., Sarti, G., 2004. Palaeogeographic and palaeoclimatic evolution of the Po Plain from 150-ky core records. Global and Planetary Change 40, 55-78.

Amorosi, A., Colalongo, M.L., 2005. The linkage between alluvial and coeval nearshore marine succession: evidence from the Late Quaternary record of the Po River Plain, Italy. In: Blum, M.D., Marriott, S.B., Leclair S.F. (Eds.), Fluvial Sedimentology VII. Special Publication. International Association of Sedimentologists, pp. 257-275.

Amorosi, A., Centineo, M.C., Colalongo, M.L., Fiorini, F., 2005. Millennial-scale depositional cycles from the Holocene of the Po Plain, Italy. Marine Geology 222-223, 7-18.

Amorosi, A., Dinelli, E., Rossi, V., Vaiani, S.C., Sacchetto, M., 2008. Late Quaternary paleoenvironmental evolution of the Adriatic coastal plain and the onset of the Po River Delta. Paleogeography, Paleoclimatology, Paleoecology 268, 80-90.

Amorosi, A., Bruno, L., Rossi, V., Severi, P., Hajdas, I., 2014. Paleosol architecture of a late Quaternary basin-margin sequence and its implications for high-resolution, non-marine sequence stratigraphy. Global and Planetary Change 112, 12-25

Amorosi, A., Bruno, L., Campo, B., Morelli, A., 2015a. The value of pocket penetration tests for the high-resolution paleosol stratigraphy of late Quaternary deposits. Geological Journal 50, 670-682.

Amorosi, A., Maselli, V., Trincardi, F., 2015b. Onshore to offshore anatomy of a late Quaternary source-to-sink system (Po Plain-Adriatic Sea, Italy). Earth-Science Reviews, DOI:10.1016/j.earscirev.2015.10.010

Amorosi, A., Bracone, V., Campo, B., D'Amico, C., Rossi, V., Rosskopf, M., 2016. A late Quaternary multiple paleovalley system from the Adriatic coastal plain (Biferno River, Southern Italy). Geomorphology 254, 146-159.

Asioli, A., Trincardi, F., Lowe, J.J., Oldfield, F., 1999. Short-term climate changes during the Last Glacial-Holocene transition: comparison between Mediterranean records and the GRIP event stratigraphy. Journal of Quaternary Science 14, 373-381.

Athersuch, J., Horne, D.J., Whittaker, J.E., 1989. Marine and brackish water ostracods. In: Kermack, D.M., Barnes, R.S.K. (Eds.), Synopses of the British Fauna (New Series), Brill E.J., Leiden, pp. 1-345.

Bard, E., Hamelin, B., Fairbanks, R.G., Zindler, A., 1990. Calibration of the ^{14}C timescale over the past 30,000 years using mass spectrometric U-Th ages from Barbados corals. Nature 345, 405-410.

Blum, M.D., Törnqvist, T.E., 2000. Fluvial responses to climate and sea-level change: a review and look forward. Sedimentology 47, 2-48.

Blum, M.D., Martin, J., Milliken, K., Garvin, M., 2013. Paleovalley systems: Insights from Quaternary analogs and experiments. Earth-Science Reviews 116, 128-169.

Bondesan, M., Favero, V., Vinals, M.J., 1995. New evidence on the evolution of the Po-delta coastal plain during the Holocene. Quaternary International 29/30, 105-110.

Bruno, L., Amorosi, A., Severi, P., Costagli, B., 2016. Late Quaternary aggradation rates and stratigraphic architecture of the southern Po Plain, Italy. Basin Research, DOI: 10.1111/bre.12174

Castellarin, A., Vai, G.B., 1986. South alpine versus Po Plain apenninic arcs. In: Wezel, F.C. (Ed.), The Origin of the Arcs, Development in Geotectonics, Elsevier, Amsterdam, pp. 253-280.

Cattaneo, A., Trincardi, F., 1999. The late-Quaternary transgressive record in the Adriatic epicontinental sea: basin widening and facies partitioning. Society for Sedimentary Geology Special Publication 64, 127-146.

Cattaneo, A., Steel, R.J., 2003. Transgressive deposits: a review of their variability. Earth-Science Reviews 62, 187-228.

Catuneanu, O., 2006. Principles of Sequence Stratigraphy. Elsevier, New York.

Catuneanu, O., Abreu, V., Bhattacharya, J.P., Blum, M.D., Dalrymple, R.W., Eriksson, P.G., Fielding, C.R., Fisher, W.L., Galloway, W.E., Gibling, M.R., Giles, K.A., Holbrook, J.M., Jordan, R., Kendall, C.G.St.C., Macurda, B., Martinsen, O.J., Miall, A.D., Neal, J.E., Nummedal, D., Pomar, L., Posamentier, H.W., Pratt, B.R., Sarg, J.F., Shanley, K.W., Steel, R.J., Strasser, A., Tucker, M.E., Winker, C., 2009. Towards the standardization of sequence stratigraphy. Earth-Science Reviews 92, 1-33.

Catuneanu, O., Galloway, W.E., Kendal, C.G.St.C., Miall, A.D., Posamantier, H.W., Strasser, A., Tucker, M.E., 2011. Sequence stratigraphy: Methodology and Nomenclature. Newsletters on Stratigraphy, Stuttgart, pp. 173-245.

Ciabatti, M., 1967. Ricerche sull'evoluzione del delta padano. Giornale di Geologia 34, 381-410.

Clark, P.U., Marshall, A., McCabe, A.M., Mix, A.C., Weaver, A.J., 2004. Rapid rise of sea level 19,000 years ago and its global implication. Science 304, 1141-1144.

Coccioni, R., 2000. Benthic Foraminifera as Bioindicators of Heavy Metal Pollution - A Case Study from the Goro Lagoon (Italy). In: Martin, R.E. (Ed.), Environmental Micropaleontology - The Application of Microfossils to Environmental Geology. Kluwer Academic/Plenum Press Publishers, New York. Topics in Geobiology, pp. 71-103.

Collinson, J.D., 1996. Alluvial sediments. In: Reading, H.G. (Ed.), Sedimentary Environments: Processes, Facies and Stratigraphy. Blackwell Scientific Publications, Oxford, pp. 37-82.

Correggiari, A., Cattaneo, A., Trincardi, F., 2005a. The modern Po delta system: lobe switching and asymmetric prodelta growth. Marine Geology 222-223, 49-74.

Correggiari, A., Cattaneo, A., Trincardi, F., 2005b. Depositional patterns in the Holocene Po Delta system. In: Bhattacharya, J.P., Giosan, L. (Eds.), River Deltas: Concepts, Models and Examples. Society of Economic Paleontologists and Mineralogists Special Publication, pp. 365-392.

Dalrymple, R.W., Zaitlin, B.A., Boyd, R., 1992. Estuarine facies models: conceptual basis and stratigraphic implications. Journal of Sedimentary Petrology 62, 1130-1146.

Debenay, J.P., Guillou, J.J., Redois, F., Geslin, E., 2000. Distribution trends of foraminiferal assemblages in paralic environments. A base for using foraminifera as bioindicators. In: Martin, R.E. (Ed.), Environmental Micropaleontology: The Application of Microfossils to Environmental Geology. Kluwer Academic/Plenum Publishers, New York, pp. 39-67.

Demko, T.M., Currieb, B.S., Nicoll, K.A., 2004. Regional paleoclimatic and stratigraphic implications of paleosols and fluvial/overbank architecture in the Morrison Formation (Upper Jurassic), Western Interior, USA. Sedimentary Geology 167, 115-135.

Di Bella, L., Bellotti, P., Frezza, V., Bergamin, L., Carboni, M.G., 2011. Benthic foraminiferal assemblages of the imperial harbour of Claudius (Rome): further paleoenvironmental and geoarcheological evidences. The Holocene 21, 1243-1257.

Di Bella, L., Bellotti, P., Milli, S., 2013. The role of foraminifera as indicators of the Late PleistoceneeHolocene palaeoclimatic fluctuations on the deltaic environment: the example of Tiber delta succession (Tyrrhenian margin, Italy). Quaternary International 303, 191-209.

Dinelli, E., Ghosh, A., Rossi, V., Vaiani, S.C., 2012. Multiproxy reconstruction of Late Pleistocene-Holocene environmental changes in coastal successions: microfossil and geochemical evidences from the Po Plain (Northern Italy). Stratigraphy 9, 153-167.

Donnici, S., Serandrei Barbero, R., 2002. The benthic foraminiferal communities of the northern Adriatic continental shelf. Marine Micropaleontology 44, 93-123.

D'Onofrio, S., 1969. Ricerche sui Foraminiferi nei fondali antistanti il Delta del Po. Giornale di Geologia 36, 283-334.

D'Onofrio, S., Marabini, F., Vivalda, P., 1976. Foraminiferi di alcune lagune del delta del Po. Giornale di Geologia 40, 267-276.

Embry, A.F., 1993. Transgressive-regressive (T-R) sequence analysis of the Jurassic succession of the Sverdrup Basin, Canadian Arctic Archipelago. Canadian Journal of Earth Sciences 30, 301-320.

Embry, A.F., 1995. Sequence boundary and sequence hierarchies: problems and proposals. In: Steel, R.J., Felt, V.L., Johannessen E.P., Mathieu C. (Eds.), Sequence Stratigraphy on the Northwest European Margin. Norwegian Petroleum Society Special Publication, pp. 1-11.

Embry, A.F., 2002. Transgressive-Regressive (T-R) Sequence Stratigraphy, In: Armentrout, J., Rosen, N. (Eds.), Sequence stratigraphic models for exploration and production: Gulf Coast. Society for Sedimentary Geology Conference Proceedings, Houston, pp.151-172.

Embry, A.F., Johannessen, A., Owen, D., Beauchamp, B., Gianolla, P., 2007. Sequence stratigraphy as a "Concrete" Stratigraphic Discipline. Report of the International Stratigraphic Guide Task Group on Sequence Stratigraphy.

Emery, D., Myers, K.J., 1996. Sequence Stratigraphy. Oxford, U.K., Blackwell.

Fairbanks, R.G., 1989. A 17000-year glacio-eustatic sea-level record: influence of glacial melting rates on the Younger Dryas event and deep-ocean circulation. Nature 342, 637-642.

Fiorini, F., 2004. Benthic foraminiferal associations from Upper Quaternary deposits of southeastern Po Plain, Italy. Micropaleontology 50, 45-58.

Fontana, A., Mozzi, P., Marchetti, M., 2014. Alluvial fans and megafans along the southern side of the Alps. Sedimentary Geology 301, 150-171.

Forzoni, A., Hampson, G., Storms, J., 2015. Along-Strike Variations In Stratigraphic Architecture of Shallow-Marine Reservoir Analogues: Upper Cretaceous Panther Tongue Delta and Coeval Shoreface, Star Point Sandstone, Wasatch Plateau, Central Utah, U.S.A. Journal of Sedimentary Research 85, 968-989.

Galloway, W.E., 1989. Genetic stratigraphic sequences in basin analysis I: architecture and genesis of flooding-surface bounded depositional units. American Association of Petroleum Geologist Bulletin 73, 125-142.

Geological Map of Italy at 1:50,000 scale. Sheet 223 – Ravenna (2002) - Regione Emilia-Romagna Geological Survey.

Geological Map of Italy at 1:50,000 scale. Sheet 256 – Rimini (2005) - Regione Emilia-Romagna Geological Survey.

Geological Map of Italy at 1:50,000 scale. Sheet 240/241 – Forlì/Cervia (2005) - Regione Emilia-Romagna Geological Survey.

Geological Map of Italy at 1:50,000 scale. Sheet 187 – Codigoro (2009) - Regione Emilia-Romagna Geological Survey.

Geological Map of Italy at 1:50,000 scale. Sheet 205 – Comacchio (2009) - Regione Emilia-Romagna Geological Survey.

Goodbred Jr., S.L., Kuehl, S.A., 2000. The significance of large sediment supply, active tectonism, and eustacy on margin sequence development: Late Quaternary stratigraphy and evolution of the Ganges-Brahmaputra delta. Sedimentary Geology 133, 227-248.

Goodbred Jr., S.L., 2003. Response of Ganges dispersal system to climate change: a source to sink view since the last interstade. Sedimentary Geology 162, 83-104.

Hampson, G.J., Gani, M.R., Sharman, K.E., Irfan, N., Bracken, B., 2011. Along-strike and Down-Dip Variations in Shallow-Marine Sequence Stratigraphic Architecture: Upper Cretaceous Star Point Sandstone, Wasatch Plateau, Central Utah, U.S.A. Journal of Sedimentary Research 81, 159-184.

Helland-Hansen, W., Gjelberg, J., 1994. Conceptual basis and variability in sequence stratigraphy: a different perspective. Sedimentary Geology 92, 1-52.

Helland-Hansen, W., Martinsen, O.J., 1996. Shoreline trajectories and sequences; description of variable depositional-dip scenarios. Journal of Sedimentary Research 66, 670-688.

Hijma, M.P., Cohen, K.M., Hoffmann, G., Van der Spek, A.J.F., Stoutthamer, E., 2009. From river valley to estuary: the evolution of the Rhine mouth in the early to

middle Holocene (western Netherlands, Rhine-Meuse delta). Netherlands Journal of Geosciences 88, 13-53.

Hori, K., Saito, Y., Zhao, Q., Wang, P., 2002. Evolution of the coastal depositional systems of the Changjiang (Yangtze) River in response to late Pleistocene-Holocene sea-level changes. Journal of Sedimentary Research 72, 884-897.

Jorissen, F.J., 1988. Benthic Foraminifera from the Adriatic Sea; principles of phenotypic variation. Utrecht Micropaleontological Bulletin 37, 1-176.

Langone, L., Asioli, A., Correggiari, A., Trincardi, F., 1996. Age-depth modelling through the late Quaternary deposits of the central Adriatic basin. Memorie dell'Istituto Italiano di Idrobiologia 55, 177-196.

Lehman, S.J., Keigwin, L.D., 1992. Sudden changes in North Atlantic circulation during the last deglaciation. Nature 356, 757-762.

Li, C., Wang, P., Sun, H., Zhang, J., Fan, D., Deng, B., 2002. Late Quaternary incised-valley fill of the Yangtze delta (China): its stratigraphic framework and evolution. Sedimentary Geology 152, 133-158.

Maselli, V., Hutton, E.W., Kettner, A.J., Syvitski, P.M, Trincardi, F., 2011. High-frequency seal level and sediment supply fluctuations during Termination I: An intergrated sequence-stratigraphy and modeling approach from the Adriatic Sea (Central Mediterranean). Marine Geology 287, 54-70.

Maselli, V., Trincardi, F., Asioli, A., Rizzetto, F., Taviani, M., 2014. Delta growth and river valleys: the influence of climate and sea level changes on the South Adriatic shelf (Mediterranean Sea). Quaternary Science Reviews 99, 146-163.

McFarlan, Jr. E., 1961. Radiocarbon dating of Late Quaternary deposits, South Lousiana. Geological Society of American Bulletin 72, 129-158.

Miall, A.D., 1992. Alluvial deposits: In: Walker, R.G., James, N.P. (Eds.), Facies Models: Response to Sea Level Change. Geological Association of Canada, Waterloo, Ontario, pp. 119-139.

Montenegro, M.E., Pugliese, N. 1996. Autecological remarks on the ostracod distribution in the Marano and Grado Lagoons (Northern Adriatic Sea, Italy). In: Cherchi, A. (Ed.), Autecology of selected fossil organisms: Achievements and problems. Bollettino della Società Paleontologica Italiana, Special, pp. 123-132.

Muttoni, G., Carcano, C., Garzanti, E., Ghielmi, M., Piccin, A., Pini, R., Rogledi, S., Sciunnach, D., 2003. Onset of major Pleistocene glaciations in the Alps. Geology 31, 989-992.

Neal, J., Abreu, V., 2009. Sequence stratigraphy hierarchy and the accommodation succession method. Geology 37, 779-782.

Nummedal, D., Swift, D.J.P., 1987. Transgressive stratigraphy at sequence-bounding unconformities: some principles derived from Holocene and Cretaceous examples. In: Nummedal, D., Pilkey, O.H., Howard, J.D. (Eds.), Sea-Level Fluctuation and Coastal Evolution. Society of Economic Paleontologists and Mineralogists Special Publication 41, pp. 241-260.

Nummedal, D., Riley, G.W., Templet, P.L., 1993. High resolution sequence architecture: a chronostratigraphic model based on equilibrium profile studies. In: Posamentier, H.W., Summerhayes, C.P., Haq, B.U., Allen, G.P. (Eds.), Sequence Stratigraphy and Facies Associations. International Association of Sedimentologists Special Publication, pp. 55-68.

Paltier, W.L., Fairbanks, R.G., 2006. Global glacial ice volume and last glacial maximum duration from an extended Barbados sea level record. Quaternary Science Review 25, 3322-3337.

Pellegrini, C., Maselli, V., Cattaneo, A., Piva, A., Ceregato, A., Trincardi, F., 2015. Anatomy of a compound delta from the post-glacial transgressive record in the Adriatic Sea. Marine Geology 362, 43-59.

Pieri, M., Groppi, G., 1981. Subsurface geological structure of the Po Plain, Italy. Pubblicazione del Progetto Finalizzato alla Geodinamica, CNR 414, pp. 1-23.

Plint, A.G., Nummendal, D., 2000. The falling stage systems tract: recognition and importance in sequence stratigraphic analysis. In: Gawthorpe, R.L., Hunt, D. (Eds.), Sedimentary Responses to Forced Regression. Geological Society of London Special Publication, pp. 1-17.

Plint, A.G., McCarthy, P.J., Faccini, U.F., 2001. Nonmarine sequence stratigraphy: Updip expression of sequence boundaries and systems tracts in a high-resolution framework, Cenomanian Dunvegan Formation, Alberta foreland basin, Canada. American Association of Petroleum Geologists Bulletin 85, 1967-2001.

Posamentier, H.W., Vail, P.R., 1988. Eustatic controls on clastic deposition II - Sequence and systems tract models. In: Wilgus, C.K., Hastings, B.S., Kendall, C.G.C., Posamentier, H.W., Ross, C.A., Van Wagoner, J.C. (Eds.), Sea-Level Changes: An Integrated Approach. Society for Sedimentary Geology Special Publication, pp. 125-154.

Posamentier, H.W., Jervey, M.T., Vail, P.R., 1988. Eustatic controls on clastic deposition I - conceptual framework. In: Wilgus, C.K., Hastings, B.S., Kendall, C.G.C., Posamentier, H.W., Ross, C.A., Van Wagoner, J.C. (Eds.), Sea-Level Changes: An Integrated Approach. Society for Sedimentary Geology Special Publication, pp. 109-124.

Posamentier, H.W., Allen, G.P., James, D.P., Tesson, M., 1992. Forced regressions in a sequence stratigraphic framework: concepts, examples and sequence stratigraphic significance. American Association of Petroleum Geologists Bulletin 76, 1687-1709.

Ramsey, B., 2009. Bayesian analysis of radiocarbon dates. Radiocarbon, 51, 337-360.

Regione Emilia-Romagna, ENI-AGIP, 1998. Riserve idriche sotterranee della Regione Emilia-Romagna. S.EL.CA., Firenze.

Reinson, G.E., 1992. Transgressive barrier island and estuarine systems. In: Walker, R.G., James, N.P. (Eds.), Facies Models: Response to Sea Level Change. Geological Association of Canada, Waterloo, Ontario, pp. 179-194.

Reimer, P.J., Bard, E., Bayliss, A., Beck, J.W., Blackwell, P.G., Bronk Ramsey, C., Grootes, P. M., Guilderson, T.P., Haflidason, H., Hajdas, I., Hatt, C., Heaton, T.J., Hoffmann, D.L., Hogg, A.G., Hughen, K.A., Kaiser, K.F., Kromer, B., Manning, S.W., Niu, M., Reimer, R.W., Richards, D.A., Scott, E.M., Southon, J.R., Staff, R.A., Turney, C.S.M., Van der Plicht, J., 2013. IntCal13 and Marine13 Radiocarbon Age Calibration Curves 0-50,000 Years cal BP. Radiocarbon 55.

Rizzini, A., 1974. Holocene sedimentary cycle and heavy mineral distribution, Romagna-Marche coastal plain, Italy. Sedimentary Geology 11, 17-37.

Rossi, V., Horton, B.P., 2009. The application of subtidal foraminifera-based transfer function to reconstruct Holocene paleobathymetry of the Po Delta, northern Adriatic Sea. Journal of Foraminiferal Research 39, 180-190.

Sarti, G., Rossi, V., Amorosi, A., 2012. Influence of Holocene stratigraphic architecture on ground surface settlements: A case study from the City of Pisa (Tuscany, Italy). Sedimentary Geology 281, 75-87

Scarponi, D., Kowalewski, M., 2004. Stratigraphic paleoecology: Bathymetric signatures and sequence overprint of mollusk associations from upper Quaternary sequences of the Po Plain, Italy. Geology 32, 989-992.

Scarponi, D., Angeletti, L., 2008. Integration of paleontological patterns in the sequence stratigraphy paradigm: a case study from Holocene deposits of the Po Plain (Italy). GeoActa 7, 1-13.

Scarponi, D., Kaufman, D., Amorosi, A., Kowalewski, M., 2013. Sequence stratigraphy and the resolution of the fossil record. Geology 41, 239-242.

Sgarrella, F., Moncharmont Zei, M., 1993. Benthic Foraminifera of the Gulf of Naples (Italy): systematics and autoecology. Bollettino della Società Paleontologica Italiana 32, 145-264.

Soil Survey Staff, 2014. Keys to Soil Taxonomy. 12th edition. Natural Resources Conservation Service. U.S. Department of Agriculture Handbook.

Stefani, M., Vincenzi, S., 2005. The interplay of eustasy, climate and human activity in the late Quaternary depositional evolution and sedimentary architecture of the Po Delta system. Marine Geology 222-223, 19-48.

Storms, J.E.A., Weltje, G.J., Terra, G.J., Cattaneo, A., Trincardi, F., 2008. Coastal dynamics under conditions of rapid sea-level rise: Late Pleistocene to Early Holocene evolution of barrier-lagoon systems on the northern Adriatic shelf (Italy). Quaternary Science Review 27, 1107-1123.

Ta, T.K.O., Nguyen, V.L., Tateishi, M., Kobayashi, I., Saito, Y., 2005. Holocene delta evolution and depositional models of the Mekong delta, southern Vietnam. Society for Sedimentary Geology Special Publication 83, 453-466.

Tanabe, S., Saito, Y., Vu, Q.L., Hanebuth, T.J.J., Ngo, Q.L., Kitamura A., 2006. Holocene evolution of the Song Hong (Red River) delta system, northern Vietnam. Sedimentary Geology 187, 29-61.

Tanabe, S., Nakanishi, T., Ishihara, Y., Nakashima, R., 2015. Millennial-scale stratigraphy of tide-dominated incised valley during the last 14 kyr: Spatial and quantitative reconstruction in the Tokyo Lowland, central Japan. Sedimentology 62, 1837-1872.

Taylor, K.C., Mayewski, P.A., Alley, R.B., Brook, E.J., Gow, A.J., Grootes, P.M., Meese, D.A., Saltzman, E.S., Severinghaus, J.P., Twickler, M.S., White, J.W.C., Whitlow, S. Zielinski, G.A., 1997. The Holocene/Younger Dryas transition recorded at Summit, Greenland. Science 278, 825-827.

Trincardi, F., Correggiari, A., Roveri, M., 1994. Late Quaternary transgressive erosion and deposition in a modern epicontinental shelf: the Adriatic Semienclosed Basin. Geo-Marine Letters 14, 41-51.

Trincardi, F., Asioli, A., Cattaneo, A., Correggiari, A., Vigliotti, L., Accorsi, C.A., 1996. Transgressive offshore deposits on the central adriatic shelf: architecture complexity and the record of the Younger Dryas short-term event. Il Quaternario, Italian Journal of Quaternary Sciences 9, 753-762.

Vaiani, S.C., 2010. Miliolidae (benthic foraminifera) distribution and relative sea-level variation during the Holocene transgression from subsurface deposits of the Po River delta (Italy). GeoActa 9, 57-66.

Vail, P.R., 1987. Seismic stratigraphy interpretation procedure. In: Bally, A. W. (Ed.), Atlas of Seismic Stratigraphy. Tulsa, OK. American Association of Petroleum Geologists Studies in Geology 27, pp. 1-10.

Vail, P.R., Audemard, F., Bowman, S.A., Eisner, P.N., Perez-Cruz, C., 1991. The stratigraphic signatures of tectonics, eustasy and sedimentology - an overview. In:

Einsele, G., Ricken, W., Seilacher, A. (Eds.), Cycles and Events in Stratigraphy, Springer-Verlag, Berlin, pp. 617-659.

Van Wagoner, J.C., Posamantier, H.W., Mitchum, R.M., Vail, P.R., Sarg, J.F., Loutit, T.S., Hardenbol, J., 1988. An overview of the fundamentals of sequence stratigraphy and key definitions. In: Wilgus, C.K., Hastings, B.S., Kendall, C.G., Posamentier, H.W., Ross, C.A., Van Wagoner, J.C. (Eds.), Sea-level changes: an integrated approach. Society for Sedimentary Geology Special Publication, pp. 39-45.

Van Wagoner, J.C., Mitchum, R.M., Campion, K.M., Rahmanian, V.D., 1990. Siliciclastic sequence stratigraphy in well logs, cores, and outcrops: concepts for high-resolution correlation of time and facies. American Association of Petroleum Geologists Methods in Exploration, Series 7, pp. 55.

Van der Zwaan, G.J., Jorissen, F.J., 1991. Biofacial patterns in river-induced shelf anoxia. In: Tyson, R.V., Pearson, T.H. (Eds.), Modern and Ancient Continental Shelf Anoxia, Geological Society Special Publication, London, pp. 65-82.

Veggiani, A., 1974. Le variazioni idrografiche del basso corso del Fiume Po negli ultimi 3000 anni. Padusa 1-2, 30-60.

5.2. Paper 2 (Study area 2)

Contrasting alluvial architecture of Late Pleistocene and Holocene deposits along a 120-km transect from the central Po Plain (northern Italy)*

Bruno Campo, Alessandro Amorosi, Luigi Bruno

*Submitted to ***Sedimentary Geology***

Contrasting alluvial architecture of Late Pleistocene and Holocene deposits along a 120-km transect from the central Po Plain (northern Italy)

Bruno Campo[a2], Alessandro Amorosi[a], Luigi Bruno[a]

[a] *Dipartimento di Scienze Biologiche, Geologiche e Ambientali, University of Bologna, Via Zamboni 67, 40127 Bologna, Italy*

Abstract

High-resolution investigation of a ~120 km-long transect along the course of the modern Po River revealed marked changes in alluvial architecture across the Pleistocene-Holocene boundary. Along the whole transect, a 20-30 m thick, sheet-like succession of Late Pleistocene fluvial sands is invariably overlain by silt and clay deposits, with isolated fluvial bodies of Holocene age (< 9.4 cal ka BP). The Holocene succession displays consistent downstream changes in facies architecture: well-drained floodplain deposits are replaced at distal locations by increasingly organic, poorly-drained floodplain to swamp facies associations. Thick paludal facies extend continuously up to 60 km landward of the Holocene maximum marine ingression, about 90 km from the modern shoreline. Based on 28 radiocarbon dates, the abrupt change in lithofacies and channel stacking pattern occurred at the transition from the last glacial period to the present interglacial, under conditions of rapid sea-level rise. The architectural change from amalgamated, Late Pleistocene sand bodies to overlying, mud-dominated Holocene units represent an example of chronologically well-constrained fluvial response to combined climate and relative sea-level change. The overall aggradational stacking pattern of individual channel-belt sand bodies indicates that high subsidence rates continuously created accommodation in the Po Basin, even during phases of falling sea level and lowstand.

Keywords: alluvial architecture, climate change, sea-level variations, accommodation, Po Plain, Quaternary

[2] Corresponding author. Fax +39 051 2094522. Phone +39 051 2094564.
E-mail addresses: bruno.campo2@unibo.it (B. Campo), alessandro.amorosi@unibo.it (A. Amorosi), luigi.bruno4@unibo.it (L. Bruno).

1. Introduction

Subsurface investigation of alluvial and coastal plains is critical to a number of applications, including exploitation of natural resources, planning of new infrastructures and overall land-use management. In the past decades, alluvial deposits have been extensively studied to highlight the response of fluvial systems to base-level variations (Shanley and McCabe 1991, 1993; Schumm, 1993; Holbrook et al., 2006), and more specifically to climate and sea-level changes (Shanley and McCabe, 1994; Smith, 1994; Legarreta and Uliana, 1998; Blum and Price, 1998; Amorosi et al., 1999a, 2003; Blum and Törnqvist, 2000; Törnqvist et al., 2000, 2003; Goodbred, 2003; Busschers et al., 2007; Rittenour et al., 2007; Macklin et al., 2012; Shen et. al, 2012; Blum et al., 2013; Starkel et al., 2015).

Strict relationships between climate change, sea-level fluctuations and alluvial stratigraphic architecture have been assessed for several late Quaternary successions, for which well-constrained chronological framework is available. Many of these studies have documented that dramatic changes in depositional style, fluvial channel geometries and stacking patterns commonly occur at the transition from glacial to interglacial periods (Aslan and Blum, 1999; Amorosi and Milli, 2001; Amorosi et al., 2008; Ishihara et al., 2012; Blum at al., 2013; Tanabe et al., 2015). Late Pleistocene strata from the Colorado River area have revealed that glacial-related units consist of amalgamated channel-belt sands with subordinate overbank deposits, whereas the overlying Holocene interglacial succession is made up mostly of silts and clays, with isolated sand bodies (Blum, 1993; Blum and Valastro, 1994; Blum et al., 1994; Blum and Törnqvist, 2000). A similar stratigraphic motif was reported from the Lower Mississippi Valley (Autin et al., 1991; Aslan and Autin, 1999; Rittenour et al., 2007), and beneath the Trinity and Brazos coastal plains (Blum and Aslan, 2006; Blum and Womack, 2009). In South America, a comparable stratigraphic framework was illustrated for the Rio de la Plata, Parana and Uruguay rivers (Violante and Parker, 2004), while it was documented in Asia for the Yangtze River (Hori et al., 2002; Wellner and Bartek, 2003), the Qiantangjang River (Zhang and Li, 1996; Li et al., 2012), the Gulf of Thailand (Reijestein et al., 2011), the Mekong River (Ta et al., 2005), the Red River (Tanabe et al., 2006), Tonegawa and Arakawa rivers (Ishihara et al., 2012), and the Tokyo Lowland (Tanabe et al., 2008, 2015). In Europe, amalgamated coarse-grained sand bodies overlain by fine-grained estuarine-alluvial deposits have been reported from the Loire River (Blum and Törnqvist, 2000; Straffin et al, 2000), the Gironde estuary (Allen and Posamentier, 1992), the Rhine-Meuse system (Törnqvist et al., 2003; Busschers et al., 2005), the Tagus River (Vis et al., 2008), the Ebro River

(Somoza et al., 1998) the Po River (Amorosi and Colalongo 2005; Stefani and Vincenzi, 2005; Amorosi et al., 2008; Bruno et al., 2016) the Tiber River Delta (Milli et al., 2013) and the Roma Basin (Milli, 1997; Milli et al., 2008; Mancini et al., 2013).

In general, few studies have focused on the role of allogenic forcing factors (i.e. climate, sea-level changes) in shaping stratigraphy in the “purely alluvial realm” (the upstream alluvial valleys *sensu* Gibling et al., 2011). At this location, where marine influence is poor due to the distance from the shoreline (backwater length effect), the role played by sea-level oscillations is debated (Paola and Mohrig, 1996; Blum and Törnqvist, 2000). On the other hand, as pointed out by Li et al. (2006) and Blum et al. (2013), backwater conditions can significantly extend upstream from any other indicator of contemporaneous marine conditions, and the effects of sea-level change may propagate inland for hundreds of kilometers from the present shoreline (ca. 600 km for the Lower Mississippi Valley - Shen et al., 2012).

In the Po Plain (northern Italy), numerous studies focused on the late Quaternary stratigraphic architecture of the coastal area showed the vertical stacking of transgressive-regressive (T-R) cycles (Amorosi et al., 2004). Based on pollen data, these T-R cycles were traced landwards, into the alluvial system, as distinct cyclic changes in lithofacies and channel stacking patterns (Amorosi et al., 2004, 2008). However, high-resolution stratigraphy and detailed facies analysis of fluvial deposits have never been performed. Through a ca. 120 km-long transect, transversal to the coastline and coincident with the middle reaches of the modern Po River (Fig. 1), this study aims at depicting for the first time the late Quaternary stratigraphy of a fluvial-dominated section, from the Last Glacial Maximum to the Present. Based on 28 radiocarbon dates, we focus on the contrasting stratigraphic architecture of Late Pleistocene and Holocene deposits, and try to establish the link between facies architecture, changing sea-level (lowstand vs highstand), climate (glacial vs interglacial conditions) and sedimentation rates.

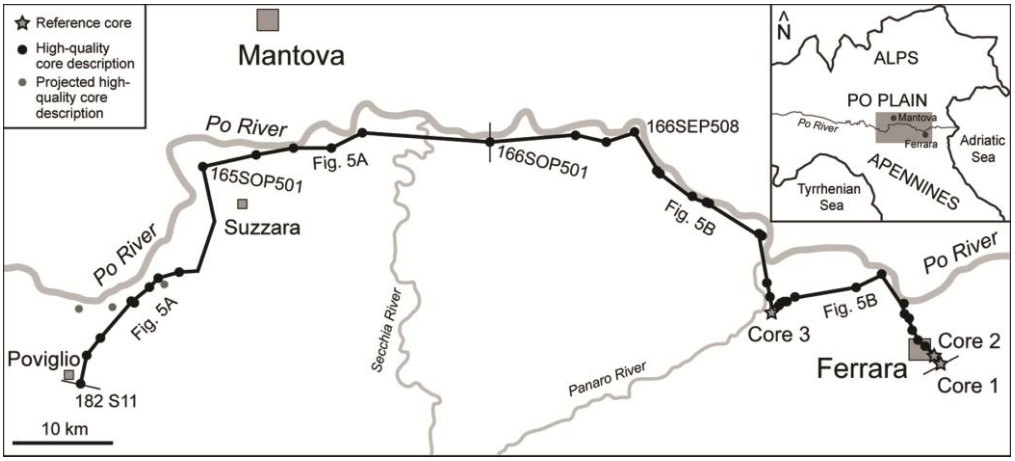

Fig. 1 - Study area, with location of Cores 1, 2 and 3 (Fig. 3) and of the two transects in Fig. 5.

2. Geological setting

The Po Plain, one of the largest alluvial plains in Europe, represents the morphologic expression of the Po River basin. This rapidly subsiding foreland basin, delimited to the north by the Alpine chain and to the south by the Apennines, originated in response to the collision between the Adria microplate and the European Plate (Ghielmi et al., 2013). Since the early formation of the Apenninic fold-and-thrust belt, in the Late Oligocene, the evolution of the Po Basin was strongly driven by tectonics (Pieri and Groppi, 1981; Dondi and D'Andrea, 1986; Muttoni et al., 2003; Carminati and Doglioni 2012). Tectonic subsidence in the Po Plain is on the order of ca. 1 mm/a (Carminati et al., 2005), and the thickness of the Pliocene-Quaternary succession attains 8 km in the depocenters (Ori et al., 1986; Doglioni, 1993; Mazzoli et al., 2006).

The large-scale stratigraphic architecture of the Po Basin has been reconstructed on the basis of integrated seismic and well log data, which led to the identification of six unconformity-bounded stratigraphic units or UBSU (Regione Emilia-Romagna and Eni-Agip, 1998; Regione Lombardia and Eni-Divisione Agip, 2002). Each unconformity marks a phase of dramatic basin reorganization due to intense tectonic activity. The uppermost UBSU (Emilia-Romagna Supersynthem of Regione Emilia-Romagna and Eni-Agip, 1998), consists of Middle-Late Pleistocene and Holocene deposits, and exhibits maximum thickness of 800 m. The lower boundary of this unit is a major unconformity dated at 870 ka on the basis of magnetostratigraphic data (Muttoni et al., 2003). The Emilia-Romagna Supersynthem is subdivided into a series of transgressive regressive (T-R) sequences (Fig. 2) showing evidence of Milankovitch-scale (~100 ka) ciclicity. In the coastal sector, littoral and shallow-marine deposits have been linked genetically to interglacial periods on the basis of long-core pollen profiles (Amorosi et al., 1999b; 2004). On the other hand, widespread development of alluvial environments was associated with return to glacial condition. Landward of the maximum marine ingression, in the central Po Plain (Po channel belt area in Fig. 2) each T-R sequence consists of basal overbank muds, with lenticular fluvial-channel sand bodies, overlain by high net-to-gross, amalgamated fluvial-channel deposits (Amorosi et al., 2008). These latter cover hundreds of square kilometers and show high degree of channel clustering. Pollen characterization, and more specifically the imprint of *thermophilous* forest expansion within the basal overbank fines, has suggested that the major phases of channel abandonment and floodplain aggradation in the Central Po Plain took place under rapid sea-level rise (Amorosi et al., 2008). The laterally extensive channel belt sand bodies have been interpreted as braided river deposits testifying periods of high sediment supply (and relatively low accommodation) during lowstand and possibly

early-transgressive phases. Other studies correlating grain size distribution to the $\delta^{18}O$ curve support this interpretation (Vittori and Ventura, 1995).

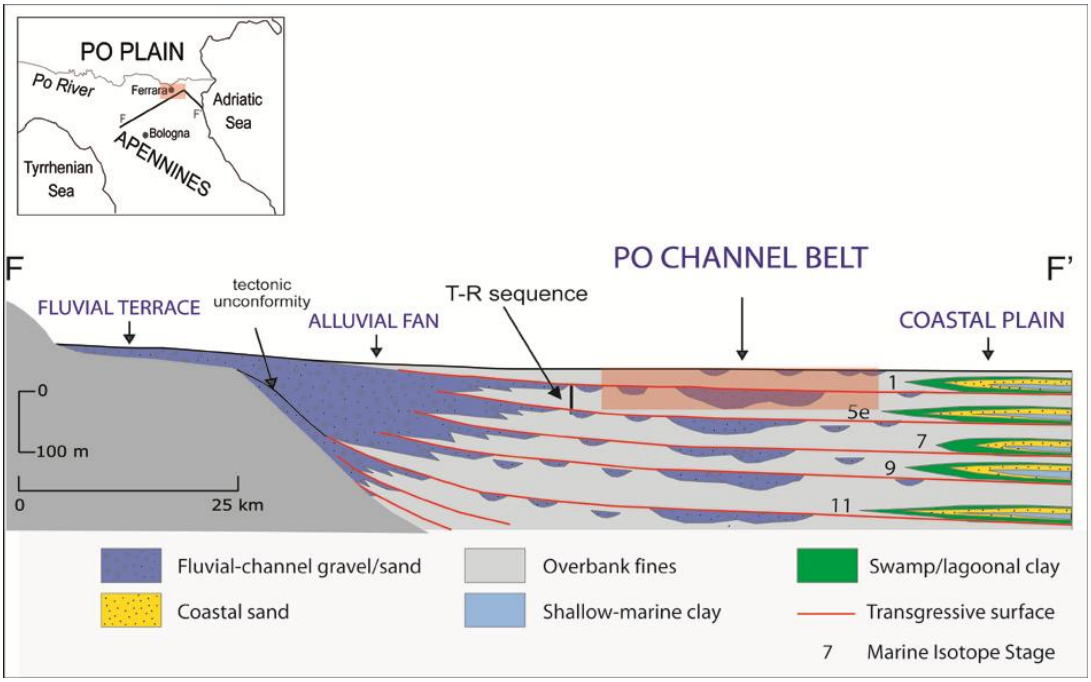

Fig. 2 – Schematic cross section through the Po Basin, showing the linkage between coastal and alluvial deposits. The red lines are transgressive surfaces dividing the Upper Po Supersynthem into T-R cycles. The red rectangle approximately highlights the study area. Modified from Amorosi et al., 2014.

3. Methods

In this work, we used the stratigraphic datasets of Emilia-Romagna and Lombardy Geological Surveys. Both datasets include sedimentological, geophysical, hydrogeological and geotechnical data, acquired over time in disparate formats. More specifically, we used stratigraphic information from:

high-quality sedimentological descriptions of continuously-cored boreholes (30-50 m deep). These data offer detailed lithologic information, including color, accessory materials (roots, wood and plant fragments, carbonate nodules, fossils), pedogenic features, pocket penetrometer and torvane test values, radiocarbon dates. We used these data as supporting tools for facies interpretation.

Water wells (30-150 m deep), which provide poor-quality stratigraphic descriptions, mostly restricted to basic grain-size (clay/sand) information. These data were utilized to identify the upper and lower boundaries of thick fluvial-channel sand bodies.

Cone penetration tests (CPT, < 15 m deep) and piezocone tests (CPTU, < 35 m deep). These data are commonly utilized for geotechnical investigations, but recent studies on late Quaternary deposits have proved that cone penetration tests can also

be efficiently employed for facies characterization and subsurface stratigraphic correlations (Amorosi and Marchi, 1999; Styllas, 2014; Amorosi et al., 2015).

The above data were calibrated using three freshly drilled continuous cores along the transect (Figs. 1 and 3), namely “Core 1” (55 m deep), “Core 2” (26.6 m) and “Core 3” (50 m).

A total of 56 continuous cores, 44 CPTU-CPT tests and 101 water wells were selected along a 123-km long and 50-m thick cross-section roughly parallel to the Po River, between Poviglio and Ferrara (Fig. 1).

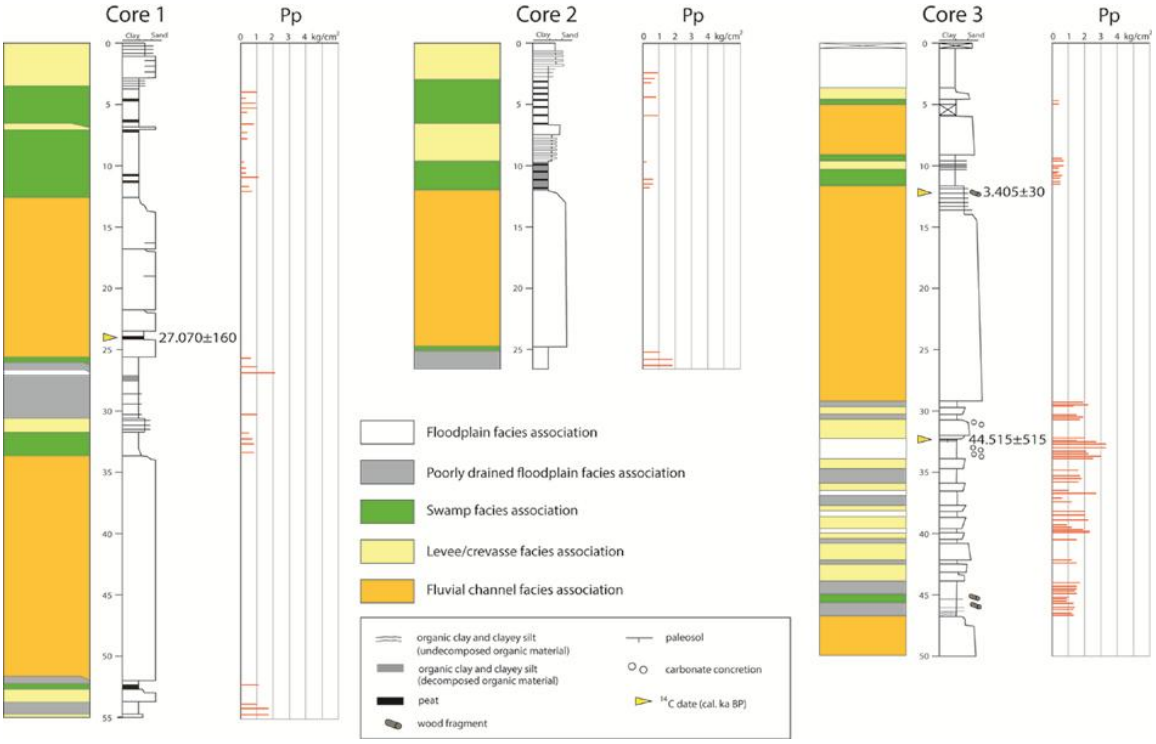

Fig. 3 - Facies interpretation and pocket penetration (Pp) values of reference cores 1-3 (see Fig. 1, for location).

Fourteen new radiocarbon dates, along with 14 published dates (Geological Map of Italy 1:50,000 scale – Sheet 182; Pavesi, 2009; Table 1) were used to validate our stratigraphic correlation scheme. Samples from cores “1” and “3” were dated at the Laboratory of Ion Beam Physics (ETH, Zurich, Switzerland). The ^{14}C dates were calibrated using Oxcal 4.2 (Ramsey, 2009) with the Intcal13 calibration curve (Reimer et al., 2013).

Table 1 – List of radiocarbon dated samples.

Core	Depth in core (m)	Conventional ^{14}C age (ka BP)	Calibrated age 2σ range (ka BP)	Calibrated age mean (ka BP)	σ	Dated material	Laboratory	Reference
165SOP503	20,2	8.240±50	9.402-9.032	9.210	±90	organic clay	ENEA (Bologna, Italy)	This paper
166SEP501	16,9	3.850±50	4.417-4.100	4.270	±85	organic clay	ENEA (Bologna, Italy)	This paper
166SEP501	24	8.330±50	9.473-9.142	9.350	±75	organic clay	ENEA (Bologna, Italy)	This paper
185010P501	20,3	5.980±50	6.943-6.679	6.820	±65	organic clay	ENEA (Bologna, Italy)	This paper
185010P501	23,2	7.260±50	8.175-7.980	8.085	±55	organic clay	ENEA (Bologna, Italy)	This paper
185020P501	19,8	1.600±50	1.606-1.382	1.485	±60	wood	ENEA (Bologna, Italy)	This paper
185020P501	22,9	7.290±50	8.190-8.000	8.100	±55	organic clay	ENEA (Bologna, Italy)	This paper
185070P507	6,3	1.240±50	1.283-1.060	1.180	±65	organic clay	ENEA (Bologna, Italy)	This paper
185070P507	12,44	7.030±80	7.982-7.690	7.860	±80	organic clay	ENEA (Bologna, Italy)	This paper
185120P505	5,6	3.015±45	3.347-3.072	3.210	±75	organic clay	ENEA (Bologna, Italy)	This paper
185120P505	11,6	6.360±50	7.419-7.175	7.300	±60	organic clay	ENEA (Bologna, Italy)	This paper
Core 3	12,2	3.180±30	3.456-3.356	3.405	±30	organic clay	ETH (Zurich, Switzerland)	This paper
Core 3	32,4	40.915±550	45.451-43.417	44.455	±515	organic clay	ETH (Zurich, Switzerland)	This paper
Core 1	23,6	22.695±75	27.326-26.697	27.070	±160	organic clay	ETH (Zurich, Switzerland)	This paper
182080P501	10,3	4.930±80	5.896-5.485	5.680	±95	organic soil	ENEA (Bologna, Italy)	Pavesi, 2009
182080P501	19,5	15.450±130	18.967-18.429	18.715	±130	wood	ENEA (Bologna, Italy)	Pavesi, 2008
182080P501	34,7	27.300±600	32.961-30.371	31.380	±640	wood	ENEA (Bologna, Italy)	Pavesi, 2009
182080P501	45	>45.000	>45.000 no cal.	-	-	organic soil	ENEA (Bologna, Italy)	Pavesi, 2009
182110P501	9	8.420±150	9.732-9.012	9.395	±180	organic clay	ENEA (Bologna, Italy)	Pavesi, 2009
182110P501	19,8	16.250±230	20.169-19020	19.620	±290	wood	ENEA (Bologna, Italy)	Pavesi, 2009
182110P501	22,8	17.550±280	21.496-20.511	21.230	±370	wood	ENEA (Bologna, Italy)	Pavesi, 2009
182110P501	23	22.100±330	27.168-25.806	26.400	±360	organic clay	ENEA (Bologna, Italy)	Pavesi, 2009
182110P501	32,9	39.900±650	44.803-42.640	43.630	±560	peat	ENEA (Bologna, Italy)	Pavesi, 2009
182110P502	33,1	40.300±550	44.937-42.998	43.920	±500	peat	ENEA (Bologna, Italy)	Geological Map of Italy – Sheet 182
182110P503	11,1	15.450±130	18.967-18.429	18.715	±130	organic soil	ENEA (Bologna, Italy)	Geological Map of Italy – Sheet 182
182 S11	13,3	13.150±180	16.268-15.240	15.770	±270	organic soil	ENEA (Bologna, Italy)	Geological Map of Italy – Sheet 182
182 S11	16	14.550±120	18.017-17.425	17.725	±150	organic soil	ENEA (Bologna, Italy)	Geological Map of Italy – Sheet 182
183050P503	45,5	>45.000	>45.000 no cal.	-	-	wood	ENEA (Bologna, Italy)	Pavesi, 2009

4. Facies analysis

A total of five non-marine facies associations (Table 2) were identified in core and correlated across the transect. They are described from high-energy to low-energy deposits.

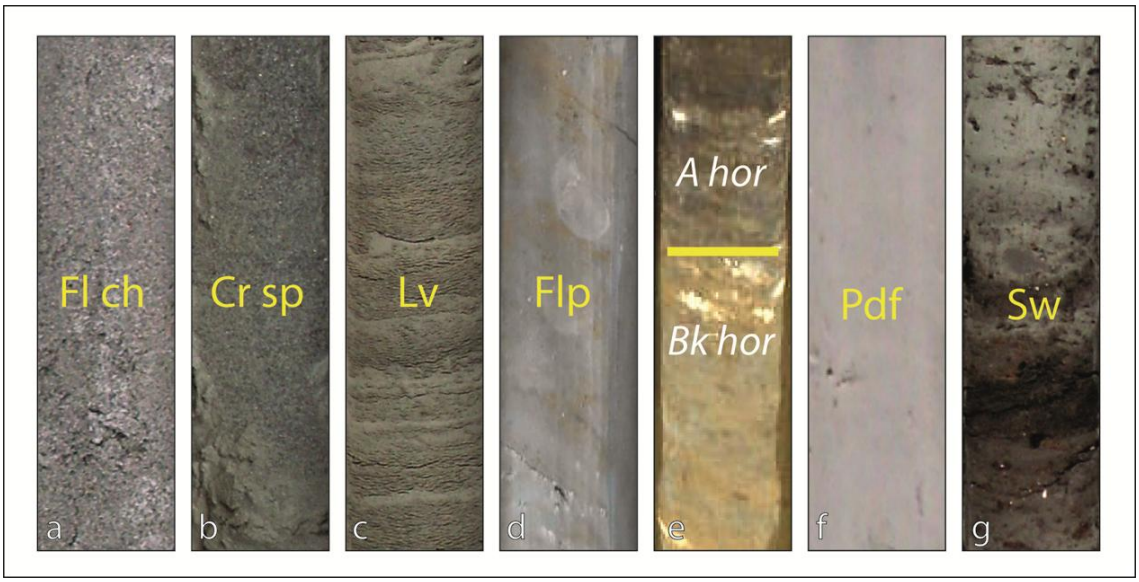

Fig. 4 - Representative photographs of facies associations identified in cores 1-3. a - Medium to coarse fluvial-channel sands (Fl ch); b - coarsening upward trend within a crevasse splay deposit (Cr sp); c - silty sand-mud alternations within a levee deposit (Lv); d - mottled floodplain silty clays(Fp); e - pedogenized floodplain clays with distinctive A (organic-rich) and Bk (calcic) horizons; f - massive poorly drained-floodplain clays (Pdf); g – organic-rich, swamp clay (Sw) .

4.1. Fluvial-channel facies association

4.1.1. Description

This facies association is made up of grey, fine to very-coarse sand (Fig. 4a). Individual sand bodies, ca. 10 m thick, are characterized by erosional lower boundaries and overall fining-upward (FU) tendency. Grain size changes are highlighted by the cone penetration (CPT and CPTU) profiles, which show distinctive upward decrease in tip-resistance values. The upper boundary to the overlying mud is either sharp or transitional, and organic-rich layers or peats commonly cap the FU succession. Pebbles and gravels are locally concentrated at the base of the sand bodies. Clays and silty clays are strongly subordinate. Commonly, sand bodies are vertically amalgamated into thicker multy-storey bodies (> 50 m), including repeated FU sequences. Wood fragments, up to 15 cm long, and clayey, organic-enriched intervals are locally encased in the sands. No fossils were recognized within this facies association. Piezocone tests display low/negative pore pressure values and tip-resistance (*Qc*) > 5 MPa.

4.1.2. Interpretation

The combination of lithology, thickness, grain size trends, type of boundaries, and negative excess pore pressure of this facies association is peculiar to fluvial-channel deposits (Allen, 1983; Miall, 1992). The gradational or sharp boundaries to the overlying muds are interpreted to reflect gradual or abrupt channel abandonment, respectively. The presence of peats and organic layers above the fluvial sands suggests the development of paludal environments following channel abandonment. As a whole, the amalgamated individual channel bodies form a thick channel-belt sand body (*sensu* Gibling, 2006) that is invariably encountered beneath the modern Po River.

4.2. Crevasse and levee facies association

4.2.1. Description

In this facies association, we included two depositional facies. One facies consists of sand bodies, up to 2 m thick, showing either (i) gradual base, sharp top and internal coarsening-upward (CU) trend (Fig. 4b) or (ii) sharp base, gradual top and internal FU trend. The other facies, 0.5 to 2 m thick, is composed of cm-alternations of very fine sand and bioturbated muds (Fig. 4c). Colors vary from grey to brownish. Root fragments, iron and manganese oxides and carbonate nodules are common in the silty intervals.

4.2.2. Interpretation

This facies association reflects a broad variety of depositional sub-environments formed as channel-related facies. In particular, sand bodies with sharp base, gradual transition to overlying muds and FU tendency are interpreted as crevasse channels, whereas sand bodies with gradual base, sharp top and CU trend reasonably represent crevasse splays (Miall, 1992; Collinson, 1996). The sand-mud alternations most likely reflect traction-plus-fallout deposition, and are interpreted as natural levee deposits, whose thickness and sand/mud ratio decrease with the distance from the channel axis (Amorosi et al., 2014).

4.3. Floodplain facies association

4.3.1. Description

This facies association, up to 12 m thick, consists of a repetitive succession of deeply bioturbated, gray silts and clays with dark-yellowish mottles of iron and manganese oxides (Fig. 4d). Mud is mostly structureless or shows faint horizontal laminations. Thin (cm-scale) intercalations of very fine sand are locally present. Scattered shell fragments of land mollusks were observed. Organic-rich horizons commonly overlie gray clays with carbonate concretions (Fig. 4e). Pocket penetration values generally are in the range of 1.8-3 kg/cm². In the carbonate-rich clays, these values are invariably higher (up to 3-5 kg/cm²). Cone tip resistance (*Qc*) in CPTU tests falls in the range of 1.2-3 MPa. Sleeve friction (*fs) is* > 0.5 MPa.

4.3.2. Interpretation

This facies association is interpreted as floodplain deposits. The dominance of massive, bioturbated silt and clays and the presence of carbonate nodules and oxides are typical of low-energy depositional environments characterized by frequent episodes of subaerial exposure under well-drained conditions (Amorosi et al., 2014, 2015). Organic-rich and calcic horizons are interpreted to represent the ‘A’ and ‘Bk’ horizons of weakly developed paleosols (Inceptisols of Soil Survey Staff, 2014), respectively. These paleosols are inferred to represent periods of non-deposition of a few thousand years. Pocket penetrometer and CPTU tip resistance values from this facies association are both characteristic of unconsolidated floodplain deposits (Amorosi and Marchi, 1999; Sarti et al., 2012; Amorosi et al. 2015).

4.4. Poorly-drained floodplain facies association

4.4.1. Description

This facies association is made up of gray to dark gray clay and silty clay (ca. 1 m thick; Fig. 4f). Organic matter is commonly decomposed in mm- to cm- dark layers or associated to mm-sized plant fragments. Carbonate concretions, iron and manganese nodules are absent. Shells fragments belonging to land mollusk species were encountered. Pocket penetrometer values range between 1.2 and 1.8 kg/cm². Cone tip resistance is between 0.8 and 1.2 MPa. Sleeve friction *fs* is < 0.5 MPa.

4.4.2. Interpretation

The dominance of fine-grained deposits, along with lack of carbonate concretions and oxides and the presence of land mollusks, are characteristic of a low-energy alluvial environment, such as a poorly drained floodplain (Amorosi et al., 2016) where the persistent effect of water (high water table) hinders processes of eluviation/illuviation and oxidation. Pocket penetrometer, *Qc* and *fs* values also support this interpretation, revealing lower consistency than the well-drained floodplain facies.

4.5. Freshwater swamp facies association

4.5.1. Description

This facies association, up to 12 m thick, consists of soft gray to dark-black, organic-rich clay with mm to cm-sized plant debris and wood fragments (Fig. 4g). Peat layers, up to 0.3 m thick, are commonly observed, along with shell fragments of terrestrial gastropods. Sand layers, a few cm thick, with sharp lower boundaries are also present. Subtle grain-size variations, from clay to silty clay or concentration of organic matter are revealed by horizontal lamination. This facies association is generally characterized by very low pocket penetration values (< 1.2 kg/cm^2), associated with low *Qc* (< 0.8 MPa) and *fs* (< 0.5 MPa). These values are slightly higher within peat layers.

4.5.2. Interpretation

Organic, soft clay-dominated deposits with abundant wood fragments, plant debris and diffuse peat layers and fossils are interpreted to have been deposited in swamps, under predominantly reducing conditions (Amorosi et al., 2015). Where this facies association is thicker than 5 m, persistent undrained conditions may reflect a wider depositional environment, such as the inner part of an estuary (Dalrymple et al., 1992). Horizontal lamination is likely to reflect the slow and gradual accumulation of organic matter, occasionally interrupted by flood events. The low penetration values are coherent with this interpretation, suggesting typically undrained conditions.

Table 2 - Summary of sedimentary facies in the Central Po Plain.

Facies Association	Lithology	Grain-size trend	Thickness (m)	Accessory materials	Pocket penetration values (kg/cm²)	Tip resistance (Qc) values (MPa)
Fluvial channel	Medium to coarse sand (subordinate pebble and gravel layers)	Fining-upward (erosional base)	5-20 (multy-storey >50)	No fossils; wood fragments; clayey organic enriched intervals	-	> 5
Crevasse and levee	cm alternations of very fine sand and silt Very fine to medium sand	None Coarsening-upward (splay) Fining-upward (channel)	0.5-2	Root fragments; bioturbation; iron and manganese oxides; carbonate nodules	-	-
Floodplain	Silt and clay	None	Max. 12	Bioturbation, iron and manganese oxides; scarce shell fragments of terrestrial mollusks; organic-rich horizons; carbonate concretions; paleosols	1.8-3 (> 3 in paleosols)	1.2-3
Poorly-drained floodplain	Clay and silt	None-	1	Decomposed organic matter (mm-cm-layers); plant fragments; shell fragments of land mollusks	1.2-1.8	0.8-1.2
Freshwater swamp	Clay (subordinate silty clay)	None	Max. 12	Peat layers (dm); terrestrial gastropods and shell fragments	<1.2 (up to 1.8 in peats)	<0.8 (up to 1.8 in peats)

5. Late Quaternary alluvial stratigraphy in the central Po Plain

The 123 km-long transect of Figure 5, roughly coincident with the southern bank of the modern Po River, depicts the Late Pleistocene to Holocene facies architecture of the central Po Basin, at significant (> 50 km) distance from the modern Adriatic coastline (see inset in Fig. 1). In the study area, the cross-section entirely cuts through non-marine deposits, and can be subdivided into two sub-transects (A and B, in Fig. 5) based on remarkable downstream changes in stratigraphy.

Two lithologically distinct stratigraphic intervals are recognized at proximal locations (Fig. 5A): the lower one, broadly assigned to the Late Pleistocene, is dominated by amalgamated (20-30 m thick), coarse-grained fluvial deposits that show very high continuity in downstream direction. Radiometric dates from this multi-storey sand body range between about 44 and 19 ka cal. BP (the deepest part is beyond the limit of the ^{14}C method - Fig. 5A). Crevasse/levee, swamp and floodplain deposits are highly subordinate. On the other hand, the uppermost interval, 10-15 m thick, is characterized by widespread fine-grained alluvial deposits, among which the well-drained floodplain facies association is largely dominant. At the SW tip of Section A, a few weakly

developed paleosols were identified. Poorly-drained floodplain or swamp deposits are scarce and typically developed atop the fluvial channel-belt sand bodies. These organic-rich facies associations, commonly 2-4 m thick, are of early Holocene age (9.4-9.2 ka cal. BP in Fig. 5A).

Similar to its proximal equivalent, sub-transect B exhibits in its lower part a continuous body of amalgamated fluvial-channel sands, with average thickness of 20-30 m (Fig. 5B). These fluvial sands yielded two radiocarbon dates of 44 and 27 ka cal. BP, confirming a Late Pleistocene age. The amalgamated sand bodies are overlain by a Holocene (< 9.4 ka) fine-grained succession, 15-20 m thick, dominated by freshwater swamp facies, with subordinate poorly-drained floodplain muds and rare floodplain deposits.

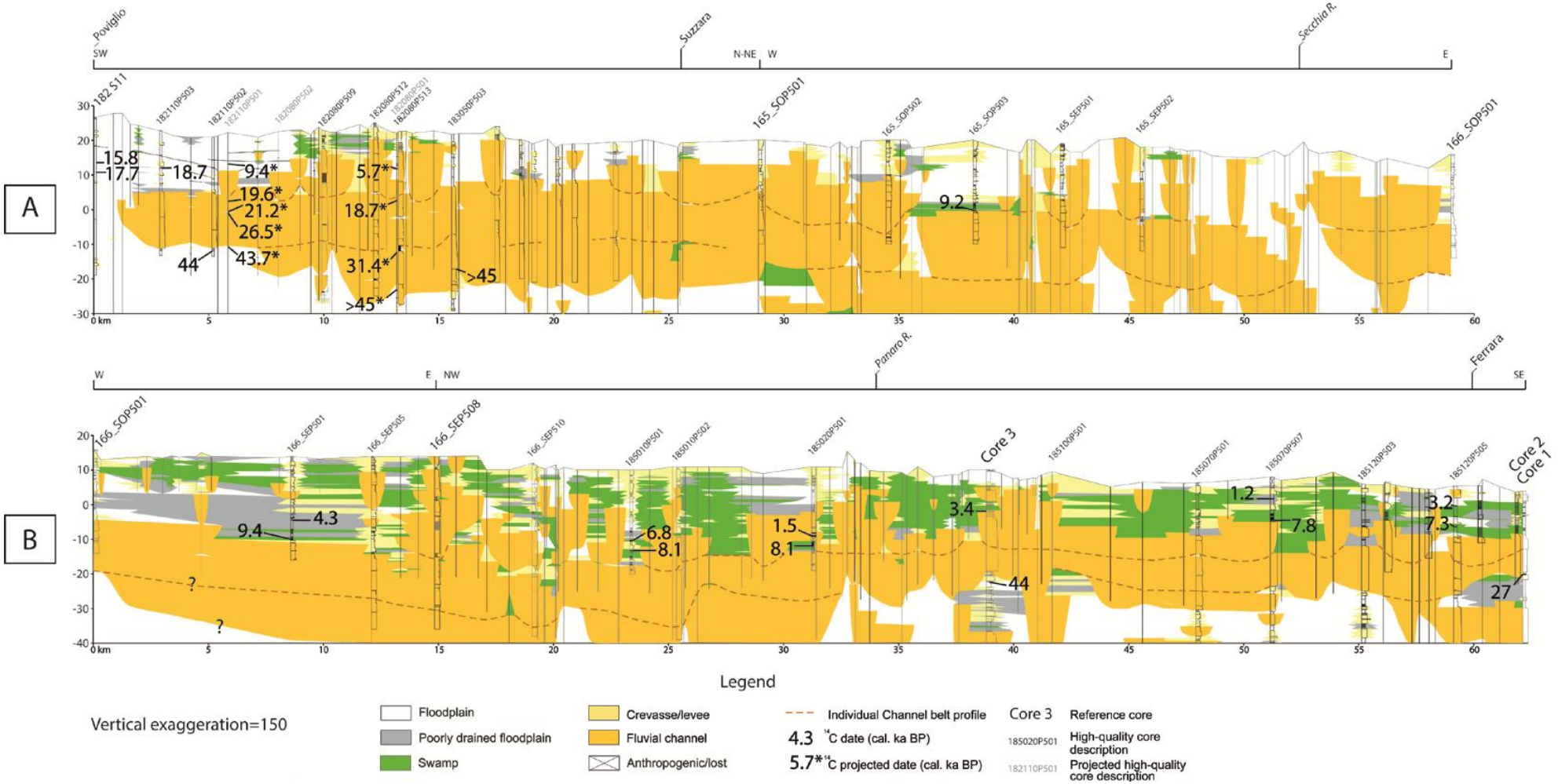

Fig. 5 - Stratigraphic panel depicting facies architecture along the 120 km-transect. A): proximal section; B) distal section (for location, see Fig. 1).

6. Factors controlling alluvial stratigraphy

The late Quaternary stratigraphic architecture along the course of the modern Po River shares remarkable similarities with many coeval alluvial plain successions worldwide. The sharp change in fluvial architecture at the transition from the Last Glacial Maximum to the Present Interglacial, postulated by numerous late Quaternary examples (Lewis et al., 2001; Macklin et al., 2002; Briant et al., 2005) is clearly reconstructed from the subsurface of the Po Plain, where Late Pleistocene, sheet-like fluvial-channel bodies with high degree of interconnectedness are replaced up-section by a mud-dominated Holocene succession with lens-shaped fluvial bodies.

Radiocarbon dates prove that the amalgamated fluvial-channel bodies were deposited between about 40 and 9.5 cal. ka BP (Fig. 5), i.e. during Marine Isotope Stage - MIS 3, the Last Glacial Maximum (MIS 2) and the following Lateglacial (early MIS 1). The abrupt transition from these glacial sands to the overlying mud-prone succession of Holocene age is marked by prominent organic-rich layers (9.4-9.2 ka cal. BP) that formed in response to widespread channel abandonment and generalized swamp development at the onset of warm-temperate (interglacial) climate conditions.

Climate and base-level variations have been called into question as driving factors of changes in alluvial architecture by several Quaternary studies (Blum and Valastro, 1994; Blum and Törnqvist, 2000; Aguzzi et al., 2007). Consistent with the general view of Blum and Törnqvist (2000), we argue that the stratigraphic modifications observed in the Po Basin at the glacial-interglacial transition, a period of generalized rapid sea-level rise, were controlled by changes in two main parameters: sediment supply and accommodation.

6.1. Influence of climate on sediment supply

Climate change can influence the production of sediment through the action of glaciers on the mountain slopes, and indirectly through the extent of vegetation cover (Vandenberghe, 2003). Glacial periods were characterized by significant ice sheet growth, mountain glaciers expansion (Benn and Evans, 2013), and reduction in arboreal-vegetation cover (Whitlock and Bartlein, 1997). Strong erosional activity and high sediment transport capability (large amount of debris for hundreds of km) make glaciers play a key role in the sediment production and dispersion processes. On the other hand, during interglacials, rapid ice-decay followed by the expansion of the arboreal-vegetation cover reduced erosion, and lower volumes of coarse-grained material were removed from the source areas.

In the Po Plain, sediment production was enhanced both in the Alpine and Apenninic catchments around the Last Glacial Maximum. The Alpine glaciers extended for kilometers through the Po Plain (Voges, 1995; Bini and Zuccoli, 2004), feeding their related fluvio-glacial systems (Fontana et al., 2014). In the northern Apennines, where the presence of glaciers was restricted to small areas (Giraudi, 2015), vegetation was mainly herbaceous (Vescovi et al., 2010). The Apenninic catchments, largely composed of weak rocks, were subject to erosion and slope instability. The coarser sediment fraction supplied by the Alpine and Apenninic sources accumulated in large alluvial fan gravel systems close to the valley outlets (Amorosi et al., 1996; Fontana et al., 2008; 2014). The sandy portion, instead, was delivered to the Po River, where partly accumulated into wide channel-belt sand bodies (Figs. 5 and 6).

Under lowstand conditions, the bulk of sediment accumulation was confined to the deepest parts of the Po-Adriatic basin (Amorosi et al., in press). The large sediment volumes of the lowstand systems tract also reflect the two-fold increase of the catchment area due to sea-level fall (Maselli et al., 2011).

At the end of the LGM, following the decay of ice sheets, glacial lakes formed at the Alpine margin of the Po Basin, trapping large amounts of sediment. Due to consequent reduction in sediment supply, most Alpine tributary rivers started to incise into the underlying glacial deposits (Fontana et al., 2014), delivering coarse-grained sediment to the Po River. Similarly, at the Apenninic margin fluvial systems spread out large volumes of coarse-grained material through the alluvial plain because of the ice melting, as testified by alluvial fan growth between 19 and 13 ka BP (Lowe, 1992; Amorosi et al., 1996). At that time, a braided Po River system was still active in the central Po Plain (Fig. 5).

The widespread development of *Quercus* and *Fagus* forests at the onset of warm conditions, around 9 cal. ka BP, (Vescovi et al., 2010), strongly reduced the erosive power and the transport capability of both Apenninic and Alpine rivers. As a result, significantly finer-grained material was supplied to the Po River during the Holocene, leading to the accumulation of a mud-dominated succession (Figs. 5 and 6). The development of a denser vegetation cover and the subsequent reduction in sediment yield under warmer and wetter climate conditions favored the shift from braided to sinuous, single-channel river systems at the Pleistocene-Holocene transition (Blum and Törnqvist, 2000; Leigh, 2006), as highlighted by the abrupt decrease in channel-belt width and thickness.

6.2. Accommodation and base-level control on stratigraphic architecture

Vertical changes in fluvial-channel stacking patterns are considered fundamental indicators for variations in the relationships between sediment supply, base-level fluctuations and accommodation space. Classic models (Shanley and McCabe, 1994; Legarreta and Uliana, 1998; Martinsen et al., 1999) have linked amalgamated and laterally extensive fluvial sands to low-accommodation (lowstand) conditions; on the other hand, poorly interconnected fluvial bodies encased into low net-to-gross successions have been inferred to reflect high accommodation settings. Experiments (Martin et al., 2009) have additionally shown that channel-belts formation is genetically related to base-level fall.

The stratigraphic architecture displayed in Fig. 5 is in line with the above models. According to radiocarbon dating, laterally extensive, amalgamated sand bodies were deposited by the Po River in the Late Pleistocene, between about 45 and 9.5 ka BP, under falling sea level, lowstand and early transgressive conditions (Low Accommodation Systems Tract or LAST of Catuneanu et al., 2009, in Fig. 6). Lateral migration during sea-level lowstand allowed deposition and preservation of the coarser portion of the sediment (i.e., sands) only, while the muddy component was carried away toward distal areas.

The overall aggradational stacking pattern of Late Pleistocene fluvial sand bodies (Fig. 5) is interpreted to reflect the high subsidence rates of the Po Basin (Carminati et al., 2005). As documented by Amorosi and Milli (2001) and Fontana et al. (2014) from the Po coastal plain and the Alpine piedmont area, respectively, high tectonic subsidence in the Po Basin resulted in continuous creation of accommodation, which enhanced fluvial aggradation and the anomalously high preservation of forced-regressive and lowstand deposits. Individual fluvial-channel units are 10-15 m thick, while the Pleistocene channel-belt sand bodies may exceed 30 m in composite thickness (Figs. 3 and 5). Radiocarbon dates show that MIS 2 channel belt sands (i.e. lowstand deposits) are piled up onto older fluvial bodies (MIS 3), formed during the latest stage of sea-level fall. Based on the diagnostic pollen signature of laterally correlative channel-belt sand bodies from adjacent areas (Amorosi et al., 2008), the amalgamated sand bodies beyond the limit of radiocarbon dating (Fig. 5) are assigned tentatively to the onset of the Late Pleistocene glacial period (MIS 4).

On the other hand, high-accommodation conditions accompanied the post-glacial sea-level rise (Liu and Milliman, 2004; Storms et al., 2008; Bruno et al., 2016) and strongly affected river behavior (Hijma et al., 2009; Hijma and Cohen, 2011). Two subsequent phases of sea-level rise associated with meltwater pulses MWP 1A and 1B

induced the NNW shoreline migration across the North Adriatic shelf, hundreds of kilometers far from the LGM Po lowstand delta (Trincardi et al., 1994; Amorosi et al., in press). Only around 9.5 ka cal. BP the study area experienced the direct influence of sea-level rise, with the development of an inner estuarine environment, dominated by coastal wetlands (Fig. 5B). Because of the rapid backstepping of the shoreline in a low-gradient setting, avulsion became the dominant fluvial process in the central Po Plain. Owing to increased accommodation, large volumes of overbank fines were preserved, resulting in a systematic change of fluvial architecture from braided to meandering styles (Törnqvist, 1993), with preservation of channel bodies isolated in fines (High Accommodation Systems Tract or HAST, Fig. 6).

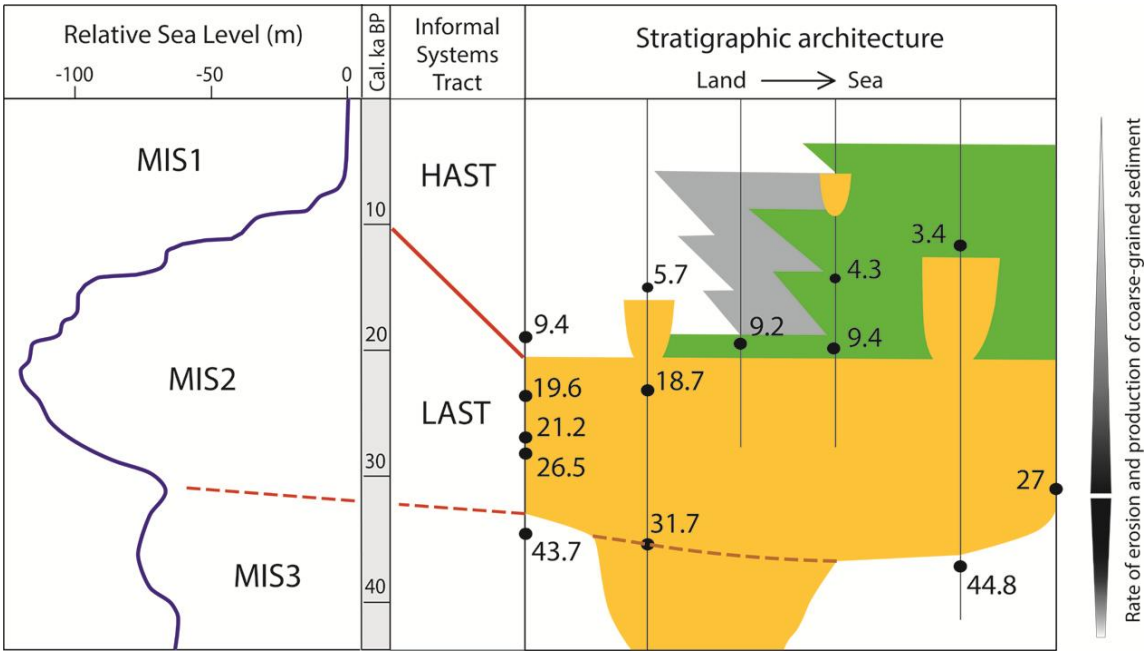

Fig. 6 – Schematic sketch showing the relationships between stratigraphic architecture, relative sea-level curve and sediment supply. LAST = low accommodation systems tract; HAST = high accommodation systems tract.

7. Conclusions

The late Quaternary stratigraphic architecture of a fluvial-dominated section transversal to the present shoreline has been depicted through a ca. 120 km-long transect, coincident with the middle reaches of the modern Po River. Based on changes in lithofacies and channel stacking patterns, chronologically calibrated through 28 radiocarbon dates, we highlighted the contrasting alluvial architecture of Late Pleistocene amalgamated fluvial-channel sands and overlying, Holocene mud-dominated deposits, with isolated fluvial-channel bodies. This prominent architectural

change, continuously traceable 130 km inland relative to the modern Adriatic coastline, is the result of changes in sediment supply and accommodation.

Radiocarbon dates proved that deposition of the multi-storey sand sheet took place between about 45 and 9.5 ka BP, i.e. during MIS 3, the LGM (MIS 2) and the Lateglacial (and probably earlier, during MIS 4). The sharp transition from the amalgamated sands to the overlying, mud-dominated deposits is marked by laterally extensive, organic-rich facies associations, testifying to regional fluvial-channel abandonment at the onset of warm-temperate (interglacial) climate conditions. Along the entire transect, the Holocene succession shows consistent variations in facies architecture, with well-drained floodplain facies that are replaced downstream by increasingly organic-rich (poorly-drained floodplain to swamp) clays. Thick paludal deposits extend almost continuously, ca. 60 km upstream of the maximum marine ingression.

The abrupt stratigraphic transition from glacial sands to interglacial mud-dominated units was controlled by combined climate change and relative sea-level rise. Because of increasing erosion under glacial conditions, huge volumes of coarse-grained material were delivered to the Po River from the Alpine and the Apenninic catchments during the LGM and the following Lateglacial. Gravels built up alluvial fan complexes in piedmont areas, whereas sands accumulated into the Po channel belts, and the muddy portion was removed from the study area and transported basinwards. On the other hand, warmer climate conditions favored widespread forest expansions, which strongly reduced erosive processes in the cactchment areas and the transport capability of the rivers. As a consequence, predominantly finer-grained material was supplied to the Po during the Holocene, leading to deposition of a clay-dominated succession.

The Po channel belt sand bodies were deposited mainly under falling-stage, lowstand and early transgressive conditions (Low Accommodation Systems Tract). Once rapid sea-level rise increased accommodation, starting from ca. 9.5 ka BP deposition of isolated fluvial bodies took place in association with low net-to-gross deposits (High Accommodation Systems Tract), and avulsion became the dominant fluvial process in the study area. The overall aggradational stacking pattern of the entire sedimentary succession was driven, instead, by high subsidence rates, which continuously created accommodation even during falling sea level and lowstand conditions.

Through a chronologically well constrained case study, we assessed the role of late Quaternary climate and base-level variations on fluvial architecture. The stratigraphic succession of the Po Plain, thus, may serve as modern analog for the interpretation of

ancient fluvial successions, and can be used to make predictive models of fluvial architecture under the influence of changes in climate and sea level.

Acknowledgements

We are grateful to Paolo Severi and Luca Martelli (Geological Survey of Regione Emilia Romagna), Lorella Dall'Olio (Servizio Ambiente, Comune di Ferrara) for the access to database.

We also thank Silvia Rosselli for the precious and professional support during the recovery of the cores.

References

Adams, M.M., Bhattacharya, J.P., 2005. No change in fluvial style across a sequence boundary, Cretaceuos Blackhawk and Castelgate formations of Central Utah, U.S.A. Journal of Sedimentary Research 75, 1038-1051.

Aguzzi, M., Amorosi, A., Colalongo, M.L., Ricci Lucchi, M., Rossi, V., Sarti, G., Vaiani, S.C., 2007. Late quaternary climatic evolution of the Arno coastal plain (Western Tuscany, Italy) from subsurface data. Sedimentary Geology 202, 211-229.

Allen, J.R.L., 1983. Studies in fluviatile sedimentation: bars, bar complexes and sandstone sheets (low-sinuosity braided streams) in the brownstones (L. Devonian), Welsh Borders. Sedimentary Geology 33, 237-293.

Allen, J.P., Posamentier, H.W., 1992. Sequence stratigraphy and facies model of an incised valley fill: the Gironde Estuary, France. Journal of Sedimentary Petrology 63, 378-391.

Amorosi, A., Farina, M., Severi, P., Preti, D., Caporale, L., Di Dio, G., 1996. Genetically related alluvial deposits across active fault zones: an example of alluvial fan-terrace correlation from the upper Quaternary of the southern Po Basin, Italy. Sedimentary Geology 102, 275-295.

Amorosi, A., Marchi, N., 1999. High-resolution sequence stratigraphy from piezocone tests: an example from the Late Quaternary deposits of the southeastern Po Plain. Sedimentary Geology 128, 67-81.

Amorosi, A., Colalongo, M.L., Pasini, G., Preti, D., 1999a. Sedimentary response to Late Quaternary sea-level changes in the Romagna coastal plain (northern Italy). Sedimentology 46, 99-121.

Amorosi, A., Colalongo, M.L., Fusco, F., Pasini, G., Fiorini, F., 1999b. Glacio-eustatic control of continental-shallow marine cyclicity from Late Quaternary deposits of the south-eastern Po-Plain (Northern Italy). Quaternary Research 52, 1-13.

Amorosi, A., Milli, S., 2001. Late Quaternary depositional of Po and Tevere river deltas (Italy) and worldwide comparison with coeval deltaic successions. Sedimentary Geology 128, 357-375.

Amorosi, A., Centineo, M.C., Colalongo, M.L., Pasini, G., Sarti, G., Vaiani, S.C., 2003. Facies architecture and Latest Pleistocene-Holocene Depositional history of the Po Delta (Comacchio Area), Italy. The Journal of Geology 11, 39-56.

Amorosi, A., Colalongo, M.L., Fiorini, F., Fusco, F., Pasini, G., Vaiani, S.C., Sarti, G., 2004. Paleogeographic and paleoclimatic evolution of the Po Plain from 150-ky core records. Global and Planetary Change 40, 55-78.

Amorosi, A., Colalongo, M.L., 2005. The linkage between alluvial and coeval nearshore marine succession: evidence from the Late Quaternary record of the Po River Plain, Italy. In: Blum, M.D., Marriott, S.B., Leclair, S.F., (Eds.), Fluvial Sedimentology VII. International Association of Sedimentologists, Special Publication, 35, pp. 257-275.

Amorosi, A., Pavesi, M., Ricci Lucchi, M., Piccin, A., 2008. Climatic signature of cyclic fluvial architecture from the Quaternary of the central Po Plain, Italy. Sedimentary Geology 209, 58-68.

Amorosi, A., Pavesi, M., 2010. Aquifer stratigraphy from the middle-late Pleistocene succession of the Po Basin. Memorie Descrittive della Carta Geologica d'Italia XC, 7-20.

Amorosi, A., Bruno, L., Rossi, V., Severi, P., Hajdas, I., 2014. Paleosol architecture of a late Quaternary basin-margin sequence and its implications for high-resolution, non-marine sequence stratigraphy. Global and Planetary Change 112, 12-25.

Amorosi, A., Bruno, L., Campo, B., Morelli, A., 2015. The value of pocket penetration tests for the high-resolution paleosol stratigraphy of late Quaternary deposits. Geological Journal 50, 670-682.

Amorosi, A., Bracone, V., Campo, B., D'Amico, C., Rossi, V., Rosskopf, M., 2016. A late Quaternary multiple paleovalley system from the Adriatic coastal plain (Biferno River, Southern Italy). Geomorphology 254, 146-159.

Amorosi, A., Maselli, V., Trincardi, F., in press. Onshore to offshore anatomy of a late Quaternary source-to-sink system (Po Plain-Adriatic Sea, Italy). Earth-Science Reviews, doi:10.1016/j.earscirev.2015.10.010

Aslan, A., Autin, W.J., 1999. Evolution of the Holocene Mississippi River floodplain, Ferriday, Louisiana: insights on the origin of the fine-grained floodplains. Journal of Sedimentary Research 69, 800-815.

Aslan, A., Blum, M.D., 1999. Contrasting styles of Holocene avulsions, Texas Gulf Coastal Plain. In: Smith, N.D., Rogers, J.J., (Eds.), Current Research in Fluvial Sedimentology: Proceedings of 6th International Conference on Fluvial Sedimentology. International Association of Sedimentologists, Special Publication 28, 193-209.

Autin, W.J., Burns, F.S., Saucier, R.T., Snead, J.J., 1991. Quaternary geology of the lower Mississippi Valley. In: Morrison, R.B. (Ed.), Quaternary Nonglacial Geology: Conterminous U.S. The Geological Society of America. The Geology of North America, K-2, pp. 547-582.

Benn, D.I., Evans, D.J.A., 2014. Glaciers and glaciations. Second edition. Routledge (Ed.), New York, USA.

Bini, A., Zuccoli, L., 2004. Glacial history of the southern side of the central Alps, Italy. In: Ehlers, J., Gibbard, P.L., (Eds.), Quaternary Glaciations – Extent and chronology. Elsevier, Amsterdam, The Netherlands, pp. 195-200.

Blum, M.D., 1993. Genesis and architecture of incised valley fill sequences: a Late Quaternary example from Colorado River, Gulf Coastal Plain of Texas. In: Weimer, P., Posamentier, H.P. (Eds.), Siliciclastic Sequence Stratigraphy: Recent Developments and Applications. American Association of Petroleum Geologists, 58, pp. 259-283.

Blum, M.D., Valastro, S. Jr., 1994. Late Quaternary sedimentation, Lower Colorado River, Gulf Coastal Plain of Texas. Geological Society of American Bulletin 106, 1002-1016.

Blum, M.D., Toomey III, R.S., Velastro, S. Jr., 1994. Fluvial response to Late Quaternary climatic and environmental change, Edwards Plateau of Texas. Paleogeography, Paleoclimatology and Paleoecology 108, 1-21.

Blum, M.D., Price, D.M., 1998. Quaternary alluvial plain construction in response to glacio-eustatic and climatic controls, Texas gulf coastal plain. In: Shanley, K.W., McCabe, P.J., (Eds.), Relative Role of Eustacy, Climate and Tectonism in Continental Rocks. Society for Sedimentary Geology, Special Publication 59, pp. 31-48.

Blum, M.D., Törnqvist, T.E., 2000. Fluvial responses to climate and sea-level change: a review and look forward. Sedimentology 47, 2-48.

Blum, M.D., Aslan A., 2006. Signatures of climate vs. sea-level change within incised valley-fill successions: Quaternary examples from the Texas Gulf Coast. Sedimentary Geology 190, 177-211.

Blum, M.D., Womack, J.H., 2009. Climate change, sea-level change, and fluvial sediment supply to deepwater systems. In: Kneller, B., Martinsen, O.J., McCaffrey, B.,

(Eds.), External Controls on Deep Water Depositional Systems: Climate, Sea-Level, and Sediment Flux. Society for Sedimentary Geology, Special Publication 92, pp. 15-39.

Blum, M.D., Martin, J., Milliken, K., Garvin, M., 2013. Paleovalley systems: Insights from Quaternary analogs and experiments. Earth-Science Reviews 116, 128-169.

Briant, R.B., Bateman, M.D., Coope, G.R., Gibbard, P.L., 2005. Climatic control on Quaternary fluvial sedimentology of a Fenland Basin river, England. Sedimentology 52, 1397-1423.

Bruno, L., Amorosi, A., Severi, P., Costagli, B., 2016. Late Quaternary aggradation rates and stratigraphic architecture of the southern Po Plain, Italy. Basin Research, doi: 10.1111/bre.12174

Busschers, F.S., Weerts, H.J.T., Wallinga, J., Cleveringa, P., Kasse, C., de Wolf, H., Cohen, K.M., 2005. Sedimentary architecture and optical dating of Middle and Late Pleistocene evolution of the Rhine-Meuse deposits – fluvial response to climate change, sea level fluctuation and glaciation. Netherlands Journal of Geosciences 84, 25-41.

Busschers, F.S., Kasse, C., Van Balen, R.T., Vandenberghe, J., Cohen, K.M., Weerts, H.J.T., Wallinga, J., Johns, C., Cleveringa, P., Bunnik, F.P.M., 2007. Late Pleistocene evolution of the Rhine-Meuse system in the southern North Sea basin: imprints of climate change, sea-level oscillation and glacio-isostacy. Quaternary Science Review 26, 3216-3248.

Carminati, E., Doglioni, C., Scrocca, D., 2005. Magnitude and causes of long-term subsidence of the Po Plain and Venetian region. In: Fletcher, C.A., Spencer, T., (Eds.), Flooding and environmental challenges for Venice and its lagoon: state of knowledge. Cambridge, pp. 697.

Carminati, E., Doglioni, C., 2012. Alps vs. Apennines: The paradigm of a tectonically asymmetric Earth. Earth Sciences Review 112, 67-96.

Catuneanu, O., Abreu, V., Bhattacharya, J.P., Blum, M.D., Dalrymple, R.W., Eriksson, P.G., Fielding, C.R., Fisher, W.L., Galloway, W.E., Gibling, M.R., Giles, K.A., Holbrook, J.M., Jordan, R., Kendall, C.G.St.C., Macurda, B., Martinsen, O.J., Miall, A.D., Neal, J.E., Nummedal, D., Pomar, L., Posamentier, H.W., Pratt, B.R., Sarg, J.F., Shanley, K.W., Steel, R.J., Strasser, A., Tucker, M.E., Winker, C., 2009. Towards the standardization of sequence stratigraphy. Earth-Science Reviews 92, 1-33.

Chang, K.H., 1975. Unconformity-bounded stratigraphic units. Geological Society of America Bulletin 86 (11), 1544-1552.

Collinson, J.D., 1996. Alluvial sediments. In: Reading, H.G. (Ed.), Sedimentary Environments: Processes, Facies and Stratigraphy. Blackwell Scientific Publications, Oxford, pp. 37-82.

Currie, B.S., 1997. Sequence stratigraphy of nonmarine Jurassic-Cretaceous rocks, central Cordilleran foreland-basin system. Geological Society of American Bulletin 109, 1206-1222.

Dalrymple, R.W., Zaitlin, B.A., Boyd, R., 1992. Estuarine facies models: conceptual basis and stratigraphic implications. Journal of Sedimentary Petrology 62, 1130-1146.

Doglioni, C., 1993. Some remarks of the origin of foredeeps. Tectonophysics 228, 1-20.

Dondi, L., D'Andrea, M.G., 1986. La Pianura Padana e Veneta dall'Oligocene superiore al Pleistocene. Giornale di Geologia 48, 197-225.

Fontana, A., Mozzi, P., Bondesan, A., 2008. Alluvial megafans in the Venetian-Friulian Plain (north-eastern Italy): evidence of sedimentary and erosive phases during Late Pleistocene and Holocene. Quaternary International 189, 71-90.

Fontana, A., Mozzi, P., Marchetti, M., 2014. Alluvial fans and megafans along the southern side of the Alps. Sedimentary Geology 301, 150-171.

Ford, M., 2004. Depositional wedge tops: interaction between low basal friction external orogenic wedges and flexural foreland basins. Basin Research 16, 361-375.

Geological Map of Italy at 1:50,000 scale. Sheet 182 – Guastalla (in press) - Regione Emilia-Romagna Geological Survey.

Ghielmi, M., Minervini, M., Nini, C., Rogledi, S., Rossi, M., 2013. Late Miocene-Middle Pleistocene sequences in the Po Plain-Northern Adriatic Sea (Italy): the stratigraphic record of modification phases affecting a complex foreland basin. Marine and Petroleum Geology 42, 50-81.

Gibling, M.R., 2006. Width and thickness of fluvial channel bodies and valley fills in the geological record: a literature compilation and classification. Journal of Sedimentary Research 76, 731-770.

Gibling, M.R., Fielding, C.R., Sinha, R., 2011. Alluvial valleys and alluvial sequences: towards a geomorphic assessment. In: Davidson, S.K., Leleu, S., North, C.P. (Eds.), From river to rock record: the Preservation of fluvial sediments and their subsequent interpretation. Society for Sedimentary Geology, Special Publication 97, pp. 423-447.

Giraudi, C., 2015. The upper Peistocene deglaciation on the Apennines (peninsular Italy). Cuadernos de Investigación Geográfica 41, 337-358.

Goodbred, S.L., 2003. Response of the Ganges dispersal system to climate change: a source-to-sink view since the last interstate. Sedimentary Geology 162, 83-104.

Hijma, M.P., Cohen, K.M., Hoffmann, G., Van der Spek, A.J.F., Stouthamer, E., 2009. From river valley to estuary: the evolution of the Rhine mouth in the early to middle Holocene (western Netherlands, Rhine-Meuse delta). Netherlands Journal of Geosciences - Geologie en Mijnbouw 88, 13-53.

Hijma, M.P., Cohen, K.M., 2011. Holocene transgression of the Rhine river mouth area, The Netherlands/Southern North Sea: palaeogeography and sequence stratigraphy. Sedimentology 58, 1453-1485.

Holbrook, J., Scott, R.W., Oboh-Ikuenobe, F.E., 2006. Base-level buffers and buttresses: a model for upstream versus downstream control on fluvial geometry and architecture within sequences. Journal of Sedimentary Research 76, 162-174.

Hori, K., Saito, Y., Zhao, Q., Wang, P., 2002. Evolution of the coastal depositional systems of the Changjiang (Yangtze) River in response to late Pleistocene-Holocene sea-level changes. Journal of Sedimentary Research 72, 884-897.

Ishihara, T., Sugai, T., Hachinohe, S., 2012. Fluvial response to sea-level changes since the latest Pleistocene in the near-coastal lowland, central Kanto Plain, Japan. Geomorphology 147-148, 49-60.

Kettner, A.J., Syvitsky, J.P.M., 2008. Predicting discharge and sediment flux of the Po River, Italy since the Last Glacial Maximum. International Association of Sedimentologists, Special Publication, 40, 171-189.

Kjemperud, A., Schomacker, E., Brendsdal, A., Fält, L.M., Jahren, J.S., Nystuen, J.P., Puigfàbragas, C., 2004. The fluvial analogue Escanilla Formation, Ainsa basin, Spanish Pyrenees: revisited. Adapted from “Extended Abstract” for Presentation at the AAPG International Conference, Barcelona, Spain, September 21-24, 2003. Search and Discovery Article # 30026.

Lambeck, K., Yokoyama, Y., Purcell, T., 2002. Into and out of the Last Glacial Maximum: sea-level change during Oxygen Isotope Stages 3 and 2. Quaternary Science Reviews 21, 343-360.

Legarreta, L., Uliana, M.A., 1998. Anatomy of hinterland depositional sequences: Upper Cretaceous fluvial strata, Neuquen Basin, West-Central Argentina. In: Shanley, K.W., McCabe, P.J., (Eds.), Relative Role of Eustacy, Climate, and Tectonism in Continental Rocks. Society of Economic Paleontologists and Mineralogists, Special Publication, 59, pp. 83-92.

Leigh, D.S., 2006. Terminal Pleistocene braided to meandering transition in rivers of the Southeastern USA. Catena 66, 155-160.

Lewis, S.G., Maddy, D., Scaife, R.G., 2001. The fluvial system response to abrupt climate change during the last cold stage: the Upper Pleistocene River Thames fluvial succession at Ashton Keynes, U K. Global and Planetary Change 28, 341-359.

Li, C., Wang, P., Fan, D., Yang, S., 2006. Characteristics and formation of Late Quaternary incised-valley-fill sequences in sediment-rich deltas and estuaries: a case studies from China. In: Dalrymple, R.W., Leckie, D.A., Tilliman, R.W. (Eds.), Incised Valleys in Time and Space. Society for Sedimentary Geology, Special Publication, 85, 141-160.

Liu, J.P., Milliman, J.D., 2004. Reconsidering Melt-water Pulses 1A and 1B: Global Impacts of Rapid Sea-level Rise. Journal of Ocean University of China, 3, 183-190.

Lowe, J.J., 1992. Lateglacial and early Holocene lake sediments from the northern Apennines, Italy-pollen stratigraphy and radiocarbon dating. Boreas 21, 193-208.

Macklin, M.G., Fuller, I.C, Lewin, J., Maas, G.S., Passmore, D.G., Rose, J., Woodward, J.C., Black, S., Hamblin, R.H.B., Rowan, J.S., 2002. Correlation of fluvial sequences in the Mediterranean basin over the last 200 ka and their relationship to climate change. Quaternary Science Review 21, 1633-1641.

Macklin, M.G., Lewin, J., Woodward, J.C., 2012. The fluvial record of climate change. Philosophical transactions of The Royal Society 370, 2143-2172.

Mancini, M., Moscatelli, M., Stigliano, F., Cavinato, G.P., Milli, S., Pagliaroli, A., Samionato, M., Brancaleoni, L., Cipolloni, I., Coen, G., Di Salvo, C., Garbin, F., Lanzo, G., Napoleoni, Q., Scarapazzi, M., Storoni Ridolfi, S., Vallone, R., 2013. The Upper Pleistocene-Holocene fluvial deposits of the Tiber River in Rome (Italy): lithofacies, geometries, stacking pattern and chronology. Journal of Mediterranean Earth Sciences Special Issue, 5, 95-101.

Martin, J.M., Abreu, V., Neal, J., Sheets, B., 2009. Sequence stratigraphy of experimental strata under known conditions of differential subsidence and variable base level. Bulletin of the American Association of Petroleum Geologists 93, 503-533.

Martinsen, O.J., Ryseth, A., Helland-Hansen, W., Flesche, H., Torkildsen, G., Idil, S., 1999. Stratigraphic base level and fluvial architecture. Ericson Sandstone (Campanian), Rock Springs Uplift, W. Wyoming, U.S.A. Sedimentology 46, 235-260.

Maselli, V., Hutton, E.W., Kettner, A.J., Syvitsky, J.P.M., Trincardi, F., 2011. High-frequency sea level and sediment supply fluctuations during Termination I: an integrated sequence-stratigraphy and modelling approach from the Adriatic Sea (Central Mediterranean). Marine Geology 287, 54-70.

Maselli, V., Trincardi, F., Asioli, A., Ceregato, A., Rizzetto, F., Taviani, M., 2014. Delta growth and river valleys: the influence of climate and sea level changes on the South Adriatic shelf Mediterranean Sea. Quaternary Science Review 99, 146-163.

Mazzoli, D., Koyi, H.A., Barchi, M.R., 2006. Structural evolution of a fold and thrust belt generated by multiple décollements: analogue models and natural examples from the northern Apennines (Italy). Journal of Structural Geology 28, 185-199.

McLaurin, B.T., Steel, R.J., 2000. Fourth-order nonmarine to marine sequences, middle Castelgate Formation, Book Cliffs, Utah. Geology 28, 359-362.

Miall, A.D., 1992. Alluvial deposits: In: Walker, R.G., James, N.P. (Eds.), Facies Models: Response to Sea Level Change. Geological Association of Canada, Waterloo, Ontario, pp. 119-139.

Milli, S., 1997. Depositional setting and high-frequency sequence stratigraphy of the middle-upper Pleistocene to Holocene deposits of the Roman basin. Geologica Romana, 33, 99-136.

Milli, S., Moscatelli, M., Palombo, M.R., Parlagreco, R., Paciucci, M., 2008. Incised-valleys, their filling and mammal fossil record: a case study from Middle-Upper Pleistocene deposits of the Roman Basin (Latium, Italy). GeoActa, Special Publication, 1, 67-88.

Milli, S., D'Ambrogi, C., Bellotti, P., Calderoni, G., Carboni, M.G., Celant, A., Di Bella, L., Di Rita, F., Frezza, V., Magri, D., Pichezzi, R.M., Ricci, V., 2013. The transition from wave-dominated estuary to wave-dominated delta. The Late Quaternary stratigraphic architecture of Tiber River deltaic succession (Italy). Sedimentary Geology 284–285, 159-180.

Muttoni, G., Carcano, C., Garzanti, E., Ghielmi, M., Piccin, A., Pini, R., Rogledi, S., Sciunnach, D., 2003. Onset of major Pleistocene glaciations in the Alps. Geology 31, 989-992.

Ori, G.G., Vannoni, F., 1986. Plio-Pleistocene sedimentation in the Apenninic-Adriatic foredeep (central Adriatic Sea, Italy). In: Allen, P.A., Homewood, P. (Eds.), Foreland Basins. International Association of Sedimentologists, Special Publication, 8, 183-198.

Paola, C., Mohorig, D., 1996. Paleohydraulics revisited: paleoslope estimation in coarse-grained braided rivers. Basin Research 8, 243-254.

Pavesi, M., 2009. Architettura stratigrafica dei depositi medio e tardoquaternari del bacino padano, finalizzata alla caratterizzazione geometrica degli acquiferi. PhD Thesis, Dipartimento di Scienze della Terra e Geologico Ambientali, University of Bologna, pp. 210.

Pieri, M., Groppi, G., 1981. Subsurface geological structure of the Po Plain, Italy. Consiglio Nazionale delle Ricerche. Progetto Finalizzato Geodinamica, 414, pp. 1-23.

Ramsey, C.B., 2009. Bayesian analysis of radiocarbon dates. Radiocarbon, 51 (1), 337-360.

Regione Emilia-Romagna, ENI-AGIP, 1998. Riserve idriche sotterranee della Regione Emilia-Romagna. S.EL.CA. (Firenze).

Regione Lombardia, ENI Divisione AGIP, 2002. Geologia degli Acquiferi Padani della Regione Lombardia. S.EL.CA. (Firenze).

Reijenstein, H.N., Posamantier, H.W., Bhattacharya, J.P., 2011. Seismic geomorphology and high-resolution seismic stratigraphy of inner-shelf fluvial, estuarine, deltaic, and marine sequences, Gulf of Thailand. Bulletin of the American Association of Petroleum Geologists 95, 1955-1990.

Reimer, P. J., Bard, E., Bayliss, A., Beck, J. W., Blackwell, P. G., Bronk Ramsey, C., Grootes, P. M., Guilderson, T. P., Haflidason, H., Hajdas, I., Hatt, C., Heaton, T. J., Hoffmann, D. L., Hogg, A. G., Hughen, K. A., Kaiser, K. F., Kromer, B., Manning, S. W., Niu, M., Reimer, R. W., Richards, D. A., Scott, E. M., Southon, J. R., Staff, R. A., Turney, C. S. M., Van der Plicht, J., 2013. IntCal13 and Marine13 Radiocarbon Age Calibration Curves 0-50,000 Years cal BP. Radiocarbon, 55 (4).

Rittenour, T.M., Blum, M.D., Globe, R.J., 2007. Fluvial evolution of the lover Mississippi River valley during the last 100-kyr glacial cycle: response to glaciations and sea-level change. Geological Society of America Bullettin 119, 586-608.

Sarti, G., Rossi, V., Amorosi, A., 2012. Influence of Holocene stratigraphic architecture on ground surface settlements: A case study from the City of Pisa (Tuscany, Italy). Sedimentary Geology 281, 75–87

Schumm, S.A., 1993. River response to base level change: implications for sequence stratigraphy. Journal of Geology 101, 279-294.

Shanley, K.W., Mc Cabe, P.J., 1991. Predicting facies architecture through sequence stratigraphy: an example from the Kaiparowits Plateau. Utah. Geology 19, 742-745.

Shanley, K.W., Mc Cabe, P.J., 1993. Alluvial architecture in a sequence stratigraphic framework: a case study from the Upper Cretaceous of southern Utah, U.S.A. In: Flint, S.S., Bryant, I.D. (Eds.), The Geological Modelling of Hydrocarbon Reservoirs and Outcrop Analogues. International Association of Sedimentologists, Special Publication, 15, pp. 21-56.

Shanley, K.W., Mc Cabe P.J., 1994. Perspectives on the sequence stratigraphy of continental strata: report of a working group at the 1991 NUNA Conference on High Resolution Sequence Stratigraphy. Bulletin of the American Association of Petroleum Geologists 74, 544-568.

Shen, Z., Törnqvist, T.E., Autin, W.J., Straub, K.M., Mauz, B., 2012. Rapid and widespread response of the Lower Mississippi River to eustatic forcing during the last glacial-interglacial cycle. Geological Society of America Bulletin 124, 690-704

Smith, G.A., 1994. Climatic influences on continental deposition during late-stage filling of an extensional basin, south-eastern Arizona. Geological Society of America Bulletin 74, 93-113.

Soil Survey Staff, 2014. Keys to Soil Taxonomy, 12th edition. USDA-Natural Resources Conservation Service, Washington, DC.

Somoza, L., Barnolas, A., Arasa, A., Maestro, A., Rees, J.G., Hernandez-Molina, F.J., 1998. Architectural stacking patterns of the Ebro delta controlled by Holocene high-frequency eustatic fluctuations, delta-lobe switching and subsidence processes. Sedimentary Geology 117, 11-32.

Starkel, L., Michczyńska, D.J., Gębica, P., Kiss, T., Panin, A., Perşoiu, I., 2015. Climatic fluctuations reflected in the evolution of fluvial systems of Central-Eastern Europe (60-8 ka cal BP). Quaternary International 388, 97-118.

Stefani, M., Vincenzi, S., 2005. The interplay of eustacy, climate and human activity in the late Quaternary depositional evolution and sedimentary architecture of the Po Delta system. Marine Geology 222-223, 19-48.

Storms, J.E.A., Weltje, G.J., Terra, G.J., Cattaneo, A., Trincardi, F., 2008. Coastal dynamics under conditions of rapid sea-level rise: Late Pleistocene to Early Holocene evolution of barrier-lagoon systems on the northern Adriatic shelf (Italy). Quaternary Science Reviews 27, 1107-1123.

Straffin, E.C., Blum, M.D., Colls, A., Stokes S., 2000. Alluvial stratigraphy of the Loire and Arroux Rivers, Burgundy, France. Quaternaire 10, 271-282.

Styllas, M., 2014. A simple approach to define Holocene sequence stratigraphy using borehole and cone penetration test data. Sedimentology 61, 444-460.

Ta, T.K.O., Nguyen, V.L., Tateishi, M., Kobayashi, I., Saito, Y., 2005. Holocene delta evolution and depositional models of the Mekong River delta, southern Vietnam. Society for Sedimentary Geology, Special Publication, 83, 453-466.

Tanabe, S., Saito, Y., Vu, Q.L., Hanebuth, T.J.J., Ngo, Q.L., Kitamura, A., 2006. Holocene evolution of the Song Hong (Red River) delta system, northern Vietnam. Sedimentary Geology 187, 29-61.

Tanabe, S., Saito, Y., Kimura, K., Hachinohe, S., Nakayama, T., 2008. Basal topography of the alluvium under the northern area of the Tokyo Lowland and Nakagawa Lowland, central Japan. Bulletin of the Geological Survey of Japan 59, 497-508.

Tanabe, S., Nakanishi, T., Ishihara, Y., Nakashima, R., 2015. Millennial-scale stratigraphy of tide-dominated incised valley during the last 14 kyr: Spatial and quantitative reconstruction in the Tokyo Lowland, central Japan. Sedimentology 62, 1837-1872.

Törnqvist, 1993. Holocene alternation of meandering and anastomosing fluvial systems in the Rhine-Meuse delta (central Netherlands) controlled by sea-level rise and subsoil erodibility. Journal of Sedimentary Research 63, 683-693.

Törnqvist, T.E., Wallinga, J., Murray, A.S., DeWolf, H., Cleverlinga, P., De Gans, W., 2000. Response of the Rhine-Meuse system (west-central Netherlands) to the last Quaternary glacio-eustatic cycles: a first assessment. Global and Planetary Change 27, 279-282.

Törnqvist, T.E., Wallinga, J., Busschers, F.S., 2003. Timing of the last sequence boundary in a fluvial setting near the highstand shoreline-insights from optical dating. Geology 31, 279-282.

Trincardi, F., Correggiari, A., Roveri, M., 1994. Late Quaternary transgressive erosion and deposition in a modern epicontinental shelf: the Adriatic Semienclosed Basin. Geo-Marine Letters 14, 41-51.

Vandenberghe, J., 2003. Climate forcing of fluvial system development: an evolution of ideas. Quaternary Science Reviews 22, 2053-2060.

Van Wagoner, J.C., 1995. Sequence stratigraphy and marine to non-marine facies architecture of foreland basin strata. Book Cliffs, Utah, U.S.A. In: Van Wagoner, J.C., Bertram, G.T. (Eds.), Sequence Stratigraphy of Foreland Basin Deposits. American Association of Petroleum Geologists Memoir, 64, pp. 137-223.

Vescovi, E., Kaltenrieder, P., Tinner, W., 2010. Late-Glacial and Holocene vegetation history of Pavullo nel Frignano (Northern Apennines, Italy). Review of Paleobotany and Palynology 160, 32-45.

Violante, R.A., Parker, G., 2004. The post-glacial maximum transgression in the de la Plata River and adjacent inner continental shelf, Argentina. Quaternary International 114, 167-181.

Vis, G.J., Kasse, C., Vandenberghe, J., 2008. Late Pleistocene and Holocene paleogeography of the Lower Tagus Valley (Portugal): effects of relative sea level, valley morphology and sediment supply. Quaternary Science Reviews 27, 1682-1709.

Vittori, E., Ventura, G., 1995. Grain size of fluvial deposits and late Quaternary climate: a case study in the Po River valley (Italy). Geology 23, 735-738.

Voges, A., 1995. International quaternary map of Europe. Bundestalt für Geowissenschaften und Rohstoffe (Unesco), Hannover, Germany.

Wellner, R.W., Bartek, L.R., 2003. The effect of sea-level, climate, and shelf physiography on the development of incised-valley complexes: a modern example from the East China Sea. Journal of Sedimentary Research 73, 926-940.

Whitloock, C., Bartlein, P.J., 1997. Vegetation and climate change in northwest America during the past 125 kyr. Nature 388, 57-61.

Zhang, G., Li, C., 1996. The fill and stratigraphic sequences in the Qintangjiang incised paleo-valley, China. Journal of Sedimentary Research 66, 406-414.

5.3. Paper 3 (Study area 3)

The value of pocket penetration tests for the high-resolution stratigraphy of late Quaternary deposits*

Alessandro Amorosi, Luigi Bruno, ***Bruno Campo***, Anese Morelli

* Geological Journal, v. 50 (2015), pp. 670-682

The value of pocket penetration tests for the high-resolution stratigraphy of late Quaternary deposits

Alessandro Amorosi[a]*, Luigi Bruno[a], ***Bruno Campo***[a], Anese Morelli[a]

[a]*Dipartimento di Scienze Biologiche, Geologiche e Ambientali, University of Bologna, Bologna, Italy*

*Correspondence to: A. Amorosi, Dipartimento di Scienze Biologiche, Geologiche e Ambientali, University of Bologna, Via Zamboni 67, 40127 Bologna, Italy. E-mail: alessandro.amorosi@unibo.it

Telephone: +39 - 0512094586

FAX: + 39 - 0512094522

Abstract

Pocket penetrometer measurements, though commonly listed as accessory components of core descriptions, are almost totally ignored in shallow subsurface stratigraphic analysis. In this study, we prove that, if properly calibrated with core data, pocket penetration tests may serve as a quick and inexpensive tool to enhance high-resolution (palaeosol-based) stratigraphy of unconsolidated, late Quaternary non-marine deposits. A palaeosol sequence, made up of 12 vertically stacked, weakly developed palaeosols (Inceptisols) dated to the last 40 ky cal BP, is reconstructed from the subsurface of the southern Po Plain. The individual palaeosols exhibit flat to slightly undulating geometries and several of them can be tracked over distances of tens of km. They show substantially higher compressive strength coefficients than all other fine-grained, alluvial (floodplain) facies, being typified by distinctive penetration resistance, in the range of 3.5-5 kg/cm^2. Along the palaeosol profiles, A and Bk horizons demonstrate consistent difference in relative compressive strengths, the highest values being invariably observed at the A/Bk boundary. Palaeosols are rarely described in conventional stratigraphic logs, and just a small proportion of them is likely to be identified by geologists with no specific sedimentological training. Through core-log calibration techniques, we document that vertical profiles of penetration resistance measured in the field can be used as an efficient method for palaeosol identification, and thus may represent a strategy for predicting stratigraphic architecture from limited core descriptions or poor-quality field logs. This technique allows to optimize the contribution of all available stratigraphic information, expanding significantly the coverage of well-described, one-dimensional core data.

Keywords: pocket penetrometer; palaeosol; alluvial stratigraphy; Quaternary; Po Plain

1. Introduction

Reconstructing the high-resolution facies architecture of the late Quaternary successions buried beneath the modern alluvial plains is an increasingly important issue for stratigraphic modeling of more ancient successions (Blum and Törnqvist, 2000; Blum *et al.*, 2013). In shallow subsurface exploration programs, however, extensive core data are needed to obtain sufficient stratigraphic information, and

drilling commonly represents the most expensive part of the whole exploration campaign. In this regard, the acquisition of a comprehensive dataset including all available stratigraphic information is essential to plan future investigations, and an appropriate level of detail of the stratigraphic description can have far-reaching implications for the success of a project.

In densely populated areas, such as the modern alluvial and coastal plains, a large number of core descriptions is commonly available. However, the overall quality of field logs may vary appreciably. Geotechnical core logging generally incorporates simple lithologic descriptions that are hardly suitable for facies interpretation and, consequently, for high-resolution stratigraphy. Delineating subsurface stratigraphy through indirect methods of subsurface investigation, such as those based upon geotechnical engineering properties of soils, may partly compensate for this lack of appropriate stratigraphic descriptions.

The high potential of geotechnical data for the high-resolution stratigraphy of unconsolidated Quaternary deposits has been illustrated by Amorosi and Marchi (1999), who showed that piezocone penetration tests can be used for the detailed characterization of distinct coastal plain, deltaic and shallow-marine facies associations. The same technique was successfully applied by Lafuerza *et al.*, (2005), Choi and Kim (2006), Sarti *et al.* (2012), and Styllas (2014), proving to be useful for the high-resolution sequence stratigraphic analysis and three-dimensional reconstruction of alluvial to coastal successions. Based on the same conceptual criteria, we document in this paper that, if proper calibration with core data is carried out, the use of simple pocket penetrometer resistance, a supplementary information normally available from most core descriptions, can be of use to a log analyst for stratigraphic profiling. Pocket penetrometer may provide almost continuous record of *in situ* properties of soils. This tool has been used for reliable assessment of the effects of compaction on soil productivity (Steber *et al.*, 2007), to estimate threshold friction velocity of wind erosion in the field (Li *et al.*, 2010), and for stratigraphic and geotechnical investigations (Brideau *et al.*, 2011).

Palaeosols have long been recognized as key features for subdivision and mapping of continental strata on a variety of time scales (Bown and Kraus, 1981; Retallack *et al*., 1987; Besly and Fielding, 1989; Joeckel, 1991; Kraus, 1999; Atchley *et al*., 2004; Rossetti, 2004; Choi, 2005; Buck *et al*., 2010), and sequence-stratigraphic models have predicted the presumed position of palaeosols within non-marine deposits (Van Wagoner *et al.*, 1990; Hanneman and Wideman, 1991; Wright and Marriott, 1993; Cleveland *et al.*, 2007; Mack *et al.*, 2010; Gibling *et al*., 2011; Varela *et al.,* 2012). One of the most prominent features are palaeosols formed at interfluve sequence

boundaries, i.e., adjacent to palaeovalley systems (Aitken and Flint, 1996; McCarthy and Plint, 1998).

In this paper, we demonstrate that late Quaternary palaeosols can often be identified on the basis of geotechnical properties generated from simple pocket penetrometer values (Bradford, 1980). The southern Po Plain, for which a palaeosol-based stratigraphic framework has been recently made available (Bruno *et al.*, 2013; Amorosi *et al.*, 2014), represents an intriguing opportunity to investigate subsurface stratigraphy based on this approach. To this purpose, we selected a mud-prone, distal alluvial succession between the basin margin and the Po channel belt, with specific focus on the interfluve between Panaro and Reno rivers (Fig. 1). We strategically chose this area because of lack of laterally continuous fluvial bodies that could be utilized as stratigraphic markers.

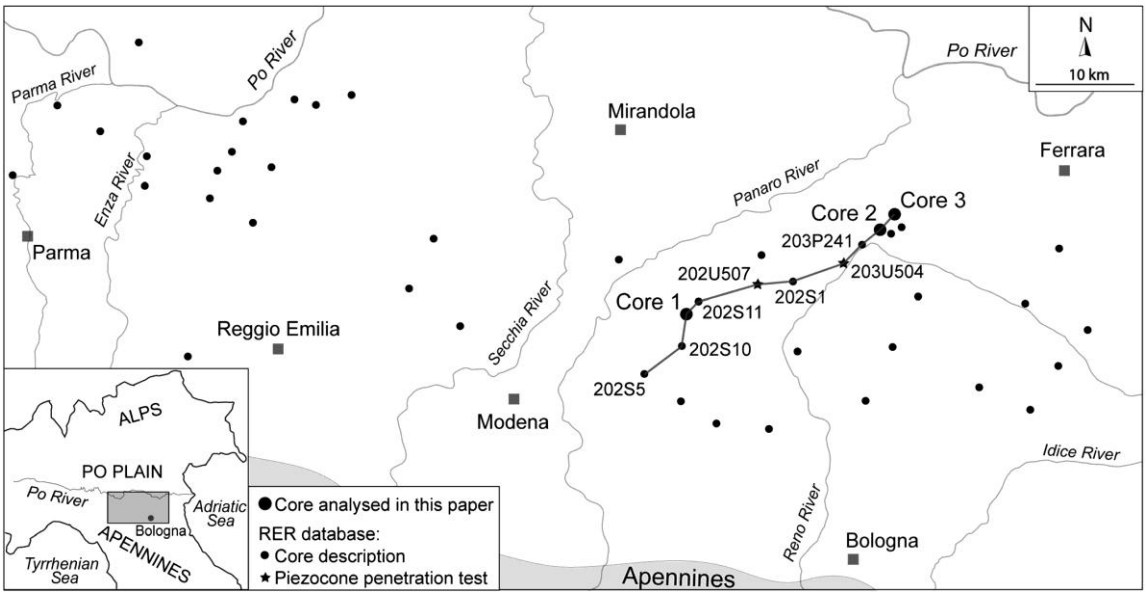

Fig. 1 - Study area, with indication of the section trace of Figures 5 and 6. The RER (Emilia-Romagna Geological, Seismic and Soil Survey) database was used to assess the engineering properties of palaeosols in Figure 7.

2. Regional geological setting

The Po Plain is a rapidly subsiding foreland basin, bounded by the Alps to the north and the Apennines to the south (Fig. 1). The formation of the Apenninic fold-and-thrust belt took place since the Late Oligocene (Ricci Lucchi, 1986; Boccaletti *et al*., 1990) in the framework of the collision of the European plate with the Adria microplate (Boccaletti *et al.*, 1971; Ghielmi *et al.*, 2013), when the sedimentary successions of the subducting margin of Adria were piled up to form the Apenninic accretionary prism (Carminati and Vadacca, 2010). The filling of the Pliocene-Pleistocene Apennineic foredeep has been estimated to exceed 7,000 meters in the thickest depocentres (Pieri and Groppi, 1981). The North Apenninic frontal thrust system, buried below the

southern margin of the Po Plain makes this area seismically active, as confirmed by the recent M 5.9-6.0 earthquakes of May-June 2012. Several active thrust faults have been recognized, such as the Ferrara and Mirandola growing anticlines, this latter with an uplift of ca. 0.16 mm/y in the last 125 ky (Carminati and Vadacca, 2010).

Extensive subsurface investigations carried out during the last two decades with the aim of establishing a general framework of aquifer distribution have led to accurate reconstruction of the large-scale, subsurface stratigraphic architecture of the Pliocene-Quaternary basin fill (Di Dio, 1998; Carcano and Piccin, 2002). Six depositional sequences were identified south of Po River (Di Dio, 1998; Molinari *et al.*, 2007) and four north of Po River (Carcano and Piccin, 2002). These depositional sequences, recognized on a seismic basis and typically bounded by stratigraphic unconformities of tectonic origin, correspond to 3rd-order depositional sequences in the sense of Mitchum *et al.* (1977). The lower boundary of the youngest depositional sequence (Po Supersynthem of Amorosi *et al.*, 2008) has an estimated age of 0.87 My (Muttoni *et al.*, 2003), and is partitioned into eight lower-rank (4th-order) depositional cycles (transgressive-regressive – T-R – cycles of Amorosi and Colalongo, 2005 – see Fig. 2).

Pollen characterization of the youngest two T-R cycles has documented a glacio-eustatic control on facies architecture, with a major influence of Milankovitch-scale eccentricity (ca. 100 ky) cycles (Amorosi *et al.*, 1999, 2004, 2008). The T-R cycles are best recognized beneath the modern coastal plain and the delta, where typical transgressive-regressive coastal wedges form the transgressive and highstand systems tracts (TST+HST in Fig. 2). These shallow-marine bodies are separated by thick packages of alluvial deposits (falling-stage and lowstand systems tracts – FST+LST), the accumulation of which was favoured by tectonic subsidence.

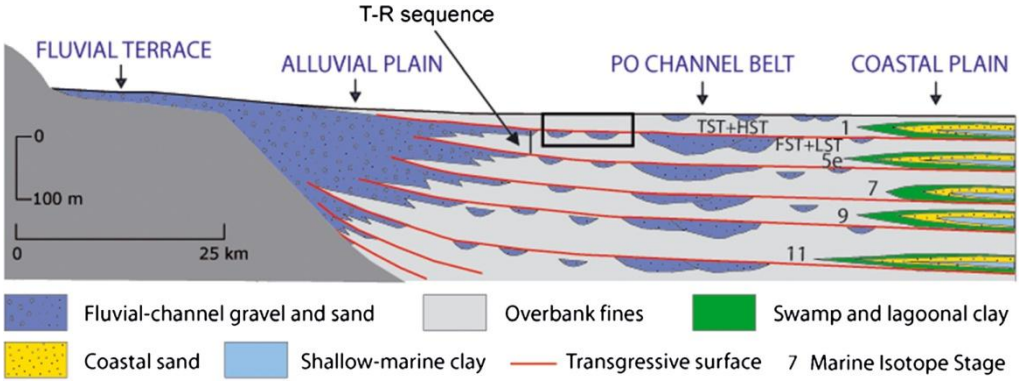

Fig. 2 - Transgressive-regressive (T-R) cycles in the subsurface of the Po Plain and their sequence-stratigraphic interpretation (from Amorosi et al., 2014). The red lines represent the transgressive surfaces. The lower parts of the T-R cycles have a typical interglacial (transgressive/highstand systems tracts - TST+HST) signature, and are marked by diagnostic coastal wedges in lateral transition to mud-prone alluvial deposits. The upper parts of the T-R cycles, formed under glacial conditions (falling stage/lowstand systems tracts - FST+LST), display increasingly amalgamated fluvial bodies. The black rectangle shows approximate position of the stratigraphic correlation panel of Figure 5.

In proximal positions, close to the basin margin, the T-R cycles consist of basal overbank facies with isolated fluvial-channel sand deposits. Upwards, the fluvial bodies become increasingly abundant, amalgamated and laterally continuous. Based upon pollen data (Amorosi *et al.*, 2008), the transgressive surfaces (or maximum regressive surfaces of Catuneanu *et al.*, 2009) separate lowstand, glacial deposits from overlying deepening-upward (brackish to shallow-marine) successions formed under interglacial conditions. Landwards, these surfaces can be traced approximately at the boundary between laterally-amalgamated and isolated fluvial bodies (Fig. 2). The lower parts of the T-R cycles are interpreted to represent the response of fluvial systems to rapid sea-level rise (equivalent of marine isotope stages 1, 5e, 7, 9 and 11, respectively, in Fig. 2 – Amorosi *et al*., 2004, 2008).

3. Materials and methods

Pocket penetrometer is a lightweight, handy tool that is commonly used for geotechnical purposes during coring operations. Its primary source of information is for evaluating consistency and approximate unconfined compressive strength. When pushing the loading piston into a freshly cut core, the pin encounters a force. A friction ring is taken along during this operation, which shows on the scale the maximum force that has been encountered. The direct reading scale, commonly ranging between 0 and 5 kg/cm^2 (up to 10), corresponds to equivalent unconfined compressive strength.

In order to test our approach of using penetration tests for palaeosol identification and high-resolution stratigraphic reconstructions, we selected a distal, mud-dominated portion of the alluvial plain, away from the influence of the major rivers (i.e., the Po channel belt) and far from the thick, fluvial gravel bodies of the Apenninic margin (Fig. 2). Three freshly drilled cores from the Modena and Ferrara alluvial plain (Cores 1-3 in Figs. 1 and 3), 40-50 m long, were used as reference for facies analysis and palaeosol characterization. Coring was performed through a continuous perforating system, which guaranteed an undisturbed core stratigraphy. We also selected 40 out of 250 detailed field logs from the database of the Emilia-Romagna Geological, Soil and Seismic Survey (RER), covering a wider area (Fig. 1). Lithology, colour, and accessory components is the typical information available for each borehole. We adopted availability of the following key aspects as decisive for borehole selection: (i) pocket penetration values, (ii) colour description, (iii) reaction to HCl, (iv) ^{14}C dating, (v) pollen data, (vi) photographs. Pocket penetration values, available uniquely from fine-grained (silt and clay) stratigraphic intervals, were stored in a specific, geo-referenced database and plotted as vertical profiles on the individual logs. In order to perform stratigraphic

correlations within the time window of radiocarbon dating, we adopted a 40 m depth cut-off. Beyond this depth, penetration values appear to be affected by over-compaction.

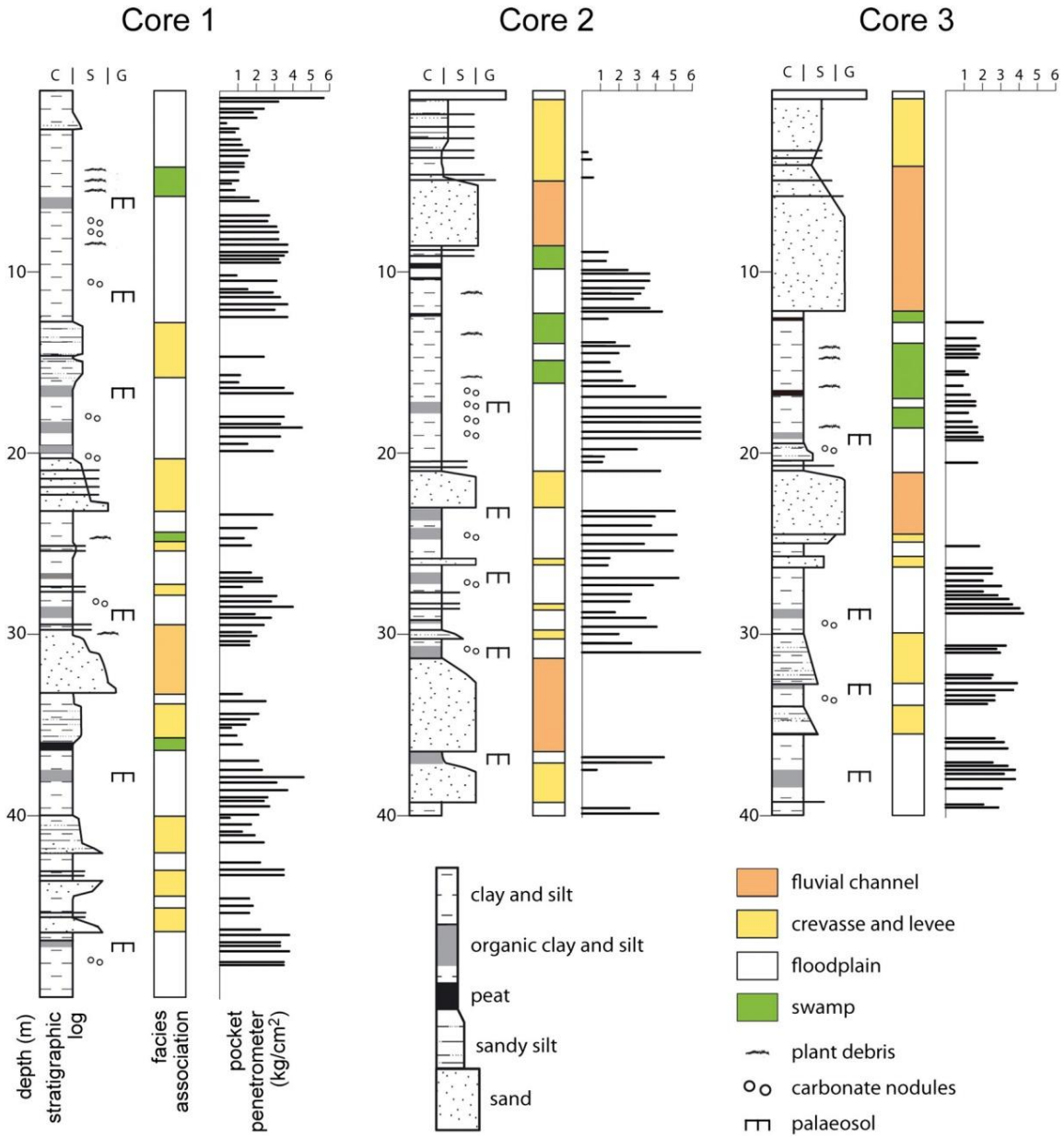

Fig. 3 - Detailed stratigraphy of reference cores 1 to 3, including facies interpretation, pocket penetration profiles and stratigraphic position of the 15 palaeosols identified. See Figure 1, for location. Paleosols are fingerprinted by the highest penetration values. C: clay, S: sand, G: gravel.

4. Sedimentary facies

In order to evaluate the relationships between depositional facies and resistance to penetration, detailed facies analysis and pocket penetrometer measurements were undertaken on three reference cores (cores 1-3 in Fig. 3). Five facies associations

were distinguished on the basis of grain size trends, accessory components, colour and consistency.

4.1. Fluvial-channel facies association

Description. This facies association is made up of single-storey, coarse to medium sand bodies, up to 6 m thick, with erosional lower boundaries (Fig. 4a) and internal fining-upward (FU) trends. The upper boundary to the overlying muds is either sharp or gradational. Pebble layers and wood fragments are locally abundant in the lower part of the unit. No fossils were observed in this facies association. Locally preserved sedimentary structures include unidirectional high-angle cross-stratification. Pocket penetration tests do not operate in sands, and for this reason no penetration values are available from this facies association.

Interpretation. The combination of textural properties, FU trends, erosional base and sedimentary structures enables interpretation of this facies association as fluvial-channel deposits. This interpretation is supported by the presence of unidirectional flow structures and abundance of floated wood. The sharp boundary to the overlying mud-prone deposits reflects abrupt channel abandonment, whereas transitional contacts suggest gradual abandonment. Simple core examination does not allow subdivision of this facies. As a whole, single-storey sand bodies are likely to represent point bar deposits.

4.2. Crevasse and levee facies association

Description. This facies association consists of fine sand bodies, generally less than 1.5 m thick, and silts and silty sands alternating on a cm scale (Fig. 4b). The sand layers exhibit (i) sharp base and gradual top, with internal FU trends, or (ii) gradual transition from the underlying muds, with sharp top and coarsening-upward (CU) tendency. Compressive strength coefficients derived from pocket penetration tests measured on silt intervals are invariably < 2.5 kg/cm^2.

Interpretation. The highest sand/mud ratios recorded within this facies association are interpreted to reflect proximity to fluvial channels. In particular, sand layers with sharp base and gradual transition to the overlying muds are interpreted to have been deposited in crevasse channels, while sand layers with gradual base and sharp top are likely to reflect crevasse splays. Heterolithic units made up of silt-sand intercalations

are interpreted as natural levee deposits, with sand proportion decreasing with increasing distance from the channel axis.

4.3. Floodplain facies association

Description. This facies association is made up of a monotonous succession, up to 9 m thick, of thoroughly bioturbated, variegated (5YR 8/1, 2.5Y 7/2-5, 5Y 6/1) silts and clays (Fig. 4b). Roots and plant remains are commonly encountered. Iron and manganese oxides are abundant. No sedimentary structures were observed, with the exception of faint horizontal lamination. Concentration of organic matter is locally encountered. Thin very fine sand beds with sharp base were occasionally seen. Pocket penetration values for this facies association commonly are in the range of 1.5 and 2.5 kg/cm^2 (average value 2.0 kg/cm^2).

Interpretation. Based on the dominance of bioturbated and oxidized muds, this facies association is interpreted to reflect background deposition of mud from suspension, in a low-energy, subaerially exposed depositional environment (floodplain). Lack of sedimentary structures is due to bioturbation. Local grey, organic-rich clays are likely to reflect areas of low topographic relief with poor drainage and high water table. The thin sand layers reflect the distal fringes of either crevasse splays or levee deposits.

4.4. Freshwater swamp facies association

Description. Soft grey and dark grey clays (7.5YR 7/1, 5YR 5/1), with subordinate silts and sandy silts compose this facies association, up to 1.8 m thick. Plant debris, wood fragments and peat layers are frequently encountered (Fig. 4c). Vertical variations in grain size, at a few cm scale, and thin organic-rich layers confer a characteristic horizontal lamination to this facies association. Extremely rare carbonate concretions are encountered. Iron and manganese oxides are absent. This facies association is typified by very low pocket penetrometer values, almost invariably lower than 1.2 kg/cm^2 (Fig. 3).

Interpretation. Organic soft clays with abundant plant fragments are interpreted to have been deposited in paludal environments under predominantly reducing conditions. Horizontal lamination is inferred to be the result of the progressive accumulation of organic material, interrupted by occasional flood events. Very low

resistance penetration values reflect undrained conditions and submergence. Temporary phases of subaerial exposure, with consequent lowering of the water table, are inferred to have been responsible for local hardening of the clay and the formation of scattered carbonate concretions.

4.5. Palaeosols

Description. Visual examination and manipulation of cores 1-3 with respect to colour, texture and plasticity led to recognition of 15 relatively stiff clay horizons, intercalated at various stratigraphic levels within floodplain deposits (Fig. 3). These clay horizons are commonly identified by the combination of dark, brownish (10YR 3/2, 2.5Y 3/1) colour and no reaction with acid. The organic clay generally overlies, with gradual transition, lighter (10YR 8/2, 2.5Y 8/2), iron mottled clays and silts, rich in carbonate concretions (Fig. 4d-e). The organic horizons and the associated carbonate-rich clays are typified by substantially higher penetration values than those recorded in the overlying and underlying floodplain clays (Fig. 3). In particular, the darker horizons display average coefficients of compressive strength around 3.5 kg/cm^2, while the underlying carbonate-rich horizons are even more consolidated (average penetration values 3.9 kg/cm^2). An abrupt increase in compressive strength, of at least 1 kg/cm^2 relative to the overlying deposits, commonly marks the upper boundary of the organic layers (Fig. 3).

Interpretation. Based on field observations, the indurated horizons are interpreted as weakly developed palaeosols (Inceptisols of Soil Survey Staff, 1999), marking short-lived phases of subaerial exposure, on the order of 3,000-4,000 thousands of years (Amorosi et al., 2014). The Inceptisols are mostly developed on floodplain muds and seem to alternate rhythmically with non-pedogenized, heterolithic intervals of small channel belts and crevasse/overbank facies. The dark, organic-rich clays reflect accumulation of organic matter and leaching of calcium carbonate in topsoil (A) horizons. The underlying clays include pedogenic calcium carbonate, and are inferred to represent Bk or calcic horizons, subject to fluctuating redox conditions and processes of iron dissolution and redeposition. Highly compacted sediments of pedogenic origin, with similar sedimentological features and unconfined compressive strength coefficients of about 4-5 kg/cm^2, have been reported about 120 km NE of the study area, from the subsurface of the Venice lagoon (Donnici *et al*., 2011). In humid to subhumid climates, Inceptisols similar to those observed in cores 1 to 3 have been

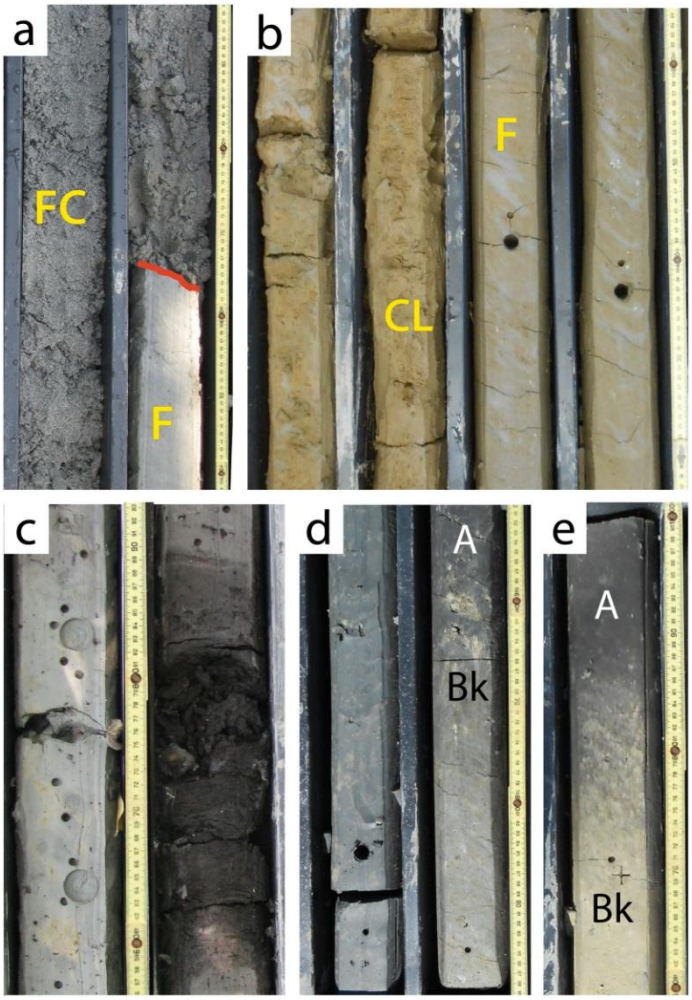

interpreted to represent subaerial exposure of a few thousands of years only (Retallack, 2001; Buol *et al.*, 2011).

Fig. 4 - Representative core photographs of the study succession (bottom: lower right corner). a: Erosional lower boundary of a fluvial-channel sand body (FC) above floodplain clays (F). b: Floodplain clays (F) gradually overlain by crevasse/levee sandy silts (CL). c: Freshwater swamp clays and peat. d: Inceptisol (with differentiation into A and Bk horizons) overlain by floodplain silts and clays. Core 2, 17-18 m depth (palaeosol D in Fig. 6). e: Close-up of an Inceptisol, with subdivision into A and Bk horizons. Core 2, 27 m depth (palaeosol G in Fig. 6). Core width is 10 cm.

5. Stratigraphic architecture

Reconstructing the stratigraphic architecture of distal alluvial plain successions is a very difficult task. In this particular fluvial setting, sand bodies are mostly ribbon-shaped and lack of laterally continuous marker horizons may represent a strongly inherent limitation to stratigraphic correlations. Subsurface stratigraphy in the study area was tentatively reconstructed along an approximately SW-NE oriented, 35 km-long transect (Fig. 5), on the basis of accurate facies analysis of three continuous cores (Fig. 3), and with the aid of five conventional field logs. Standard core descriptions were converted to facies association (Fig. 5) using sedimentological concepts that incorporated the simple lithologic information available with a list of accessory components. The chronological framework was partly constrained by eight radiocarbon dates (Fig. 5).

Strong uncertainties associated with stratigraphic correlation affect the accuracy of facies architecture reconstruction in Figure 5. In particular, low data density combined

with poor-quality stratigraphic data make the reconstruction of subsurface stratigraphy problematic, and several alternative stratigraphic scenarios could be generated on the basis of the data available. Palaeosols, distinctive features that could potentially act as marker horizons, are clearly identified within reference cores 1-3, where their relatively low maturity indicates short stratigraphic breaks in rapidly aggrading deposits. In contrast, they are almost totally neglected by the available core descriptions, with the sole exception of core 202S1 (Fig. 5). Owing to difficult correlation between wells, palaeosols appear as highly discontinuous features and cannot be integrated into a well-defined architectural framework.

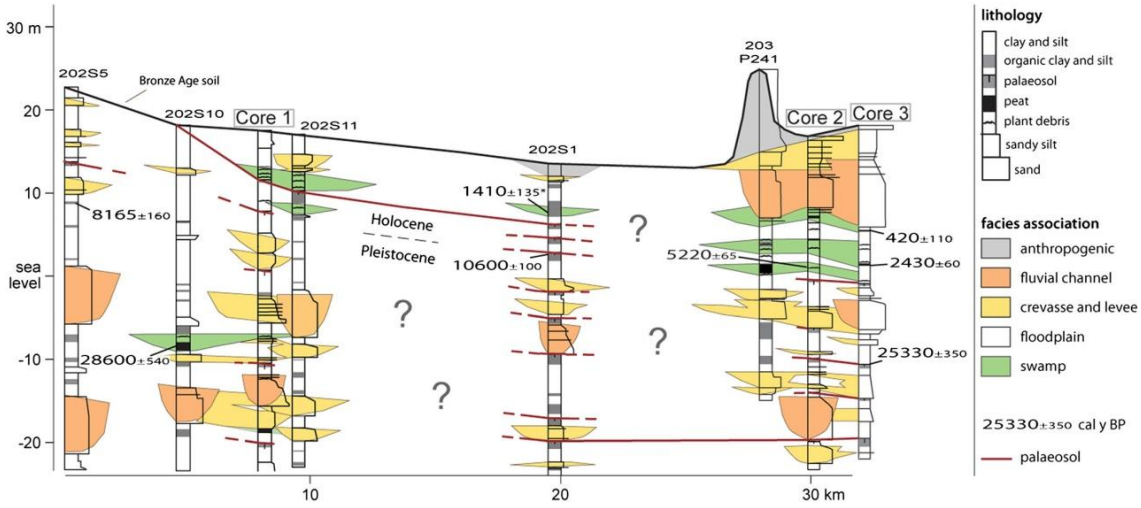

Fig. 5 - Stratigraphic correlation panel across the study area, showing stratigraphic architecture of distal alluvial plain deposits based upon facies analysis of cores 1-3, facies interpretation of five core descriptions, and eight radiocarbon dates (the asterisk indicates one radiocarbon date projected from outside the section profile). Palaeosols are poorly identified by standard core descriptions (with the sole exception of core 202S1), and cannot be used as reliable stratigraphic markers. For section trace, see Fig. 1.

A marked change in fluvial architecture is observed approximately across the Pleistocene-Holocene boundary (Fig. 5), which marks an abrupt upward decrease in the proportion of fluvial-channel bodies (and related overbank and crevasse sandy deposits). The individual sand bodies are generally 3-8 m thick and appear to cluster at two distinct stratigraphic levels (between +2 and -6 m a.s.l., and between -12 m and –20 m a.s.l., respectively, in Fig. 5). Fluvial bodies are mostly isolated in the overlying Holocene section, where they are associated to an abundance of swamp clays. The greater lateral continuity of the late Pleistocene channel-related deposits suggests deposition during phases of slowed accommodation. Based on the age of these deposits (Fig. 5), we assign the major sand bodies to the last phases of sea-level fall (late forced-regressive systems tract or FST in Fig. 2) and to the lowstand systems tract (LST in Fig. 2). Owing to poor data coverage (average borehole spacing is ca. 4.5 km, i.e., remarkably greater than the width of the individual channel bodies), we cannot constrain precisely the lateral extension of fluvial sand bodies, nor their hypothetical

connectivity. As a consequence, channel-belt geometries in the cross-sections of Figure 5 represent a main uncertainty, and are highly speculative.

Upwards, the abrupt change from sand bodies with possible high degree of interconnectedness, to predominantly muddy units, with mostly isolated, ribbon-shaped sand bodies, reflects a sudden drop in the sediment supply/accommodation ratio (Dreyer, 1993; Shanley and McCabe, 1994; Martinsen *et al.*, 1999; Huerta *et al.*, 2011), which may testify the sedimentary response to the Holocene sea-level rise (cf. Olsen *et al.*, 1995; Posamentier et Allen, 1999; Ainsworth, 2010). In terms of sequence stratigraphy, this part of the sedimentary succession includes the TST+HST (Fig. 2).

6. Inferring palaeosols from conventional core descriptions

It is readily apparent from the stratigraphic panel of Figure 5 that key features for alluvial architecture, such as palaeosols, can be easily missed in conventional field logs. As a result, standard core descriptions have considerably lower potential for cross-correlations of alluvial deposits than those performed by an experienced sedimentologist (see reference cores 1-3 in Fig. 3). In this context, specific physical characteristics and engineering properties that can be extracted from routine core descriptions, such as simple lists of pocket penetration values, appear as a powerful tool to reduce significantly stratigraphic uncertainty. With specific reference to the 15 weakly developed palaeosols identified in cores 1-3, attributes that are commonly reported by geotechnical data sheets and that can be used for palaeosol identification include (Fig. 3):

1. Colour. All Inceptisols identified in the study area have dark brown to black coloured ‘A’ horizons, underlain by lighter, calcic ‘Bk’ horizons (Fig. 4d-e). This diagnostic palaeosol horizonation can often be deduced from conventional stratigraphic descriptions.
2. Soil reaction to dilute hydrochloric acid. In the visual classification scheme developed by the Emilia-Romagna Geological, Soil and Seismic Survey for testing the carbonate content by effervescence of reaction, which incorporates five categories (from 0 = acid unreactive, to 4 = violent HCl reaction, with bubbles forming immediately), the ‘A’ horizons invariably fall into lowest category (0), while the underlying ‘Bk’ horizons show the highest reaction with acid (class 4). As a consequence, where ‘0’ category is found to overlie a ‘4’ class, the two adjacent horizons are strongly suspected to represent an Inceptisol.

3. Diagnostic penetration values. A wide range of compressive strength coefficients typifies the alluvial succession investigated in this study. However, while non-pedogenized floodplain deposits invariably display pocket penetration values lower than 3 kg/cm^2, with average value of 2.0 kg/cm^2 (Fig. 3), the 15 palaeosols recognized in cores 1-3 display remarkably higher average values, of 3.5 kg/cm^2 (A horizon) and 3.9 kg/cm^2 (Bk horizon), respectively (Fig. 3).

Re-examination of the existing stratigraphic logs on the basis of the above features, with special emphasis on vertical pocket penetration profiles, results in identification of a significantly higher number of potential palaeosols. The correlation panel of Figure 6, which traces out the same cross-section of Figure 5, highlights the influence of penetration test interpretation on well-to-well palaeosol correlations. If plotted as vertical profiles, pocket penetration values within alluvial deposits reveal a clearly defined set of stiff, highly compacted horizons, where compressive strengths are generally > 3 kg/cm^2, and across which penetration values show abrupt increase of 1 to 2 kg/cm^2 (Fig. 6). The palaeosols recognized on the basis of compressive strength profiles are stratigraphically well correlatable with those identified in cores 1-3 (Fig. 6).

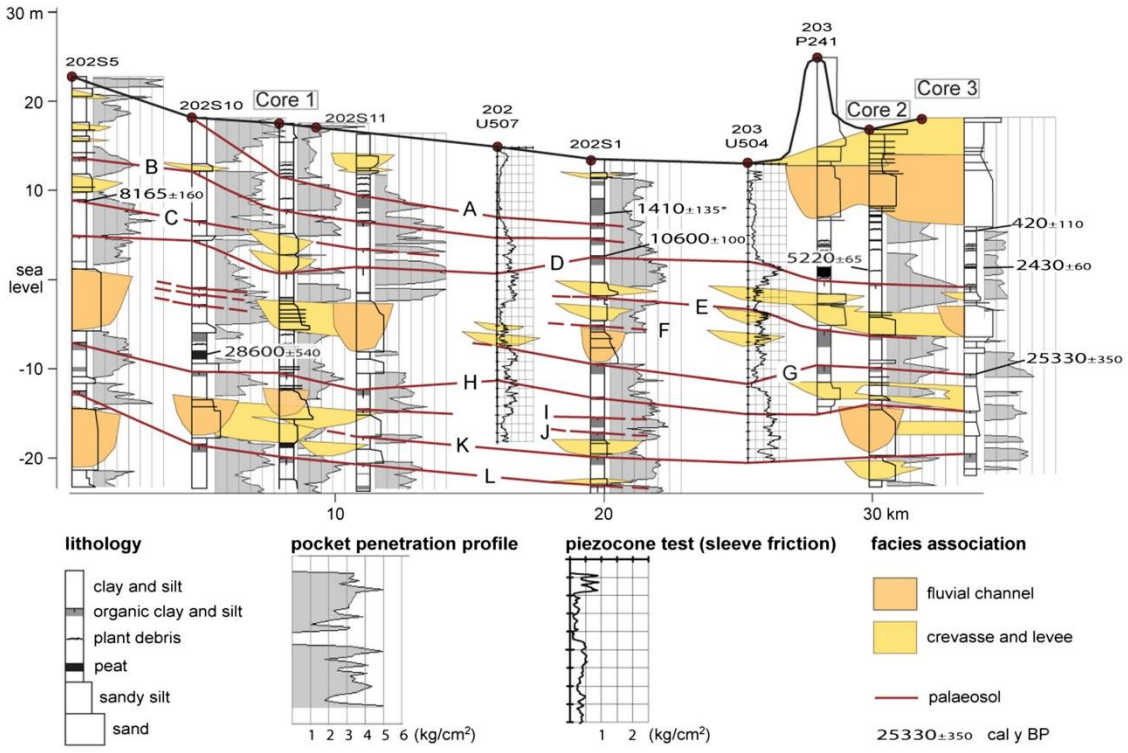

Fig. 6 - Same cross-section as Figure 5, with re-interpretation of stratigraphic architecture on the basis of palaeosol stratigraphy. Palaeosols are identified via pocket penetration profiles calibrated with reference cores 1-3. For section trace, see Fig. 1.

Consistent with recent observations from the subsurface of Bologna (Amorosi *et al*., 2014), about 30 km SE of the study area, twelve prominent Inceptisols (A to L in Fig. 6)

represent the key stratigraphic features of the study succession. These palaeosols display relatively flat to slightly undulating geometries, which may reflect antecedent topography, lateral changes in sediment compaction, or both. Several palaeosols can be tracked over distances of tens of km on the basis of pedogenic features, stratigraphic position and radiometric dating (see the caranto palaeosol of the adjacent Venetian-Friulian Plain – Fontana *et al*., 2008; Donnici *et al*., 2011). In general, palaeosols assessed using pocket penetration values represent laterally extensive marker horizons that can be used for bracketing packages of stratigraphic significance.

The resulting palaeosol-bounded depositional units are approximately 3-5 m thick, and appear to have been developed during time intervals of a few thousand years, which could reflect interacting millennial-scale glacio-eustatic and climatic control during the late Quaternary (see Blum and Price, 1998). In this stratigraphic scenario, where palaeosols are used to guide interpretation of facies distribution, channel bodies appear to be clustered at more than two stratigraphic intervals (compare Figures 5 and 6), hence providing the basis for a more realistic stratigraphic scenario and for detailed reconstruction of channel migration pathways through time. When traced laterally over lenticular fluvial bodies, palaeosols become progressively less pronounced, appear to merge in a complex manner, and eventually disappear (Fig. 6). Unfortunately, limited data density and lack of geophysical profiles (see the use of ground-penetrating radar of Bennett *et al.*, 2006, as an example) hamper the accurate investigation of the relationships between palaeosol formation and channel-belt development.

Using the same combination of colour, carbonate content and distinctive pocket penetrometer signature as diagnostic criteria for palaeosol identification, we performed the re-interpretation of 40 core descriptions from the Regione Emilia-Romagna database (see Fig. 1, for cores location), from which a total of 39 palaeosols had been reported. This re-interpretation led to recognition of 118 (inferred) Inceptisols. Compressive strength coefficients across both non-pedogenized floodplain deposits and interpreted ‘A’ and ‘Bk’ horizons are consistent with those observed from reference cores 1-3 (Fig. 7). In particular, pocket penetration values from organic-rich (‘A’) horizons are centered at 3.0 kg/cm^2, whereas calcic (‘Bk’) horizons show a modal value of 3.5 kg/cm^2. The ‘normal’, non-pedogenized floodplain deposits exhibit remarkably lower compressive strength (average value 2.0 kg/cm^2).

Although we cannot place absolute confidence in our interpretations of the geotechnical dataset, and thus slight palaeosol overestimation is possible, the remarkably (three times) higher number of palaeosols recognized through our technique suggests that simple re-examination of available core descriptions in terms

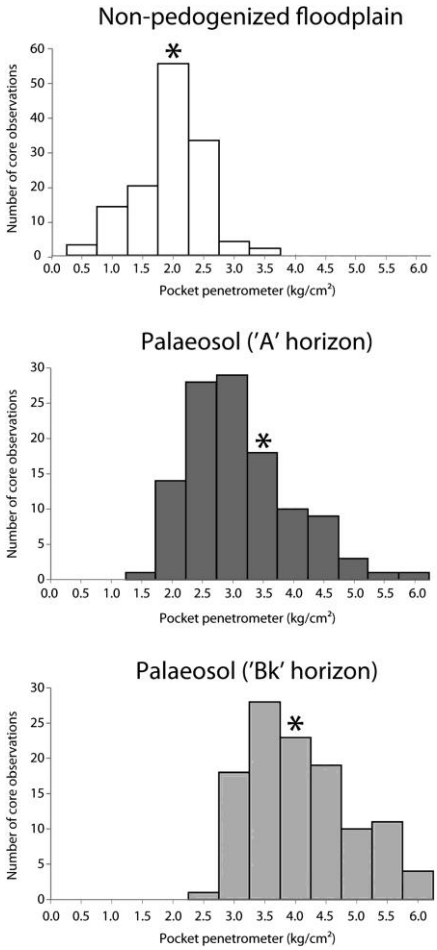

of colour, carbonate content and pocket penetration profiles might lead to considerable refinement of stratigraphic architecture in the study area (compare Fig. 6 with Fig. 5).

Fig. 7 - Histograms of soil strength (pocket penetrometer) estimates obtained from 40 core descriptions of the RER database (see Fig. 1 for cores location), including 120 non-pedogenized floodplain core observations and 118 palaeosols, subdivided by A/Bk horizons. Asterisks refer to the average pocket penetration values obtained from the same depositional facies in reference cores 1-3.

7. Compressive strength properties of palaeosols

We have documented that the late Quaternary Inceptisols of the southern Po Plain exhibit distinctive geotechnical signature, being characterized invariably by higher penetration values than non-pedogenized floodplain deposits. A sharp increase in penetration values is generally recorded atop the pedogenized horizons: this feature is due to exposure to a few thousand years of subaerial conditions, which made the sediment surface desiccated and unsaturated, resulting in considerable increase in compressive strength.

Pedogenically modified muds with high compressive strengths have been reported from several papers, with values 2-4 times higher than that of the overlying unexposed deposits (Park *et al.*, 1998; Choi and Kim, 2006). In the study area, pocket penetration tests proved to be highly sensitive to palaeosol identification (Donnici *et al.*, 2011), with compressive strengths commonly 1.5-2.5 times higher than those recorded from the overlying/underlying floodplain deposits (Figs. 3 and 7).

Although, in general, palaeosols are easy to identify by their highly consolidated nature, vertical changes in physical properties through individual palaeosol horizons appear to follow complex patterns. Previous interpretations of (piezo)cone penetration tests across palaeosol-bearing successions have shown that the upper boundaries of palaeosols may appear as gradational and defined as zones, rather than sharp surfaces (Amorosi and Marchi, 1999; Choi and Kim, 2006). The same can be said for the pocket penetration signature of palaeosols (compare with Figs. 3 and 6). Despite a certain variability of soil types and wide range of penetrometer resistance, a consistent increase of penetrometer measurements is recorded at the boundary between non-

pedogenized and pedogenized deposits (top A horizon – Figs. 7 and 8). The compressive strength, however, is even higher at the boundary between the A horizons and the underlying Bk horizons (Figs. 7 and 8).

Owing to this two-step increase in pocket penetrometer resistance, palaeosols are likely to offer two slightly offset images (on the order of 30-50 cm), each representing the different perspective of a distinct viewer. While on one hand a soil specialist would define a palaeosol on the basis of its horizonation, thus placing its top at the upper boundary of the A horizon, an interpreter of geotechnical profiles could be inclined to place the top of the same palaeosol in a lower position, at the A/Bk boundary, i.e., where compressive strength is highest (Fig. 8). The lower compressive strengths values invariably recorded in the A horizons relative to the Bk horizons could reflect: (i) temporary re-saturation of the uppermost palaeosol at time of burial, (ii) a simple weathering effect, which would contribute to the softening of the soil through an increase in soil moisture and physical disruption (Choi and Kim, 2006), (iii) the presence of diffuse carbonate concretions, which might enhance the resistance values of the Bk horizon.

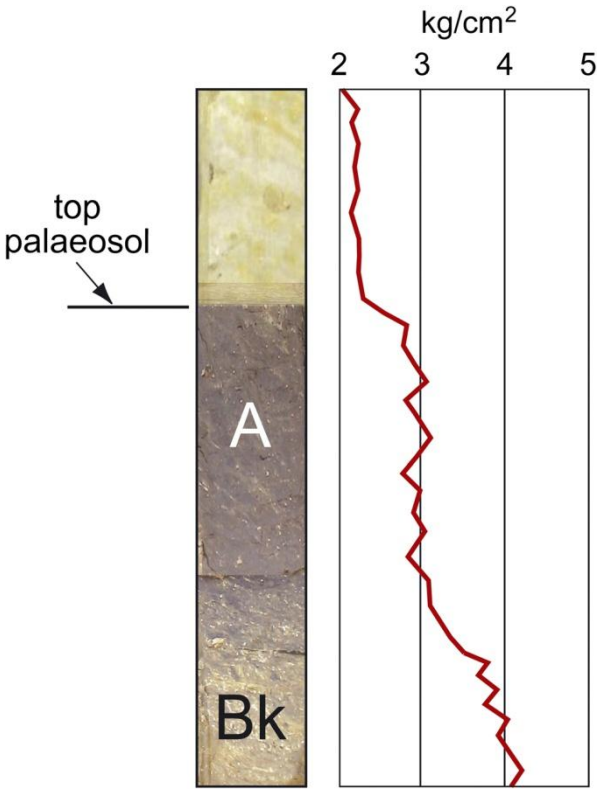

Fig. 8 - Idealized penetrometer readings of A and Bk horizons from in-situ measurements in the study area (based on the histograms of Fig. 7). Note the two-step increase of mean penetrometer resistance atop horizons A and Bk. The highest values invariably mark the A/Bk boundary.

The overall consistency between penetration profiles recorded under different operating conditions (the 40 cores of Figs 1 and 7 were recovered over a time interval of 10 years by distinct drilling companies) indicates that the inherent quantitative nature of penetration tests can provide reliable constraints to palaeosol stratigraphy in the study area and, in general, comparable results, even when penetration tests are carried out with different equipment and following different procedures. The robustness of this method suggests that pocket penetrometer values from summary logs can be used as an inexpensive, powerful tool in the alluvial stratigraphy of unconsolidated Quaternary deposits to enhance the detection and successful prediction of palaeosols.

Conversely, reliance on correlations based uniquely on pocket penetration profiles can be problematic, and we strongly encourage to carry out detailed calibration with cores before any interpretation of penetration profiles is performed with confidence. It should be kept in mind that a simple increase in pocket penetration values has little objective sedimentological expression. Not all shifts in compressive strength are unequivocally related to palaeosol development, and abrupt changes in penetration values may simply reflect sharp facies changes. In this regard, additional information, such as dark colour, occurrence of organic material and carbonate accumulation, should not be overlooked in palaeosols estimation.

8. Conclusions

In order to save money and increase research capability, optimizing the contribution of all available data is a primary need for subsurface stratigraphic interpretation. When facies analysis is carried out uniquely through point data (cores, stratigraphic logs) with poor spatial information, re-interpretation under a sedimentological perspective of pre-existing core descriptions, such as field logs from municipalities or private drilling companies, may be crucial to increase the accuracy of stratigraphic analysis before a new exploration campaign is undertaken.

Palaeosol identification is an essential part of the stratigraphic interpretation process. However, the presence of palaeosols is often neglected by an untrained observer. Descriptive logs can be highly subjective, especially when the geologist's experience is limited. In some instances, stratigraphic descriptions are performed directly by drillers, and are very unlikely to contain information useful for a sedimentologist. In such instances, pocket penetration tests, a set of data normally available from most core descriptions, may provide objective information on sedimentological characteristics not recognized at time of core description.

This study, by focusing on the late Quaternary deposits of the southern Po Plain, shows that integration of simple geotechnical (pocket penetrometer resistance) data with accurate facies analysis from even a limited number of cores can be effective in identifying pedogenically modified muds, thus enlarging significantly the number of control points and increasing their value in building a reliable high-resolution stratigraphic framework for unconsolidated alluvial sediments.

Through calibration with facies analysis and radiometric dating from three late Quaternary cored successions of the southern Po Plain, we documented the repeated alternation of 12 pedogenized horizons (Inceptisols A-L) within non-pedogenized, alluvial strata. These palaeosol-bounded packages, 3-5 m thick and spanning intervals

of a few thousand years, can be physically traced over distances of tens of km, allowing the identification of sedimentary packages of chronostratigraphic significance. Palaeosol horizonation plays a fundamental role in shaping the geotechnical response of palaeosols to pocket penetration, the maximum increase in penetration resistance being observed at the boundary between the A and Bk horizons.

In spite of simple identification of heavily overconsolidated horizons via pocket penetration tests, the interpretation of compressive strength profiles is not unequivocal, and this technique should never replace visual inspection of cores. To be of maximum benefit when setting up a comprehensive stratigraphic study, pocket penetration tests should necessarily be calibrated with accurate core descriptions at selected study sites.

Acknowledgements

We are grateful to R. Pignone, L. Martelli and P. Severi (Regione Emilia-Romagna – RER - Geological, Seismic and Soil Survey) for access to cores 1-3 and to the RER core database. We are indebted to two anonymous reviewers for their constructive criticism.

References

Ainsworth, R.B. 2010. Prediction of stratigraphic compartmentalization in marginal marine reservoirs. In: Reservoir Compartmentalization, Jolley, S.J., Fisher, Q.J., Ainsworth, R.B., Vrolijk, P.J., Delisle, S. (eds.). Geological Society, London, Special Publication 347, 199-218.

Aitken, J.F., Flint, S.S. 1996. Variable expressions of interfluvial sequence boundaries in the Breathitt Group (Pennsylvanian), eastern Kentucky, USA. In: High Resolution Sequence Stratigraphy: Innovations and Applications, Howell, J.A., Aitken, J.F. (eds.). Geological Society, London, Special Publication 104, 193-206.

Amorosi, A., Marchi, N. 1999. High-resolution sequence stratigraphy from piezocone tests: an example from the Late Quaternary deposits of the SE Po Plain. Sedimentary Geology 128, 69-83.

Amorosi, A., Colalongo, M.L., Fusco, F., Pasini, G., Fiorini, F. 1999. Glacio-eustatic control of continental-shallow marine cyclicity from Late Quaternary deposits of the south-eastern Po Plain (Northern Italy). Quaternary Research 52, 1-13.

Amorosi, A., Colalongo, M.L., Fiorini F., Fusco, F., Pasini, G., Vaiani, S.C., Sarti, G. 2004. Palaeogeographic and palaeoclimatic evolution of the Po Plain from 150-ky core records. Global and Planetary Change 40, 55-78.

Amorosi, A., Colalongo, M.L. 2005. The linkage between alluvial and coeval nearshore marine successions: evidence from the Late Quaternary record of the Po River Plain, Italy. In: Fluvial Sedimentology VII, Blum, M.D., Marriott, S.B., Leclair, S.F. (eds.). International Association of Sedimentologists Special Publication 35, 257-275.

Amorosi, A., Pavesi, M., Ricci Lucchi, M., Sarti, G., Piccin, A. 2008. Climatic signature of cyclic fluvial architecture from the Quaternary of the central Po Plain, Italy. Sedimentary Geology 209, 58-68.

Amorosi, A., Bruno, L., Rossi, V., Severi, P., Hajdas, I. 2014. Paleosol architecture of a late Quaternary basin-margin sequence and its implications for high-resolution, non-marine sequence stratigraphy. Global and Planetary Change 112, 12-25.

Atchley, S.C., Nordt, L.C., Dworkin, S.I. 2004. Eustatic control on alluvial sequences stratigraphy: a possible example from the Cretaceous-Tertiary transition of the Tornillo Basin, Big Bend National Park, West Texas, U.S.A. Journal of Sedimentary Research 74, 391-404.

Bennett, G.L., Weissmann, G.S., Baker, G.S., Hyndman, D.W. 2006. Regional-scale assessment of a sequence-bounding paleosol on fluvial fans using ground-penetrating radar, eastern San Joaquin Valley, California. Geological Society of America Bulletin 118, 724-732.

Besly, B.M., Fielding, CR. 1989. Palaeosols in Westphalian coal-bearing and red-bed sequences, central and northern England. Palaeogeography, Palaeoclimatology, Palaeoecology 70, 303-330.

Blum, M.D., Price, D.M. 1998. Quaternary alluvial plain construction in response to interacting glacio-eustatic and climatic controls, Texas Gulf Coastal Plain. In: Relative Role of Eustasy, Climate and Tectonism in Continental Rocks, Shanley, K., McCabe, P. (eds.). Society for Sedimentary Geology (SEPM) Special Publication 59, 31-48.

Blum, M.D., Törnqvist, T.E. 2000. Fluvial response to climate and sea-level change: a review and look forward. Sedimentology 47, 2-48.

Blum, M.D., Martin, J., Milliken, K., Garvin, M. 2013. Paleovalley systems: Insights from Quaternary analogs and experiments. Earth Science Reviews 116, 128-169.

Boccaletti, M., Elter, P., Guazzone, G. 1971. Plate tectonics models for the development of the western Alps and northern Apennines. Nature 234, 108-111.

Boccaletti, M., Calamita, F., Deiana, G., Gelati, R., Massari, F., Moratti, G., Ricci Lucchi, F. 1990. Migrating foredeep-thrust belt system in the Northern Apennines and Southern Alps. Palaeogeography, Palaeoclimatology, Palaeoecology 77, 3-14.

Bown, T.M., Kraus, M.J. 1981. Lower Eocene alluvial paleosols (Willwood Formation, Northwest Wyoming) and their significance for paleoecology, paleoclimatology and basin analysis. Palaeogeography, Palaeoclimatology, Palaeoecology 34, 1-30.

Bradford, J.M. 1980. The penetration resistance in a soil with well-defined structural units. Soil Science Society of America Journal 40, 965-966.

Brideau, M.-A., Stead, D., Bond, J.D., Lipovsky, P.S., Ward, B.C. 2011. Preliminary stratigraphic and geotechnical investigations of the glaciolacustrine and loess deposits around the city of Whitehorse (NTS 105D/11), Yukon. In: Yukon Exploration and Geology 2010, MacFarlane, K.E., Weston, L.H., Relf, C. (eds.). Yukon Geological Survey, 33-53.

Bruno, L., Amorosi, A., Curina, R., Severi, P., Bitelli, R. 2013. Human-landscape interactions in the Bologna area (northern Italy) during the mid-late Holocene, with focus on the Roman period. The Holocene 23, 1560-1571.

Buck, B.J., Lawton, T.F., Brock, A.L. 2010. Evaporitic paleosols in continental strata of the Carroza Formation, La Popa Basin, Mexico: Record of Paleogene climate and salt tectonics. Geological Society of America Bulletin 122, 1011-1026.

Buol, S.W., Southard, R.J., Graham, R.C., McDaniel, P.A. 2011. Soil Genesis and Classification, 6th Edition. Wiley-Blackwell: Chichester.

Carcano, C., Piccin, A. 2002. Geologia degli acquiferi Padani della Regione Lombardia. Regione Lombardia and ENI Divisione AGIP, S.EL.CA: Firenze.

Carminati, E., Vadacca, L. 2010. Two- and three-dimensional numerical simulations of the stress field at the thrust front of the Northern Apennines, Italy. Journal of Geophysical Research 115, DOI: 10.1029/2010JB007870.

Catuneanu, O., Abreu, V., Bhattacharya, J.P., Blum, M.D., Dalrymple, R.W., Eriksson, P.G., Fielding, C.R., Fisher, W.L., Galloway, W.E., Gibling, M.R., Giles, K.A., Holbrook, J.M., Jordan, R., Kendall, C.G.S.t.C., Macurda, B., Martinsen, O.J.,Miall, A.D., Neal, J.E., Nummedal, D., Pomar, L., Posamentier, H.W., Pratt, B.R., Sarg, J.F., Shanley, K.W., Steel, R.J., Strasser, A., Tucker, M.E., Winker, C. 2009. Towards the standardization of sequence stratigraphy. Earth Science Reviews 92, 1-33.

Choi, K. 2005. Pedogenesis of late Quaternary deposits, northern Kyonggi bay, Korea: Implications for relative sea-level change and regional stratigraphic correlation. Palaeogeography, Palaeoclimatology, Palaeoecology 220, 387-404.

Choi, K., Kim, J.H. 2006. Identifying late Quaternary coastal deposits in Kyonggi Bay, Korea, by their geotechnical properties. Geo-Marine Letters 26, 77-89.

Cleveland, D.M., Atchley, S.C., Nordt, L.C. 2007. Continental sequence stratigraphy of the Upper Triassic (Norian–Rhaetian) Chinlestrata, northern New Mexico, U.S.A.: Allocyclic and autocyclic origins of paleosol-bearing alluvial successions. Journal of SedimentaryResearch 77, 909-924.

Di Dio, G. 1998. Riserve idriche sotterranee della Regione Emilia-Romagna. Regione Emilia-Romagna and ENI-AGIP, S.EL.CA: Firenze.

Donnici, S., Serandrei-Barbero, R.,Bini, C., Bonardi, M., Lezziero, A. 2011. The caranto paleosol and its role in the early urbanization of Venice. Geoarchaeology 26, 514-543

Dreyer, T. 1993. Quantified fluvial architecture in ephemeral stream deposits of the Esplugafreda Formation (Palaeocene), Tremp-Graus Basin, northern Spain. In: Alluvial Sedimentation, Marzo, M.,Puigdefabregas, C. (eds.). International Association of Sedimentologists Special Publication 17, 337-362.

Fontana, A., Mozzi, P., Bondesan, A. 2008. Alluvial megafans in the Venetian-Friulian Plain (north-eastern Italy): Evidence of sedimentary and erosive phases during Late Pleistocene and Holocene. Quaternary International 189, 71-90.

Ghielmi, M., Minervini, M., Nini, C., Rogledi, S., Rossi, M. 2013. Late Miocene-Middle Pleistocene sequences in the Po Plain - Northern Adriatic Sea (Italy): The stratigraphic record of modification phases affecting a complex foreland basin. Marine and Petroleum Geology 42, 50-81.

Gibling, M.R., Fielding, C.R., Sinha, R. 2011. Alluvial valleys and alluvial sequences: Towards a geomorphic assessment. In: From River to Rock Record: The Preservation of Fluvial Sediments and their Subsequent Interpretation, Davidson, S.K., Leleu, S.,

North, C.P. (eds.). SEPM Society for Sedimentary Geology Special Publication 97, 423-447.

Hanneman, D.L., Wideman, C.J. 1991. Sequence stratigraphy of Cenozoic continental rocks, southwestern Montana. Geological Society of America Bulletin 103, 1335-1345.

Huerta, P., Armenteros, I., Silva, P.G. 2011. Large-scale architecture in non-marine basins: the response to the interplay between accommodation space and sediment supply. Sedimentology 58, 1716-1736.

Joeckel, R.M. 1991. Paleosol stratigraphy of the Eskridge Formation; Early Permian pedogenesis and climate in southeastern Nebraska. Journal of Sedimentary Research 61, 234-255

Kraus, M.J. 1999. Paleosols in clastic sedimentary rocks: their geologic applications. Earth Science Reviews 47, 41-70.

Lafuerza, S., Canals, M., Casamor, J.L., Devincenzi, J.M. 2005. Characterization of deltaic sediment bodies based on in situ CPT/CPTU profiles: a case study on the Llobregat delta plain, Barcelona, Spain. Marine Geology 222-223, 497-510.

Li, J., Okin, G.S., Herrick, J.E., Belnap, J., Munson, S.M., Miller, M.E. 2010. A simple method to estimate threshold friction velocity of wind erosion in the field. Geophysical Research Letters 37, DOI: 10.1029/2010GL043245.

Mack, G.H., Tabor, N.J., Zollinger, H.J. 2010. Palaeosols and sequence stratigraphy of the Lower Permian Abo Member, south-central New Mexico, USA. Sedimentology 57, 1566-1583.

Martinsen, O.J., Ryseth, A., Helland-Hansen, W., Flesche, H., Torkildsen, G., Idil, S. 1999. Stratigraphic base level and fluvial architecture: Ericson Sandstone (Campanian), Rock Sorings Uplift, SW Wyoming, USA. Sedimentology 46, 235-259.

McCarthy, P.J. and Plint, A.G. 1998. Recognition of interfluve sequence boundaries: Integrating paleopedology and sequence stratigraphy. Geology 26, 387-390.

Mitchum Jr, R.M., Vail, P.R., Thompson III, S. 1977. The depositional sequence as a basic unit for stratigraphic analysis. In: Seismic stratigraphy - Application for Hydrocarbon Exploration Payton C.E. (ed.). American Association of Petroleum Geologists Memoir 26, 53-62.

Molinari, F.C., Boldrini, G., Severi, P., Dugoni, G., Rapti Caputo, D., Martinelli, G. 2007. Risorse idriche sotterranee della Provincia di Ferrara. In: Risorse Idriche Sotterranee della Provincia di Ferrara, Dugoni, G., Pignone R. (eds.). Ferrara, 7-61.

Muttoni, G., Carcano, C., Garzanti, E., Ghielmi, M., Piccin, A., Pini, R., Rogledi, S., Sciunnach, D. 2003. Onset of major Pleistocene glaciations in the Alps. Geology 31, 989-992.

Olsen, T., Steel, R., Hogseth, K., Skar, T., Roe, S.L. 1995. Sequential architecture in a fluvial succession: sequence stratigraphy in the Upper Cretaceous Mesaverde Group, Price Canyon, Utah. Journal of Sedimentary Research B65, 265-280.

Park, Y.A., Lim, D.I., Khim, B.K., Choi, J.Y., Doh, S.J. 1998. Stratigraphy and subaerial exposure of late Quaternary tidal deposits in Haenam Bay, Korea (South-eastern Yellow Sea). Estuarine, Coastal and Shelf Science 47, 523-533.

Pieri, M., Groppi, G. 1981. Subsurface geological structure of the Po Plain, Italy. In: Progetto finalizzato alla geodinamica 414, Pieri, M., Groppi, G. (eds.). C.N.R: Roma, 1-23.

Posamentier, H.W., Allen, G.P. 1999. Siliciclastic Sequence Stratigraphy: Concepts and Applications. SEPM Concepts in Sedimentology and Paleontology 7. Society for Sedimentary Geology, 204 pp.

Retallack, G.J. 2001. Soils of the Past: An Introduction to Paleopedology. 2nd Edition. Blackwell Science Ltd: Oxford.

Retallack, G.J., Leahy, G.D., Spoon, M.D. 1987. Evidence from paleosols for ecosystem changes across the Cretaceous/Tertiary boundary in eastern Montana. Geology 15, 1090-1093.

Ricci Lucchi, F. 1986. Oligocene to Recent foreland basins of northern Apennines. In: Foreland Basins, Allen P., Homewood P. (eds.). International Association of Sedimentologists Special Publication 8, 105-139.

Sarti, G., Rossi, V., Amorosi, A. 2012. Influence of Holocene stratigraphic architecture on ground surface settlements: A case study from the City of Pisa (Tuscany, Italy). Sedimentary Geology 281,75-87.

Shanley, K.W., McCabe, P.J. 1994. Perspectives on the sequence stratigraphy of continental strata. American Association of Petroleum Geologists Bulletin 78, 544-568.

Steber, A., Brooks, K., Perry, C.H., Randy, K. 2007. Surface Compaction Estimates and Soil Sensitivity in Aspen Stands of the Great Lakes States. Northern Journal of Applied Forestry 24, 276-281.

Styllas, M. 2014. A simple approach for defining Holocene sequence stratigraphy using borehole and cone penetration test data. Sedimentology 61, 444-460.

Van Wagoner, J.C., Mitchum, R.M., Campion, K.M., Rahmanian, V.D. 1990. Siliciclastic sequence stratigraphy in well logs, cores and outcrops: concepts for high resolution correlations of time and facies. In: Methods in Exploration 7, Barbara H. Lidtz (ed.), American Association of Petroleum Geologists, Tulsa: U.S.A.

Varela, A.N., Veiga, G.D., Poiré, D.G. 2012. Sequence stratigraphic analysis of Cenomanian greenhouse palaeosols: A case study from southern Patagonia, Argentina. Sedimentary Geology 271-272, 67-82.

Wright, V.P., Marriott, S.B. 1993. The sequence stratigraphy of fluvial depositional systems: the role of floodplain storage. Sedimentary Geology 86, 203-210.

5.4. Paper 4 (Study area 4)

A late Quaternary multiple paleovalley system from the Adriatic coastal plain (Biferno River, Southern Italy)*

Alessandro Amorosi, Vito Bracone, ***Bruno Campo***, Carmine D'Amico, Veronica Rossi, Carmen M. Rosskopf

*Geomorphology, v. 254 (2016), pp. 146-159

A late Quaternary multiple paleovalley system from the Adriatic coastal plain (Biferno River, Southern Italy)

Alessandro Amorosi, Vito Bracone, ***Bruno Campo***, Carmine D'Amico, Veronica Rossi, Carmen M. Rosskopf

Abstract

A buried paleovalley system, up to 2 km wide and exceeding 50 m in relief, made up of multiple cross-cutting depressions incised into the Lower Pleistocene bedrock, is reported from the Central Adriatic coastal plain at the mouth of Biferno River. Through a multi-proxy approach that included geomorphological, stratigraphic, sedimentological and paleontological (benthic foraminifers, ostracods and molluscs) investigations, the facies architecture of distinct, superposed valley fills is reconstructed and their relative chronology established along a transverse profile with extremely high data density (average borehole spacing 75 m). Regional tectonic uplift appears as the major controlling factor of initial (Middle Pleistocene) river down-cutting and paleovalley formation. In contrast, glacio-eustatic fluctuations drove fluvial-system response over the last 120 ky, when valley incision was primarily induced by the last glacial base-level lowering and climatic forcing. A fragmented record of coastal and shallow-marine deposits is available for the lower paleovalley fill, which is penetrated by a limited borehole dataset. Multiple erosion phases probably related to the post-MIS 5e sea-level fall are reconstructed from the upper paleovalley fill, where a buried fluvial terrace succession is identified a few tens of meters below the ground surface. The flat surfaces of two buried fluvial terraces suggest longer-term, stepped relative sea-level fall, and are correlated with fluvial incisions that took place possibly at the MIS 5/4 transition and at the MIS 3/2 transition, respectively. A laterally extensive gravel body developed on the valley floor during the Last Glacial Maximum. During the ensuing, latest Pleistocene-early Holocene sea-level rise the Biferno paleovalley was transformed into an estuary. Upstream from the maximum shoreline ingression, the vertical succession of well-drained floodplain, poorly-drained floodplain, and swamp deposits evidences increasing marine influence in the estuary, in response to continuing sea-level rise. The interfluves were drowned around 8 cal. ky BP, when brackish conditions developed in study area. Decreasing marine influence in the uppermost 15 m of the paleovalley fill suggests the onset of the modern delta: when

the rate of sea-level rise was overwhelmed by sediment supply, delta progradation took place.

Keywords: Paleovalley, Sequence stratigraphy, Biferno coastal plain, Adriatic Sea, Quaternary.

1. Introduction

Incised-valley fill systems are widely known from the end of the last century, when these large stratigraphic features were found to contain abundant hydrocarbon reserves and became a significant key to the identification of sequence-bounding unconformities (Posamentier and Vail, 1988; Dalrymple et al., 1994). The stratigraphic organization of incised-valley systems associated with relative sea-level change and the role of estuarine sedimentation within incised-valley fills were then documented at length in several papers (e.g., Zaitlin et al., 1994; Hori et al., 2002; Boyd et al., 2006; Tanabe et al., 2006). Several studies have highlighted the stratigraphic importance of paleovalley fills of Quaternary age (Blum and Törnqvist, 2000), for which the time-transgressive nature of the sequence boundary was clearly documented (Blum and Price, 1998; Blum et al., 2013). In the recent context of source-to-sink analysis, it has been shown that Quaternary incised-valley systems may help improve understanding of basin-scale sediment transport pathways, from the hinterland drainage areas to the depositional basin, thus providing the basis for reliable sediment budget calculations (Mattheus and Rodriguez, 2014).

Thick paleovalley systems in Italy have been described in detail from the high-gradient Tyrrhenian Sea coast. These studies include the Tiber (Tevere) River Delta near Rome (Milli et al., 2013), the Arno and Serchio river mouths in Tuscany, west of Pisa (Amorosi et al., 2009a; 2013), and the Volturno coastal plain, north of Naples (Amorosi et al., 2012). Similar studies have also been carried out along the Ionian Sea coast by Tropeano et al. (2013). Contrary to the abundance of incised-valley systems from the Tyrrhenian Sea coast, poor documentation of paleovalley systems exists from the Adriatic area. Despite the dense grid of geophysical data available, no major valley systems attributable to the Po River have been observed along the low-gradient Adriatic shelf (Trincardi et al., 1994). Post-LGM incised-valley systems have been described uniquely from the Alpine sector (Tagliamento, Piave and Brenta incised valleys; Fontana et al., 2008; 2013). Recently, a huge erosional feature (Manfredonia incised-valley system) was recognized in the Adriatic offshore, below the Apulian shelf,

70 km south of the study area (Maselli and Trincardi, 2013; De Santis and Caldara, 2014; Maselli et al., 2014).

Aim of this paper is to present the first detailed stratigraphic and geomorphological documentation of a multiple paleovalley system from the western-central Adriatic coastal area, beneath the modern Biferno River coastal plain (Fig. 1). This study is based on a transect oriented parallel to the Adriatic coast, and transversal to the Apenninic river network. Detailed reconstruction of facies architecture along the transect was ensured by an exceptionally high density of borehole data: 29 stratigraphic logs along a 2,100 m transect, at 75 m average spacing. Such subsurface data density along an individual line is comparable to that of the well-known Rhine-Meuse system, which represents the highest-density mapped and dated Holocene delta in the world (Berendsen and Stouthamer, 2001; Hijma et al., 2009). Given the paucity of data on the lower valley fill, we focus in this paper on the upper sedimentary package, related to the last cycle of sea-level fall and rise.

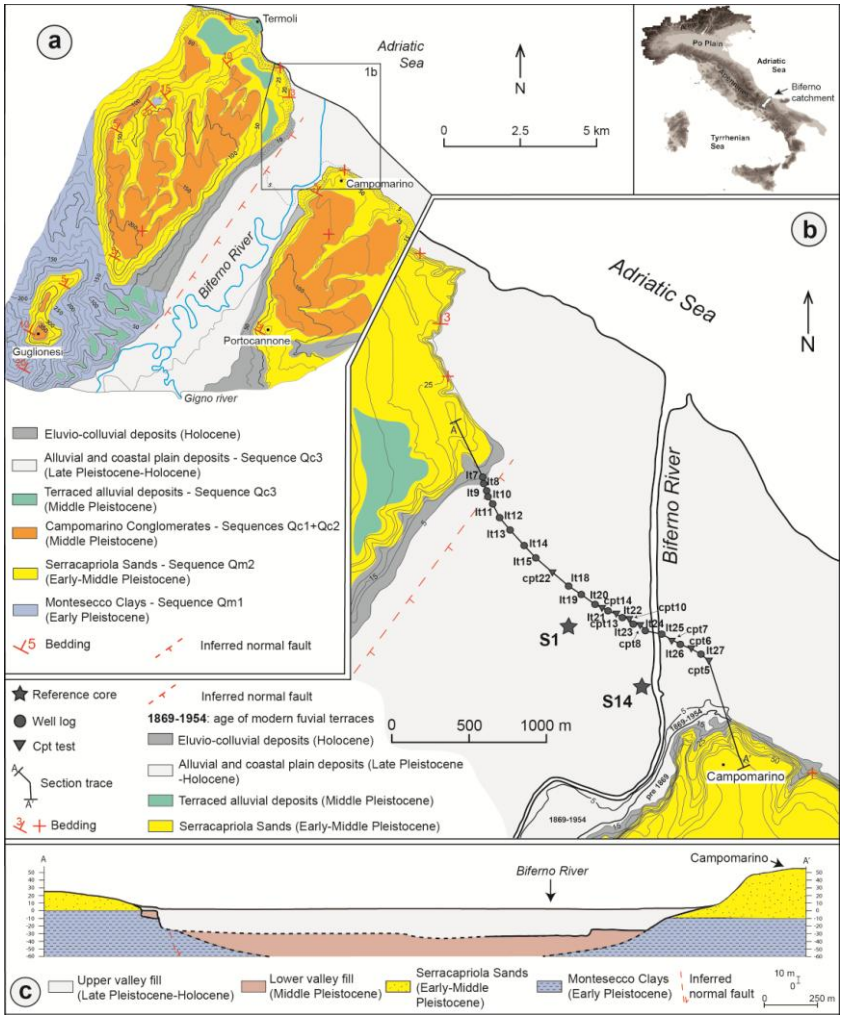

Fig. 1 – The Biferno coastal plain. a) Geological sketch map of the Biferno River valley. b) The study transect, with location of reference cores S1 and S14. c) Transversal section across the Biferno River valley.

2. Regional setting

The Biferno River catchment is spread over 1300 km^2 across the Apennines, in Southern Italy. Total length is 93 km, from springs (Matese Mountains) to river mouth into the Adriatic Sea (Aucelli et al., 2009; Rosskopf and Scorpio, 2013). The Biferno River has a longitudinal steep gradient (0.68 %, on average) in the upper-middle portion of valley, whereas in the lower portion its channel cuts across a nearly flat alluvial plain (longitudinal channel gradient 0.24 %, on average) that grades into a coastal plain, up to 2.5 km wide near the river mouth (Rosskopf and Scorpio, 2013; Fig. 1a).

In the lower portion of the Biferno valley, the surrounding foothills are made up of Pliocene-Pleistocene rocks (Fig. 1a), forming the local infill of the Apenninic foredeep and wedge-top basin, as part of a foreland basin (Amorosi et al., 2009b; Bracone et al., 2012a; b).

The Pleistocene succession in the study area shows an overall “regressive” tendency (Fig. 1a): open-marine deposits (Montesecco Clays) are overlain by nearshore facies (Serracapriola Sands), which in turn are capped by a fluvial conglomerate lithofacies (Campomarino Conglomerates of Amorosi et al., 2009b; Vezzani et al., 2010; Bracone et al., 2012b). The lithofacies boundaries are marked by angular unconformities that enable stratigraphic subdivision into depositional sequences (Bracone et al., 2012a). Sequence Qm1 (Montesecco Clays) has a Pliocene to Lower Pleistocene (late Piacenzian to Santernian) age, while the overlying sequence Qm2 (Serracapriola Sands) has a Lower to Middle Pleistocene (Emilian-Sicilian) age. Two depositional sequences (Qc1 and Qc2) have been identified within the Middle Pleistocene Campomarino Conglomerates. A prominent, laterally extensive reddish paleosol developed under warm and humid climate (interglacial) conditions marks the top of sequence Qc2 (Bracone et al., 2012a). Close to the study area, this paleosol correlates with marine isotope stage (MIS) 9 (Di Celma et al., 2015).

Sequence Qc3 (Middle Pleistocene-Holocene) is mainly made up of alluvial deposits (Bracone et al., 2012a). In the distal portion of the Biferno valley, flights of terraces indicate at least four incision/aggradation cycles at different heights above sea level, while another three fluvial terraces are observed on the valley floor. Fluvial-channel gravels and floodplain silts and clays are the dominant lithofacies, but amalgamated, alluvial fan gravel bodies are present at the confluence with the largest tributary valleys (Rosskopf and Scorpio, 2013). Fluvial scarps are covered by clay-sand colluvial deposits at the valley margin. In the coastal plain, alluvial, paludal and nearshore deposits represent the Holocene succession. Remnants of two beach-ridge complexes

cropping out NE of the study transect and dated to the Roman Age and the XVI Century, respectively (Aucelli et al. 2009), mark the historical shoreline progradation.

Early Pleistocene sedimentation in the study area was controlled by thrust tectonics at the main thrust front of the Apennines. In particular, tectonic activity drove the development of progressive unconformities at sequence boundaries (Bracone et al., 2012a). In contrast, the Middle Pleistocene evolution of this sector was controlled by a generalized, regional uplift, affecting the frontal part of the Apenninic chain. The interaction between uplift and glacio-eustatic sea-level fluctuations drove the major paleolandscape changes that are represented by progressive river downcutting, paleosol development on top of sequence Qc2, and the ultimate deposition of sequence Qc3 (Bracone et al., 2012a). The tectonic setting of the distal portion of the Biferno valley is shown in Fig. 1c.

3. Materials and methods

The subsurface stratigraphy of the Biferno coastal plain was reconstructed along a shore-parallel, NW-SE oriented transect crossing the Biferno valley, about 1.5 km from the modern coastline (Fig. 1b). The dataset, provided by Italferr S.p.A. (*Ferrovie dello Stato Italiane* Group), consists of 19 boreholes (depth range 20-60 m) and 8 cone penetration tests (CPT, 15-25 m deep). Following the criteria illustrated in Amorosi et al. (2014a), facies interpretation was also based upon compressive strength (pocket penetration) values, typically associated to fine-grained (silt and clay) deposits.

Detailed facies characterization was achieved through integrated sedimentological and paleontological (molluscs, benthic foraminifers and ostracods) analyses, which were undertaken on two reference cores, S1 and S14 (Fig. 1b), 38 and 40 m long, respectively. The two boreholes, 3 m above sea level, were drilled 200 m (S1) and 400 m (S14) SW of the study transect (Fig. 1b). Core S1 was acquired specifically as part of this study, while core S14 was provided by Cosib (*Consorzio per lo sviluppo industriale della valle del Biferno*). The two cored successions were described in terms of mean grain size, texture, color, sedimentary structures and accessory materials, such as plant remains, wood fragments, calcareous nodules and fossils.

A total of 90 samples (40 from core S1 and 50 from core S14) were collected for malacofauna and meiofauna analyses, which furnished detailed information in terms of paleosalinity, substrate characteristics and organic matter concentration. Samples (~150-200 g) were dried in oven for 8 h at 60°C, soaked in water and 4% H_2O_2, wet sieved on 63 μm screens (240 mesh) and weighed again. For each sample all molluscs were identified, whenever possible, to species level and counted. Forty samples

containing well-preserved meiofauna were dry sieved and quantitatively analyzed in the size fraction >125 μm to avoid problematic taxonomic identification of juvenile ostracods and foraminifers. Standardized procedures for counting (Buzas, 1990) were followed and relative percentages were calculated for each species. All valves of ostracods and all foraminifer individuals were counted within samples containing scarce meiofauna (n<300). Fossil counts are available as supplementary material in Table 1 (core S1) and Table 2 (core S14). Identification and autoecological information of the benthic species were based upon the original descriptions and several key papers dealing with modern assemblages (Pérès and Picard, 1964; Bonaduce et al., 1975; Breman, 1975; Jorissen, 1988; Athersuch et al., 1989; Albani and Serandrei Barbero, 1990; Henderson, 1990; Sgarrella and Moncharmont Zei, 1993; Meisch, 2000; Fiorini and Vaiani, 2001; Murray, 2006; Scaperrotta et al., 2009; Welter-Schultes, 2012).

Following Amorosi and Marchi (1999), core data were also used to calibrate CPT profiles, with specific focus on tip resistance and sleeve friction values. The tip resistance (*qc*) is determined by the force required to push the tip of the cone through the soil, while the sleeve friction is determined by the force required to push the sleeve. In this study, the tip resistance was used as a powerful tool for prompt identification of coarse-grained sedimentary bodies in the subsurface (Fig. 2).

Finally, outcrop stratigraphy was reconstructed through detailed field surveys along the modern Biferno valley flanks (Fig. 1b). Integration with subsurface data enabled the reconstruction of Middle Pleistocene to Holocene landscape evolution of the study area.

The chronological framework is furnished by seven AMS ^{14}C dates performed on carbon-rich samples (organic matter, wood, mollusc shells) at the CIRCE laboratory (Caserta, Italy). Conventional ages were calibrated using the CALIB 7.1 calibration program (referenced as Stuiver and Reimer, 1993), along with the Intcal13 and Marine13 datasets (Reimer et al., 2013). In order to compensate for the reservoir effect, mollusc samples were calibrated using the value of DeltaR (420±30) available for the central Adriatic Sea area from online databases (http://calib.qub.ac.uk/marine; Siani et al 2000; Reimer and McCormac, 2002). All ages are reported in text and figures as calibrated years BP.

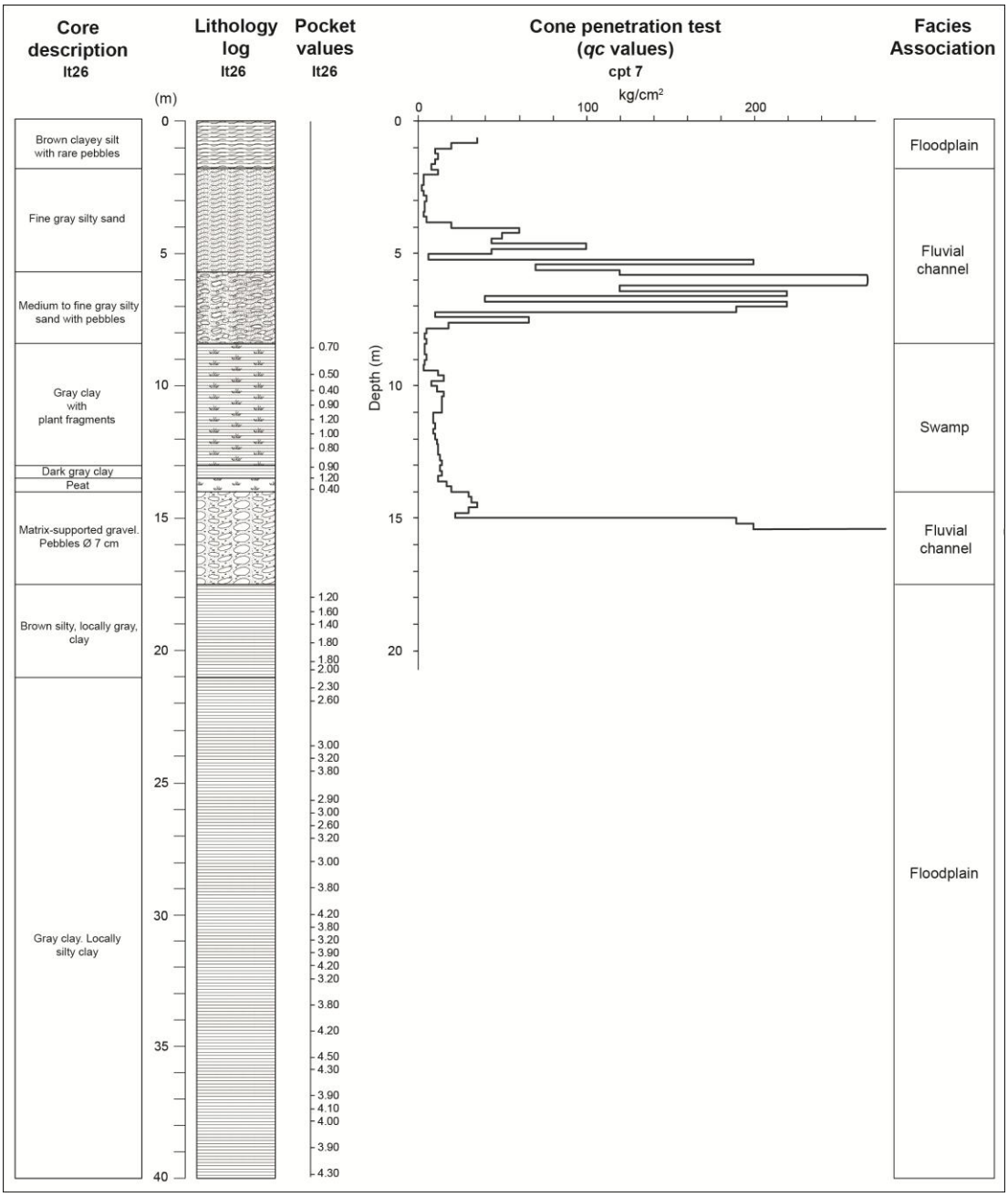

Fig. 2 – Different lithofacies response to pocket penetration and cone penetration tests. The Qc profile shows increasing values in sandy and sandy-gravelly intervals. Cone penetration is stopped by thick gravel bodies. Facies association interpretation is also shown.

4. Depositional facies

Identification of buried paleovalley systems commonly relies upon recognition of high-relief erosional surfaces that are larger than the thickness of individual channel belts within the valley (Zaitlin et al., 1994; Gibling, 2006; Gibling et al., 2011). These surfaces separate younger from older deposits, and are typically associated to abrupt facies changes, especially where marine deposits are in contact with non-marine

facies. Beneath the Biferno River valley, the Lower Pleistocene, marine Montesecco Clays exhibit lateral contacts with a variety of considerably younger continental to coastal deposits (Fig. 1c), thus highlighting the presence of an incised-valley fill. The abrupt facies boundaries between the Pleistocene bedrock and the valley fill represent the subsurface prolongation of the modern valley flanks (Fig. 1c).

Eight major facies associations were identified from integrated sedimentological and paleontological analysis of cores S1 and S14 (Figs. 3, 4).

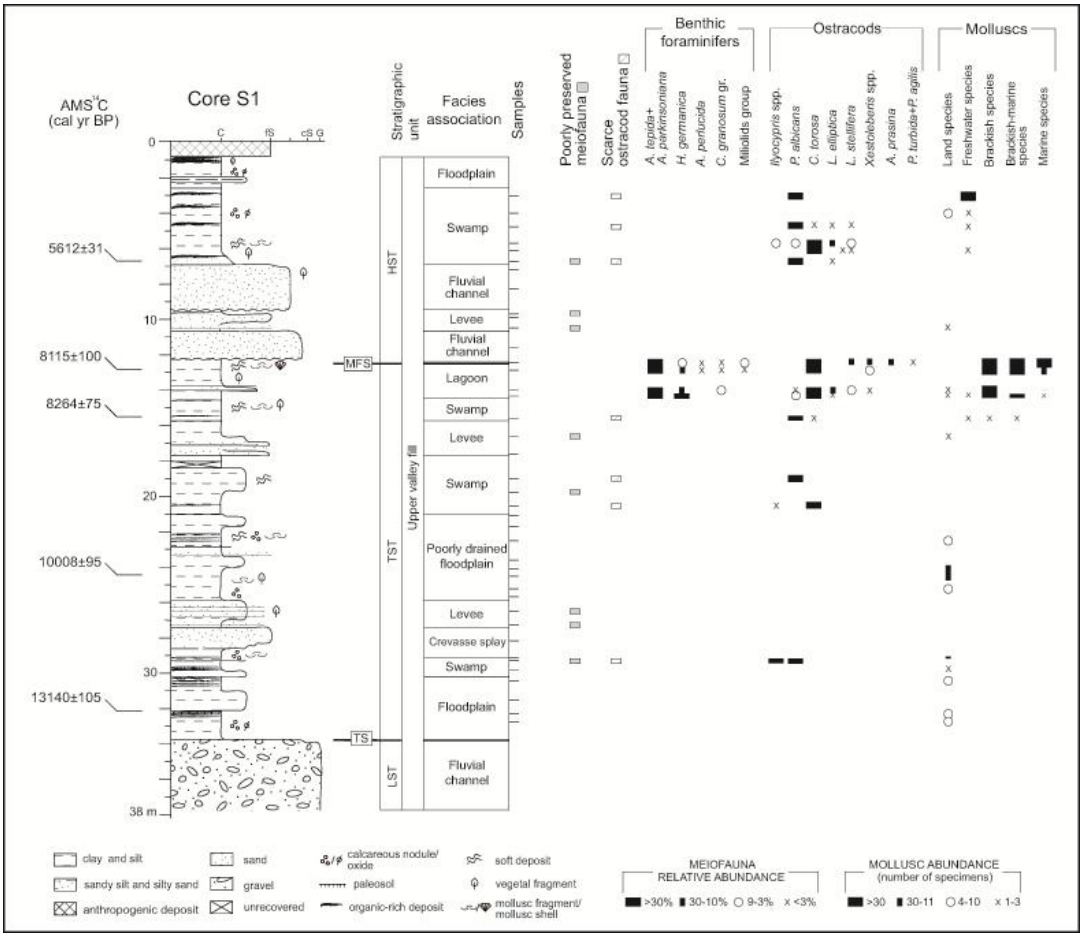

Fig. 3 – Integrated sedimentology (facies analysis) and paleontology (benthic foraminifers, ostracods and molluscs) of core S1. Samples containing a scarce ostracod fauna (< 50 ostracod valves) and a poorly preserved meiofauna are highlighted. Fossil counts are reported in Table 1 (supplementary material). Radiocarbon dates (cal. yr BP) are shown on left. LST = Lowstand systems tract; TST = Transgressive systems tract; HST = Highstand systems tract. TS = Transgressive surface; MFS = Maximum flooding surface.

In general, a clear stratigraphic distinction is observed between (i) the lower valley fill, which is dominated by shallow-marine and coastal facies (Fig. 4), with sparse alluvial deposits reported by the stratigraphic database, and (ii) the upper valley fill, which is entirely non-marine and typically gravel-dominated at the base (Figs. 3, 5).

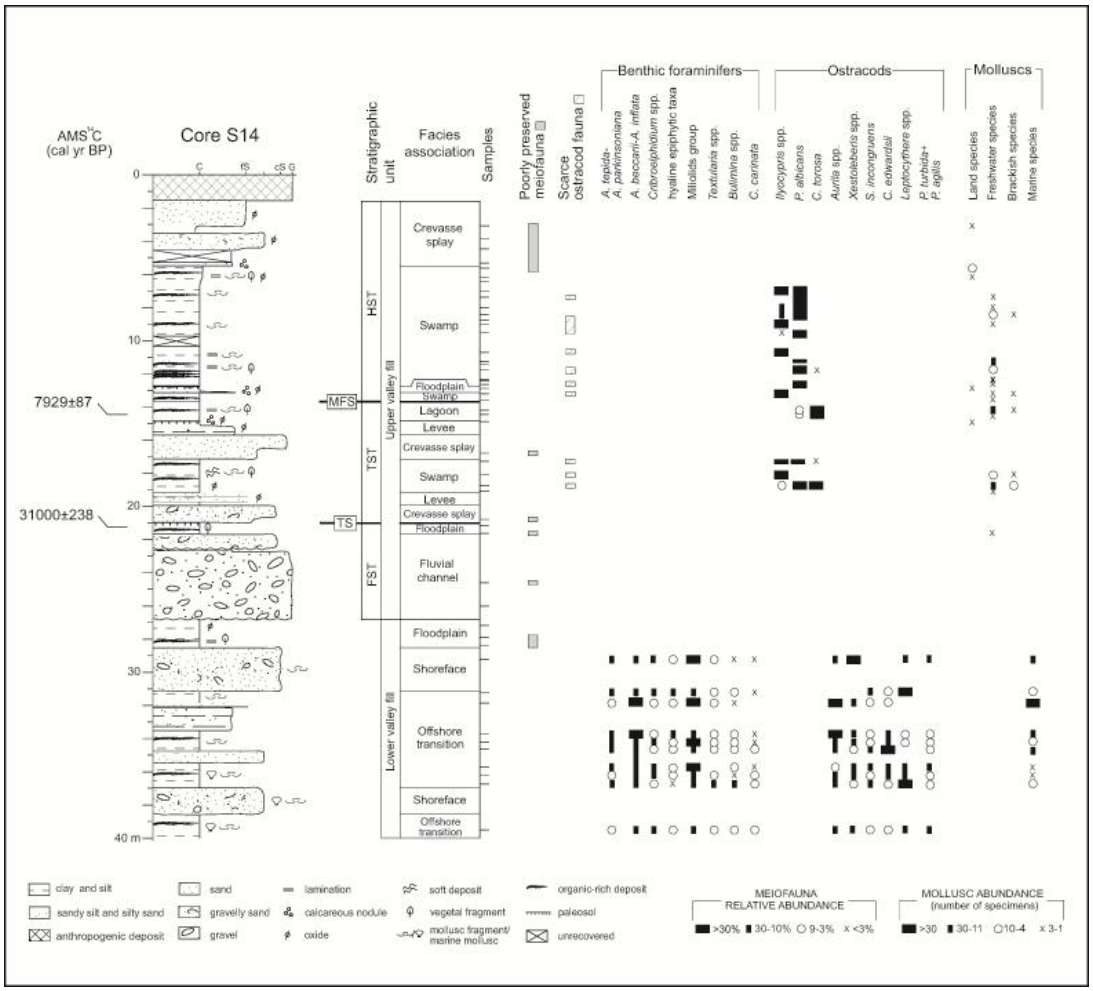

Fig. 4 – Integrated sedimentology (facies analysis) and paleontology (benthic foraminifers, ostracods and molluscs) of core S14. Hyaline ephiphytic taxa include Asterigerinata mamilla, Buccella granulata, Elphidium advenum, Elphidium crispum, Lobatula lobatula and Reussella spinulosa. Samples containing scarce ostracod fauna (< 50 ostracod valves) and poorly preserved meiofauna are highlighted. Fossil counts are reported in Table 2 (supplementary material). Radiocarbon dates (cal. yr BP) are shown on left. Key as in Fig. 2. FST = Forced regressive systems tract.

Owing to reduced borehole depth, the available stratigraphic data prevented us from identifying the paleovalley floor and performing an adequate stratigraphic description of the lower valley fill. For this reason, the lower sedimentary package is undifferentiated. In contrast, the upper valley fill is stratigraphically well constrained, and facies architecture can accurately be described (Fig. 5). Detailed facies description (including sedimentological features, meiofauna and mollusc content, and geotechnical proprieties) and interpretation are reported below.

4.1. Lower valley fill

4.1.1. Shallow marine facies association

Description

This facies association, observed in core S14 only, consists of gray silty clay with cm- to dm-thick sand intercalations, whose thickness and frequency increase upwards. Two distinct coarse-grained bodies, up to 2.5 m thick, composed of medium-coarse sand with rare rounded pebbles are recorded around 38 m and 30 m core-depth, the latter capping the facies association (Fig. 4). Mollusc fragments and shells are locally associated to vegetal remains. On the whole, the mollusc assemblage is composed by marine species (Fig. 4), mainly *Corbula gibba* and *Bittium reticulatum*, with subordinate *Spisula subtruncata* and *Odostomia* sp. Other marine species, including *Abra alba*, *Anomia ephippium*, *Dosinia lupinus*, *Glycymeris* sp., *Myrtea spinifera*, *Nuculana pella*, *Mitrella minor*, *Nassarius mutabilis*, *Neverita josephinia* and *Turbonilla delicata*, are represented by relatively few specimens.

The meiofauna is abundant and exhibits remarkable species richness. The benthic foraminiferal assemblage is dominated by Miliolids (mainly *Quinqueloculina* and *Triloculina* species), *Ammonia beccarii* and *Ammonia inflata*, with the secondary occurrence (commonly <10%) of *Textularia* species and hyaline epiphythic taxa, mainly including *Elphidium crispum*, *Elphidium advenum* and *Buccella granulata*. Variable amounts of *Ammonia tepida* and *Ammonia parkinsoniana*, *Cribroelphidium* species (mainly *C. granosum* and *C. decipiens*), *Bulimina* species and *Cassidulina carinata* are also recorded (Fig. 4). Specifically, high amounts of *Ammonia tepida* and *A. parkinsoniana* are paralleled by low abundances of *Bulimina* species and *Cassidulina carinata* in the 2.5 m-thick gravelly sand interval (Fig. 4). These deposits also show a scarce ostracod fauna, dominated by *Xestoleberis communis*. A more abundant ostracod fauna, with several dominant taxa (*Xestoleberis* and *Aurila* species, *Costa edwardsii* and *Leptocythere* species), is recorded within the clayey succession.

Interpretation

The sedimentological features and the fossil content of the clay fraction document the establishment of a shallow-marine environment subject to moderate fluvial influence, such as an offshore transition zone. A comparable modern foraminiferal assemblage, with high amounts of *Ammonia*, *Cribroelphidium* and Miliolid species, has been observed along the Adriatic coast at < 25 m water depth, on mixed sandy and clayey substrates rich in calcium carbonate (Jorissen, 1988), and within late Quaternary shallow-marine successions buried beneath several Mediterranean delta plains (Fiorini and Vaiani, 2001; Rossi and Vaiani, 2008; Milli et al., 2013; D'Amico et al., 2013). Moreover, the occurrence of remarkable percentages of epiphythic taxa suggests vegetation cover at the sea bottom and low turbidity conditions, possibly far from the river outlets. This interpretation is consistent with the highly-diversified

ostracod fauna and the mollusc marine assemblage (mainly *Corbula gibba* and *Bittium reticulatum*; Fig. 4), commonly found on vegetated sandy and clayey bottoms of the infralittoral zone (Pérès and Picard, 1964; Bonaduce et al., 1975; Athersuch et al., 1989; Scaperrotta et al., 2009). In the gravelly sands of core S14, the dominance of *Xestoleberis communis*, a phytal ostracod species preferring coarse-grained substrates (Bonaduce et al., 1975), and the increase in mollusc species living on sandy bottoms of the infralittoral zone (*Nassarius mutabilis*, *Neverita josephinia*, *Spisula subtruncata*) document the establishment of a high-energy, littoral depositional setting (shoreface).

4.2. Upper valley fill

4.2.1. Fluvial-channel (gravel) facies association

Description

This facies association consists of amalgamated, poorly sorted gravel bodies, up to 6 m thick, with rounded cobbles (up to 8 cm in diameter) and gravelly sand embedded in a silty-sandy tawny matrix (Figs. 3, 4). The gravel bodies exhibit fining-upward (FU) trends and erosional lower boundaries. The upward transition to sand-silt deposits is abrupt (Figs. 3, 4). No fossils or plant debris were observed. The gravel bodies were not penetrated by piezocone penetration tests, except for their uppermost finer-grained portions, which furnished tip penetration resistance values lower than 200 kg/cm^2 (CPT 7 in Fig. 2).

Interpretation

The coarse texture of the deposit and its erosional base suggest that this facies association is a high gradient and high-energy fluvial-channel deposit. In particular, grain size, poor sorting and the presence of amalgamation surfaces indicate a braided stream facies formed under high-energy flow conditions. Mass transport was likely favored by the high topographic gradient and the strong confinement within the narrow Biferno River valley. The overall FU tendency indicates waning energy over time as the system moved to depositional environments dominated by suspension fallout.

4.2.2. Fluvial-channel (sand) facies association

Description

This facies association, a few metres thick, includes well sorted, medium to very fine gray sand bodies with internal FU trends and sharp erosional lower boundaries (Figs.

3, 4). The cm-thick silt-clay intervals and scattered pebbles are locally preserved. Thin, organic-rich fine-grained layers may cap the sandy succession. Plant debris is common, while fossils were not observed. CPT measurements indicate high tip penetration resistance (*qc* = 200 kg/cm²), with typical upward decreasing values.

Interpretation

Sedimentary characteristics, including lithology, grain-size trends and erosional lower boundary are fully consistent with a sandy fluvial-channel deposit. The abundance of plant fragments and the lack of fossils are also indicative of a non-marine, high-energy environment. Isolated sand bodies (see Fig. 5) are interpreted as dominantly recording ribbon-shaped fluvial bodies, while laterally amalgamated sand bodies are inferred to reflect lateral migration of the river channel, likely during periods of low accommodation.

4.2.3. Levee and crevasse facies association

Description

This facies association, up to 4 m thick, consists of sandy-silty deposits containing few shells of land molluscs (*Carychium minimum, Punctum pygmaeum, Vallonia pulchella, Vertigo angustior*), with scarce and poorly preserved planktonic and benthic foraminifers (Figs. 3, 4). Nodules of Fe, Mn and $CaCO_3$, as well as plant fragments, are locally encountered. Rhythmical alternations, mm- to cm-thick, of gray to brownish silty sand, silt and clayey silt are the most common feature. The individual layers show distinctive FU trends, sharp bases and gradational tops, and are capped locally by indurated horizons (core S14 in Fig. 4). *Qc* values range between 40 and 80 kg/cm². Very fine to medium sand bodies, with subordinate silty sand and sandy silt, may occur. These sedimentary bodies, 1 to 1.5 m thick, display either fining-upward (FU) or coarsening-upward (CU) internal trends accompanied by erosional or gradational lower boundaries, respectively. Scattered pebbles may be encountered (core S14 in Fig. 4). *Qc* values range between 90 and 120 kg/cm².

Interpretation

Because of its sedimentological-paleontological characteristics and stratigraphic relationships with fluvial-channel deposits, this facies association is interpreted to have formed in a variety of alluvial sub-environments close to the river channel. The occurrence of land-mollusc species commonly found in alluvial wet habitats (Welter-Shultes, 2012; D'Amico et al., 2014) is consistent with overbank sub-environments

subject to frequent river floods. In particular, the rhythmical alternation of silty sand and silt is interpreted as a proximal overbank (levee) deposit, recording traction-plus-fallout deposition. Lower sand/silt ratios indicate relatively more distal positions, reflecting decreasing flow strength as the distance from the channel increased. Thin sand bodies with erosional base and FU trends are interpreted as crevasse channels. CU silty sand to sand deposits showing gradational lower boundaries are argued to represent crevasse splays.

4.2.4. Floodplain facies association

Description

This facies association is made up of massive gray clay and silty clay, with brownish and yellowish mottles due to iron and manganese oxides. Bioturbation, root traces and pedogenic features are widespread. Paleosols are typically observed (core S1 and core S14 in Figs. 3, 4), with dark-gray organic-rich clay (A-horizon) overlying gray clay containing oxides and carbonate nodules (Bk-horizon). The meiofauna is absent, while scarce shells of land molluscs (*Pomatias elegans*, *P. pygmaeum* and Hygromiinae) are locally encountered. This monotonous muddy succession forms two laterally continuous stratigraphic intervals, the thickness of which varies between 5 and 8 m (Fig. 5). This facies association, which shows lateral transition to pedogenized levee/crevasse deposits and poorly drained organic-rich clays, is also characterized by moderate *qc* values (14-24 kg/cm²) and pocket penetration values in the range of 1.5-3 kg/cm². Two samples, from core S1 and core S14, yielded radiometric ages of 13140±105 and 31000±238 cal. yr BP, respectively (Figs. 3, 4).

Interpretation

This facies association is interpreted as floodplain deposits. In particular, the fine-grained texture, the color (yellowish and brownish mottles due to iron oxides) and the occurrence of bioturbation and paleosols testify to a low-energy interfluvial setting, subject to overbank deposition and frequent episodes of subaerial exposure under well-drained conditions. The occurrence of land molluscs (*P. pygmaeum*, Hygromiinae) with high flood tolerance and populating floodplain environments (Ilg et al., 2009) supports this interpretation. Paleosols with distinctive A-Bk horizons are interpreted as Inceptisols (Soil Survey Staff, 1999), and are likely to represent phases of non-deposition (*i.e. hiatus*) of a few thousand years of duration. Penetration tip resistance values in the range of 15-25 kg/cm^2 and pocket penetrometer values of 1.5-3 kg/cm^2

are both diagnostic of floodplain deposits (Amorosi & Marchi, 1999; Sarti et al., 2012; Amorosi et al., 2014a).

4.2.5. Poorly drained floodplain facies association

Description

This facies association was observed in core S1 only (Fig. 3), and consists of massive clay and silty clay ranging in color from gray to dark gray. Organic matter is quite common and may locally form mm- to cm-thick black layers; mm-sized plant fragments are also found. Neither Fe-Mn nodules nor paleosols were observed in this facies association. A relatively highly diversified malacofauna consisting of land mollusc species, such as *C. minimum*, *Cecilioides acicula*, *Daudebardia brevipes*, *P. elegans*, *P. pygmaeum* and *Vitrea diaphana* is encountered (Figs. 3, 4). The meiofauna is absent. Pocket penetrometer values fall in the very narrow interval of 1.2-1.8 kg/cm², whereas tip resistance measurements are around 10-22 kg/cm². One radiocarbon date from the lower part of this facies association offered an age of 10008±95 cal. yr BP (core S1 in Fig. 3).

Interpretation

The absence of paleosols and yellowish-brownish mottles, along with the occurrence of land mollusc species preferring humid habitats are indicative of low-energy alluvial environments, such as a poorly drained floodplain, where episodes of subaerial exposure were lacking due to the persistent influence of water (i.e., low topography, high water table, frequent river floods). This interpretation is supported by the presence of *C. minimum*, an amphibious and drought-sensitive species usually living close to calm water bodies (Welter-Shultes, 2012). Pocket penetrometer and *qc* measurements also favor this interpretation, documenting lower penetration values, and consequently lower consistency than well-drained floodplain facies.

4.2.6. Swamp facies association

Description

This facies association, up to 6 m thick, is made up of dark gray to black bioturbated, organic-rich clay with abundant mm-sized plant debris and leaf fragments. Peat layers, commonly less than 0.5 m thick, and fragments of gastropod shells are observed locally (Figs. 3, 4). Sand layers, a few centimeters thick, are also present. The organic-rich clays are very soft, as documented by the peculiar CPT (5-12 kg/cm²,

CPT 6, 7, 13, 14, 22) and pocket penetration values (0.1-1.2 kg/cm²). With the exception of few samples containing poorly preserved planktonic and benthic foraminifers, a scarce to relatively abundant autochthonous ostracod fauna characterizes this facies association. Freshwater-hypohaline taxa, such as *Pseudocandona albicans* and *Ilyocypris* species dominate this assemblage. Remarkable percentages (>30%) of holoeuryhaline ostracod *Cyprideis torosa* are locally encountered (Figs. 3, 4). Similarly, freshwater species (*Acroloxus lacustris*, *Galba truncatula*, *Gyraulus crista*, *Gyraulus laevis*) with subordinate land species (*C. minimum*, *P. pygmaeum*, *P. elegans*, *Vertigo pygmaea*) commonly dominate the malacofauna. Few samples are barren of molluscs, while others contain rare specimens of brackish molluscs (*Abra segmentum*, *Ventrosia ventrosa*; Figs. 3, 4). The middle and upper part of this facies association were radiocarbon dated to 8.264±75 and 5612±31 cal. yr BP, respectively (core S1 in Fig. 3).

Interpretation

Sedimentological features (fine-grained soft texture, dark color, abundant organic matter, presence of peat) and the fossil content testify to the development of an organic-rich, freshwater-hypohaline environment, like a swamp. More specifically, the widespread abundance of *Pseudocandona albicans*, a mesohaline species typical of shallow, slow-moving waters (Henderson, 1990; Meisch, 2000), and freshwater-oligohaline mollusc species preferring vegetated standing bodies (*A. lacustris*, *G. truncatula, G. crista*, *G. laevis*; Welter-Shultes, 2012) is indicative of paludal, stagnant conditions. The local high abundance of opportunistic holoeuryhaline species *C. torosa*, typically found within lagoon basins (Athersuch et al., 1989; Meisch, 2000), suggests the establishment of ephemeral brackish conditions. The thin silty sand layers record occasional river floods in the paludal basin.

4.2.7. Lagoon facies association

Description

This facies association, up to 2 m thick, is made up of a monotonous succession of soft gray clay with mollusc shells and vegetal remains, locally forming mm- to cm-thick organic-rich layers. Faint lamination and mm-thick sandy-silt layers are locally observed (Figs. 3, 4). CPT measurements and pocket penetration values range between 5-11 kg/cm² and 0.2-1 kg/cm², respectively. The abundant well-preserved fauna exhibits a moderate to high species richness. In core S1, the meiofauna is mainly composed of typical brackish ostracods and benthic foraminifers (Fig. 3). The ostracod

assemblage is dominated by *Cyprideis torosa* with the secondary occurrence of *Loxoconcha elliptica* and *Loxoconcha stellifera*. *Pseudocandona albicans* is also locally encountered with low relative abundances (<10%). The euryhaline species *Ammonia tepida* and *Ammonia parkinsoniana* (>30%) dominate the foraminiferal association, with variable amounts of *Haynesina germanica*, *Aubignyna perlucida*, *Cribroelphidium granosum* and *Cribroelphidium lidoense*. In the upper part of the succession, brackish-marine ostracods (*Xestoleberis dispar*, *Aurila prasina* and *Palmoconcha turbida – P. agilis*) and foraminifers (Miliolid species) are observed (Fig. 3). The mollusc assemblage is dominated by the brackish species *V. ventrosa* and the brackish-marine species *A. segmentum*, *Cerastoderma glaucum* and *Loripes lucinalis*. The upward increase of euryhaline gastropod *Bittium reticulatum* and several other marine mollusc species (*Gibbomodiola adriatica*, *Spisula subtruncata, Bulla striata, Chrysallida interstincta, Eulimella ventricosa, Hemilepton nitidum, Retusa truncatula,* Rissoidae spp.) are observed (Fig. 3). At slightly more proximal location (core S14; Fig. 1b), the meiofauna is less diverse and composed almost entirely of valves of *C. torosa*, with secondary occurrence of *P. albicans* (Fig. 4). No benthic foraminifers were encountered. Among the molluscs, only rare specimens of *V. ventrosa* and freshwater species *A. lacustris*, *G. truncatula* and *G. crista* occur (Fig. 4). Two radiocarbon dates from this facies association indicate an age range between 8.115±100 and 7.929±87 cal. yr BP (Figs. 3, 4).

Interpretation

The dominance of the euryhaline species *C. torosa*, *Ammonia tepida* and *A. parkinsoniana* (Athersuch et al., 1989; Murray, 2006) accompanied by high amounts of brackish (*V. ventrosa*) and brackish-marine (*A. segmentum*, *Cerastoderma glaucum* and *Loripes lucinalis*) species indicate the establishment of a semi-closed, brackish-water environment subject to salinity changes, such as a lagoonal basin with slight to moderate marine influence. The secondary occurrence of opportunistic ostracod and foraminiferal species tolerant to relatively restricted conditions and ample food availability, such as *L. elliptica*, *H. germanica*, *A. perlucida* and *C. granosum*, is consistent with this interpretation (Jorissen, 1988; Ruiz et al., 1997, 2000; Meisch, 2000; Debenay et al., 2005; Carboni et al., 2009). Comparable microfossil assemblages have been reported from several Mediterranean lagoons (D' Onofrio et al., 1976; Albani and Serandrei Barbero, 1990; Montenegro and Pugliese, 1996; Coccioni, 2000; Ruiz et al., 2000; Debenay and Guillou, 2002; Murray, 2006; Carboni et al., 2009; Frontalini et al., 2009), as well as from Holocene lagoonal successions buried beneath the Mediterranean coasts (Barra et al., 1999; Carboni et al., 2002,

2010; Amorosi et al., 2004, 2014; Fiorini, 2004). In core S1, a significant marine influence within the lagoon is documented by the association between brackish-marine ostracod/foraminiferal species and marine mollusc species (Fig. 3). In contrast, generally more restricted conditions developed relatively far from the open sea, at proximal locations (core S14), as shown by the absence of benthic foraminifers and the constant co-occurrence of the typical brackish ostracod *C. torosa* with the hypohaline ostracod *P. albicans*, which prefers shallow, slow-moving waters with high organic matter content (Meisch, 2000; Fig. 4). The mollusc fauna, represented only by rare specimens of the brackish *V. ventrosa* and the freshwater *A. lacustris*, *G. truncatula* and *G. crista* is also consistent with this interpretation.

5. The compound Biferno paleovalley

5.1. The onset of the Biferno paleovalley and the lower valley fill

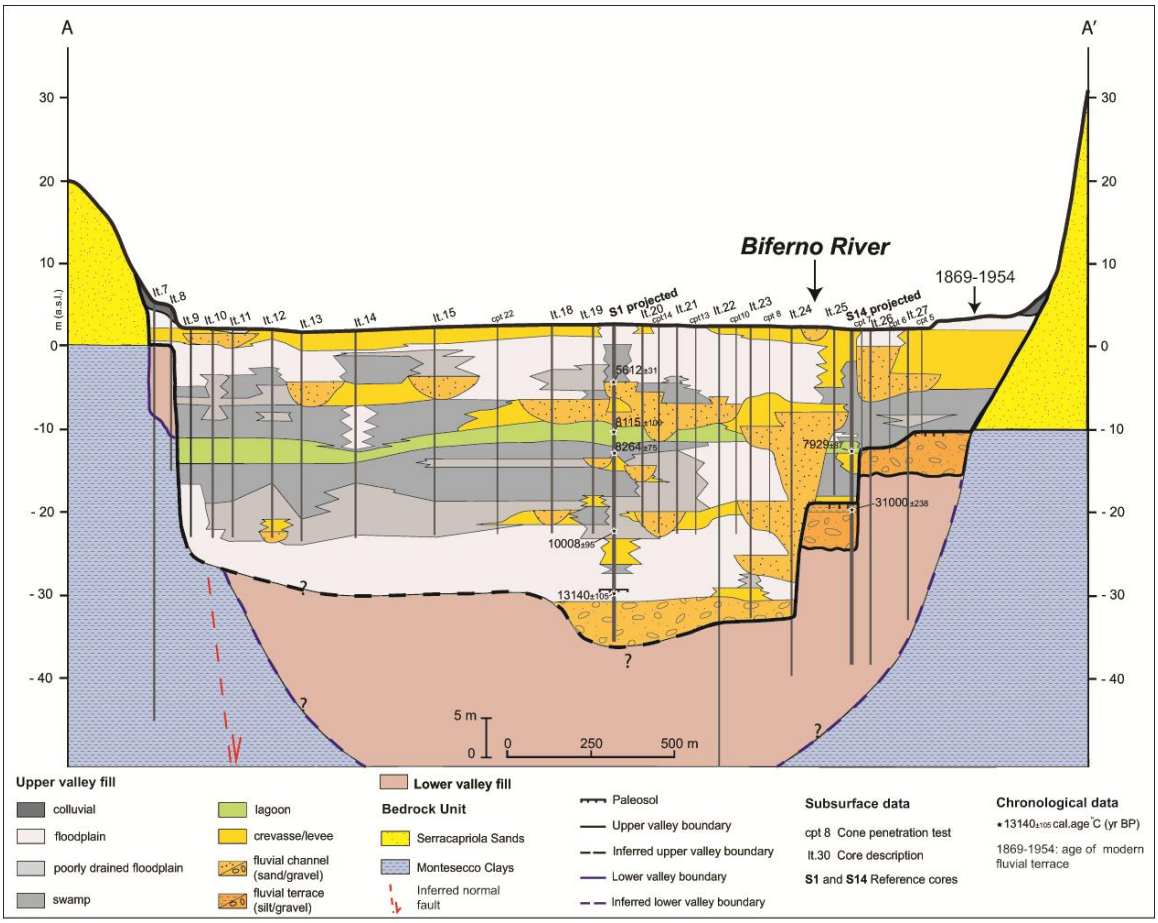

Fig. 5 – Facies architecture of the Biferno valley fill. The lower valley fill is undifferentiated.

The late Quaternary stratigraphic architecture of the Biferno coastal plain reveals a story of multiple valley incisions that persisted in the same area over the last 350 ky, under the combined effect of antecedent topography, tectonics and sea-level change. The steep and narrow Biferno River paleovalley is approximately 2 km wide and its total relief exceeds 50 m (Fig. 5).

Abrupt changes in stratigraphy at the paleovalley margins reveal sharply bound valley walls, incised into the Lower Pleistocene bedrock (Montesecco Clays and Serracapriola Sands – Fig. 5). Above the basal surface, the alternation of marine and continental deposits represents the basic motif of the valley fill. This characteristic stacking pattern of facies is inferred to represent successive fluvial incisions during distinct sea-level lowerings, the older valley fill being truncated by renewed fluvial incision (Li et al., 2006). At least two distinct, superposed paleovalley systems are recognized within the Biferno valley fill (Fig. 5). The erosional boundary that separates coastal and shallow-marine deposits (lower valley fill) from the overlying, essentially non-marine facies (upper valley fill) in Core S14 (Fig. 4) suggests a characteristic compound architecture, where remnants of distinct depositional sequences are stacked upon each other (Zaitlin et al., 1994; Thomas and Anderson, 1994; Törnqvist et al., 2003; Greene et al., 2007; Tesson et al., 2011; Roy et al., 2012; Tropeano et al., 2013).

Absolute age constraints for the initial incision of the Biferno valley are not available. Based on the MIS 9 age assignment of the mature red argillic paleosol identified at the Apenninic margin (Di Celma et al., 2015), we infer that Biferno River excavated a deep incision in the bedrock after ca. 350 ky BP. It has been documented at length that the study area and the adjacent coastal plains experienced generalized tectonic uplift during the Middle Pleistocene (Bracone et al., 2012a), and then remained stable up to the Holocene (Antonioli et al., 2009; Parlagreco et al., 2011; D'Amico et al., 2013). In that scenario, it is likely that tectonic uplift triggered the onset of the Biferno River paleovalley, inducing river down-cutting, widespread terrace formation, and prolonged pedogenesis on the adjacent Apenninic interfluves.

Glacio-eustatic fluctuations drove fluvial-system response over the Middle-Late Pleistocene, when channel incision was primarily induced by the glacial base-level lowering and climatic forcing. It is widely held by the Quaternary fluvial community that climate change has been a key driver in terrace formation during this time period (Gibbard and Lewin, 2009; Lewin and Gibbard, 2010; Bridgland and Westaway, 2014). In the case of the Biferno River, MIS 7 appears as the most plausible timeframe for deposition of the lower valley fill (shallow-marine and coastal facies in core S14). Most of these shallow-marine deposits were eroded during the subsequent sea-level lowering, associated with MIS 6. Above the partly preserved MIS 7 coastal facies, the

upper valley fill would record the recent, prominent phase of fluvial incision and fill that took place during the last glacial phase of sea-level fall, when MIS 7 and MIS 5e marine deposits became vulnerable to later erosion in a continental setting.

5.2. The upper valley fill: post-MIS 5e sedimentary evolution

Multiple strath terraces are a common feature of paleovalleys (Cassel and Graham, 2011), and regular patterns in which incision occurs at the beginning of glacial periods have been highlighted from several regions (Antoine et al., 2000; Vandenberghe, 2008). The remnants of two distinct, buried fluvial terrace gravel deposits at successively lower elevations in the Biferno upper valley fill (Fig. 5) suggest multiple phases of valley excavation and aggradation. Repeated fluvial deposition and incision following initial down-cutting at the MIS 5e/MIS 5d transition has been widely documented from modern shelf systems (e.g., the Trinity/Sabine incised valley system of Thomas and Anderson, 1994). This compound paleovalley architecture is consistent with the post-115 ky BP sea-level curve (Waelbroeck et al., 2002), which shows a stepwise sea-level fall punctuated by short-lived episodes of stillstand or even sea-level rise (Blum et al., 2013).

A comprehensive chronology for the older buried surface of the Biferno paleovalley is not available, whereas the youngest terrace deposit yielded an age of about 31 cal. ky BP (Figs. 4, 5). Based upon this radiometric age, we assume that the last phase of valley incision culminated in the Late Pleniglacial (MIS 3/2 transition in Fig. 6), between 28 and 23 cal. ky BP, possibly in association with increased flood magnitudes (Hanson et al., 2006). Coeval episodes of fluvial incision, with fluvial terrace development and pedogenesis on the interfluves, have been recently documented from two buried incised-valley systems of Italy, in Tuscany and close to Naples (Amorosi et al., 2012; 2013), as well as from several paleovalley systems worldwide (Dabrio et al., 2000; Wellner and Bartek, 2003; Cordier et al., 2006; Busschers et al., 2007; Blum et al., 2008; Kasse et al., 2010; Liu et al., 2010; Amorosi et al., 2014b). Similarly, although aspects of this interpretation are open to question, the older terrace might represent the remnant of fluvial erosion during the Early Pleniglacial (MIS 5/4 transition in Fig. 6). Generalized erosion with soil development at the MIS 5/4 transition has been documented by Cordier et al. (2006) and Rittenour et al. (2007).

The lowermost gravel deposit, at about 30 m depth, is a laterally extensive fluvial body that contains the same lithologies as the above fluvial terrace deposits. Poor or no preservation of overbank deposits suggests that silts and clays were removed by

erosion as a (braided?) river system migrated laterally under sea-level lowstand conditions.

A significant change in fluvial sedimentation is recorded close to the Pleistocene-Holocene transition. While Pleistocene fluvial sedimentation resulted in coarse-grained, laterally amalgamated gravel bodies, the Holocene fluvial deposits consist of isolated and narrow sand bodies embedded in muds, with rare (< 500 m wide) channel-belt sand bodies at distinct stratigraphic levels. Changes in fluvial architecture and the abrupt decrease in grain size at the glacial/interglacial transition reflect a period of rapid floodplain aggradation, with notably decreased stream competence of Holocene rivers relative to their high-energy, lowstand counterparts (Fuller et al., 1998; Aslan and Autin, 1999; Macklin et al., 2002). Apparently, the Biferno River migrated laterally within the valley at lowstand times, whereas the locus of fluvial deposition did not change significantly during the Holocene.

The latest Pleistocene-Holocene valley fill is about 30 m thick and consists almost entirely of non-marine deposits. Above fluvial gravels, the vertical succession of well-drained floodplain facies, poorly-drained floodplain deposits, swamp and then brackish-water clays is interpreted to reflect the progressive flooding of the valley that took place between about 13 and 8 cal. ky BP under conditions of rapid sediment accumulation (about 4 mm/y, on average). When the sea invaded the former river valley, an estuary developed in the modern Biferno coastal plain, as depicted in sequence-stratigraphic models (Dalrymple et al., 1992; Hori et al., 2002; Tanabe et al., 2006), and its related depositional environments can be correlated to the segment 2 of Zaitlin et al. (1994), i.e. the muddy central portion of the estuary. In general, the early Holocene facies sequence of the Biferno valley depicts increasingly marine influence, as observed in the coeval paleovalley systems from the Tyrrhenian Sea coast (Amorosi et al., 2012, 2013). Based upon scattered borehole data from outside the study transect, the maximum landward extent of the Holocene shoreline was about 1 km south of the present-day coastline, i.e. just few hundred of meters north of the study transect (Fig. 1b). As sea level rose to the elevation of the relatively flat fluvial terraces, these areas were flooded, the estuary became progressively wider, and more extensive paludal and lagoonal areas could develop (Anderson et al., 2008). During the middle-late Holocene the Biferno coastal plain experienced progradation. A reverse facies trend characterizes the uppermost 15 m, with swamp clays overlain by discontinuous poorly-drained floodplain facies, capped in turn by the present-day, well-drained alluvial plain.

5.3. Sequence stratigraphy

The Biferno valley fill provides full documentation of the depositional history during the last glacial-interglacial cycle. In terms of sequence stratigraphy, the Late Pleistocene-Holocene depositional sequence exhibits diagnostic facies architecture, which enables prompt identification of the four component systems tracts (Figs. 3, 4, 6).

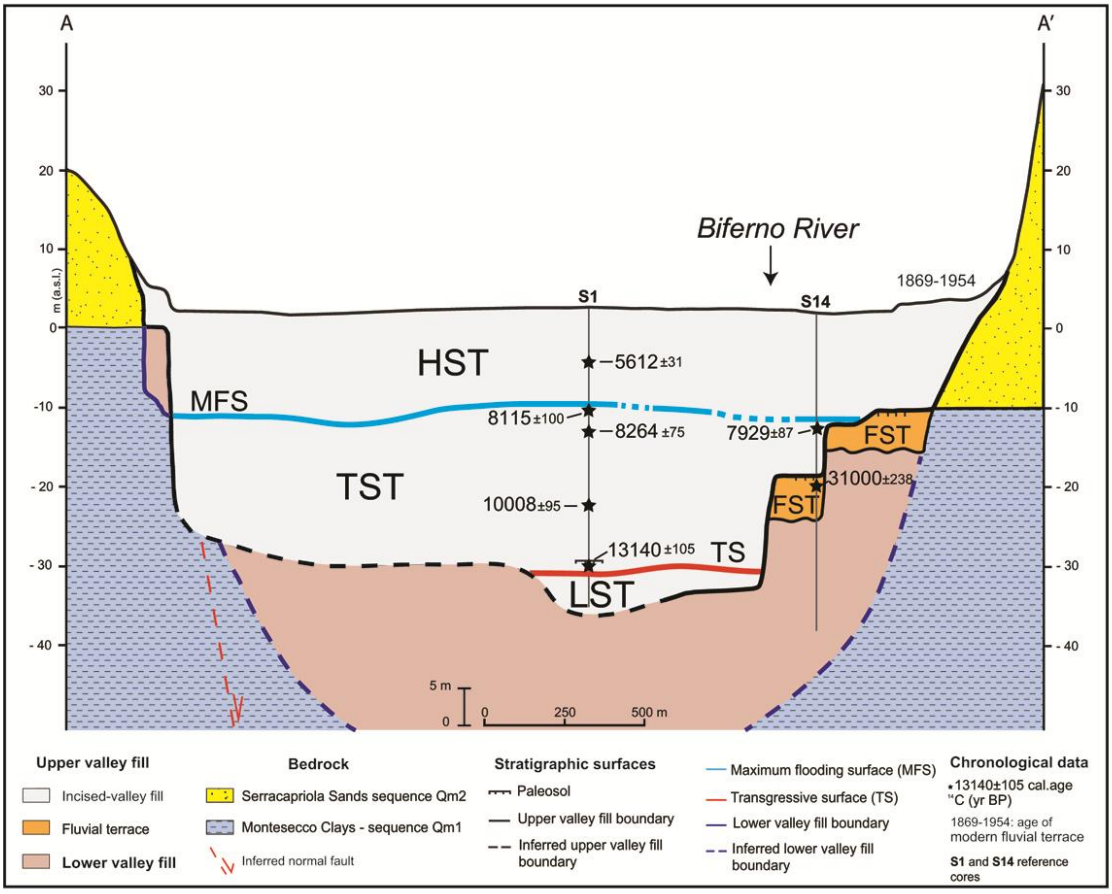

Fig. 6 – Sequence stratigraphic interpretation of the upper valley fill. FST = Forced regressive systems tract; LST = Lowstand systems tract; TST = Transgressive systems tract; HST = Highstand systems tract.

In particular, the sequence boundary appears as a highly diachronous surface in cross-valley direction (Blum and Price, 1998; Korus et al., 2008; Blum et al., 2013), and the buried fluvial terrace deposits developed between about 125 ky (?) and 30 ky BP are interpreted to reflect the forced regressive systems tract (FST) (Fig. 7). This systems tract, albeit discontinuous, is therefore an important component of the Biferno paleovalley fill.

The laterally extensive gravel body that unconformably overlies the marine deposits of the underlying sequence, given its position at the valley floor is very likely to represent the lowstand systems tract (LST). The deepening-upward succession of latest Pleistocene-early Holocene age represents the transgressive systems tract by

definition, while the overlying shallowing-upward tendency records sedimentation under recent sea-level highstand conditions (HST).

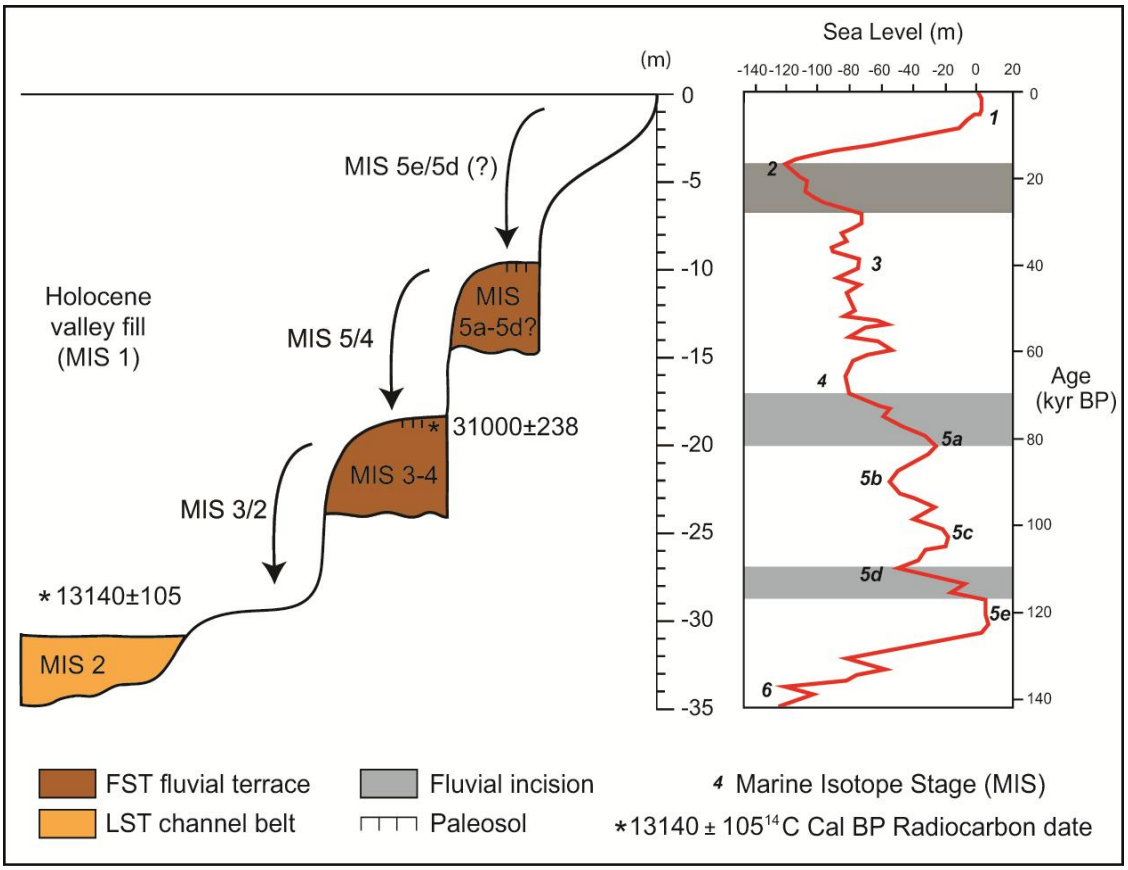

Fig. 7 – Inferred timing of upper valley incision and fill. Multiple channel incision (in grey) was primarily induced by the post-MIS 5e ky glacial base-level lowering, which left (buried) fluvial terraces along the paleovalley flanks. The sea-level curve is drawn from Bard et al. (1990).

The transgressive surface marks an abrupt change in fluvial architecture and lithology, from laterally amalgamated gravels to isolated sand bodies. Based on radiometric dates from Core S1, this surface is slightly older than 13 cal. ky BP, and can tentatively be correlated to the meltwater pulse 1A (Fairbanks et al., 1989; Bard et al., 1990, 1996). Finally, the maximum flooding surface is readily identified at the turnaround from deepening to shallowing-upward conditions, around 8 cal. ky BP.

Despite generalized interest of sequence stratigraphy in compound paleovalley systems, relatively little attention has been directed specifically at coastal-plain compound paleovalleys and their facies architecture (Busschers et al., 2007; Blum et al., 2013). Only by extending stratigraphic analysis to a wider set of post-MIS 5e incised-valley fills will it be possible to develop a predictive model that depicts the effects of repeated glacio-eustatic changes on coastal systems accurately.

6. Conclusions

Beneath 15 m of middle-late Holocene deposits, the Biferno River coastal plain, in southern Italy exhibits considerable stratigraphic complexity and records multiple episodes of valley incision and infilling that took place over the last 350 ky. A combination of stratigraphic, sedimentological, geomorphological and paleontological data was used to reconstruct facies and sediment body geometries along a transverse cross-section through the Biferno paleovalley. Extremely high data density (75 m spacing, on average) ensured reliable reconstructions of facies architecture for the upper valley fill.

Fluvial incision during the Middle Pleistocene was probably triggered by regional tectonic uplift in a rejuvenating landscape, but the overprint of the Late Pleistocene-Holocene sea-level fluctuations onto the overall facies architecture is clearly identified. Successive cycles of base-level fall are recorded in the Biferno coastal plain, and a complex set of older incised-valley-fill deposits was partially eroded by younger valley incisions. The nearshore to shallow-marine lower valley fill is correlated with MIS 7. Subsequent river erosion through unconsolidated material, though loosely constrained by few radiocarbon ages, appears to have been controlled by climate and base-level drop during the last glacial (post-125 ky) sea-level fall, when river valley deeply dissected the previous (MIS 7 and MIS 5e) highstand coastal wedges.

A detailed stratigraphic panel transverse to the paleovalley direction highlights that the Late Pleistocene-Holocene valley was shaped with lateral terraces (buried at various depths, and with typically flat surfaces) and a deeper channel. Two fluvial terraces provide timelines to constrain the valley development. Above lowstand fluvial gravels, the most landward portion of the post-glacial upper valley fill succession displays a transgressive-regressive succession of non-marine deposits. In response to the rapid latest Pleistocene-Holocene sea-level rise, the Biferno valley in the study area was no longer active as a river valley, and during the early Holocene was transformed into an estuary, with characteristic landward shift of facies. At time of maximum marine ingression, the marine influence into the valley extended 1.5 km landward of the present-day coastline, and the study area experienced sedimentation under brackish-water (estuarine) conditions. The return to paludal, poorly-drained floodplain and then well-drained alluvial conditions reflect highstand progradation during the middle-late Holocene.

As predicted by the recent most sequence-stratigraphic models, the sequence boundary appears as a highly time-transgressive surface. The associated buried fluvial

terraces, which document repeated cycles of fluvial incision and aggradation, represent a distinctive feature of the forced-regressive systems tract.

Acknowledgements

We thank Italferr S.p.A. (*Ferrovie dello Stato Italiane* Group) and Cosib (*Consorzio per lo sviluppo industriale della valle del Biferno*) for providing most of stratigraphic and geotechnical data used in study. We are strongly indebted to both reviewers and editor Andrew J. Plater, for their careful review of our manuscript.

References

Albani, A.D., Serandrei Barbero, R., 1990. I foraminiferi della Laguna e del Golfo di Venezia. Mem. Sci. Geol., Padova.

Amorosi, A., Marchi, N., 1999. High-resolution sequence stratigraphy from piezocone tests: An example from the Late Quaternary deposits of the southeastern Po Plain. Sediment. Geol. 128, 67-81.

Amorosi, A., Colalongo, M.L., Fiorini, F., Fusco, F., Vaiani, S.C., Sarti, G., 2004. Paleogeographic and paleoclimatic evolution of the Po Plain from 150-ky records. Glob. Planet. Change 40, 55-78.

Amorosi, A., Ricci Lucchi, M., Rossi, V., Sarti, G., 2009a. Climate change signature of small-scale parasequences from Lateglacial-Holocene transgressive deposits of the Arno valley fill. Palaeogeogr. Palaeocl. Palaeoecol. 273, 142-152.

Amorosi, A., Bracone, V., Di Donato, V., Rosskopf, C.M., Aucelli P.P.C., 2009b. The Plio-Pleistocene succession between Trigno and Fortore rivers (Molise and Apulia Apennines): stratigraphy and facies characteristics. GeoActa 8, 1-12.

Amorosi A., Pacifico, A., Rossi, V., Ruberti, D., 2012. Late Quaternary incision and deposition in an active volcanic setting: The Volturno valley fill, southern Italy. Sediment. Geol. 282, 307-320.

Amorosi, A., Rossi, V., Sarti, G., Mattei, R., 2013. Coalescent valley fills from the late Quaternary record of Tuscany (Italy). Quat. Int. 288, 129-138.

Amorosi, A., Bruno L., Campo, B., Morelli, A., 2014a. The value of pocket penetration tests for the high-resolution palaeosol stratigraphy of late Quaternary deposits. Geol. J. DOI: 10.1002/gj.2585.

Amorosi, A., Bruno, L., Rossi, V., Severi, P., Hajdas, I., 2014b. Paleosol architecture of a late Quaternary basin–margin sequence and its implications for high-resolution, non-marine sequence stratigraphy. Glob. Planet. Change 112, 12-25.

Anderson, J.B., Rodriguez, A.B., Milliken, K.T., Taviani, M., 2008. The Holocene evolution of the Galveston estuary complex, Texas: Evidence for rapid change in estuarine environments. In: Anderson, J.B., Rodriguez, A.B. (Eds.), Response of Upper Gulf Coast Estuaries to Holocene Climate Change and Sea. Geol. Soc. Am., Spec. Paper 443, pp. 89-104.

Antoine, P., Lautridou, J.P., Laurent, M., 2000. Long-term fluvial archives in NW France: response of the Seine and Somme rivers to tectonic movements, climatic variations and sea-level changes. Geomorphology 33, 183-207.

Antonioli, F., Ferranti, L., Fontana, A., Amorosi, A., Bondesan, A., Braitenberg, C., Dutton A., Fontolan, G., Furlani, S., Lambeck, K., Mastronuzzi, G., Monaco, C., Spada, G., Stocchi P., 2009. Holocene relative sea-level changes and vertical movements along the Italian and Istrian coastlines. Quat. Int. 206, 102-133.

Aslan, A., Autin, W.J., 1999. Evolution of the Holocene Mississippi River floodplain, Ferriday, Louisiana: insights on the origin of fine-grained floodplains. J. Sediment. Res. 69, 800-815.

Athersuch, J., Horne, D.J., Whittaker, J. E., 1989. Marine and brackish water ostracods (Superfamilies Cypridacea and Cytheracea). In: Kermack, D. M. and Barnes, R. S. K. (Eds.), Synopsis of the British Fauna. New Series 43. Brill, Leiden, pp. 1-350.

Aucelli, P.P.C., Faillace, P.I., Rosskopf, C.M., 2009. Evoluzione geomorfologica del tratto finale del fondovalle del fiume Biferno (Molise) dal 1800 ad oggi. Mem. Soc. Geograf. Ital. 87, 367-378.

Bard, E., Hamelin, B., Fairbanks, R.G., Zindler, A., 1990. Calibration of the ^{14}C timescale over the past 30,000 years using mass spectrometric U-Th ages from Barbados corals. Nature 345, 405-410.

Bard, E., Hamelin, B., Arnold, M., Montaggioni, L., Cabioch, G., Faure, G., Rougerie, F., 1996. Deglacial sea-level record from Tahiti corals and the timing of global meltwater discharge. Nature 382, 241-244.

Barra, D., Calderoni, G., Cipriani, M., De La Geniere, J., Fiorillo, L., Greco, G., Mariotti Lippi, M., Mori Secci, M., Pescatore, T., Russo, B., Senatore, M.R., Tocco Sciarelli, G., Thorez, J., 1999. Depositional history and palaeogeographic reconstruction of Sele coastal plain during Magna Grecia settlement of Hera Argiva (Southern Italy). Geol. Rom. 35, 151-166.

Berendsen, H.J.A., Stouthamer, E., 2001. Palaeogeographic development of the Rhine-Meuse delta, the Netherlands. Koninklijke van Gorcum, Assen.

Blum, M.D., Price, D.M., 1998. Quaternary alluvial plain construction in response to interacting glacio-eustatic and climatic controls, Texas Gulf Coastal Plain. In: Shanley,

K.W., and McCabe, P.J., (Eds.), Relative Role of Eustacy, Climate, and Tectonism in Continental Rocks. Publ. Soc. Econ. Paleont. Miner. 59, pp. 31-48.

Blum, M.D., Törnqvist, T.E., 2000. Fluvial responses to climate and sea-level change: a review and look forward. Sedimentology 47, 2-48.

Blum, M.D., Tomkin, J.H., Purcell, A., Lancaster, R.R., 2008. Ups and downs of the Mississippi Delta. Geology 36, 675-678.

Blum, M.D., Martin, J., Milliken, K., Garvin, M., 2013. Paleovalley systems: Insights from Quaternary analogs and experiments. Earth-Sci. Rev. 116, 128-169.

Bonaduce, G., Ciampo, G., Masoli, M., 1975. Distribution of Ostracoda in the Adriatic Sea. Pubblicazioni della Stazione Zoologica, Napoli.

Boyd, R., Dalrymple, R.W., Zaitlin, B.A., 2006. Estuarine and incised-valley facies models. In: Posamentier, H.W., Walker, R.G., (Eds.), Facies models revisited. SEPM Special Publication 84, pp. 171-235.

Bracone, V., Amorosi, A., Aucelli, P.P.C., Rosskopf, C.M., Scarciglia, F., Di Donato, V., Esposito P., 2012a. The Pleistocene tectono-sedimentary evolution of the Apenninic foreland basin between Trigno and Fortore rivers (Southern Italy) through a sequence stratigraphic perspective. Basin Res. 24, 213-233.

Bracone, V., Amorosi, A., Aucelli, P., Ciampo, G., Di Donato, V., Rosskopf, C., 2012b. Palaeoenvironmental evolution of the Plio-Pleistocene Molise Periadriatic Basin (Southern Apennines, Italy): insight from Montesecco Clays. Ital. J. Geosciences 131, 272-285.

Bremen, E., 1975. The distribution of ostracodes in the bottom sediments of the Adriatic Sea. Ph.D Thesis. Vrije Universiteit, Amsterdam.

Bridgland, D.R., Westaway, R., 2014. Quaternary fluvial archives and landscape evolution: a global synthesis. Proc. Geol. Assoc. 125, 600-629.

Busschers, F.S., Kasse, C., van Balen, R.T., Vandenberghe, J. Cohen, K.M., Weerts, H.J.T., Wallinga, J., Johns, C., Cleveringa, P., Bunnik, F.P.M., 2007. Late Pleistocene evolution of the Rhine-Meuse system in the southern North Sea basin: imprints of climate change, sea-level oscillation, and glacio-isostacy. Quat. Sci. Rev. 26, 3216-3248.

Buzas, M.A., 1990. Another look at confidence limits for species proportions. J. Paleontol. 64, 842-843.

Carboni, M.G., Bergamin, L., Di Bella, L., Iamundo, F., Pugliese, N., 2002. Palaeoecological evidences from foraminifers and ostracods on Late Quaternary sea-level changes in the Ombrone river plain (central Tyrrhenian coast, Italy). Geobios Mem. Spec. 24, 40-50.

Carboni, M.G., Succi, M.C., Bergamin, L., Di Bella, L., Frezza, V., Landini, B., 2009. Benthic foraminifera from two coastal lakes of southern Latium (Italy). Preliminary evaluation of environmental quality. Mar. Pollut. Bull. 59, 268-280.

Carboni, M.G., Bergamin, L., Di Bella, L., Esu, D., Pisegna Cerone, E., Antonioli, F., Verrubi, V., 2010. Palaeoenvironmental reconstruction of late Quaternary foraminifera and molluscs from the ENEA borehole (Versilian plain, Tuscany, Italy). Quat. Res. 74, 265-276.

Cassel, E.J., and Graham, S.A., 2011, Paleovalley morphology and fluvial system evolution of Eocene-Oligocene sediments ('auriferous gravels'), northern Sierra Nevada, California: Implications for climate, tectonics, and topography. Geol. Soc. Am. Bull. 123, 1699-1719.

Coccioni, R., 2000. Benthic Foraminifera as Bioindicators of Heavy Metal Pollution - A Case Study from the Goro Lagoon (Italy). In: Martin, R.E., (Ed.), Environmental Micropaleontology - The Application of Microfossils to Environmental Geology. Kluwer Academic/Plenum Press Publishers, New York. Topics in Geobiology, 15, pp. 71-103.

Cordier, S., Harmand, D., Frechen, M., Beiner, M., 2006. Fluvial system response to Middle and Upper Pleistocene climate change in the Meurthe and Moselle valleys (Eastern Paris Basin and Rhenish Massif). Quat. Sci. Rev. 25, 1460-1474.

Dabrio, C.J., Zazo, C., Goy, J.L., Sierro, F.J., Borja, F., Lario, J., González, J.A., Flores, J.A., 2000. Depositional history of estuarine infill during the last postglacial transgression (Gulf of Cadiz, Southern Spain). Mar. Geol. 162, 381-404.

Dalrymple, R.W., Zaitlin, B.A., Boyd, R., 1992. Estuarine facies models: conceptual basis and stratigraphic implications. J. Sediment. Petrol. 62, 1130-1146.

Dalrymple, R.W., Boyd, R., Zaitlin, B.A., 1994. Incised-Valley Systems: Origin and Sedimentary Sequences. SEPM Special Publication 51, pp. 1-391.

D'Amico, C., Aiello, G., Barra, D., Bracone, V., Di Bella, L., Esu, D., Frezza, V., Rosskopf, C.M., 2013. Late Quaternary foraminiferal, molluscan and ostracod assemblages from a core succession in the Trigno River mouth area (Central Adriatic Sea, Italy). Boll. Soc. Paleontol. Ital. 52, 197-205.

D'Amico, C., Esu, D., Magnatti, M., 2014. Land mollusc palaeocommunity dynamics related to palaeoclimatic changes in the Upper Pleistocene alluvial deposits of Marche Apennines (central Italy). Ital. J. Geosciences 133, 235-248.

Debenay, J.P., Guillou, J.J., 2002. Ecological transitions indicated by foraminiferal assemblages in paralic environments. Estuaries 25, 1107-1120.

Debenay, J.P., Millet, B., Angelidis, M. O., 2005. Relationships between foraminiferal assemblages and hydrodynamics in the Gulf of Kalloni, Greece. J. Foramin. Res. 35, 327-343.

De Santis, V., Caldara, M., 2014. Evolution of an incised valley system in the Southern Adriatic Sea (Apulian margin): an onshore-offshore correlation. Geol. J. DOI: 10.1002/gj.2628.

Di Celma, C., Pieruccini, P., Farabollini, P., 2015. Major controls on architecture, sequence stratigraphy and paleosols of middle Pleistocene continental sediments ("Qc Unit"), eastern central Italy. Quat. Res. 83, 3, 565-581. doi:10.1016/j.yqres.2015.01.006

D'Onofrio, S., Marabini, F., Vivalda, P., 1976. Foraminiferi di alcune lagune del delta del Po. G. Geol. 40, 267-276.

Fairbanks, R.G., 1989. A 17,000-year glacio-eustatic sea level record: influence of glacial melting rates on the Younger Dryas event and deep-ocean circulation. Nature 342, 637-642.

Fiorini, F., Vaiani, S.C., 2001. Benthic foraminifers and transgressive-regressive cycles in the Late Quaternary subsurface sediments of the Po Plain near Ravenna (Northern Italy). Boll. Soc. Paleontol. Ital. 40, 357-403.

Fiorini, F., 2004. Benthic foraminiferal associations from Upper Quaternary deposits of southeastern Po Plain, Italy. Micropaleontology 50, 45-58.

Fontana, A., Mozzi, P., Bondesan, A., 2008. Alluvial megafans in the Venetian-Friulian Plain (north-eastern Italy): Evidence of sedimentary and erosive phases during Late Pleistocene and Holocene. Quat. Int. 189, 71-90.

Fontana A., Ferrarese F., Mozzi P., 2013. Integrating digital elevation models and stratigraphic data for the reconstruction of the post-LGM unconformity in the Brenta alluvial megafan (North-eastern Italy). Alpine Mediterr. Quat. 3, 41-54.

Foyle, A.M., Oertel, G.F., 1997. Transgressive systems tract development and incised-valley fills within a quaternary estuary-shelf system: Virginia inner shelf, U.S.A. Mar. Geol. 137, 227-249.

Frontalini, F., Buosi, C., Da Pelo, S., Coccioni, R., Cherchi, A., Bucci, C., 2009. Benthic foraminifera as bio-indicators of trace element pollution in the heavily contaminated Santa Gilla lagoon (Cagliari, Italy). Mar. Pollut. Bull. 58, 858-877.

Fuller, I.C., Macklin, M.G., Lewin, J., Passmore, D.G., Wintle, A.G., 1998. River response to high-frequency climate oscillations in Southern Europe over the past 200 k.y. Geology 26, 275-278.

Gibbard, P.L., Lewin, J., 2009. River incision and terrace formation in the Late Cenozoic of Europe. Tectonophysics 474, 1-2, 41-55.

Gibling, M.R., 2006. Width and thickness of fluvial channel bodies and valley fills in the geological record: a literature compilation and classification. J. Sediment. Res. 76, 731-770.

Gibling, M.R., Fielding, C.R., Sinha, R., 2011. Alluvial valleys and alluvial sequences: towards a geomorphic assessment. In: Davidson, K.S., Leleu, S., North, C.P. (Eds.), From River to Rock Record: The Preservation of Fluvial Sediments and Their Subsequent Interpretation. Tulsa, Oklahoma. SEPM Special Publication 97, pp. 423-447.

Greene, D.L., Rodriguez, A.B., Anderson, J.B., 2007. Seaward-branching coastal-plain and piedmont incised valley systems through multiple sea-level cycles: Late Quaternary examples from Mobile Bay and Mississippi Sound, USA. J. Sediment. Res. 77, 139-158.

Hanson, P.R., Mason, J.A., Goble, R.J., 2006. Fluvial terrace formation along Wyoming's Laramie Range as a response to increased late Pleistocene flood magnitudes. Geomorphology 76, 12-25.

Henderson, P.A., 1990. Freshwater Ostracods. Synopses of the British Fauna. E. J. Brill. (New Series), Leiden

Hijma, M.P., Cohen, K.M., Hoffmann, G., Van der Spek, A.J.F., Stouthamer, E., 2009. From river valley to estuary: the evolution of the Rhine river mouth in the early to middle Holocene (western Netherlands, Rhine-Meuse delta). Netherlands J. Geosciences 88, 13-53.

Hori, K., Saito, Y., Zhao, Q., Wang, P., 2002. Evolution of the coastal depositional systems of the Changjiang (Yangtze) in response to late Pleistocene-Holocene sea-level changes. J. Sediment. Res. 72, 884-897.

Ilg, C., Foeckler, F., Deichner, O., Henle, K., 2009. Extreme flood events favour floodplain mollusc diversity. Hydrobiologia 621, 63-73.

Jorissen, F.J., 1988. Benthic foraminifera from the Adriatic Sea; principles of phenotypic variation. Utrecht Micropaleontol. Bull. 37, 1-176.

Kasse, C., Bohncke, S.J.P., Vandenberghe, J., Gábris, G., 2010. Fluvial style changes during the last glacial–interglacial transition in the middle Tisza valley (Hungary). Proc. Geol. Assoc. 121, 180-194.

Korus, J.T., Kvale, E.P., Eriksson, K.A., Joeckel, R.M., 2008. Compound valley fills in the Lower Pennsylvanian New River Formation, West Virginia, USA. Sediment. Geol. 208, 15-26.

Lewin, J., Gibbard, P.L., 2010. Quaternary river terraces in England: Forms, sediments and processes. Geomorphology 120, 293-311.

Li, C., Wang, P., Fan, D., Yang, S., 2006. Characteristics and formation of late Quaternary incised-valley-fill sequences in sediment-rich deltas and estuaries: case study from China. In: Dalrymple, R.W., Leckie, S. A., Tilliman, R.W. (Eds.), Incised

valleys in time and space. Tulsa, Oklahoma. SEPM Special Publication 85, pp. 141-160.

Liu, J., Saito, Y., Kong, X., Wang, H., Wen, C., Yang, Z., Nakashima, R., 2010. Delta development and channel incision during marine isotope stages 3 and 2 in the western South Yellow Sea. Mar. Geol. 278, 54-76.

Macklin, M.G., Fuller, I.C., Lewin, J., Maas, G.S., Passmore, D.J., Rose, J., Woodward, J.C., Black, S., Hamlin, R.H.B., Rowan, J.S., 2002. Correlation of fluvial sequences in the Mediterranean basin over the last 200 ka and their relationship to climate change. Quat. Sci. Rev. 21, 1633-1641.

Maselli, V., Trincardi, F., 2013. Large-scale single incised valley from a small catchment basin on the western Adriatic margin (central Mediterranean Sea). Glob. Planet. Change 100, 245-262.

Maselli, V., Trincardi, F., Asioli, A., Rizzetto, F., Taviani, M., 2014. Delta growth and river valleys: the influence of climate and sea level changes on the South Adriatic shelf (Mediterranean Sea). Quat. Sci. Rev. 99, 146-163.

Mattheus, C.R., Rodriguez, A.B., 2014. Controls on lower-coastal-plain valley morphology and fill architecture. J. Sediment. Res. 84, 314-325.

Meisch, C. 2000. Freshwater Ostracoda of Western and Central Europe. Spektrum Academischer, Heidelberg, Berlin.

Milli, S., D'Ambrogi, C., Bellotti, P., Calderoni, G., Carboni, M.G., Celant, A., Di Bella L., Di Rita, F., Frezza, V., Magri, D., Pichezzi, R.M., Ricci, V., 2013. The transition from wave-dominated estuary to wave-dominated delta. The Late Quaternary stratigraphic architecture of Tiber River deltaic succession (Italy). Sediment. Geol. 284–285, 159-180.

Montenegro, M.E., Pugliese, N., 1996. Autoecological remarks on the ostracod distribution in the Marano and Grado Lagoons (Northern Adriatic Sea, Italy). Boll. Soc. Paleont. Ital. 3, 123-132.

Murray, J. W., 2006. Ecology and applications of benthic foraminifera. Cambridge University Press, Cambridge.

Parlagreco, L., Mascioli, F., Miccadei, E., Antonioli, F., Gianolla, D., Devoti, S., Leoni, G., Silenzi, S., 2011. New data on Holocene relative sea level along the Abruzzo coast (central Adriatic, Italy). Quat. Int. 232, 179-186.

Pérès, J.M., Picard, J., 1964. Nouveau manuel de bionomie benthique de la Mer Méditerranée. Recueil des travaux de la Station Marine d'Endoume, pp. 1-137.

Posamentier, H.W., Vail, P.R., 1988. Eustatic controls on clastic deposition II - Sequence and systems tract models. In: Wilgus, C.K., Hastings, B.S., Kendall, C.G.St.C., Posamentier, H.W., Ross, C.A., Van Wagoner, J.C. (Eds.), Sea Level

Changes: An Integrated Approach. Tulsa, Oklahoma. SEPM Special Publication 42, pp. 125-154.

Reimer, P.J., Bard, E., Bayliss, A., Beck, J.W., Blackwell, P.G., Bronk Ramsey, C., Buck, C.E., Cheng, H., Edwards, R.L., Friedrich, M., Grootes, P.M., Guilderson, T.P., Haflidason, H., Hajdas, I., Hatté, C., Heaton, T.J., Hoffmann, D.L., Hogg, A.G., Hughen, K.A., Kaiser, K.F., Kromer, B., Manning, S.W., Niu, M., Reimer, R.W., Richards, D.A., Scott, E.M., Southon, J.R., Staff, R.A., Turney, C.S.M., Van der Plicht, J., 2013. Intcal13 and Marine13 radiocarbon age calibration curves 0 – 50,000 years cal BP. *Radiocarbon 55*, 1869-1887.

Reimer, P.J., McCormac, F.G., 2002. Marine radiocarbon reservoir corrections for the Mediterranean and Aegean Seas, Radiocarbon 44, 159-166.

Rittenour, T.M., Blum, M.D., Goble, R.J., 2007. Fluvial evolution of the lower Mississippi river valley during the last 100 k.y. glacial cycle: Response to glaciation and sea-level change. Geol. Soc. Am. Bull. 119, 586-608.

Rossi, V., Vaiani, S.C., 2008. Benthic foraminiferal evidence of sediment supply changes and fluvial drainage reorganization in Holocene deposits of the Po Delta, Italy. Mar. Micropaleontol. 69, 106-118.

Rosskopf, C.M., Scorpio, V., 2013. Geomorphologic map of the Biferno River valley floor system (Molise, Southern Italy). J. Maps 9, 106-114.

Roy, N.G., Sinha, R., Gibling, M.R., 2012. Aggradation, incision and interfluve flooding in the Ganga Valley over the past 100,000 years: Testing the influence of monsoonal precipitation. Palaeogeogr. Palaeocl. Palaeoecol. 356–357, 38-53.

Ruiz, F., Gonzalez-Regalado, M.L., Muñoz, J.M., 1997. Multivariate analysis applied to total and living fauna: seasonal ecology of recent benthic Ostracoda off the North Cádiz Gulf coast (southwestern Spain). Mar. Micropal. 31, 183-203.

Ruiz, F., Gonzalez-Regalado, M.L., Baceta, J.I., Menegazzo-Vitturi, L., Pistolato, M., Rampazzo G., Molinaroli, E. 2000. Los ostrácodos actuales de la laguna de Venecia (NE de Italia). Geobios 33, 447-454.

Sarti, G., Rossi, V., Amorosi, A., 2012. Influence of Holocene stratigraphic architecture on ground surface settlements: A case study from the City of Pisa (Tuscany, Italy). Sediment. Geol. 281, 75-87.

Scaperrotta, M., Bartolini, S., Bogi, C., 2009. Accrescimenti. Stadi di accrescimento dei molluschi marini del Mediterraneo. L'Informatore Piceno, Ancona.

Sgarrella, F., Moncharmont-Zei, M., 1993. Benthic Foraminifera of the Gulf of Naples (Italy): systematics and autoecology. Boll. Soc. Paleont. Ital. 32, 145-264.

Siani, G., Paterne, M., Arnold, M., Bard, E., Métivier, B., Tisnerat, N., Bassinot, F., 2000. Radiocarbon reservoir ages in the Mediterranean Sea and Black Sea. Radiocarbon 42, 2, 271-280.

Soil Survey Staff. 1999. Soil Taxonomy: A basic system of soil classification for making and interpreting soil surveys. Second ed. USDA-SCS Agric. Handb. 436. US Gov. Print. Office, Washington, DC.

Stuiver, M., Reimer, P.J., 1993. Extended 14C database and revised CALIB radiocarbon calibration program, Radiocarbon 3, 215-230.

Tanabe, S., Saito, Y., Vu, Q.L, Hanebuth, T.J.J., Ngo, Q.L, Kitamura, A., 2006. Holocene evolution of the Song Hong (Red River) delta system, northern Vietnam. Sediment. Geol. 187, 29-61.

Tesson, M., Labaune, C., Gensous, B., Suc, J.P., Melinte-Dobrinescu, M., Parize, O., Imbert, P., Delhaye-Prat, V., 2011. Quaternary “compound” incised valleys in a microtidal environment, Roussillon continental shelf, Western Gulf of Lions, France. J. Sediment. Res. 81, 708-729.

Thomas, M.A., Anderson, J.B., 1994. Sea-level controls on the facies architecture of the Trinity/Sabine incised valley system, Texas continental shelf. In: Dalrymple, R.W., Boyd, R., Zaitlin, B.A. (Eds.), Incised-Valley Systems: Origin and Sedimentary Sequences. SEPM Special Publication 51, 63-82.

Törnqvist, T.E., Wallinga, J., Busschers, F.S., 2003. Timing of the last sequence boundary in a fluvial setting near the highstand shoreline – Insights from optical dating. Geology 31, 279-282.

Trincardi, F., Correggiari, A., Roveri, M., 1994. Late Quaternary transgressive record and deposition in a modern epicontinental shelf: the Adriatic semi-enclosed basin. Geo-Mar. Lett. 14, 41-51.

Tropeano, M., Cilumbriello, A., Sabato, L., Gallicchio, S., Grippa, A., Longhitano, S.G., Bianca, M., Gallipoli, M.R., Mucciarelli, M., Spilotro, G., 2013. Surface and subsurface of the Metaponto Coastal Plain (Gulf of Taranto – Southern Italy): Present-day-vs LGM-landscape. Geomorphology 203, 115-131.

Vandenberghe, J., 2008. The fluvial cycle at cold-warm-cold transitions in lowland regions: A refinement of theory. Geomorphology 98, 275-284.

Vezzani, L., Festa, A., Ghisetti F., 2010. Geology and tectonic evolution of Central-Southern Apennines, Italy. Geol. Soc. Am. Special Paper, 469, 1-58.

Waelbroeck, C., Labeyrie, L., Michel, E., Duplessy, J.C., McManus, J.F., Lambeck, K., Balbon, E., Labracherie, M., 2002. Sea-level and deep water temperature changes derived from benthic foraminifera isotopic records. Quat. Sci. Rev. 21, 295-305.

Wellner, R.W., Bartek, L.R., 2003. The effect of sea level, climate, and shelf physiography on the development of incised-valley complexes: a modern example from the East China Sea. J. Sediment. Res. 73, 926-940.

Welter-Schultes, F.W., 2012. European non-marine molluscs, a guide for species identification. Planet Poster Editions, Göttingen.

Zaitlin, B.A., Dalrymple, R.W., Boyd, R., 1994. The stratigraphic organization of incised valley systems associated with relative sea-level change. In: Dalrymple, R.W., Boyd, R., Zaitlin, B.A. (Eds.), Incised-Valley Systems: Origin and Sedimentary Sequences. SEPM Special Publication 51, pp. 45-60.

5.5. Paper 5 (Study area 5)

Origin of VC-only plumes from naturally enhanced dechlorination in a peat-rich hydrogeologic setting*

Maria Filippini, Alessandro Amorosi, ***Bruno Campo***, Sara Herrero-Martìn, Ivonne Nijenhuis, Beth L. Parker, Alessandro Gargini

*Submitted to Journal of ***Contaminant Hydrology***

Origin of VC-only plumes from naturally enhanced dechlorination in a peat-rich hydrogeologic setting

Maria Filippini, Alessandro Amorosi, ***Bruno Campo***, Sara Herrero-Martìn, Ivonne Nijenhuis, Beth L. Parker, Alessandro Gargini

Abstract

The occurrence of vinyl chloride (VC) is often a main concern at sites contaminated with chlorinated solvents due to its high degree of toxicity and carcinogenicity. VC occurrence in aquifers is most often related to the degradation of higher chlorinated ethenes or ethanes and it is generally detected in plumes along with parent contaminants. However, specific combination of hydrogeologic and stratigraphic conditions can enhance the degradation of parents and lead to the formation of plumes almost entirely composed by VC (i.e. VC-only plumes). This paper investigates the causes of VC-only plumes in the aquifers below the city of Ferrara (northern Italy) by combining hydrogeological and stratigraphic lines of evidence. The City of Ferrara is located on an alluvial lowland, built by the River Po, and made up of alternating unconsolidated sandy aquifer and silt-clay aquitard deposits of fluvial origin. This region has been strongly impacted by prior industrial activities, with the occurrence of chlorinated compounds at several sites. VC-only plumes with uncertain source location were found in two contaminated sites. The source zone of a third plume composed of chloroethenes from PCE down to VC was investigated for high resolution depositional facies architecture and contaminant distribution (contaminant concentration and Compound Specific Isotope Analysis – CSIA). The investigation showed that reductive dechlorination of PCE and TCE takes place during contaminant migration through peat-rich (swamp) layers related to the Holocene transgression, which locally act as a “reactor” for stimulating biodegradation down to VC but accumulation of VC given the strongly reducing conditions. Regional-scale stratigraphic architecture showed the ubiquitous occurrence of swamp layers at distinct stratigraphic levels in the investigated system and their apparent linkage with the in situ creation of the VC-only plumes due to distinct hydrochemical conditions.

Keywords: Vinyl Chloride, plume, depositional facies, Swamp deposits, reductive dechlorination

1. Introduction

Chlorinated hydrocarbons are the most prevalent organic contaminants found in groundwater (Stroo et al., 2003). Among them, Vinyl Chloride (VC) is often of greater concern than higher chlorinated compounds, since it is more mobile in liquid and gas phases (Mackay et al., 2006) and a known human carcinogen (IARC, 2007). VC can be found in aquifers as result of direct dumping or most often as the product of partial reductive dechlorination of high chlorinated ethenes and ethanes (Barrio-Lage et al., 1986; Chen et al., 1996; Lorah and Olsen, 1999; Vogel and McCarty, 1985). VC from partial dechlorination generally occurs in groundwater along with its associated high chlorinated parent compounds. However, under certain biogeochemical conditions the dechlorination of parents can be enhanced and lead to the formation of plumes almost entirely composed of VC (i.e. VC-only plumes). The occurrence of VC-only plumes can cause the potential for severe human health concerns related to groundwater quality and vapor intrusion. It is therefore essential to identify the kinds of setting where the phenomenon could be expected. A robust stratigraphic model based on detailed characterization and interpolation of the contaminant constituents and concentrations in association with distinct depositional environments can help identify zones where dechlorination of contaminants and potential production of hazardous metabolites (e.g. VC) could be enhanced. The association between chlorinated hydrocarbon constituents, isotopic composition, hydrochemical and depositional environments is particularly relevant in the case of unconsolidated porous settings comprised of layered sediments (e.g. alluvial plains) where the contaminants have intimate and pervasive contact with the lower permeability and organic-rich matrix and average groundwater flow rates are relatively low (e.g. Allen-King et al., 2006; Chapman and Parker, 2005; Guilbeault et al., 2005; Kalinovich et al., 2012; Parker et al., 2004; Ritzi et al., 2013). Gilmore (2010) and Sale et al. (2013) observed the importance of studying contaminant mass storage in depositional zones corresponding to lower K sediment layers, where contrasting hydrochemical conditions and strongly variable physicochemical properties of sediments can influence contaminant degradation.

The main objective of this study was to understand the origin of VC-only plumes in an unconsolidated alluvial setting. To achieve the objective, detailed stratigraphic and hydrogeological investigations have been carried out in a complex multilayered aquifer system (southeastern sector of the Po Plain, Ferrara, northern Italy), where contamination by chlorinated ethenes occurs at several sites, showing peculiar accumulations of the degradation product VC, but lack of the parent compounds suspected to have been released as DNAPLs decades ago. In particular, two VC-only

plumes with uncertain source location were detected in contaminated sites “A” and “B” (Fig. 1). The study focused at the source of contamination of a third site (“Caretti site”) where the whole series of chloroethenes (from PCE to VC) occurs in groundwater at concentrations up to $1x10^4$ µg/L. Detailed depositional facies analysis and high-resolution vertical hydrogeological investigations (i.e. reconstruction of contaminant architecture, in the same manner as Adamson et al., 2015; Guilbeault et al., 2005; Parker et al., 2003) have been carried out along with investigation of groundwater geochemical conditions and application of Compound-Specific Isotope Analyses (CSIA). A detailed conceptual model developed at the Caretti source zone allowed interpretation of the accumulation of by-products in relation with the regional stratigraphy, and therefore to understand the genesis and persistence of VC-only plumes in the Ferrara region.

2. Geological setting

The Po Plain, one of the largest alluvial plains in Europe, has been widely investigated during the last three decades in terms of basin formation and evolution (Dalla et al., 1992; Dondi and D'Andrea, 1986; Muttoni et al., 2003; Pieri and Groppi, 1981). These early studies showed the Po Plain as a rapidly subsiding foreland basin bounded by two mountain chains, the Alps to the north and the Apennines to the south.

South of Po River, the large-scale stratigraphic architecture of the Pliocene-Quaternary basin fill displays vertically stacked, third-order depositional sequences (sensu Mitchum et al., 1977), identified on a seismic basis and mapped as unconformity-bounded stratigraphic units (UBSU - Molinari et al., 2007; Regione Emilia-Romagna and ENI-AGIP, 1998). A tectonic unconformity within the uppermost unit (Emilia-Romagna Supersynthem) allows its subdivision into two lower-rank units: Lower and Upper Emilia-Romagna Synthems. The latter shows the characteristic alternation of continental/marine deposits (Amorosi et al., 2004; Amorosi et al., 1999) or distinctive fluvial-channel stacking patterns (Amorosi et al., 2008). The Upper Emilia-Romagna Synthem is subdivided into four fourth-order depositional cycles (subsynthems), 50 to 100 m thick, which have been interpreted to reflect transgressive-regressive (T-R) cycles falling in the Milankovitch band (ca. 100 kyr), and that are inferred to represent regional hydrostratigraphic units (aquifer systems A0 to A4 of Molinari et al., 2007; Regione Emilia-Romagna and ENI-AGIP, 1998; Regione Lombardia and ENI Divisione AGIP, 2002).

In the study area (Fig. 1), landward of the maximum marine ingression, the T-R cycles are made up entirely of continental deposits. Above basal, overbank clays and

silts with highly lenticular fluvial sand bodies, each fourth-order cycle exhibits increasingly amalgamated and laterally extensive channel-belt sand bodies (Amorosi et al., 2008). The sheet-like fluvial bodies represent the major aquifer systems, while the overbank fines are considered low permeability barriers. The youngest channel belt, which is assigned to the Würm period (Marine Isotope Stages 4 to 2), is of latest Pleistocene age and corresponds to aquifer A1 of Molinari et al. (2007). The aquifer is overlain by aquitard Q1. At the Caretti site (Fig.1) the A1 aquifer consists of two distinct, locally amalgamated sand bodies (lower A1 and upper A1 aquifers, overlain by lower Q1 and upper Q1 aquitards, respectively). The overlying Holocene deposits are mud-dominated, with lens-shaped sand bodies of fluvial origin (aquifer A0, overlain by aquitard Q0). Recent unpublished work in the study area has focused on the stratigraphic architecture of the Holocene succession, identifying a thick interval of transgressive swamp deposits (peats and organic-rich clays) in the Q0 and Q1 aquitards (Q0 and upper Q1 at the Caretti site).

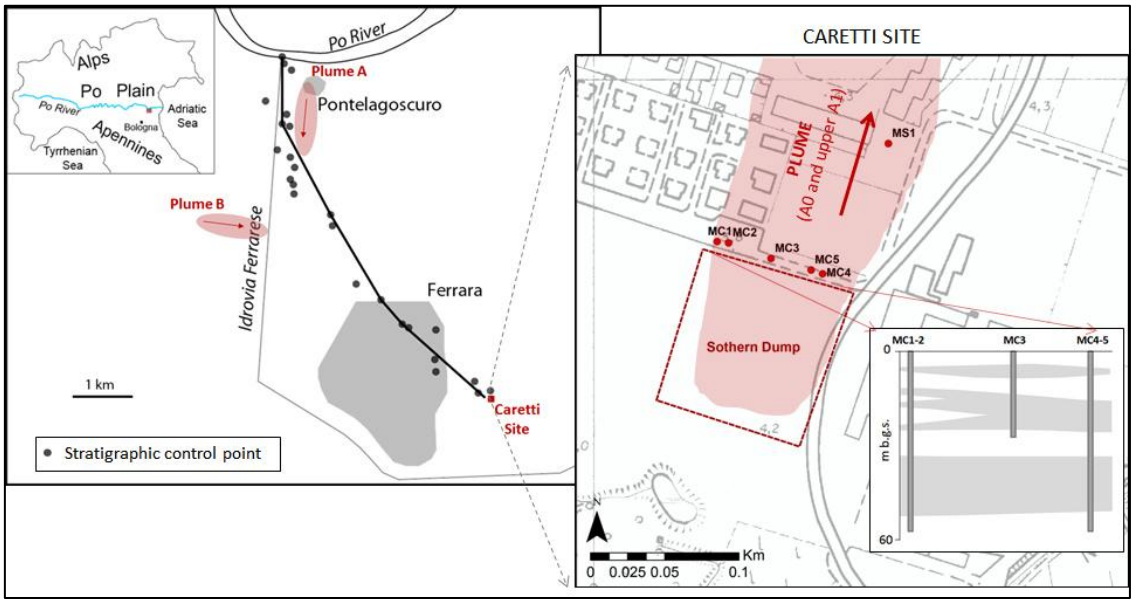

Fig.1 - Location of the study area. The left box depicts the VC-only plumes A and B, their main flow direction and the points used for stratigraphic reconstruction across the Ferrara region. Details about the Caretti site (configuration of the monitoring cross-section in relation with the source of contamination) are schematized on the right: profiles MC1 + MC2 are considered as one single vertical profile named MC1-2; likewise profiles MC4 + MC5 are jointed in the MC4-5 profile.

3. The issue of Vinyl Chloride in Ferrara

The aquifers below Ferrara are burdened by a groundwater contamination peculiar in terms of severity and chemical composition. Chlorinated solvents with concentrations up to $1x10^4$ µg/L occur below industrial, residential or agricultural areas. Vinyl Chloride dominates the composition of contaminant plumes (Gargini et al., 2011). The origin of

the plumes is related to local sources directly or indirectly linked with industrial activities (Nijenhuis et al., 2013). Highly chlorinated compounds were spilled in the environment as industrial wastes, while VC must represent a product of dechlorination of former compounds. The high VC concentrations show strong propensity for PCE, TCE and cDCE to degrade but not for the VC itself. The common occurrence of VC accumulation and persistence within the region suggests strong association with the local hydrogeologic setting.

At least two VC-only plumes (A and B in Fig. 1) flow in the totally confined and strongly reducing A1 aquifer below Ferrara. Plume A was detected by Pasini et al. (2008), while plume B was detected by Nijenhuis et al. (2013) and thoroughly investigated by a private company that will remain anonymous for privacy issues. Both plumes are markedly developed along their main flow directions (up to distances of 1.2 km), while showing limited transverse spreading (up to 300 m in the case of plume A, the largest plume). Maximum detected concentrations of VC are in the order of $1x10^4$ µg/L and $1x10^2$ µg/L in plumes A and B, respectively. The vertical distribution of VC was investigated for both plumes (see Fig. 7). Since it was not possible to identify the exact location, geometry and composition of the primary source of contamination for either plumes A or B, the mechanism of VC accumulation as a function of local stratigraphy was investigated at another known source of contamination (Caretti site), located 5 to 6 km southwestward.

4. Methods

4.1. Stratigraphic reconstruction and facies interpretation

In order to reconstruct a reliable stratigraphic framework for the study area, the whole stratigraphic database hosted at the Emilia-Romagna Geological Survey (RER) was considered. From the RER dataset, we selected 24 core descriptions and 1 piezocone penetration (CPTU) test (Fig. 1). Stratigraphic descriptions include color, lithology, accessory material and, in a few instances, pocket penetrometer values. Cores recovered from three boreholes (MC1-2, MC3 and MC4-5) during summer 2013, were investigated for detailed sedimentology. The three cores were recovered along a 60 m long cross-section, 60 m thick at the Caretti site (Fig. 1) and are currently stored at the Environmental Survey of the Ferrara Municipality. Only the uppermost 30 m of the cross-section were taken into account for the purposes of this paper.

Facies interpretation from the three cores was used for calibration of stratigraphic data extracted from the RER dataset. As a result, each stratigraphic description was tentatively converted into facies data. For stratigraphic interpretation of the CPTU test,

a combination of Q_c (cone penetration resistance), sleeve friction (f_s) and pore water pressure (u) values were used, as suggested by Amorosi and Marchi (1999). Pocket penetrometer values, where available, were also used for facies characterization (Amorosi et al., 2014). Facies analysis was used as a basis for stratigraphic correlations, allowing reconstruction of facies architecture at regional scale (i.e. transect extended from Caretti site to the Po River; Fig. 6).

4.2. Groundwater sampling and sample preparation

Five multilevel systems (Solinst® CMT System; Einarson and Cherry (2002)) were installed into the five boreholes used for the stratigraphic reconstruction at the Caretti site (MC1-2, MC3 and MC4-5 from Fig. 1; MC1-2 and MC4-5 consist of two coupled boreholes spaced 4 to 5 m apart). The CMT multilevel systems were exploited to create a detailed profile of groundwater concentrations with depth, allowing sampling ports in distinct facies and layers. The monitoring cross-section is located on the downgradient fringe of a known source of contamination (i.e. Southern dump, Fig. 1).

Groundwater samples were collected from the CMT systems in aquifer and aquitard units, and used to determine concentration distributions of chlorinated ethenes and dissolved gases (i.e. ethene, methane).

Prior to sampling, three times the volume of water contained in the tubing and in the sandpacks surrounding the screens was purged (between 5-120 L), using a low flow peristaltic pump (Model 410 Peristaltic Pump, Solinst®). Groundwater samples were collected after stabilization of physico-chemical parameters monitored via a flow-cell equipped with electrodes for the determination of temperature, specific electricconductivity, pH and Eh (QuantaD, Hydrolab®).

For samples dedicated to contaminant concentration analyses, 1 L Schott glass bottles were filled completely (no headspace) with groundwater and sealed with Teflon™ lined screw caps. For concentration analysis of dissolved gases, 220 mL serum bottles were filled to the top, acidified immediately (hydrochloric acid to pH 2) and closed with butyl rubber stoppers capped with aluminum crimp seals. Samples were stored upside down at 4 °C until analysis.

4.3. Sediment Core subsampling

Core subsamples were collected from continuous cores of MC4-5 (Fig. 1) and analyzed for chlorinated ethene concentrations and determination of their respective compound specific isotope composition ($\delta^{13}C$). MC4-5 was selected since it was expected to be the most contaminated profile (Gargini et al., 2011; Nijenhuis et al., 2013).

The core subsampling technique provides point information and a high level of vertical resolution (e.g. dm scale), which cannot be gained from groundwater samples, especially concerning pore water concentrations in lower permeability layers (Chapman and Parker, 2005; Parker et al., 2004). This also allows assessment of the total concentration of the different contaminant phases present in the subsoil (i.e. DNAPL, dissolved and sorbed). Isotopic analyses were performed on sediment samples in order to obtain high-resolution information to be compared with contaminant concentrations along the same profile. The core subsampling procedure is described in detail by Parker et al. (2003) and Parker et al. (2004) (see Sup. Mat. for further details).

Four subsamples were collected at each depth, one dedicated to contaminant concentration analysis and three dedicated to CSIA. The samples for contaminant concentration were extruded into a pre-weighed 25 mL glass VOA (volatile organic analysis) bottle, containing a known volume of HPLC-grade methanol (around 15 mL) for preservation and contaminant extraction. Samples for isotopic analyses were extruded into 20 mL headspace (HS) crimp vials, containing 9.5 mL of NaCl water saturated solution (for preservation and salting out of the contaminants); each sediment subsample was approximately 9.5 g in order to maintain a ratio g sediment/mL solution at least equal to 1 and the sediment sample completely covered with the solution (as recommended by Pavón et al., 2009). With this sampling procedure the HS volume inside the vial was ≥ 5 mL.

4.4. Analytical methods

Concentration analyses of volatile contaminants on groundwater samples (i.e. chlorinated ethenes) were performed by a private certified laboratory, using the analytical method “EPA 5030 C” (U.S. EPA, 2003) and “EPA 8260 C” (U.S. EPA, 2006).

Dissolved gases were analyzed on groundwater samples at the Department of Isotope Biogeochemistry, at the Helmholtz Centre for Environmental Research in Leipzig (Germany). Gas chromatography with flame ionization detection (GC-FID) was applied to analyze methane and ethene (see Sup. Mat. for further details).

Sediment subsamples dedicated to chlorinated ethene concentration were analyzed at the Parker research lab at the University of Guelph, following the technique described by Parker et al. (2003). This analytical technique provides the total analyte content per mass of wet sediment, and therefore does not distinguish between concentrations present in the aqueous, sorbed and/or NAPL phases. Calculations were used to distinguish the three phases, modified from Feenstra et al. (1991) in the same

manner as Parker et al. (2003). Details about the analytical technique and the phase calculations are reported in the Supplementary Material.

Gas chromatography combustion isotope ratio mass spectroscopy (GC-C-IRM-MS) was applied to determine the stable carbon isotope composition of the volatile organic contaminants (i.e. chlorinated ethenes) in the sediment samples. A novel pre-concentration technique, consisting on large volume injection of headspace samples into the Programmed Temperature Vaporizing (PTV) injector, was used for the precise determination of the carbon isotope composition of volatile contaminants present in many of the samples at low concentrations (in µg/g range, Fig. 2). The method was validated for the carbon isotope analysis of volatile organic compounds in water samples (Herrero-Martín et al., 2014), and has been adapted here to the extraction of volatile compounds from sediment samples. More details about the CSIA analytical method and the pre-concentration technique are reported in the Supplementary Material.

5. Results

5.1. Depositional facies

Detailed sedimentological analysis of cores collected at the Caretti site (MC1-2, MC3 and MC4-5) enabled the identification of five facies associations on the basis of sediment lithology, stratigraphic boundaries, grain size trends, sediment color, thickness, and accessory materials (e.g., fossil content, organic matter, plant debris). Additional data include in situ pocket penetrometer tests from core MC1-2.

The fluvial-channel facies association consists of well-sorted, generally amalgamated, grey coarse-to-fine sand and locally silty-sand bodies, with thin clay-organic rich intervals, erosional lower boundary and fining-upward (FU) trend. The upper boundary is sharp to slightly gradational.

The levee and crevasse facies association locally shows lateral transition to fluvial-channel deposits. It consists of: (i) rhythmic alternations of grey to brownish silty sand, silt and clayey silt in few mm- to few cm-thick layers. The silty-sand layers show fining-upward trends, distinctive sharp bases and gradational tops. These where interpreted as (natural) levee deposits; (ii) very fine to medium sand, silty sand and sandy silt, with FU trend, erosional base and gradational/sharp top (interpreted as crevasse channels), or coarsening-upward (CU) successions, with gradational lower boundary and sharp top (argued to represent crevasse splays).

The floodplain facies association is composed of massive grey clay and silty clay deposits. Pocket penetrometer values are in the range of 1.8-3.1 kg/cm^2. This

monotonous muddy succession may be interbedded with pedogenically modified levee/crevasse deposits, or softer and grey silty-clay, locally organic-rich. Within this stratigraphic interval a paleosol was identified in clay deposits, with pocket penetration value of 3.1 kg/cm² (core MC1-2). The relatively high pocket penetrometer values and pedogenic features testify to episodes of subaerial exposure under well-drained conditions.

The poorly-drained floodplain facies association consists of massive clay and silty clay ranging in color from grey to dark grey. Organic matter may locally form mm- to cm-thick very dark layers. Pocket penetrometer values fall invariably in the narrow interval of 1.2-1.8 kg/cm², with very few exceptions.

The swamp facies association is made up of dark grey to black organic-rich clay, with abundant mm-sized plant debris and leaf fragments. The black and dark gray colors indicate an abundance of organic matter. A characteristic peat horizon, about 1 m thick, forms a prominent marker bed in the basal portion of this facies association. The dark clay is commonly very soft, as revealed by its very low pocket penetrometer values (0.2 to 1.2 kg/cm²).

5.2. Distribution of contaminants

The total concentration of contaminants obtained from sediment core subsamples along profile MC4-5 (C_t, µg/g wet sediment; Fig. 2) shows changes in concentration of over 2 orders of magnitude at dm scale, i.e. the scale of sampling. A similar concentration variability was observed by Parker et al. (2003) and Guilbeault et al. (2005) in different geological settings with less extreme lithologic variability. Chlorinated ethenes were labeled as parent (i.e. PCE and TCE, spilled at the source) or daughter compounds (i.e. cDCE and VC, produced by biodegradation). Parent compounds occur along the whole profile (0 to 30 m bgs), with the highest concentrations located in A0 aquifer and at the top of upper Q1 and lower Q1 aquitards, suggesting substantial contaminant accumulation at these interfaces, which serve as important hydrologic unit boundaries. Daughter products are present exclusively within the uppermost 11 m, showing peaks of concentration at the bottom of Q0 aquitard (3 to 5.5 m bgs) and at the top of upper Q1 (8 to 11 m bgs). In A0 aquifer, cDCE and VC occur in concentrations 50% and 90% lower, respectively, than in the surrounding aquitards. Estimated dissolved concentrations (C_w), determined from the total contaminant concentrations (C_t) using the partitioning calculations described in the Supplementary Material, excluded DNAPL presence. C_w concentrations of parent compounds show lower maxima compared to C_t, consistent with significant sorption of PCE and TCE mass into the solid matrix (Fig. 2).

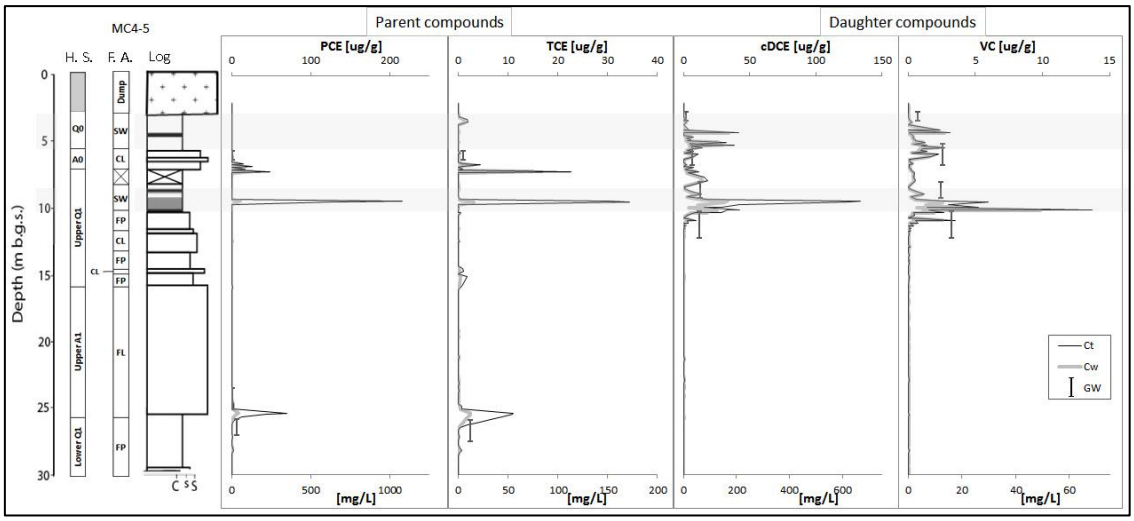

Fig. 2 - Vertical distribution of chlorinated ethenes obtained from numerous subsamples from continuous cores and groundwater samples along profile MC4-5. The total concentrations of the main analytes (Ct; ug/g wet soil) are reported together with estimated dissolved concentrations (Cw; mg/L). Dissolved concentrations obtained by groundwater samples are referred to as GW, and expressed in mg/L. The hydrostratigraphic subdivision in aquifers and aquitards ("H. S.") and the depositional facies associations ("F. A.") are reported beside the stratigraphic log (where: "CL" is Crevasse and Levee F. A.; "FL" is Fluvial Channel F. A.; "FP" is Floodplain F. A.; "pd FP" is poorly drained floodplain F. A.; "SW" is Swamp F. A.). The location of swamp deposits is highlighted in light grey along the graphs.

Along MC1-2 and MC3 profiles, where the distribution of contaminants was investigated only via groundwater sampling, substantial variations in the vertical distribution of parents and daughter compounds were also observed, but each with its own variability (Fig. 3). In detail, cDCE and VC are spread down to the upper A1 aquifer both along MC1-2 and MC3 profiles, with maximum concentrations in groundwater of 61.4 and 25.0 mg/L, respectively. At MC1-2 the contamination is almost absent in the A0 aquifer and the surrounding aquitards and PCE, which is the most chlorinated compound, shows relatively low concentrations along the entire profile (maximum concentration of 0.4 mg/L).

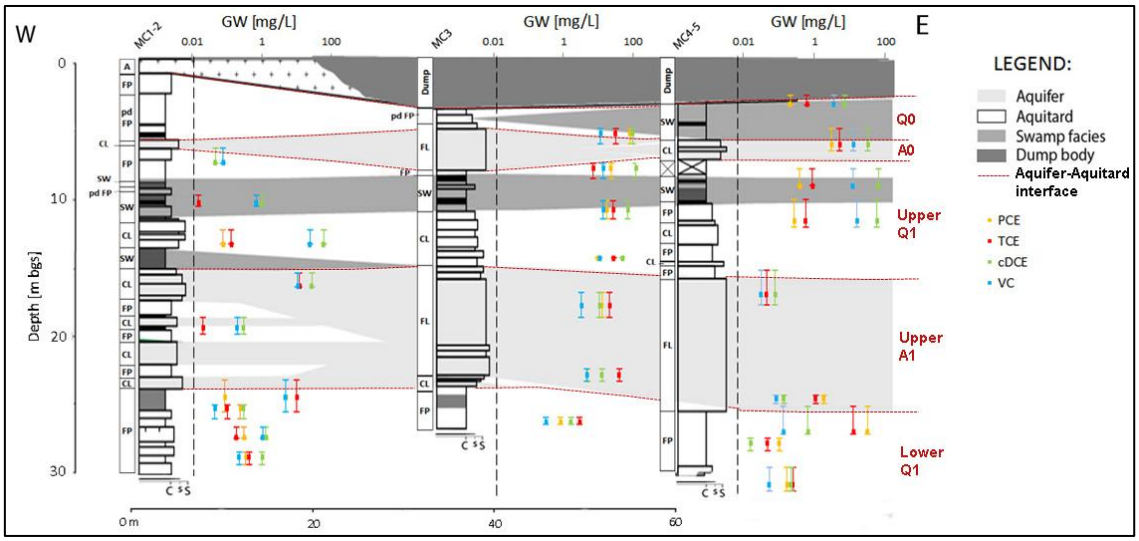

Fig. 3 - Distribution of contaminants from groundwater samples collected along the whole monitoring cross section (profiles MC1-2, MC3 and MC4-5). The concentrations are expressed in mg/L and displayed in log scale. The hydrostratigraphic subdivision in aquifers and aquitards is reported on the right and the depositional facies associations

("F. A.") are reported beside each stratigraphic log (where: "CL" is Crevasse and Levee F. A.; "FL" is Fluvial Channel F. A.; "FP" is Floodplain F. A.; "pd FP" is poorly drained floodplain F. A.; "SW" is Swamp F. A.; "A" is Anthropogenic F. A.).

A residual thickness of wastes (i.e. dump body) was identified at the top of the MC3 and MC4-5 stratigraphic logs, which was absent at MC1-2 (Fig. 3). This indicates that a marginal fringe of the source of contamination occurs directly on the monitoring cross-section and disappears westward.

5.3. Redox conditions and dissolved gases

Markedly negative values of Eh were detected in groundwater along the whole cross-section (range from -278 to -160 mV) (results from profile MC4-5; Fig. 4). Methane was found in all groundwater samples analyzed, with concentrations ranging from 31 to 1296 mg/L. The average concentration of methane within the upper 11 m is 224 mg/L, around two orders of magnitude higher than the average background value at the regional scale (6.6 mg/L; Sciarra et al., 2013).

Ethene was detected exclusively in groundwater collected from swamp deposits (Fig. 4).

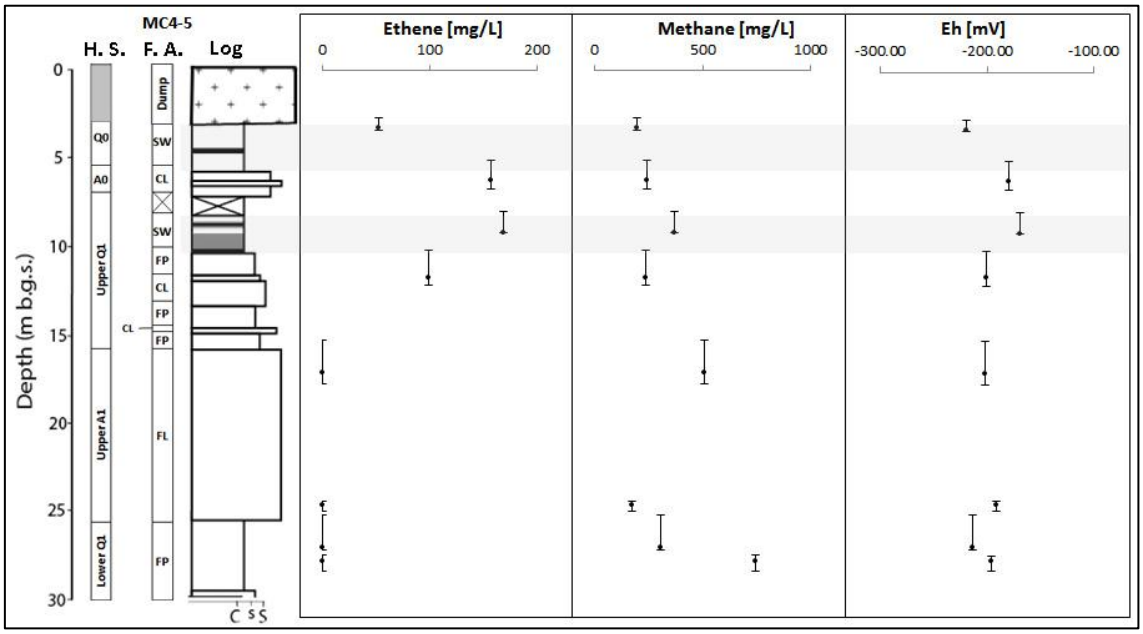

Fig. 4 - Distribution of dissolved gases (ethene and methane) and Eh along profile MC4-5. The hydrostratigraphic subdivision in aquifers and aquitards ("H. S.") and the depositional facies associations ("F. A.") are reported beside the stratigraphic log (see F. A. legend from Fig. 2).

5.4. CSIA of chlorinated ethenes

The general depleted $\delta^{13}C$ values obtained for chlorinated ethenes in the study area (-76‰ < $\delta^{13}C$ < -51 ‰; Fig. 5), in comparison to those values common to commercial products (-37‰ < δ13C < -23‰; Hunkeler et al., 2005; Sherwood Lollar et al., 2000; Shouakar-Stash et al., 2003), are related to the characteristics of the primary source of

contamination, described by Nijenhuis et al. (2013). The $\delta^{13}C$ corresponding to the main peaks of contaminant concentrations (Fig. 5) allowed the identification of two main isotopic pattern types: pattern type I represents only parent contaminants present (no daughters detected), with isotopic signatures between -75‰ and -68‰, and corresponds with the peak concentrations of PCE and TCE; pattern type II represents both parent and daughter compounds present, with the parents showing less negative signatures in comparison with pattern type I (-56‰ < $\delta^{13}C$ < -50‰) and daughters being similar to parents in pattern type I (-76‰ < $\delta^{13}C$ < -61‰). This corresponds with the peak concentrations of daughter compounds in the peaty swamp layers.

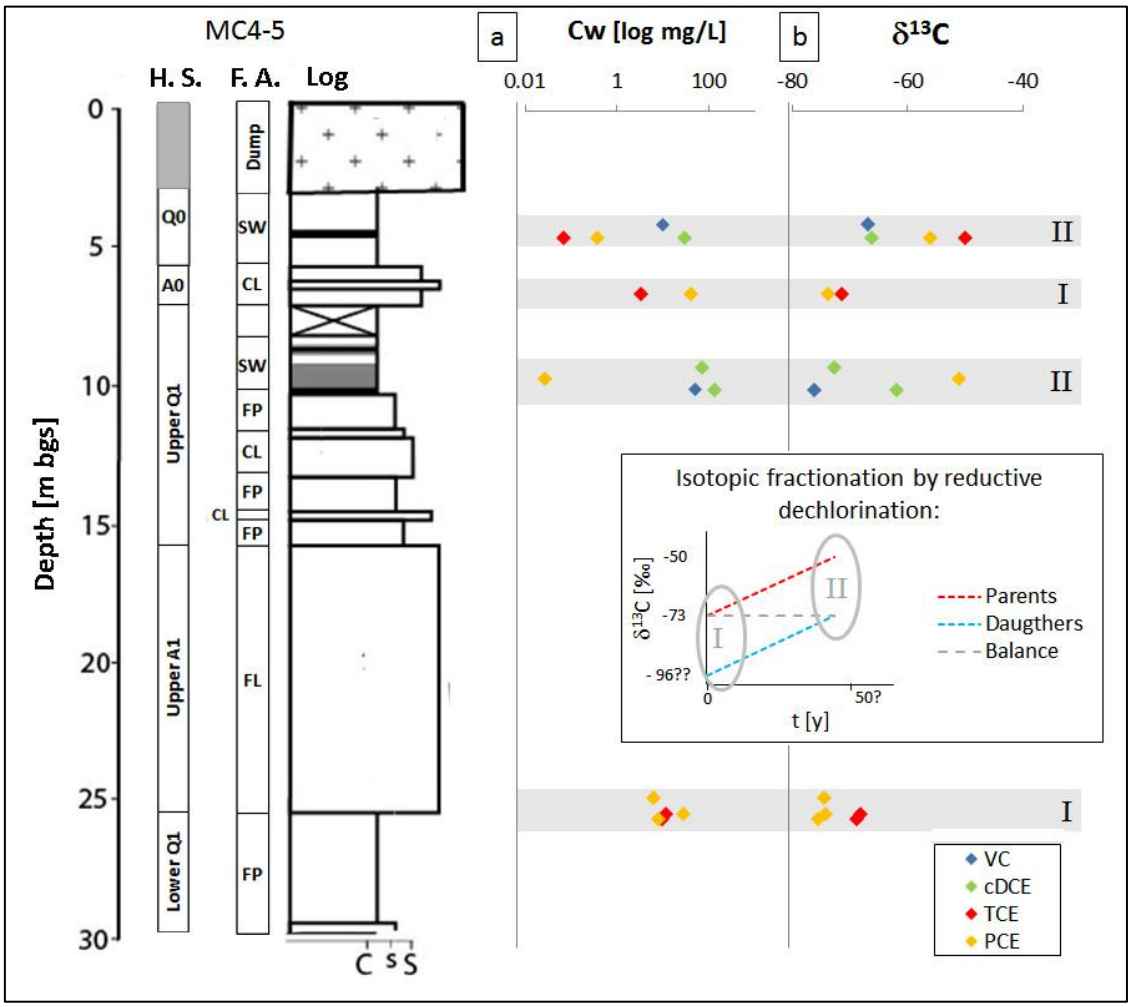

Fig. 5 - $\delta^{13}C$ of chlorinated ethenes corresponding to dissolved contaminant concentration (C_w) peaks along profile MC4-5 (b). The grey stripes identify different concentration peak zones from core subsampling (see Fig. 2). The estimated C_ws are reported for reference (a). "I" and "II" indicate two different isotopic pattern types corresponding to two distinct steps of the isotope fractionation pathway produced by reductive dechlorination. The hydrostratigraphic subdivision in aquifers and aquitards ("H. S.") and the depositional facies associations ("F. A.") are reported beside the stratigraphic log (see F. A. legend from Fig. 2). Isotopic pattern type I occurs inside the FL, FP and CL F. A.; pattern type "II" occurs inside the SW F.A.

6. Discussion

6.1. Origin of VC at the Caretti site

Evidence for reductive dechlorination inside swamp deposits

Comparison between the MC4-5 facies associations and the distribution of contaminants (C_t and C_w; Fig. 2) shows that peak concentrations of daughter compounds occur within the shallow peat-rich swamp deposits, suggesting that production of VC via reductive dechlorination of parent compounds (Vogel et al., 1987) occurs inside these layers. High methane concentration and markedly negative Eh (likely over-depressed by the contamination itself) indicate the occurrence of methanogenic conditions along the whole system (Fig. 4). This geochemical condition is the most favorable for reductive dechlorination (Stroo and Ward, 2010) and was previously observed at the same field site (Nijenhuis et al., 2013).

Isotopic pattern types I and II (Fig. 5) are related to two different steps in the isotopic dechlorination pathway (Bloom et al., 2000; Hunkeler et al., 2005; Slater et al., 2001): pattern type I corresponds with the beginning stage of dechlorination, when no (or very low) concentrations of products are present, and the parents preserve the isotopic signature of the source (in agreement with the findings of Hunkeler et al., 2004, for plumes in context of low organic carbon content); pattern type II corresponds to the end of the dechlorination pathway when the majority of the parent compounds have been converted to daughter products with isotopic signatures similar to the original parents. The observed $\delta^{13}C$ pattern (Fig. 5) confirms the occurrence of strong biodegradation activity via reductive dechlorination within the organic-rich swamp layers. In contrast, no dechlorination activity can be inferred in the layers with much lower natural solid-phase organic carbon.

The vertical distribution of ethene (Fig. 4) suggests that some complete dechlorination occurs inside the peaty layers. It is well known from literature that reductive dechlorination is the most important anaerobic biodegradation process for the higher chlorinated ethenes (Bouwer, 1994; Freedman and Gossett, 1989; Vogel and McCarty, 1985) however the in situ reduction of VC to the non-chlorinated product ethene appears to be considerably slower than dechlorination of PCE, TCE and cDCE (Ballapragada et al., 1995; Barrio-Lage et al., 1987; Bouwer, 1994; Carter and Jewell, 1993; De Bruin et al., 1992; Di Stefano et al., 1991; Fennell et al., 1995; Freedman and Gossett, 1989; Maymó-Gatell et al., 1995; Odum et al., 1995; Vogel and McCarty, 1985; Wu et al., 1995). The significant difference in the reductive biodegradation rates

of higher and lower chlorinated compounds justifies the accumulation of the VC product in the investigated system.

Contaminant distribution along the cross-section

The migration of daughter products from the peat-rich deposits into the underlying upper A1 aquifer is influenced by the depositional facies architecture of the upper Q1 aquitard (Fig. 3): along MC3, the slightly permeable silty-sandy crevasse and levee deposits below the swamps allowed the migration of dissolved cDCE and VC from the organic-rich layer down into the aquifer. Differently, the less permeable clayey-silty floodplain deposits underlying the swamps in MC4-5 obstructed vertical contaminant migration towards the upper A1 aquifer.

Profile MC1-2 is uncontaminated in its shallower section (i.e. A0 and upper Q1) and no wastes were detected in the stratigraphic log. This rules out direct supply of contaminants directly from above. The contamination detected in the upper A1 aquifer must be the result of horizontal migration from upgradient. The relatively low concentrations of PCE detected in the MC1-2 profile suggest that the contamination was subjected to a higher degree of dechlorination than in the rest of the cross-section, reflecting greater distance from the source zone with natural attenuation of contaminants occurring along the flowpath (Wiedemeier et al., 1998). This is consistent with the observation for VC only/dominated plumes elsewhere in the region (i.e. not far from sources, parent compounds are depleted to VC).

6.2. Origin of VC-only plumes at regional scale

The stratigraphic transect 6 km long between the Caretti site and the Po River, shows the ubiquitous presence of swamp deposits across the entire study area (Fig. 6). This unit invariably overlies aquifer A1 (upper A1, at the Caretti site), and shows an increasing volume of peat-rich deposits toward distal locations (i.e. NE-ward). This suggests that the genesis of VC in plumes A and B is likely the same as observed at the source area of the Caretti site, with swamp deposits acting as an efficient “reactor” for the degradation of highly chlorinated compounds and further migration of daughter chlorinated ethenes, particularly VC, in the underlying aquifer (where the facies architecture allows hydrogeological connection between the aquifer and the swamps).

The vertical distributions of VC in plumes A and B (Fig. 7a, b) show the highest concentrations at the top of the aquifer. This is consistent with the hypothesis of a supply of VC from above the aquifer (where the organic-rich swamp deposits are located).

Concerning the absence of parent compounds in plumes A and B (contrastingly still present at the Caretti site), this can be attributed to the greater thickness and higher persistence of organic-rich layers in the northern part of the stratigraphic transect, which exacerbated the dechlorination process. Moreover, preferential sorption of the higher chlorinated compounds on the organic rich layers (as already observed at the Caretti site; see section 5.2) could have produced an apparent relative increase of VC concentration in groundwater samples (i.e. dissolved phase) (Mackay et al., 1986). Eventually, the greater distance of the sampling points from the source compared to the Caretti site explains a further relative increase of VC concentrations along the plume, due to differential transport rates of the compounds (where VC is the one most mobile and less reactive in strongly reductive environment, Mackay et al., 1986; Stroo and Ward, 2010) and progressive natural attenuation of parent contaminants (Wiedemeier et al., 1998). Likewise, the plumes developed in the Caretti site display a consistent increase of VC against the higher chlorinated ethenes as the distance from the source increases (as shown from data described by Gargini et al., 2011).

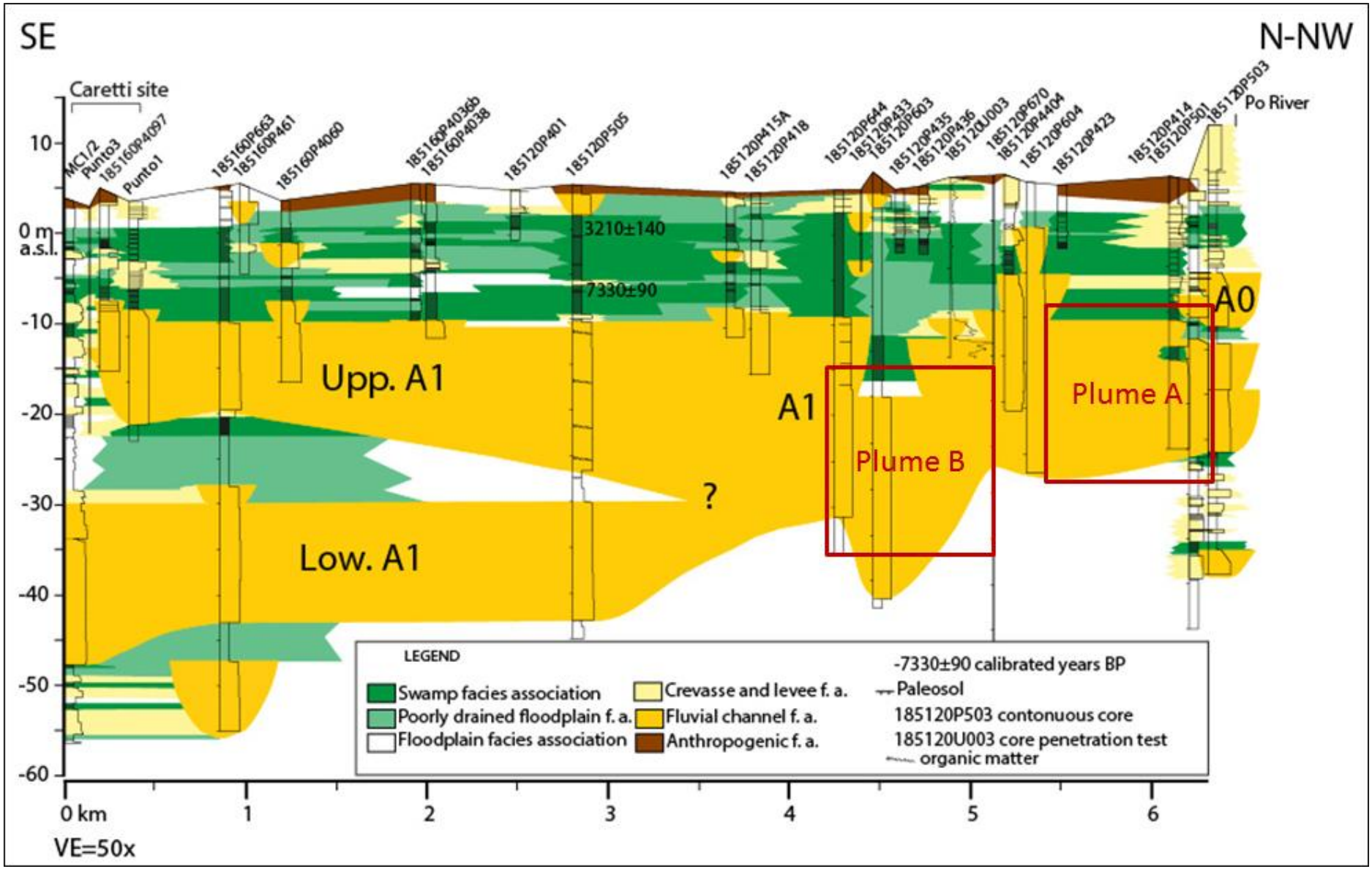

Fig. 6 - Depositional facies architecture over 6 km distance between the Caretti and the Po river. The 26 stratigraphic control points used for the transect are indicated in Fig.1. The approximate projections of the Caretti source zone (blue) and VC-only plumes A and B (red) are shown on the transect. "?" stand for uncertain stratigraphic interpolation.

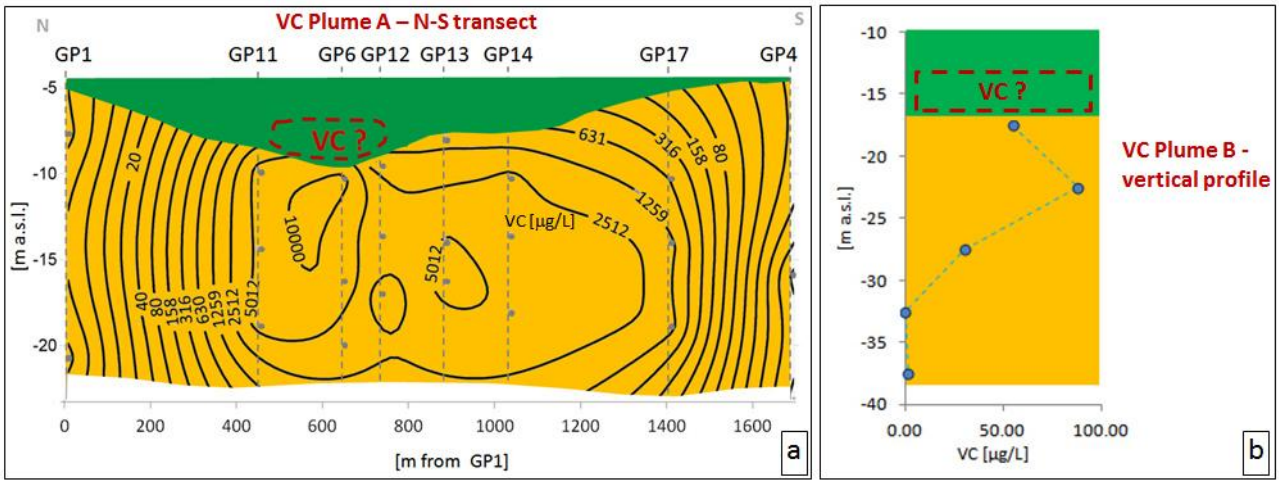

Fig. 7 - (a) isoconcentration lines of VC along a longitudinal section of plume A, obtained by direct push groundwater sampling (Pasini et al., 2008); VC concentrations are expressed in µg/L and isoconcentration lines are reported every 0.3 log VC; (b) vertical profile of VC in plume B from a single multi-level groundwater sampling (from private company's investigation). The green and orange background colors refer to the Facies legend in Fig. 6. The supposed zones of VC production ad accumulation are indicated with red dashed lines.

7. Summary and conclusions

The hydrogeological system below Ferrara is characterized by recurring accumulations of high concentration VC in groundwater. In particular, two peculiar VC-only plumes developed for more than 1 km from the sources, within the shallower confined A1 aquifer of the region. Also, significant accumulations of VC were found 3 to 11 m bgs in urbanized areas (concentrations up to 70 mg/L at the Caretti site), creating the potential for vapor intrusion issues impacting indoor air quality.

A detailed stratigraphic and hydrogeological investigation, including depth discrete data from cores and multilevel samplers for chemical and isotopic analyses, allowed creation of a hydrogeologic conceptual model for the area that explains the behavior of multiple chlorinated ethene zones in the region, with focus on the accumulation of biodegradation products in strongly reducing hydrochemical conditions not conducive for complete dechlorination. In this conceptual model, reductive dechlorination of more highly chlorinated parent compounds (PCE and TCE) occurs down to VC, during contaminants retention and migration within fine peat-rich deposits (corresponding to Holocene swamp sediments), which represent a local "reactor" for bio-transformation in strongly reducing conditions and for preferential sorption of the higher chlorinated ethenes.

The results of this study show the benefit of combining multiple and diverse paleo-environmental and hydrogeological datasets as lines of evidence for establishing a robust site conceptual model for chlorinated organic behavior in the regional groundwater.

The use of investigative tools able to provide detailed information on low permeability layers (i.e. sediment core subsampling) proved to be essential for the aim of the paper, since these layers represent the most hydrochemically and biologically active sections of the system.

Eventually, the research shows that co-occurrence of organic-rich sediments and chlorinated solvent contamination can cause the potential for severe environmental and human-health issues. Indeed, if partial biodegradation of high chlorinated compounds to VC occurs, as in the case of Ferrara hydrogeology, the threat to human health and environment are accentuated due to the increased mobility to the biosphere (both in dissolved and vapor phases) and high carcinogenicity of this compound.

Acknowledgements

We are grateful for the financial support of EU FP7 project Genesis (contract number: 226536).

We gratefully acknowledge Ursula Günther and Stefan Riedel (Helmholtz Centre for Environmental Research, Leipzig, Germany) for analytical support and technical assistance. Core sample VOC analyses at the University of Guelph were performed by analytical chemists Maria Gorecka and Rashmi Jadeja through collaboration with the University Consortium for Field-Focused Groundwater Contamination Research.

We acknowledge Environmental Service of the municipality of Ferrara for providing support to our investigation, and the geology students of the University of Bologna: Paola Posella, Giuseppe Rutigliano and Riccardo Giusti, for the essential support during field activities and sample analysis. Steven Chapman of the University of Guelph and Prof. Ramon Aravena also provided helpful review of the manuscript.

References

Adamson, D.T., Chapman, S.W., Farhat, S.K., Parker, B.L., deBlanc, P., Newell, C.J., 2015. Characterization and Source History Modeling Using Low-k Zone Profiles at Two Source Areas. Groundwater Monitoring & Remediation: n/a-n/a.

Allen-King, R.M., Divine, D.P., Robin, M.J.L., Alldredge, J.R., Gaylord, D.R., 2006. Spatial distributions of perchloroethylene reactive transport parameters in the Borden Aquifer. Water Resources Research, 42(1).

Amorosi, A., Bruno, L., Campo, B., Morelli, A., 2014. The value of pocket penetration tests for the high-resolution palaeosol stratigraphy of late Quaternary deposits. Geological Journal: n/a-n/a.

Amorosi, A., Colalongo, M.L., Fiorini, F., Fusco, F., Pasini, G., Vaiani, S.C., Sarti, G., 2004. Palaeogeographic and palaeoclimatic evolution of the Po Plain from 150-ky core records. Global and Planetary Change, 40(1–2): 55-78.

Amorosi, A., Colalongo, M.L., Fusco, F., Pasini, G., Fiorini, F., 1999. Glacio-eustatic Control of Continental–Shallow Marine Cyclicity from Late Quaternary Deposits of the Southeastern Po Plain, Northern Italy. Quaternary Research, 52(1): 1-13.

Amorosi, A., Marchi, N., 1999. High-resolution sequence stratigraphy from piezocone tests: an example from the Late Quaternary deposits of the southeastern Po Plain. Sedimentary Geology, 128(1–2): 67-81.

Amorosi, A., Pavesi, M., Ricci Lucchi, M., Sarti, G., Piccin, A., 2008. Climatic signature of cyclic fluvial architecture from the Quaternary of the central Po Plain, Italy. Sedimentary Geology, 209(1–4): 58-68.

Ballapragada, B.S., Puhakka, J.A., Stensel, H.D., Ferguson, J.F., 1995. Development of tetrachloroethene transforming anaerobic cultures from municipal digester sludge. In: Hinchee, R.E., Leeson, A., Semprini, L. (Eds.), Bioremediation of Chlorinated Solvents. Battelle Press, Columbus, OH, USA, pp. 91-97.

Barrio-Lage, G., Parsons, F.Z., Nassar, R.S., Lorenzo, P.A., 1986. Sequential dehalogenation of chlorinated ethenes. Environmental Science & Technology, 20(1): 96-99.

Barrio-Lage, G.A., Parsons, F.Z., Nassar, R.S., Lorenzo, P.A., 1987. Biotransformation of trichloroethene in a variety of subsurface materials. Environmental Toxicology and Chemistry, 6(8): 571-578.

Bloom, Y., Aravena, R., Hunkeler, D., Edwards, E., Frape, S., 2000. Carbon isotope fractionation during microbial dechlorination of trichloroethene, cis-1, 2-dichloroethene, and vinyl chloride: implications for assessment of natural attenuation. Environmental science & technology, 34(13): 2768-2772.

Bouwer, E.J., 1994. Bioremediation of Chlorinated Solvents Using Alternate Electron Acceptors. . In: Norris, R.D. et al. (Eds.), Handbook of Bioremediation. CRC Press, Boca Raton, FL, USA, pp. 149-175.

Carter, S.R., Jewell, W.J., 1993. Biotransformation of tetrachloroethylene by anaerobic attached-films at low temperatures. Water Research, 27(4): 607-615.

Chapman, S.W., Parker, B.L., 2005. Plume persistence due to aquitard back diffusion following dense nonaqueous phase liquid source removal or isolation. Water Resources Research, 41(12): W12411.

Chen, C., Puhakka, J.A., Ferguson, J.F., 1996. Transformations of 1,1,2,2-Tetrachloroethane under Methanogenic Conditions. Environmental Science & Technology, 30(2): 542-547.

Dalla, S., Rossi, M., Orlando, M., Visentin, C., Gelati, R., Gnaccolini, M., Papani, G., Belli, A., Biffi, U., Citrullo, D., 1992. Late Eocene-Tortonian tectono-sedimentary evolution in the western part of the Padan basin (northern Italy). Paleontol. y Evol., 24-25: 341-362.

De Bruin, W.P., Kotterman, M.J.J., Posthumus, M.A., Schraa, G., Zehnder, A.J.B., 1992. Complete biological reductive transformation of tetrachloroethene to ethane. Appl Environ Microbiol 58: 1996-2000.

Di Stefano, T.D., Gossett, J.M., Zinder, S.H., 1991. Reductive dechlorination of high concentrations of tetrachloroethene to ethene by an anaerobic enrichment culture in the absence of methanogenesis. Appl Environ Microbiol, 57: 2287-2292.

Dondi, L., D'Andrea, M.G., 1986. La Pianura Padana e Veneta dall'Oligocene superiore al Pleistocene (in italian; transl. The Po and Venetian plain from Upper Oligocene to Pleistocene) . Giorn. Geol., 48: 197-225.

Einarson, M.D., Cherry, J.A., 2002. A New Multilevel Ground Water Monitoring System Using Multichannel Tubing. Ground Water Monitoring & Remediation, 22(4): 52-65.

Feenstra, S., Mackay, D.M., Cherry, J.A., 1991. A Method for Assessing Residual NAPL Based on Organic Chemical Concentrations in Soil Samples. Ground Water Monitoring & Remediation, 11(2): 128-136.

Fennell, D.E., Stover, M.A., Zinder, S.H., Gossett, J.M., 1995. Comparison of alternative electron donors to sustain PCE anaerobic reductive dechlorination. In: Hinchee, R.E., Leeson, A., Semprini, L. (Eds.), Bioremediation of Chlorinated Solvents. Battelle Press, Columbus, OH, USA, pp. 9-16.

Freedman, D.L., Gossett, J.M., 1989. Biological reductive dechlorination of tetrachloroethylene and trichloroethylene to ethylene under methanogenic conditions. Appl Environ Microbiol 55: 2144-2151.

Gargini, A., Pasini, M., Picone, S., Rijnaarts, H., Van Gaans, P., 2011. Chlorinated hydrocarbons plumes in a residential area. Site investigation to assess indoor vapor intrusion and human health risks. In: Saponaro, S., Sezenna, E., Bonomo, L. (Eds.), Vapor emission to outdoor air and enclosed spaces for human health risk assessment: site dharacterization, monitoring and modelling. Nova Science Publishers, Inc., Milan, Italy, pp. 211-233.

Gilmore, A.M., 2010. High Resolution Investigation in a Heterogeneous Aquifer and Evaluation of the Membrane Interface Probe to Assess Back-Diffusion Potential, MASc Thesis, Vols 1 & 2, Univeristy of Guelph, 463 pp.

Guilbeault, M.A., Parker, B.L., Cherry, J.A., 2005. Mass and flux distributions from DNAPL zones in sandy aquifers. Ground Water, 43(1): 70-86.

Herrero-Martín, S., Nijenhuis, I., Richnow, H.H., Gehre, M., 2014. Coupling of a headspace autosampler with a programmed temperature vaporizer for stable carbon and hydrogen isotope analysis of volatile organic compounds at µg/L concentrations. Analytical chemistry.

Hunkeler, D., Aravena, R., Berry-Spark, K., Cox, E., 2005. Assessment of Degradation Pathways in an Aquifer with Mixed Chlorinated Hydrocarbon Contamination Using Stable Isotope Analysis. Environmental Science & Technology, 39(16): 5975-5981.

Hunkeler, D., Chollet, N., Pittet, X., Aravena, R., Cherry, J.A., Parker, B.L., 2004. Effect of source variability and transport processes on carbon isotope ratios of TCE and PCE in two sandy aquifers. Journal of Contaminant Hydrology, 74(1–4): 265-282.

IARC, 2007. Biennial Report 2006-2007 of the International Agency for Research on Cancer, 298 IARC, World Health Organization, Lyon, France, 141 pp.

Kalinovich, I., Allen-King, R.M., Thomas, K., 2012. Distribution of carbonaceous matter in lithofacies: Impacts on HOC sorption nonlinearity. Journal of Contaminant Hydrology, 133(0): 84-93.

Lorah, M.M., Olsen, L.D., 1999. Degradation of 1,1,2,2-Tetrachloroethane in a Freshwater Tidal Wetland: Field and Laboratory Evidence. Environmental Science & Technology, 33(2): 227-234.

Mackay, D., Shiu, W.Y., Lee, S.C., Ma, K.C., 2006. Handbook of physical–chemical properties and environmental fate for organic chemicals. . CRC, Boca Raton.

Mackay, D.M., Freyberg, D.L., Roberts, P.V., Cherry, J.A., 1986. A natural gradient experiment on solute transport in a sand aquifer: 1. Approach and overview of plume movement. Water Resources Research, 22(13): 2017-2029.

Maymó-Gatell, X., Tandoi, V., Gossett, J.M., Zinder, S.H., 1995. Characterization of an H2-utilizing enrichment culture that reductively dechlorinates tetrachloroethene to vinyl chloride and ethene in the absence of methanogenesis and acetogenesis. Appl Environ Microbiol 61: 3928-3933.

Mitchum, R.M., Vail, P.R., Thompson III, S., 1977. The depositional sequence as a basic unit for stratigraphic analysis. In: Payton C.E. (Ed.), Seismic stratigraphy - Application for Hydrocarbon Exploration. American Association of Petroleum Geologists Memoir, pp. 53-62.

Molinari, F.C., Boldrini, G., Severi, P., Dugoni, G., Rapti Caputo, D., Martinelli, G., 2007. Risorse idriche sotterranee della Provincia di Ferrara (in italian; transl. Groundwater resources of the Ferrara Province), Risorse idriche sotterranee della Provincia di Ferrara (in italian; transl. Groundwater resources of the Ferrara Province). DB-MAP printer, Florence, Italy, pp. 1-62.

Muttoni, G., Carcano, C., Garzanti, E., Ghielmi, M., Piccin, A., Pini, R., Rogeldi, S., Sciunnach, D., 2003. Onset of major Pleistocene glaciations in the Alps. Geology, 31: 989-992.

Nijenhuis, I., Schmidt, M., Pellegatti, E., Paramatti, E., Richnow, H.H., Gargini, A., 2013. A stable isotope approach for source apportionment of chlorinated ethene plumes at a complex multi-contamination events urban site. Journal of Contaminant Hydrology, 153(0): 92-105.

Odum, J.M., Tabinowski, J., Lee, M.D., Fathepure, B.Z., 1995. Anaerobic biodegradation of chlorinated solvents: Comparative laboratory study of aquifer microcosms. In: Norris, R.D. et al. (Eds.), Handbook of Bioremediation. Lewis Publishers, Boca Raton, FL, USA, pp. 17-24.

Parker, B.L., Cherry, J.A., Chapman, S.W., 2004. Field study of TCE diffusion profiles below DNAPL to assess aquitard integrity. Journal of Contaminant Hydrology, 74(1–4): 197-230.

Parker, B.L., Cherry, J.A., Chapman, S.W., Guilbeault, M.A., 2003. Review and analysis of chlorinated solvent DNAPL distributions in five sandy aquifers. Vadose Zone J 2: 116-137.

Pasini, M., Gargini, A., Aravena, R., Hunkeler, D., 2008. Use of hydrogeological and geochemical methods to investigate the origin and fate of vinyl chloride in groundwater in an urban

environment, Ferrara, Italy. In: Trefry, M.G. (Ed.), Groundwater quality: securing groundwater quality in urban and industrial environments IAHS Publication pp. 102-109.

Pavón, J.L.P., Martín, S.H., Pinto, C.G., Cordero, B.M., 2009. Programmed temperature vaporizer based method for the sensitive determination of trihalomethanes and benzene, toluene, ethylbenzene and xylenes in soils. Journal of Chromatography A, 1216(32): 6063-6070.

Pieri, M., Groppi, G., 1981. Subsurface geological structure of the Po Plain, Italy, 414. P.F. Geodinamica, C.N.R, 23 pp.

Regione Emilia-Romagna, ENI-AGIP, 1998. Riserve idriche sotterranee della Regione Emilia-Romagna (In italian; transl.: Groundwater resources of the Emilia-Romagna Region). S.EL.CA. printer, Florence.

Regione Lombardia, ENI Divisione AGIP, 2002. Geologia degli acquiferi Padani della Regione Lombardia (in Italian; transl.: Geology of the Po plain aquifers in the Lombardy Region). S.EL.CA, Firenze, Italy, 130 pp.

Ritzi, R.W., Huang, L., Ramanathan, R., Allen-King, R.M., 2013. Horizontal spatial correlation of hydraulic and reactive transport parameters as related to hierarchical sedimentary architecture at the Borden research site. Water Resources Research, 49(4): 1901-1913.

Sale, T., Parker, B.L., Newell, C.J., Devlin, J.F., 2013. Management of contaminants stored in low permeability zones - State of the science review. SERDP Project ER-1740, Strategic Environmental Research and Development Program, Alexandria, VA.

Sciarra, A., Cinti, D., Pizzino, L., Procesi, M., Voltattorni, N., Mecozzi, S., Quattrocchi, F., 2013. Geochemistry of shallow aquifers and soil gas surveys in a feasibility study at the Rivara natural gas storage site (Po Plain, Northern Italy). Applied Geochemistry, 34(0): 3-22.

Sherwood Lollar, B., Slater, G.F., Sleep, B., Witt, M., Klecka, G.M., Harkness, M., Spivack, J., 2000. Stable Carbon Isotope Evidence for Intrinsic Bioremediation of Tetrachloroethene and Trichloroethene at Area 6, Dover Air Force Base. Environmental Science & Technology, 35(2): 261-269.

Shouakar-Stash, O., Frape, S.K., Drimmie, R.J., 2003. Stable hydrogen, carbon and chlorine isotope measurements of selected chlorinated organic solvents. Journal of Contaminant Hydrology, 60(3–4): 211-228.

Slater, G.F., Sherwood Lollar, B., Sleep, B.E., Edwards, E.A., 2001. Variability in Carbon Isotopic Fractionation during Biodegradation of Chlorinated Ethenes: Implications for Field Applications. Environmental Science & Technology, 35(5): 901-907.

Stroo, H.F., Unger, M., Ward, C.H., Kavanaugh, M.C., Vogel, C., Leeson, A., Marqusee, J.A., Smith, B.P., 2003. Chlorinated solvent source zones. Environmental Science & Technology 37(11): 224-230.

Stroo, H.F., Ward, C.H., 2010. In situ remediation of chlorinated solvent plumes. Springer, New York, 802 pp.

U.S. EPA, 2003. Method 5030C, "Purge-and-trap for aqueous samples", U.S. Environmental Protection Agency.

U.S. EPA, 2006. Method 8260C "Volatile Organic Compounds By Gas Chromatography/Mass Spectrometry(GC/MS)", U.S. Environmental Protection Agency.

Vogel, T.M., Criddle, C.S., McCarty, P.L., 1987. Transformation of halogenated aliphatic compounds. Environ. Sci Technol, 21: 722-736.

Vogel, T.M., McCarty, P.L., 1985. Biotransformation of tetrachloroethylene to trichloroethylene, dichloroethylene, vinyl chloride, and carbon dioxide under methanogenic conditions. Appl Environ Microbiol, 49: 1080-1083.

Wiedemeier, T.H., Swanson, M.A., Moutoux, D.E., Gordon, E.K., Wilson, J.T., Wilson, B.W.H., Kampbell, D.H., Hansen, J.E., Hass, P., Chapelle, F.H., 1998. Technical Protocol for Evaluating Natural Attenuation of Chlorinated Solvents in Groundwater. EPA/600/R-98/128. , USEPA, Washington, DC, USA.

Wu, W.M., Nye, J., Hickey, R.F., Jain, M.K., Zeikus, J.G., 1995. Dechlorination of PCE and TCE to ethene using an anaerobic microbial consortium. In: Norris, R.D. et al. (Eds.), Handbook of Bioremediation. Lewis Publishers, Boca Raton, FL, USA, pp. 45-52.

(Paper 5) – Supplementary material

1. Additional information on sediment core subsampling

Sediment cores were recovered inside PVC tubes 1.5 m long, and placed horizontally in a wooden holder. They were split longitudinally using a circular saw for the PVC tubing and then a wire for the core material. The half core chosen for sampling was covered immediately with aluminum foil to minimize pore water evaporation and volatilization of contaminants. The other half was used for stratigraphic logging. Sediment subsamples were collected by means of small cylindrical stainless-steel samplers (12 mm diameter), with an average vertical spacing of 20 cm along the length of the core. Possible cross-contamination was minimized by avoiding advancing the sampler down to the walls of the core tube and by decontamination of samplers between each depth using a three-step wash and rinse sequence (soapy water, methanol, deionized water).

2. Additional information on analytical methods

Analysis of dissolved gasses concentration in groundwater samples

The gas chromatograph used for analyses of dissolved gas concentrations on groundwater samples is a Varian Chrompack CP-3800 (Middelburg, The Netherlands) equipped with a 30 m 0.53 mm GS-Q column (J& W Scientific, Waldbronn, Germany). The temperature program used was as follows: 2 min at 50 °C, 50 °C/ min to 225 °C, hold 2.5 min. The FID was operated at 250 °C and helium was used as the carrier gas. Air and hydrogen flows were set at 300 and 30 ml/min, respectively. The injection was automated using an HP 7694 headspace autosampler. A 10 mL HS vial was flushed with helium and hermetically sealed (aluminum cap with PTFE/butyl septa -3 mm thickness- Th. Geyer, Renningen, Germany), then 1 mL of groundwater sample was introduced through the septum using a Hamilton syringe. 1 mL headspace sample was then injected into the GC-FID system (split 1:1). Dilutions of samples (1:20) were performed as necessary based on initial analysis of the undiluted sample. Authentic standards were used for analyte identification and calibration. All samples were measured in triplicates. The data were recorded using the Varian STAR software.

Analysis of chloroethenes on sediment samples and phase partitioning

The VOA vials containing the sediment samples preserved in methanol were shaken on a vortex mixer to break up the sediment. Samples were then stored at 4°C for two weeks to allow adequate time for extraction with occasional shaking. The samples were then centrifuged to separate the sediment and methanol in the sample vial, and a small aliquot of methanol extract from the sample was diluted into pentane (capillary GC grade) containing an internal standard.

Further dilutions of samples into methanol were performed as necessary based on initial analysis of the undiluted sample. Standards were laboratory-prepared mixtures of the target analytes (typically PCE, TCE, DCE isomers) in methanol, which were spiked into pentane as described above for the samples. The pentane was then analyzed by direct injection on a gas chromatograph equipped with a micro-electron capture detector and a liquid autosampler.

The total analyte concentration provided by the analysis was converted to a porewater concentration (C_w) using the following relation (which assumes equilibrium chemical partitioning between dissolved and solid phases and no DNAPL present):

$$C_w = C_t^*(\rho_{b\text{-}wet}/(R^*\phi))$$

where C_t is the total analyte concentration in the bulk sample from lab analyses (µg/g wet sediment), $\rho_{b\text{-}wet}$ is the wet bulk sediment density (g/cm^3), ϕ is the sediment porosity and R is the estimated retardation factor due to sorption that assumes rapid, linear and reversible partitioning between the contaminant and the solid-phase organic C in the aquifer sediments. An averaged $\rho_{b\text{-}wet}$ value of 1.9 g/cm^3 was selected from the literature (Manger, 1963). ϕ was estimated using the relations between void ratio (e), particle density (ρ_s), water content (w, determined via the gravimetric method on dedicated sediment samples) and degree of water saturation (S) (Lambe and Whitman, 2008), assuming S=1 and ρ_s equal to 2.65 g/cm^3. The retardation factor (R) was estimated using the relation:

$$R = 1 + (\rho_{b\text{-}dry}/\phi)^*K_d$$

where K_d is the distribution coefficient and $\rho_{b\text{-}dry}$ is the dry bulk sediment density. The distribution coefficient was estimated using the correlation $K_d = K_{oc}^*f_{oc}$, using literature values for K_{oc} (e.g. Table A.1 in Pankow and Cherry, 1996), and measured f_{oc} values. An averaged $\rho_{b\text{-}dry}$ value of 1.2 g/cm^3 was selected from the literature (Manger, 1963).

Presence of DNAPL could be inferred for samples where the estimated pore water concentration of a compound exceeded its effective aqueous solubility in the contaminant mixture (S^e_i) determined via the Raoult's law (Banerjee, 1984):

$$S^e_i = X_i * S_i$$

where S_i is the solubility of the pure compound i and X_i is the mole fraction of the compound i in the mixture.

Compound Specific Isotope Analysis on sediment samples and analyte pre-concentration technique

An Agilent 7890A GC (Agilent Technologies, Waldbronn, Germany) coupled to an IRMS (MAT 253, Thermo Fisher Scientific, Bremen, Germany) via GC IsoLink (CNH) and ConFlo IV universal interface (Thermo Fisher Scientific, Bremen, Germany) was used. The GC was equipped with a programmed temperature vaporizer (Multimode Inlet (MMI) G3510A/G3511A, Agilent Technologies, Waldbronn, Germany) and a CombiPAL autosampler (CTC Analytics AG, Zwingen, Switzerland). The capillary column was a DB-MTBE (60 m x 0.32 mm ID x 1.80 µm FD; Agilent Technologies, Waldbronn, Germany). The temperature program started at 35 °C and was held for 10 min, then increased at a rate of 4 °C/min to 150 °C and then at 20 °C/min to 260 °C and held for 5 min.

Concerning the pre-concentration technique used to optimize the analysis on low concentration analytes (see main text), the headspace and PTV analytical conditions were the same as optimized before for water samples (Herrero-Martín et al., 2014). Different headspace injection volumes (from 250 µL to 5000 µL) were selected depending on the concentration of the target compounds in the samples in order to obtain in all cases peak amplitudes within the linear range of the IRMS system (peaks from 300 to 10000 mV were considered). All samples were analyzed at least in triplicate. A standard solution in Milli-Q water, containing the target compounds with known isotopic composition, was analyzed with the described method every 5 samples, for identification of the target compounds and to ensure accuracy and precision of the GC-C-IRMS system.

References

Banerjee, S., 1984. Solubility of organic mixtures in water. Environmental Science & Technology, 18(8): 587-591.

Herrero-Martín, S., Nijenhuis, I., Richnow, H.H., Gehre, M., 2014. Coupling of a headspace autosampler with a programmed temperature vaporizer for stable carbon and hydrogen isotope analysis of volatile organic compounds at µg/L concentrations. Analytical chemistry.

Lambe, T.W., Whitman, R.V., 2008. Soil mechanics SI version. John Wiley & Sons.

Manger, G.E., 1963. Porosity and bulk density of sedimentary rocks. 1144E, USGS.

Pankow, J.F., Cherry, J.A., 1996. Dense Chlorinated Solvents and Other DNAPLs in Groundwater. Waterloo Press, Portland, Oregon, 522 pp.

6. CONCLUSIONS

Late Quaternary stratigraphic studies have been increasingly considered and developed among the scientific community in the past 20 years, because of their significant “major control” in terms of chronological framework and impact of allogenic factors (i.e. climate, eustacy and tectonics) upon the stratigraphic record. These forcing factors, in fact, are relatively well constrained within the Quaternary successions because of: i) the improvement of dating methods (i.e. radiocarbon dating); ii) the development of paleoclimatology (acceptance of the Milankovitch theory of climatic change and superimposed sub-Milanchovitch cycles); iii) the irrelevance of tectonic deformation; iv) the high-comparability of species between late Quaternary and modern fossil records.

Furthermore, the recent increased interest for climate changes (i.e. “greenhouse effect”), hydrocarbon exploration and aquifer preservation has led to the development of conceptual models with the aim of preventing the risk of natural hazards, improving exploitation and protection of underground resources.

In this perspective, highly-subsiding basins such as the Po Plain, represent a unique laboratory for high-resolution stratigraphic studies, due to the huge sediment (i.e. rock record) preservation induced by the high subsidence rates (1 mm/y); whereas, the Pleistocene-Holocene (Pl-H) stratigraphic record allows the possibility to focus on the last Glacial-Interglacial transition and those factors (allogenic) that have been controlling the sedimentation.

This research is the result of integrated, multi-proxy (stratigraphic, paleontological, geotechnical, radiometric, pollen, petrographic) data, mostly extracted from the Regione Emilia-Romagna and Regione Lombardia databases. Stratigraphic data have been re-interpreted in the light of additional, “freshly” drilled continuous cores, carried out by the Regione Emilia-Romagna Geological Survey.

Accurate stratigraphic correlations led to the construction of high-resolution cross-sections through five study areas: these areas were specifically selected to investigate Pl-H sedimentary successions from distal to more proximal sectors of the Po Plain (study areas 1, 2 and 3); to document the stratigraphic architecture of a coeval coastal succession located 300 km to the south, along the Adriatic shoreline, close to the LGM Po lowstand Delta (study area 4); to prove how high-resolution stratigraphic studies, including reconstruction of facies architecture and sediment body geometries, can be used for practical purposes (aquifer preservation - study area 5).

The key points of this 3 year Ph.D thesis focused on the Pleistocene-Holocene transition in the Po Plain, can be summarized as follows:

- Integrated sedimentological and micropaleontological analyses, coupled with radiocarbon dating, enabled the construction of a > 90 km-long cross section, transversal to the present Adriatic

coastline. This stratigraphic transect allowed for the first time the along-strike characterization of the Late Pleistocene-Holocene coastal succession in the Po Plain. The resulting high-resolution stratigraphic framework casts new light on the geometry of the Holocene, transgressive-regressive (T-R) coastal wedge, seen from a different perspective.

The Late Pleistocene sedimentary succession (ca. 45-12.5 ky BP) is almost entirely made up of well-drained floodplain deposits. Close to the Apenninic margin, three prominent weakly-developed paleosols were identified:

i) the lower paleosol (< 34 ky BP), is genetically related to erosional-based fluvial bodies;

ii) another paleosol (18.5-16 ky BP), is locally traceable into the top of amalgamated fluvial sands;

iii) the upper paleosol (12.5-10 ky BP), assigned to the Younger Dryas cold event, is tracked discontinuously across a large part of the transect. This paleosol marks the abrupt transition from Late Pleistocene alluvial sediments to the overlying Holocene succession.

A gradual transition from poorly-drained floodplain deposits to organic-rich, paludal clays (10.9-9.2 ky cal BP) up to lagoonal sediments (ca. 9 ky cal BP) characterizes the lower part of the Holocene succession. These back-barrier deposits are replaced up-section by thin, transgressive sands (ca. 8.4 ky cal BP), which in turn are overlain by a thick succession of laterally extensive offshore/prodelta muds (4.4-3.5 ky cal BP). In the southern part of the study area 1, shallow-marine deposits are in lateral transition with nearshore and lagoonal deposits, reflecting a local, along-dip component of the cross-section. The whole sedimentary succession is capped by a laterally extensive (> 90 km), 10 m-thick sand sheet, composed of beach ridge and delta-front deposits (last 2 ky).

In a sequence stratigraphic perspective, the lower paleosol is interpreted as the Sequence Boundary (SB). Radiocarbon ages suggest a possible link between pedogenesis and the abrupt sea-level fall/climate change (onset of Last Glacial Maximum) that took place at the MIS 3-MIS 2 transition, producing river incision and soil development in the interfluves. The coeval amalgamated channel-belts (lowstand systems tract, LST) accumulated during the LGM when shoreline was located more than 300 km to the south. The underlying (pre-LGM) alluvial deposits represent the forced regressive systems tract (FSST). The Transgressive Surface (TS) marks a major phase of channel abandonment, and coincides with a weakly-developed paleosol dated at 18.5-16 ky cal BP. Most likely this paleosol records the very last episode of subaerial exposure on the interfluves before sea-level rise induced the dramatic reorganization of the drainage system. The progressive drowning of the lowstand, north Adriatic alluvial plain is reflected by the characteristic deepening-upward tendency observed in the transgressive systems tract (TST), from alluvial, up to shallow-marine deposits. The YD paleosol allows TST subdivision into lower TST (pre-YD) and upper TST (post-YD). The early stages of transgression (Late Pleistocene) saw the onset of poorly-drained floodplain conditions along vast portions of the study area. Following

deglaciation, the sea invaded the alluvial plain during the Holocene, and the upper TST consists of vertically stacked, coastal to shallow-marine deposits. The Maximum Flooding Surface (MFS), dated ca. 6.6 ky cal BP at proximal locations, is placed at the turnaround from deepening-upward to shallowing-upward trend, and marks the generalized progradation of deltaic and coastal depositional systems. Based on the very high lateral continuity (> 90 km) of the late Holocene beach-ridge systems, we provide evidence for a wave-dominated (arcuate) delta morphology, with lateral transition to prograding strandpains.

- Beneath the modern Po River, in a fully-alluvial sector (study area 2), the contrasting alluvial architecture of Late Pleistocene amalgamated fluvial channel sands and overlying, Holocene mud-dominated deposits with isolated fluvial-channel bodies has been highlighted.

This characteristic architectural change can be continuously tracked for 130 km inland relative to the modern Adriatic shoreline, and is the result of changes in accommodation and sediment supply rates.

The deposition of the multi-storey sand sheet took place between 45 and 9.5 ky BP, during MIS 3, MIS 2 (LGM) and Late Glacial. A laterally extensive, organic-rich facies association marks the sharp transition between amalgamated sands to the overlying, mud-dominated Holocene deposits. It has been associated to the regional fluvial-channel abandonment at the onset of warm-temperate (interglacial) climate conditions.

The low net-to-gross Holocene deposits show considerable variations in the lateral distribution of facies association, with well-drained floodplain deposits that are replaced downstram by increasingly organic-rich clays (poorly-drained floodplain to swamps). Thick paludal desposits continuously extend ca. 60 km upstream of the maximum marine ingression.

Combined changes in climate and sea-level rise produced the characteristic stratigraphic transition from glacial sands to interglacial clay units. High erosional rates during glacial conditions allowed the accumulation of coarse sands into the Po channel belts, whereas the muddy portion was removed and transported basinwards. Forest expansion under warmer-interglacial conditions reduced erosional processes and transport capability along the catchment areas, leading to the deposition of the clay-dominated Holocene succession.

The Po channel belt sand bodies were deposited mainly under falling-stage, lowstand and early transgressive conditions (low accommodation). Once rapid sea-level rise increased accommodation (ca. 9.5 ky BP), avulsion became the dominant fluvial process and deposition of isolated fluvial channel bodies took place within low net-to-gross deposits (high accommodation).

The overall aggradational stacking pattern of the late Pleistocene-Holocene deposits in the Po Plain was driven by high subsidence rates, which continuously created accommodation even during falling sea-level and lowstand conditions.

- Paleosol identification is an essential part of the stratigraphic interpretation process. Simple geotechnical data (pocket penetrometer resistance) coupled by accurate facies analysis may help with the identification of pedogenized horizons. In this perspective, paleosols if properly correlated (i.e. paleosol stratigraphy), can play a key role for high-resolution stratigraphic reconstruction within Pleistocene-Holocene mud-dominated areas (i.e. interfluves).

Twelve pedogenized horizons (Inceptisols) within non-pedogenized alluvial strata were documented, through the calibration with facies analysis and radiometric dating from freshly drilled cores recovered in an interfluves sector of the Po Plain (study area 3). These paleosols can be physically traced over distances of tens of km.

- The comparison between two coeval coastal plain deposits (Po and Biferno, study areas 1 and 4) has revealed similarities in the overall stratigraphic architecture of these successions (i.e. amalgamated fluvial bodies underlying mud-dominated sediments with individual fluvial sands). Despite this general similarity, high-resolution investigation of the Biferno coastal deposits has shown episodes of valley incision (Biferno paleovalley), whereas no evidence of paleovalley systems was found within the Po Plain deposits.

The Late Pleistocene-Holocene Biferno paleovalley represents the first reported onshore example of incised valley system (IVS) along the Adriatic coast of Italy. The valley was incised by the Biferno River since the last glacial (ca. 125 ky BP) sea-level fall, which progressively shaped the characteristic profile with lateral terraces and a deeper channel. Above lowstand fluvial gravels, the most landward portion of the post-glacial valley fill succession displays a transgressive-regressive succession of non-marine deposits. In response to the rapid Pleistocene-Holocene sea-level rise, the Biferno alluvial valley was progressively drowned. During the early Holocene it became an estuary, characterized by landward shift of facies. At time of maximum marine ingression, the marine influence into the valley extended 1.5 km landward of the present day shoreline, and the study area 4 experienced sedimentation under brackish (estuarine) conditions. The upward return to paludal, poorly-drained floodplain and well-drained conditions reflects highstand progradation during the middle-late Holocene.

In a sequence stratigraphic perspective, the fluvial terraces have been interpreted as falling stage systems tract (FSST); the deepest fluvial gravel body as the lowstand systems tract (LST); the deepening upward succession from alluvial to estuarine deposits as the transgressive systems tract (TST); the uppermost shallowing-upward trend from estuarine to modern alluvial deposits as the highstand systems tract (HST).

- High-resolution stratigraphic investigations can be useful for aquifer protection. A detailed stratigraphic and hydrogeological investigation of Pleistocene-Holocene deposits beneath the city of Ferrara allowed the creation of a hydrogeologic conceptual model focusing on contaminant

reduction and migration through aquifers. Facies distribution and sediment body geometries play a key role within this framework. In fact, reductive dechlorination of more highly chlorinated parent compounds (PCE and TCE) occurs down to VC, during contaminant retention and migration within fine peat-rich deposits, which correspond to Holocene swamp deposits. These organic-rich sediments represent a local “reactor” for biotransformation in strongly reducing conditions. Furthermore, distribution and migration of contaminants is driven by lateral, vertical distribution and degree of connectivity of high-permeability versus low-permeability sedimentary bodies. Amalgamated Late Pleistocene fluvial-channel sands form one of the major aquifers beneath the Ferrara subsurface (i.e. A1 aquifer); clay and silty clay floodplain deposits represent permeability barriers (i.e. aquitards).

REFERENCES

Adams M.M., Bhattacharya J.P., 2005. No change in fluvial style across a sequence boundary, Cretaceous Blackhawk and Castlegate formations of Central Utah, U.S.A. Journal of Sedimentary Research, 75, 1038-1051.

Aitken J.F., Flint S.S., 1996. Variable expression of interfluvial sequence boundaries in the Breathitt Group (Pennsylvanian), eastern Kentucky, USA. In: Howell J.A., Aitken J.F. (Eds.), High Resolution Sequence Stratigraphy: Innovation and Applications. Geological Society, London, Special Publication, 104, 193-206.

Amorosi A, Farina M., Severi P., Preti D., Caporale L., Di Dio G., 1996. Genetically related alluvial deposits across active fault zones: an example of alluvial fan-terrace correlation from the upper Quaternary of the southern Po Basin, Italy. Sedimentary Geology, 102, 275-295.

Amorosi A., Marchi N., 1999. High-resolution sequence stratigraphy from piezocone tests: an example from the Late Quaternary deposits of the SE Po Plain. Sedimentary Geology, 128, 69-83.

Amorosi A., Colalongo M.L., Fusco F., Pasini G., Fiorini F., 1999a. Glacio-eustatic control of continental-shallow marine cyclicity from Late Quaternary deposits of the south-eastern Po Plain (Northern Italy). Quaternary Research, 52, 1-13.

Amorosi A., Colalongo M.L., Pasini G., Preti, D., 1999b. Sedimentary response to Late Quaternary sea-level changes in the Romagna coastal plain (northern Italy). Sedimentology, 46, 99-121.

Amorosi A., Milli S., 2001. Late Quaternary depositional architecture of Po and Tevere river deltas (Italy) and worldwide comparison with coeval deltaic successions. Sedimentary Geology, 144, 357-375.

Amorosi A., Forlani M.L., Fusco F., Severi P., 2001. Cyclic patterns of facies and pollen associations from Late Quaternary deposits in the subsurface of Bologna. GeoActa, 1, 83-94.

Amorosi A., Centineo M.C., Dinelli E., Lucchini F., Tateo F., 2002. Geochemical and mineralogical variations as indicators of provenance changes in Late Quaternary deposits of SE Po Plain. Sedimentary Geology, 151, 273-292.

Amorosi A., Centineo M.C., Colalongo M.L., Pasini G., Sarti G., Vaiani S.C., 2003. Facies architecture and Latest Pleistocene–Holocene depositional history of the Po Delta (Comacchio area), Italy. Journal of Geology, 111, 39-56.

Amorosi A., Colalongo M.L., Fiorini F., Fusco F., Pasini G., Vaiani S.C., Sarti G., 2004. Palaeogeographic and palaeoclimatic evolution of the Po Plain from 150-ky core records. Global and Planetary Change, 40, 55-78.

Amorosi A., Colalongo M.L., 2005. The linkage between alluvial and coeval nearshore marine succession: evidence from the Late Quaternary record of the Po River Plain, Italy. In: Blum M.D.,

Marriott S.B., Leclair S.F. (Eds.), Fluvial Sedimentology VII. International Association of Sedimentologists, Special Publication, 35, 257-275.

Amorosi A., Centineo M.C., Colalongo M.L., Fiorini F., 2005. Millennial-scale depositional cycles from the Holocene of the Po Plain, Italy. Marine Geology, 222-223, 7-18.

Amorosi A., 2008. Delineating aquifer geometry within a sequence stratigraphic framework: Evidence from the Quaternary of the Po River Basin, Northern Italy. In: Amorosi A., Haq B.U., Sabato L. (Eds.), Advances in Application of Sequence Stratigraphy in Italy. GeoActa, Special Publication, 1, 1-14.

Amorosi A., Pavesi M., Ricci Lucchi M., Sarti G., Piccin A., 2008a. Climatic signature of cyclic fluvial architecture from the Quaternary of the central Po plain, Italy. Sedimentary Geology, 209, 58-68.

Amorosi A., Dinelli E., Rossi V., Vaiani S.C., Sacchetto M., 2008b. Late Quaternary palaeoenvironmental evolution of the Adriatic coastal plain and the onset of the Po River Delta. Palaeogeography, Palaeoclimatology, Palaeoecology, 268, 80-90.

Amorosi A., Sarti B., Rossi V., Fontana V., 2008c. Anatomy and sequence stratigraphy of the late Quaternary Arno valley fill (Tuscany, Italy). In: Amorosi A., Haq B.U., Sabato L. (Eds.), Advances in Application of Sequence Stratigraphy in Italy. GeoActa, Special Publication, 1, 55-66.

Amorosi A., Ricci Lucchi M., Rossi V., Sarti B., 2009. Climate change signature of small-scale parasequences from Lateglacial–Holocene transgressive deposits of the Arno valley fill. Palaeogeography, Palaeoclimatology, Palaeoecology, 273, 142-152.

Amorosi A., Pavesi M., 2010. Aquifer stratigraphy from the middle-late Pleistocene succession of the Po Basin. Memorie Descrittive della Carta Geologica d'Italia XC, 7-20.

Amorosi A., Pacifico A., Rossi V., Ruberti D., 2012. Late Quaternary incision and deposition in an active volcanic setting: The Volturno valley fill, southern Italy. Sedimentary Geology, 282, 307-320.

Amorosi A., Rossi V., Sarti G., Mattei R., 2013. Coalescent valley fills from the late Quaternary record of Tuscany (Italy). Quaternary International, 288, 129-138.

Amorosi A., Bruno L., Rossi V., Severi P., Hajdas I., 2014. Paleosol architecture of a late Quaternary basin-margin sequence and its implications for high-resolution, non-marine sequence stratigraphy. Global and Planetary Change, 112, 12-25.

Amorosi A., Bruno L., Campo B., Morelli A., 2015. The value of pocket penetration tests for the high-resolution palaeosol stratigraphy of late Quaternary deposits. Geological Journal, 50, 670-682.

Antonioli F., Ferranti L., Fontana A., Amorosi A., Bondesan A., Braitenberg C., Dutton A., Fontolan G., Furlani S., Lambeck K., Mastronuzzi G., Monaco C., Spada G., Stocchi P., 2009. Holocene relative sea-level changes and vertical movements along the Italian and Istrian coastlines. Quaternary International, 206, 102-133.

Aqrawi A.A.M., 2001. Stratigraphic signatures of climatic change during the Holocene evolution of the Tigris-Euphrates delta, lower Mesopotamia. Global and Planetary Change, 28, 267-283.

Baldi P., Casula G., Cenni N., Loddo F., Pesci A., 2009. GPS-based monitoring of land subsidence in the Po Plain (Northern Italy). Earth and Planetary Science Letters, 288, 204-212.

Behl R.J., Kennet J.P., 1996. Brief interstadial events in the Santa Barbara basin, NE Pacific, during the past 60 kyr. Nature, 379, 243-246.

Bertotti G., Picotti V., Cloetingh S., 1998. Lithospheric weakening during "retroforeland" basin formation: tectonic evolution of the central South Alpine foredeep. Tectonics, 17, 131-142.

Blum M.D., Törnqvist T.E., 2000. Fluvial response to climate and sea level change: a review and look forward. Sedimentology, 47, 2-48.

Blum M.D., Aslan A., 2006. Signatures of climate vs. sea-level change within incised valley-fill successions: Quaternary examples from the Texas Gulf Coast. Sedimentary Geology, 190, 177-211.

Blum, M.D., Martin, J., Milliken, K., Garvin M., 2013. Paleovalley systems: insights from Quaternary analogs and experiments. Earth Science Reviews, 116, 128-169.

Boccaletti M., Coli M., Eva C., Ferrari G., Giglia G., Lazzarotto A., Merlanti A., Nicolich F., Papani R., Postpischl G., 1985. Considerations on the seismotectonics of the Northern Apennines. Tectonophysics, 117, 7-38.

Boccaletti M., Bonini M., Corti G., Gasperini P., Martelli L., Piccardi L., Tanini C., Vannucci G., 2004. Seismotectonic map of the Emilia-Romagna Region, 1:250,000, Regione Emilia-Romagna-CNR, SELCA, Firenze, Italy.

Bond G., Broecker W., Johnsen S., McManus J., Labeyrie L., Jouzel J., Bonani G., 1993. Correlations between climate records from North Atlantic sediments and Greenland ice. Nature, 365, 143-147.

Bond G., Showers W., Cheseby M., Lotti R., Almasi P., DeMenocal P., Priore P., Cullen H., Haidas I., Bonani G., 1997. A pervasive millennial-scale cycle in North Atlantic Holocene and glacial climates. Science, 14, 1257-1266.

Bondesan M., Favero V., Vinals M.J., 1995. New evidence on the evolution of the Po-delta coastal plain during the Holocene. Quaternary International, 29-30, 105-110.

Boyd R., Dalrymple R.W., Zaitlin B.A., 2006. Estuarine and incised-valley facies models. In: Posamentier H.W., Walker R.G. (Eds.), Facies models revisited. SEPM, Special Publication, 84, 171-235 pp.

Bridgland D.R., 2000. River terrace systems in north-west Europe: an archive of environmental change, uplift and early human occupation. Quaternary Science Review, 19, 1293-1303.

Bruno L., Amorosi A., Curina R., Severi P., Bitelli R., 2013. Human-landscape interactions in the Bologna area (northern Italy) during the mid-late Holocene, with focus on the Roman period. The Holocene, 23, 1560-1571.

Buck B.J., Lawton T.F., Brock A.L., 2010. Evaporitic paleosols in continental strata of the Carroza Formation, La Popa Basin, Mexico: Record of Paleogene climate and salt tectonics. Geological Society of America Bulletin, 122, 1011-1026.

Burke K., Francis P., Wells G., 1990. Importance of the geological record in understanding global change, Peleogeography, Paleoclimatology, Paleoecology, 89, 193-204.

Burrato P., Ciucci F., Valensise G., 2003. An inventory of river anomalies in the Po Plain, Northern Italy: evidence for active blind thrust faulting. Annals of Geophysics, 46, 865-882.

Carminati E., Martinelli G., 2002. Subsidence rates in the Po Plain, northern Italy: the relative impact of natural and anthropogenic causation. Engineering Geology, 66, 241-255.

Carminati E., Doglioni C., Scrocca D., 2005. Magnitude and causes of long-term subsidence of the Po Plain and the Venetian region. In: Fletcher C.A. and Spencer T. (Eds.) with Da Mosto J., Campostrini P., Flooding and Environmental changes for Venice and its Lagoon: State of Knowledge. Cambridge University Press, 23-28 pp.

Carminati E., Vadacca L., 2010. Two- and three-dimensional numerical simulations of the stress field at the thrust front of the Northern Apennines, Italy. Journal of Geophysical Research, 115. DOI: 10.1029/2010JB007870

Carminati E., Doglioni C., 2012. Alps vs. Apennines: the paradigm of a tectonically asymmetric Earth. Earth-Science Reviews, 112, 67-96.

Castellarin A., Vai G.B., 1986. Southalpine versus Po Plain apenninic arcs. In: Wezel F.C. (Ed.), The Origin of Arcs. Geotectonics, 21, 253-280.

Castellarin A., Cantelli L., 2000. Neo-Alpine evolution of the Southern Eastern Alps. Journal of Geodynamics, 30, 251-274.

Cattaneo A., Trincardi F., 1999. The late-Quaternary transgressive record in the Adriatic epicontinental sea: basin widening and facies partitioning. In: Bergman K.M., Snedden J.W. (Eds.), Isolated shallow marine sand bodies: sequence stratigraphic analysis and sedimentologic interpretation. SEPM, Special Publication, 64, 127-146.

Cattaneo A., Steel R.J., 2003. Transgressive deposits: a review of their variability. Earth-Science Reviews, 62, 187-228.

Chappell J., Shackleton N.J., 1986. Oxygen isotopes and sea-level. Nature, 324, 137-140.

Choi K., 2005. Pedogenesis of late Quaternary deposits, northern Kyonggi Bay, Korea: Implications for relative sea-level change and regional stratigraphic correlation. Palaeogeography, Palaeoclimatology, Palaeoecology, 220, 387-404.

Cleveland D.M., Atchley S.C., Nordt L.C., 2007. Continental sequence stratigraphy of the Upper Triassic (Norian-Rhaetian) Chinle strata, northern New Mexico, U.S.A.: allocyclic and autocyclic origins of paleosol-bearing alluvial successions. Journal of Sedimentary Research, 77, 909-924.

Consiglio Nazionale delle Ricerche, 1992. Structural model of Italy and gravity map, Progetto Finalizzato Geodinamica. Quad. Ric. Sci., Rome, 114, 3.

Correggiari A., Roveri M., Trincardi F., 1996. Late Pleistocene and Holocene evolution of the North Adriatic Sea. Il Quaternario (Italian J. Quat. Scien.), 9, 697-704.

Correggiari A., Cattaneo A., Trincardi F. 2005. The modern Po Delta system: Lobe switching and asymmetric prodelta growth. Marine Geology, 222-223, 49-74.

Correggiari A., Cattaneo A., Trincardi F. 2005. Depositional patterns in the Late-Holocene Po Delta System. In: Bhattacharya J.P., Giosan L. (Eds.), River deltas: Concepts, models and examples. SEPM, Special Publication, 83, 365-392.

Dalla S., Rossi M., Orlando M., Visentin C., Gelati R., Gnaccolini M., Papani G., Belli A., Biffi U., Citrullo D., 1992. Late Eocene Tortonian tectono-sedimentary evolution in the western part of the Padan basin (northern Italy). Paleontologia i Evolució, 24-25, 341-362.

Dalrymple R.W., Boyd R., Zaitlin B.A., 1994. Incised-Valley Systems: Origin and Sedimentary Sequences. SEPM, Special Publication, 51, 1-391 pp.

Doglioni C., 1993. Some remarks on the origin of foredeeps. Tectonophysics, 228, 1-20.

Doglioni C., Harabaglia P., Merlini S., Mongelli F., Peccerillo A., Piromallo C., 1999. Orogens and slab vs their direction of subduction. Earth Science Reviews, 45, 167-208.

Elter P., Pertusati P., 1973. Considerazioni sul limite Alpi-Appennino e sulle sue relazioni con l'arco delle Alpi occidentali. Memorie della Società Geologica Italiana, 12, 359-375.

Embry A.F., 1993. Transgressive-regressive (T-R) sequence analysis of the Jurassic succession of the Sverdrup Basin, Canadian Arctic Archipelago. Canadian Journal of Earth Sciences, 30, 301-320.

Embry A.F., 1995. Sequence boundaries and sequence hierarchies: problems and proposals. In: Steel R.J., Felt V.L., Johannessen E.P., Mathieu C. (Eds.), Sequence Stratigraphy on the Northwest European Margin. Spec. Publ. Nor. Petrol. Soc., 5, 1-11.

Galli P., Castenetto S., Peronace E., 2012. May 2012 Emilia earthquakes (Mw6, Northern Italy): macroseismic effects distribution and seismotectonic implications. Alpine and Mediterranean Quaternary, 25, 105-123.

Gueguen E., Doglioni C., Fernandez M., 1998. On the post 25 Ma geodynamic evolution of the western Mediterranean. Tectonophysics, 298, 259-269.

Hayes J.D., Imbrie J., Shackleton N.J., 1976. Variations in the earth's orbit: Pacemaker of the ice age. Science, 194, 1121-1132.

Helland-Hansen W., Gjelberg J.G., 1994. Conceptual basis and variability in sequence stratigraphy: a different perspective. Sedimentary Geology, 92, 31-52.

Helland-Hansen W., Martinsen O.J., 1996. Shoreline trajectories and sequences: description of variable depositional-dip scenarios. Journal of Sedimentary Research, 66, 670-688.

Hickson T.A., Sheets B.A., Paola C., Kelberer M., 2005. Experimental Test of Tectonic Controls on Three-Dimensional Alluvial Facies Architecture. Journal of Sedimentary Research, 75, 710-722.

Holbrook J., Scott R.W., Oboh-Ikuenobe F.E., 2006. Base-level buffers and buttresses: amodel for upstream versus downstream control on fluvial geometry and architecture within sequences. Journal of Sedimentary Research, 76, 162-174.

Hori K., Saito Y., Zhao Q., Wang P., 2002. Evolution of the Coastal Depositional Systems of the Changjiang (Yangtze) River in Response to Late Pleistocene-Holocene Sea-Level Changes. Journal of Sedimentary Research, 72, 884-897.

Imbrie J., Imbrie K., 1979. Ace Ages. Harvard University Press, Cambridge, MA.

Imbrie J., Hays J.D., Martinson D.G., McIntyre A., Mix A.C., Morley J.J., Pisias N.J., Prell W.I., Shackleton N.J., 1984. The orbital theory of Pleistocene climate: support from a revised chronology of the marine 18O record. In: Berger A., Imbrie J., Hays J., Kukla G., Saltsman B. (Eds.), Milankovitch and Climate – Part I. Reidel Publishing, Dordrecht, Holland, 269-306 pp.

Intergovernment Panel on Climate Change (IPCC), 1990. The IPCC Scientific Assessment, In: Houghton J.T., Jenkins G.J., Ephraums J.J. (Eds.), Cambridge University Press, 310 pp.

Kettner A.J., Syvitski J.P.M., 2008. Predicting discharge and sediment flux of the Po River, Italy since the Last Glacial Maximum. International Association of Sedimentologists, Special Publication, 40, 171-189.

Jervey M.T., 1988. Quantitative geological modeling of siliciclastic rock sequences and their seismic expression. In: Wilgus C.K., Hastings B.S., Kendall C.G.S.C., Posamentier H.W., Ross C.A., Van Wagoner J.C. (Eds.), Sea-Level Changes: An Integrated Approach. Soc. Econ. Paleontol. Mineral., Spec. Publ., 42, 47-69.

Johnson J.G., Klapper G., Sandberg C.A., 1985. Devonian eustatic fluctuations in Euramerica. Geological Society of America Bulletin, 96, 567-587.

Legarreta L., Uliana M.A., 1998. Anatomy of hinterland depositional sequences: Upper Cretaceous fluvial strata, Neuquen Basin, West-Central Argentina. In: Shanley K.W., McCabe P.J. (Eds.), Relative Role of Eustasy, Climate, and Tectonism in Continental Rocks. Soc. Econ. Paleontol. Mineral., Spec. Publ., 59, 83-92.

Leeder M.R., Stewart M.D., 1996. Fluvial incision and sequence stratigraphy: alluvial responses to relative sea-level fall and their detection in the geological record. In: Hesselbo S.P., Parkinson D.N. (Eds.), Sequence Stratigraphy in British Geology. Geological Society, London, Special Publications, 103, 25-39.

Lewis S.G., Maddy D., Scaife R.G., 2001. The fluvial system response to abrupt climate change during the last cold stage: the Upper Pleistocene River Thames fluvial succession at Ashton Keynes, UK. Global and Planetary Change, 28, 341-359.

Livio F.A., Berlusconi A., Michetti A.M., Sileo G., Zerboni A., Trombino L., Cremaschi M., Mueller K., Vittori E., Carcano C., Rogledi S., 2009. Active fault-related in the epicentral area of the December 25, 1222 (Io = IX MCS) Brescia earthquake (Northern Italy): seismotectonic implications. Tectonophysics, 476, 320-335.

Makclin M.G., Fuller I.C, Lewin J., Maas G.S., Passmore D.G., Rose J., Woodward J.C., Black S., Hamblin R.H.B., Rowan J.S., 2002. Correlation of fluvial sequences in the Mediterranean basin over the last 200 ka and their relationship to climate change. Quaternary Science Reviews, 21, 1633-1641.

Mancini M., Moscatelli M., Stigliano F., Cavinato G.P., Milli S., Pagliaroli A., Samionato M., Brancaleoni L., Cipolloni I., Coen G., Di Salvo C., Garbin F., Lanzo G., Napoleoni Q., Scarapazzi M., Storoni Ridolfi S., Vallone R., 2013. The Upper Pleistocene-Holocene fluvial deposits of the Tiber River in Rome (Italy): lithofacies, geometries, stacking pattern and chronology. Journal of Mediterranean Earth Sciences Special Issue, 95-101.

Marriott S.B., 1999. The use of models in the interpretation of the effects of base-level change onalluvial architecture. In: Smith N.D. and Rogers J. (Eds.), Fluvial Sedimentology VI. International Association of Sedimentologists Special Publication, 28, 271-281.

Martinsen O.J., Ryseth A., Helland-Hansen W., Flesche H., Torkildsen G., Idil S., 1999. Stratigraphic base level and fluvial architecture Ericson Sandstone (Campanian), Rock Sorings Uplift, SW Wyoming, USA. Sedimentology, 46, 235-259.

Martinson D.G., Pisias N.G., Hayes J.D., Imbrie J., Moore T.C., Shackleton N.J., 1987. Age dating and the orbital theory of the ice ages – Development of a high-resolution 0 to 300,000 year chronostratigraphy. Quaternary Research., 27, 1-29.

Marzo M., Steel R.J., 2000. Unusual features of sediment supply dominated, transgressive-regressive sequences: Paleogene clastic wedges, SE Pyrenean foreland basin, Spain. Sedimentary Geology, 138, 3-15.

Maselli V., Hutton E.W., Kettner A.J., Syvitski J.P.M., Trincardi F., 2011. High-frequency sea level and sediment supply fluctuations during Termination I: an integrated sequence-stratigraphy and modeling approach from the Adriatic Sea (Central Mediterranean). Marine Geology, 287, 54-70.

Maselli V., Trincardi F., 2013. Large-scale single incised-valley from a small catchment basin on the western Adriatic margin (central Mediterranean Sea). Global and Planetary Change, 100, 245-262.

Maselli V., Trincardi F., Asioli A., Rizzetto F., Taviani M., 2014. Delta growth and river valleys: the influence of climate and sea level changes on the South Adriatic shelf (Mediterranean Sea). Quaternary Science Reviews, 99, 146-163.

Massironi M., Zampieri D., Caporali A., 2006. Miocene to Present major fault linkages through the Adriatic indenter and the Austroalpine-Penninic collisional wedge (Alps of NE Italy). In: Moratti G., Chalouan A. (Eds.), Active Tectonics of the Western Mediterranean Region and North Africa. Geological Society, Special Publications, London, 262, 245-258.

Mazzoli S., Santini S., Macchiavelli C., Ascione A., 2015. Active tectonics of the outer northern Apennines: Adriatic vs. Po Plain seismicity and stress fields. Journal of Geodynamics, 84, 62-76.

McCarthy P.J., Plint A.G., 1998. Recognition of interfluve sequence boundaries: Integrating paleopedology and sequence stratigraphy. Geology, 26, 387-390.

Miall A.D., 1991. Stratigraphic sequences and their chronostratigraphic correlation. Journal of Sedimentary Petrology, 61, 497-505.

Milana J.P., 1998. Sequence stratigraphy in alluvial settings: a flume-based model with applications to outcrop and seismic data. AAPG Bulletin, 82, 1736-1753.

Milli S., 1997. Depositional setting and high-frequency sequence stratigraphy of the middle-upper Pleistocene to Holocene deposits of the Roman basin. Geologica Romana, 33, 99-136.

Milli S., Moscatelli M., Palombo M.R., Parlagreco R., Paciucci M., 2008. Incised-valleys, their filling and mammal fossil record: a case study from Middle-Upper Pleistocene deposits of the Roman Basin (Latium, Italy). GeoActa, Special Publication, 1, 67-88.

Milli S., D'Ambrogi C., Bellotti P., Calderoni G., Carboni M.G., Celant A., Di Bella L., Di Rita F., Frezza V., Magri D., Pichezzi R.M., Ricci V., 2013. The transition from wave-dominated estuary to wave-dominated delta. The Late Quaternary stratigraphic architecture of Tiber River deltaic succession (Italy). Sedimentary Geology, 284-285, 159-180.

Mitchell J.F.B., 1989. The greenhouse effect and climate change, Review of Geophysics, 27, 115-139.

Mitchum Jr. R.M., Vail P.R., Thompson III S., 1977. The depositional sequence as a basic unit for stratigraphic analysis. In: Payton C.E. (Ed.), Seismic Stratigraphy – Application to Hydrocarbon Exploration, AAPG Memoir, 26, 53-62.

Mitovica J.X., Davis J., 1995. Present-day post glacial sea level change far from the Late Pleistocene ice sheets: Implications for recent analyses of tide gauge records. Geophysical Research Letters, 22, 2529-2532.

Molinari F.C., Boldrini G., Severi P., Dugoni G., Rapti Caputo D., Martinelli G., 2007. Risorse idriche sotterranee della Provincia di Ferrara. In: Dugoni G., Pignone R. (Eds.), Risorse idriche sotterranee della Provincia di Ferrara, 7-61 pp.

Muttoni G., Carcano C., Garzanti E., Ghielmi M., Piccin A., Pini R., Rogledi S., Sciunnach D., 2003. Onset of major Pleistocene glaciations in the Alps. Geology, 31, 989-992.

Olsen T., Steel R., Hogseth K., Skar T., Roe S.L., 1995. Sequential architecture in a fluvial succession: sequence stratigraphy in the Upper Cretaceous Mesaverde Group, Price Canyon, Utah. Journal of Sedimentary Research, B65, 265-280.

Peiji L., 1991. Greenhouse effect and climate change, Journal of Glaciology and Geochronology, 3.

Picotti V., Pazzaglia F.J., 2008. A new active tectonic model for the construction of the Northern Apennines mountain front near Bologna (Italy). Journal of Geophysical Research, 113. DOI: 10.1029/2007JB005307

Pieri M., Groppi G., 1975. The structure of the base of the Pliocene-Quaternary sequence in the subsurface of the Po and Veneto Plains, the Pedeapennine Basin and the Adriatic Sea. In: Ogniben L., Parotto M., Praturlon A. (Eds.), Structural model of Italy, Quaderni de “La Ricerca Scientifica”, 90, 409-415.

Pieri M., Groppi G., 1981. Subsurface geological structure of the Po Plain, Italy. In: Pieri M., Groppi G. (Eds.), Progetto Finalizzato Geodinamica 414, C.N.R, Roma, 1-23 pp.

Plint A.G., Nummedal D., 2000. The falling stage systems tract: recognition and importance in sequence stratigraphic analysis. In: Gawthorpe R.L., and Hunt D. (Eds.), Sedimentary Responses to Forced Regressions, Geological Society, London, Special Publications, 172, 1-17.

Plint A.G., McCarthy P.J., Faccini U.F., 2001. Nonmarine sequence stratigraphy: updip expression of sequence boundaries and systems tracts in a high-resolution framework, Cenomanian Dunvegan Formation, Alberta foreland basin, Canada. AAPG Bullettin, 85, 1967-2001.

Posamentier H.W., Jervey M.T., Vail P.R., 1988. Eustatic controls on clastic deposition I: Conceptual framework. In: Wilgus C.K., Hastings B.S., Kendall C.G.St.C., Posamentier H.W., Ross C.A., Van Wagoner J.C. (Eds.), Sea Level Changes: An Integrated Approach. Soc. Econ. Paleontol. Mineral., Spec. Publ., 42, 109-124.

Posamentier H.W., Vail P.R., 1988. Eustatic controls on clastic deposition II: Sequence and systems tract models. In: Wilgus C.K., Hastings B.S., Kendall C.G.St.C., Posamentier H.W., Ross C.A., VanWagoner J.C. (Eds.), Sea Level Changes: An Integrated Approach. Soc. Econ. Paleontol. Mineral., Spec. Publ., 42, 125-154.

Posamentier H.W., Allen G.P., 1999. Siliciclastic sequence stratigraphy: concepts and applications. SEPM, Concepts in Sedimentology and Paleontology, 7, 209 pp.

Ramsey B., 2009. Bayesian analysis of radiocarbon dates. Radiocarbon, 51, 337-360.

Reimer P.J., Bard E., Bayliss A., Beck J.W., Blackwell P.G., Bronk Ramsey C., Grootes P.M., Guilderson T.P., Haflidason H., Hajdas I., Hatt C., Heaton T.J., Hoffmann, D.L., Hogg A.G., Hughen K.A., Kaiser K.F., Kromer B., Manning S.W., Niu M., Reimer R.W., Richards D.A., Scott E.M., Southon J.R., Staff R.A., Turney C.S. M., van der Plicht J., 2013. IntCal13 and Marine13 Radiocarbon Age Calibration Curves 0-50,000 Years cal BP. Radiocarbon, 55, 1869-1887.

Regione Emilia-Romagna, and ENI-AGIP, 1998. Riserve idriche sotterranee della Regione Emilia-Romagna, Firenze, S.EL.CA. s.r.l., 120 pp.

Regione Lombardia, and E.N.I. Divisione A.G.I.P., 2002. Geologia degli acquiferi Padani della Regione Lombardia, Firenze, S.EL.CA. s.r.l., 130 pp.

Ricci Lucchi F., Colalongo M.L., Cremonini G., Gasperi G., Iaccarino S., Papani G., Raffi I., Rio D., 1982. Evoluzione sedimentaria e paleogeografica del margine appenninico. In: Cremonini G., Ricci Lucchi F. (Eds.), Guida alla geologia del margine appenninico-padano. Guide Geologiche Regionali So. Geol. Ital., 17-46.

Rizzini A., 1974. Holocene sedimentary cycle and heavy mineral distribution, Romagna-Marche coastal plain, Italy. Sedimentary Geology, 11, 17-37.

Schumm S.A., 1993. River response to baselevel change: implications for sequence stratigraphy. Journal of Geology, 101, 279-294.

Serpelloni E., Vannucci G., Pondrelli S., Argnani A., Casula G., Anzidei M., Baldi P., Gasperini P., 2007. Kinematics of the Western Africa-Eurasia plate boundary from focal mechanism and GPS data. Geophysical Journal International, 169, 1180-1200.

Shackleton N.J., 1987. Oxygen isotopes, ice volume and sea level. Quaternary Science Reviews, 6, 183-190.

Shackleton N.J., Opdyke N.D., 1973. Oxygen isotope and paleomagnetic stratigraphy of equatorial Pacific core V28-238: oxygen isotope temperatures and ice volume on a 105 and 106 year scale. Quaternary Research, 3, 39-55.

Shanley K.W., McCabe P.J., 1993. Alluvial architecture in a sequence stratigraphic framework: a case history from the Upper Cretaceous of southern Utah, USA. In: Flint S.S., Bryant I.D. (Eds.), The Geological Modelling of Hydrocarbon Reservoirs and Outcrop Analogues. International Association of Sedimentologists Special Publication, 15, 21-56.

Shanley K.W., McCabe P.J., 1994. Perspectives on the sequence stratigraphy of continental strata: report of working group at the 1991 NUNA Conference on High Resolution Sequence Stratigraphy. AAPG Bulletin, 78, 544-568.

Shen Z., Törnqvist T.E., Autin W.J., Mateo Z.R.P., Straub K.M., Mauz B., 2012. Rapid and widespread response of the Lower Mississippi River to eustatic forcing during the last glacial-interglacial cycle. Geological Society of America Bullettin, 124, 690-704.

Smith J.B., Tirpak D.A., 1989. The potential effects of global climate changes on the United States, United States Environmental Protection Agency, Washington DC, 642 pp.

Stefani M., Vincenzi S., 2005. The interplay of eustasy, climate and human activity in the late Quaternary depositional evolution and sedimentary architecture of the Po Delta system. Marine Geology, 222-223, 19-48.

Stefani C., Fellin M.G., Zattin M., Zuffa G.G., Dalmonte C., Mancin N., Zanferrari A., 2007. Provenance and paleogeographic evolution in a multisource foreland: the Cenozoic Venetian-Friulian Basin (NE Italy). Journal of Sedimentary Research, 77, 867-887.

Stuiver M., Reimer P.J., 1993. Extended 14C database and revised CALIB radiocarbon calibration program. Radiocarbon, 3, 215-230.

Styllas M., 2014. A simple approach for defining Holocene sequence stratigraphy using borehole and cone penetration test data. Sedimentology, 61, 444-460.

Tanabe S., Saito Y., Vu Q.L., Hanebuth T.J.J., Ngo Q.L., Kitamura A., 2006. Holocene evolution of the Song Hong (Red River) delta system, northern Vietnam. Sedimentary Geology, 187, 29-61.

Trincardi F., Correggiari A., Roveri M., 1994. Late Quaternary transgressive erosion and deposition in a modern epicontinental shelf: the Adriatic semi-enclosed Basin. Geo-Marine Letters, 14, 41-51.

Vandenberghe J., 2003. Climate forcing of fluvial system development: an evolution of ideas. Quaternary Science Reviews, 22, 2053-2060.

Vannoli P., Burrato P., Valensise G., 2015. The seismotectonics of the Po Plain (northern Italy): tectonic diversity in a blind faulting domain. Pure and Applied Geophysics, 172, 1105-1142.

Van Wagoner J.C., Mitchum R.M., Posamentier H.W., Vail P.R., 1987. An overview of sequence stratigraphy and key definition. In: Bally A.W. (Ed.), Atlas of seismic Stratigraphy (1). AAPG, Studies in geology, 27, 1, 11-14.

Van Wagoner J.C., Mitchum R.M., Campion K.M., Rahmanian V.D., 1990. Siliciclastic sequence stratigraphy in well logs, cores and outcrops: concepts for high resolution correlations of time and facies. In: Barbara H. Lidtz (Ed.), Methods in Exploration 7. AAPG, Tulsa, U.S.A, 55 pp.

Varela A.N., Veiga G.D., Poiré D.G., 2012. Sequence stratigraphic analysis of Cenomanian greenhouse paleosols: a case study from southern Patagonia, Argentina. Sedimentary Geology, 271-272, 67-82.

Wright V.P., Marriott S.B., 1993. The sequence stratigraphy of fluvial depositional systems: the role of floodplain sediment storage. Sedimentary Geology, 86, 203-210.

Zaitlin B.A., Dalrymple, R.W., Boyd, R., 1994. The stratigraphic organization of incised valley systems associated with relative sea-level change. In: Dalrymple R.W., Boyd R., Zaitlin B.A. (Eds.), Incised-Valley Systems: Origin and Sedimentary Sequences. SEPM, Special Publication, 51, 45-60 pp.